



If you have discovered material in AURA which is unlawful e.g. breaches copyright, (either yours or that of a third party) or any other law, including but not limited to those relating to patent, trademark, confidentiality, data protection, obscenity, defamation, libel, then please read our [Takedown Policy](#) and [contact the service](#) immediately

*TO THE SOUL OF MY FATHER WHO
LIVED HUMBL Y AND DIED PEACFULLY*

MODELLING OF INDUCTION MOTORS
FOR SYSTEM FAULTS AND TRANSIENT
STABILITY STUDIES

THESIS

BY

NAGI RIZIG FAHMI

Presented to the Department of Electrical
and Electronic Engineering of the
UNIVERSITY OF ASTON IN BIRMINGHAM
for the degree of

DOCTOR OF PHILOSOPHY

APRIL 1986

Acknowledgements

I wish to take the opportunity to express my sincere thanks to Dr. R. C. Johnson, my research supervisor, whose door was always open whenever I sought advice and help. Also, I would like to extend my thanks to Dr. A. L. Bowden, the research co-supervisor for the useful discussions and guidance during the course of the research.

The Author is also grateful to Mr. G. Hadwick from the CEEGB who enriched the discussions and gave advice on many technical aspects.

I would like also to express my thanks and love to my wife Raga who sacrificed time and comfort, encouraging and supporting in spite of illness. My thanks also to my daughter Nancy and my son Romani for their patient appreciation.

Thanks are also due to the Sudanese people in providing the financial support in a time of crises and famine where thousands of children are starving to death.

Most of all, I am thankful to GOD almighty for His help during the course.

THE UNIVERSITY OF ASTON IN BIRMINGHAM

MODELLING OF INDUCTION MOTORS
FOR SYSTEM FAULTS AND TRANSIENT
STABILITY STUDIES

BY NAGI RIZIG FAHMI

A thesis submitted for the degree of
Doctor of Philosophy

Summary

The research carried out in this thesis was mainly concerned with the effects of large induction motors and their transient performance in power systems. Computer packages using the three phase co-ordinate frame of reference were developed to simulate the induction motor transient performance.

A technique using matrix algebra was developed to allow extension of the three phase co-ordinate method to analyse asymmetrical and symmetrical faults on both sides of the three phase delta-star transformer which is usually required when connecting large induction motors to the supply system.

System simulation, applying these two techniques, was used to study the transient stability of a power system. The response of a typical system, loaded with a group of large induction motors, two three-phase delta-star transformers, a synchronous generator and an infinite system was analysed. The computer software developed to study this system has the advantage that different types of fault at different locations can be studied by simple changes in input data.

The research also involved investigating the possibility of using different integrating routines such as Runge-Kutta-Gill, Runge-Kutta-Fehlberg and the Predictor-Corrector methods. The investigation enables the reduction of computation time, which is necessary when solving the induction motor equations expressed in terms of the three phase variables. The outcome of this investigation was utilised in analysing an introductory model (containing only minimal control action) of an isolated system having a significant induction motor load compared to the size of the generator energising the system.

Key words

Induction Motors, Synchronous Generators, Fault Analysis,
Transient Stability, Simulation.

LIST OF CONTENTS

<u>Section</u>	<u>Caption</u>	<u>Page No.</u>
CHAPTER I	INTRODUCTION	
1.1	Background	1
1.2	Critical Review of Past Literature and Scope of Achievements	3
1.3	Aims of Present Reseach	7
1.4	Approachs in Research	7
1.5	Research Layout	9
CHAPTER II	LITERATURE SURVEY	
2.1	Introduction .	12
2.2	Types of Loads and Their Effects on Power Systems	12
2.2.1	Electrical Characteristics of Loads in Steady State	14
2.3	Induction-Motors in Power Systems	17
2.4	Transient Behaviour of Induction-Motors	19
2.5	System Fault Levels	20
2.6	Selection of Make-Break Devices	20
2.7	Induction-Motors Loading and the Choice of the Make-Break Devices	24
2.8	Stability of Systems Containing Synchronous and Induction Machines	26
2.9	Prediction of Stability in Power Systems	27
2.9.1	Step-by-Step Methods	28
2.9.2	Application of Lyapunov's Direct Method	29

<u>Section</u>	<u>Caption</u>	<u>Page No.</u>
2.9.3	Network Analysers and Analogue Computers	32
2.9.4	Digital Computers	33
2.10	Representation of Machines for Transient Analysis	34
2.10.1	Synchronous Machines	34
2.10.2	Induction Machines	37
2.11	Comparison between Synchronous and Induction machines	38
2.12	Effect of Saturation on Machine Performance	40
2.13	Effect of Inertia on Machine Performance	41
2.14	Conclusions	42
CHAPTER III	TRANSIENT PERFORMANCE OF LARGE INDUCTION MOTORS	
3.1	Introduction	44
3.2	Differential Equations of Induction Machines in Three Phase Frame of Reference	45
3.2.1	General	45
3.2.2	Assumptions and Limitations	46
3.2.3	E.M.F Equations	47
3.2.4	The Inductance Matrix	48
3.2.5	Equations of Motion	51
3.3	Determination of Machine Parameters by Test	53
3.4	System Circuit and Data	54

<u>Section</u>	<u>Caption</u>	<u>Page No.</u>
3.5	Algorithms and the Numerical Solution	57
3.6	Program Flow Chart	58
3.7	Transient Analysis	60
3.7.1	Switching	60
3.7.2	Fault Analysis	62
3.8	Discussion and Conclusions	65
CHAPTER IV	FAULT ANALYSIS OF INDUCTION MOTORS FED VIA DELTA/STAR TRANSFORMERS	
4.1	Introduction	87
4.2	Delta/Star Transformers	88
4.2.1	Voltage Analysis	89
4.2.2	Current Analysis	91
4.3	Induction Motor Equations in term of Currents	92
4.4	Transformation of Parameters from h.v Delta side to l.v Star side	95
4.5	System Modelling	96
4.5.1	Mathematical Analysis	97
4.6	Fault Analysis	100
4.7	Faults on Motor Terminals	100
4.7.1	Symmetrical Faults	101
4.7.2	Asymmetrical Faults	101
4.8	Faults on h.v Delta Terminals	102
4.9	Open-Circuit Faults	105

<u>Section</u>	<u>Caption</u>	<u>Page No.</u>
4.10	Numerical Solution	106
4.11	Analysis of The Results	109
4.12	Conclusions	110
CHAPTER V	TRANSIENT STABILITY STUDIES.	
5.1	Introduction	120
5.2	System Description	121
5.3	Requirements	123
5.4	Synchronous Generator Model	126
5.4.1	Voltage Equation	127
5.4.2	The Swing Equation	129
5.4.3	The Elements of the Generator Inductance Matrix	131
5.5	Derivation of the System Model	137
5.5.1	Modelling of the Group of the Induction Motors	138
5.5.2	Modelling of the Generator Connected to Bus-Bar 'B2'	139
5.5.3	Modelling of the Line and the Generator-Transformer 'T2'	139
5.5.4	Modelling of the Motor-Transformer 'T1'	142
5.6	Transient Stability Studies	143
5.6.1	Disturbances due to Faults on Bus-Bar 'B2'	143
5.6.1.1	Single Phase to earth Fault on Phase 'a'	144
5.6.1.2	Double Phase to eart Fault on Phases 'a& b'	145

<u>Section</u>	<u>Caption</u>	<u>Page No.</u>
5.6.1.3	Three Phase to earth Fault	145
5.6.1.4	Line-to-Line Short Circuit	146
5.6.2	Disturbances due to Faults on Bus-Bar 'B1'	147
5.7	Software Development	148
5.8	Results	156
5.9	Conclusions	158
CHAPTER VI	AN INTRODUCTION TO THE MODELLING OF ISOLATED SYSTEMS	
6.1	Introduction	169
6.2	Integration Routines	171
6.2.1	Runge-Kutta Methods	172
6.2.1.1	Gill Process	173
6.2.1.2	Runge-Kutta 4th Order	174
6.2.1.3	Kutta's Three-Eights Rules	175
6.2.1.4	Runge-Kutta-Fehlberg	175
6.2.2	Multistep Methods	178
6.2.2.1	The Implicit or Closed Methods	178
6.2.2.2	The Explicit or Open Methods	179
6.2.3	Criteria for Choice of the Step-Length	181
6.3	Investigations Made with Different Integration Routines	182
6.4	Outcome of the Investigations	184
6.5	The System and its Equations	190

<u>Section</u>	<u>Caption</u>	<u>Page No.</u>
6.5.1	Assumptions & Justification	190
6.5.2	System Mathematical Model	196
6.6	Faults and Transient Stability Studies	199
6.6.1	Sustained Solid Three-Phase-to-Earth Faults	199
6.6.2	A Transient Stability Study	201
6.7	Discussion	202
6.8	Conclusions	205
CHAPTER VII	CONCLUSIONS AND SUGGESTIONS FOR FURTHER WORK	
7.1	Conclusions	217
7.2	Suggestions for Further Work	224

APPENDICES

Appendix A1

Appendix A2

Appendix A3

LIST OF REFERENCES AND BIBLIOGRAPHY

LIST OF FIGURES

<u>Figure No.</u>	<u>Description</u>	<u>Page No.</u>
2.1	Steady-state load characteristics of the Induction Motor	15
2.2	A graph illustrating a numerical integrating technique solving for the angular velocity (ω) with an assumption of constant accelerating power	28
2.3	As fig. 2.2 with an assumption of constant power from the middle of the interval Δt	29
3.1	A diagram showing the current convention of the idealised Induction Machine	45
3.2	A vector diagram to show the relationships between the stator and rotor axes of the Induction Machine	45
3.3	A flow chart to show the steps of the solution of the flux vector of the Induction Machine equations	59
3.4	Starting current (phase A stator) of 12.6 Mva Induction Motor following simultaneous switching with the machine unloaded	71
3.5	A case of switching as in fig. 3.4 but the motor is fully loaded	72
3.6	Starting current (phase-a-rotor) of 12.6 Mva Induction Motor following simultaneous switching with the machine unloaded	73
3.7	A case of switching as in fig. 3.6 but the motor fully loaded	72

<u>Figure No.</u>	<u>Description</u>	<u>Page No.</u>
3.8	Air-Gap Torque/Time characteristics of 12.6 Mva Induction Motor following simultaneous switching with the machine unloaded	74
3.9	As fig. 3.8 but the machine fully loaded	75
3.10	Air-Gap Torque/Slip characteristics of 12.6 Mva Induction Motor following simultaneous switching with the machine unloaded	75
3.11	Speed/Time curve of 12.6 Mva Induction Motor following simultaneous switching with the machine fully loaded	76
3.12	As fig. 3. 11 but the machine unloaded	76
3.13	Starting current (phase 'A' stator) of 12.6 Mva Induction Motor following sequential switching at 90 degrees with the machine unloaded	71
3.14	Starting current (phase 'a' rotor) of 12.6 Mva Induction Motor following sequential switching at 90 degrees with the machine unloaded	73
3.15	Air-Gap Torque/Time characteristics of 12.6 Mva Induction Motor following sequential switching at 90 degrees with the machine unloaded	74
3.16	Speed/Time curve of 12.6 Mva Induction Motor following sequential switching at 90 degrees with the machine unloaded	76
3.17	Phase 'A' stator current of 12.6 Mva Induction Motor following a single phase-to-earth fault with the machine unloaded	77
3.18	As fig. 3.17 but the machine fully loaded	77

<u>Figure No.</u>	<u>Description</u>	<u>Page No.</u>
3.19	Phase 'a' rotor current of 12.6 Mva Induction Motor following a single phase-to-earth fault with the machine unloaded	78
3.20	As fig. 3.19 but the machine fully loaded	78
3.21	Air-Gap Torque/Time characteristics of 12.6 Mva Induction Motor following a single phase-to-earth fault with the machine unloaded	79
3.22	As fig. 3.21 but the machine fully loaded	79
3.23	Speed/Time curve of 12.6 Mva Induction Motor following a single phase-to-earth fault with the machine unloaded	80
3.24	As fig. 3.23 but the machine fully loaded	80
3.25, 3.26	Phase B&C stator current of 12.6 Mva Induction Motor following a line-to-line short-circuit with the machine unloaded	81
3.27, 3.28	Phase b&c rotor current of 12.6 Mva Induction Motor following a line-to-line short-circuit with the machine unloaded	82
3.29	Air-Gap Torque/Time characteristics of 12.6 Mva Induction Motor following a line-to-line short-circuit with the machine unloaded	83
3.30	Speed/Time curve of 12.6 Mva Induction Motor following a line-to-line short-circuit with the machine unloaded	83
3.31, 3.32	Phase 'A,a' Stator and rotor currents of 12.6 Mva Induction Motor following a three phase-to-earth fault with the machine fully loaded	84

<u>Figure No.</u>	<u>Description</u>	<u>Page No.</u>
3.33	Air-Gap Torque/Time characteristics of 12.6 Mva Induction Motor following a three phase-to-earth fault with the machine fully loaded	85
3.34	Speed/Time curve of 12.6 Mva Induction Motor following a three phase-to-earth fault with the machine fully loaded	85
3.35	Internal E.M.F of 12.6 Mva Induction Motor following a three phase-to-earth fault with the machine unloaded	86
3.36	Slip recovery of 12.6 Mva Induction Motor following clearance of a three phase-to-earth fault	86
4.1 (a),(b)	Diagrammatic representations of DY1 three phase transformer	88
4.2	A three phase diagram of an Induction Motor fed via a Delta/Star transformer	96
4.3	A flow chart to show the steps of solution for the current vector of the circuit of fig. 4.2	108
4.4	Phase 'A' stator current of 12.6 Mva Induction Motor following a three phase-to-earth fault on machine terminals	114
4.5	As fig. 4.4 but the fault occurs on the h.v. Delta terminals	114
4.6	Phase 'A' current of 12.6 Mva Induction Motor following a single phase-to-earth fault on machine terminals	115
4.7	As fig. 4.6 but the fault occurs on the h.v. Delta terminals	115
4.8	Phase 'B' stator current of 12.6 Mva Induction Motor following a double phase-to-earth fault on the machine terminals	116

<u>Figure No.</u>	<u>Description</u>	<u>Page No.</u>
4.9	As fig. 4.8 but the fault occurs on the h.v. Delta terminals	116
4.10	Phase 'C' current of 12.6 Mva Induction Motor following a double phase-to-earth fault on machine terminals	117
4.11	As fig. 4.10 but the fault occurs on the h.v. Delta terminals	117
4.12	Phase 'C' current of 12.6 Mva Induction Motor following line-to-line short-circuit on machine terminals	118
4.13	As fig. 4.12 but the fault occurs on the h.v. Delta terminals	118
4.14, 4.15	Phase 'B&C' currents of 12.6 Mva Induction Motor following an open-circuit fault on phase 'A' at machine terminals	119
5.1	A single-line diagram of a system having a group of Induction Motors, two three-phase transformer, an alternator and an infinite bus-bar	122
5.2	Schematic diagram of a synchronous generator	126
5.3	A three phase diagram for the system shown in fig. 5.1 with initial values	150
5.4 - 5.8	Flow charts showing the steps of the solution for the variables of the circuit shown in fig. 5.1	151-155
5.9(a)	Three phase currents and the rotor-angle speed of the synchronous generator following a three phase-to-earth fault and clearance of fault on bus-bar B2	159
5.9(b)	Three phase currents through transformer T1 under the same condition of operation as in fig. 5.9(a)	160

<u>Figure No.</u>	<u>Description</u>	<u>Page No.</u>
5.9(c)	Slip recovery of motor CWP, PAF, BFP and IDF under the same condition of operation as in fig. 5.9(a)	161
5.10(a)	Three phase currents and the rotor-angle speed of the synchronous generator following a double phase -to-earth fault and clearance of the fault at bus-bar B2	162
5.10(b)	Generator field current and currents fed by the group of Induction Motor under the same condition of operation as in fig. 5.10(a)	163
5.10(c)	Slip recovery of motor CWP, PAF, BFP and IDF under the same condition of operation as in fig. 5.10(a)	164
5.11(a)	Three phase currents and the rotor-angle speed of the synchronous generator following a three phase fault and clearance of fault at bus-bar B1	165
5.11(b)	Three phase currents through transformer T1 & the phase 'A' current contributed to the fault by motors CWP, BFP & PAF under the same condition of operation as in fig. 5.11(a)	166
5.11(c)	Phase 'B&C' currents contributed to the fault by motors CWP, BFP & PAF under the same condition of operation as in fig. 5.11(a)	167
5.11(d)	Slip recovery of motor CWP, BFP, IDF under the same condition of operation as in fig. 5.11(a)	168
6.1	A single line diagram of an isolated system	170
6.2	Graphs of Accuracy/step-length, % Improvement in speed of calculation/step-length when using different integrating routines	187

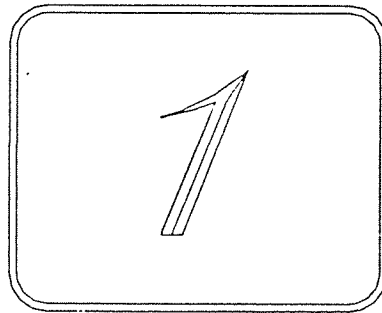
<u>Figure No.</u>	<u>Description</u>	<u>Page No.</u>
6.3	Comparison of current wave forms when using different integrating routines with step-length 0.1 & 0.13 milliseconds	188
6.4	As fig. 6.3 but with step-length of 0.185 & 0.08 milliseconds	189
6.5	Three phase diagram of the system shown in fig. 6.1	193
6.6	Generator terminal voltage and total fault current (phase 'A') for a sustained three phase fault at the 1.v bus-bar	207
6.7	Total fault current and the generator current for the first 0.5 sec. following the fault at the 1.v bus-bar	208
6.8	Generator field current and the contribution of motors HAGA2 to the fault at 1.v bus-bar	209
6.9	Generator rotor-angle speed and motor HAGA2 speed under the same condition of operation as in fig. 6.6	210
6.10	As fig. 6.6 but with the effect of the AVR approximated by a linear variation	211
6.11	A linear increase of the generator field voltage following a three phase fault	212
6.12	Generator terminal voltage and the internal E.M.F of motor HAGA2 following a three phase fault and clearance of the fault at 1.v bus-bar	213
6.13	Positive envelope of the generator terminal voltage and the internal E.M.F of motor HAGA2 under the same condition of operation as in fig. 6.12	214

<u>Figure No.</u>	<u>Description</u>	<u>Page No.</u>
6.14	Generator rotor angle swing and slip recovery of motor HAGA2 under the same condition of operation as in fig. 6.12	215
6.15	Slip recovery of motor HARCP under the same condition of operation as in fig 6.12	216

LIST OF TABLES

<u>Table No.</u>	<u>Description</u>	<u>Page No.</u>
3.1	Data for 12.6 Mva Induction Motor	56
4.1	Details of Fault Matrix, Circuit & Vector Diagrams for Faults on Motor terminals	112
4.2	As Table 4.1 Except that the Faults occur on Delta Terminals	113
5.1	Data for 776 Mva Synchronous Generator	124
5.2	Data for Motor CWP, BFP, PAF & IDF and 800, 48 Mva Three phase Transformers	125
6.1	Comparisons of Results obtained Using different Integration Routines Relative to Runge-Kutta-Fehlberg Algorithm	186
6.2	Data for 24.67 Mva Synchronous Generator	191
6.3	Data for Motor HARCP& HAGA2 and 100 Mva Three Phase Transformer	192

CHAPTER
ONE



INTRODUCTION

CHAPTER 1
INTRODUCTION

1.1 Background

In modern electrical power systems, the basic objective is to give satisfactory service to the various utility points throughout the system. In order to meet such a requirement adequately, there are many factors which need careful consideration in the planning and operation stage. It is often desirable for the system to be designed and managed to deliver the energy demanded, by each type of load at different locations, efficiently with both reliability and economy. The design should also cater for the security of supply by satisfying the following factors :

- a) improving the plant design by increasing the spare capacity margin,
- b) arranging alternative circuits to supply loads,
- c) flexibility during normal operation,
- and d) minimum dislocation following a breakdown.

In addition, it is necessary at the design stage to investigate the typical characteristics of loads that may vary from a few-watt domestic load to a multi-megawatt induction motor.

In the operational stage, it was generally thought that electrical power systems operate in a symmetrical steady-state condition where the natural tendency of the machines is to circulate power to keep in step. However, this situation was found not to be so, especially when disturbances take place that reduce the synchronising power. In some cases this change of power may be so marked that machines are unable to remain in step. Circumstances that may lead to such a situation are :

- a) major faults,
- b) an important item of plant being switched on, or tripped out due to an over-load,
- and c) conditions that require synchronous machines to operate in an under-excited mode.

The above system disturbances may all stem from an interaction between the electrical transmission capability of the system and the power injected at points of generation and that demanded by various loads. In addition, to this power balance, the stored kinetic energy of machines and the action of any controlling device will also contribute to fault levels and stability.

Apart from the modes of operation of power systems already discussed, large modern power systems represent an enormous capital investment, therefore; it is essential to consider the protection

of the whole system and its components as one of the major factors which need to be taken into the account. The vast quantities of energy released in the event of a short circuit fault, or a human error, could cause expensive damage to the system. Furthermore, if the fault condition is not removed or isolated rapidly, there may be a danger to the operating team behind the system, and possibly further system disturbances such as overloading, instability or even damage to the healthy equipment could occur. To avoid such consequences, the system faults must be sensed quickly, to initiate the remedial action to intervene and clear the fault.

In order to create a reliable system, the above mentioned factors point towards the need for a broad knowledge of the behaviour of power systems and their auxiliaries under both steady-state and transient conditions. Such knowledge helps to expose abnormalities and arrangements can be made to prevent instability before loss of supply.

1.2 Critical Review of Past Literature and Scope of Achievements

It has been mentioned in 1.1 that to design and operate a modern power system there is a need to investigate the characteristics and behaviour of loads. Of all the various parameters of an electrical power system, the load required by the consumers is the

most difficult to assess and analyse with sufficient accuracy. The statistical approach is often used to assess the load demand in power systems. In the past, for the purpose of the analysis of load behaviour, loads in general have been represented by either, constant impedances drawing constant power from the system [18] or by models with parameters derived from step response tests [52]. The former representation was extensively used for hand calculations and in A.C Network Analyzers [7]. Although the constant impedance approach can be justified for a fairly large number of loads, it is far from realistic when applied to represent loads like large induction motors. This is true especially when the improved representation of generating devices is to benefit. The large induction motor was found to have marked effects on the system performance under transient conditions [25,31,32&33]. Due to the fact that large induction motors have a large inductance to resistance ratio, the fault current produced may have an extreme off-set due to a large d.c component, and in one or possibly two phases the current may not reach zero for many cycles. Such a condition makes the duty of the circuit breaker onerous or even impossible and moreover, the operating time of the protective relays can be delayed for an undesirably long period.

In 1955, D.F Shankle and others [51], represented the induction machine by a transient voltage (e') behind a transient reactance (x'). This manner of a representation is similar to that used for

the synchronous generator but differs in that the transient voltage (e') is a function of the rotor slip and the excitation received from the system.

In 1957, J.L Gabbard and J.E Rowe [23], simulated the induction motor under transient conditions by using a digital computer. Three different representations were used in their studies :

- a) complete transient analysis, i.e including rotor and stator transient, based on the $0, \alpha, \beta$ frame of reference suggested by H.C Stanley [53]
- b) analysis using a transient equivalent circuit including rotor transient but neglecting stator transient
- and c) steady state analysis.

In both studies [23 & 51], only symmetrical system disturbances were analysed with special emphasis on transient stability, disregarding the contribution of the induction motor to the fault currents.

In 1964, an analogue computer simulation using a 'd,q' representation of the induction machine equations has been used by Hughes and Aldred [25]. Although the 'd,q' frame of reference gives a linearised mathematical model which reduces the computation time, it has the drawback of neglecting the effects due to

the change in rotor currents that give rise to the 'd.c' component in the stator current.

Asish K. DE Surkar and Gunnar J. Berg [3], considered just the simulation of an induction motor using a three phase co-ordinate method. Such a frame of reference, results in performance equations of the non-linear type due to the existence of terms including the rotor speed variation. S.S. Kalsi and others [31] devised a standard method, similar to that used for a synchronous machine with minor modifications, to determine the contribution made by the induction motor to the fault current in power systems. The method was applied [32] to study the transient stability of a power system containing both synchronous and induction machines.

In 1979, the authors of [47] applied a three phase co-ordinate frame of reference to study the dynamic characteristics of single cage deep-bar and double-cage induction motors. The analysis include the complex transient situations that arise from non-simultaneous breaker operation, system fault conditions on machine terminals, reswitching and plugging operations. None of the authors [3,47] extended the method to examine the effect of the motor transient performance on the the system at the vicinity where the motor is connected.

The preceding literature review is rather brief and a more detailed treatment of loads and, in particular, the representation of the induction and synchronous machines with transient stability analysis of power systems are high lighted in chapter 2 of this thesis.

1.3 Aims of Present Research

The work in this research is devoted to study the transient behaviour of large induction motors and their effects on power systems. The modelling includes the delta-star transformer that is often used to connect large induction motors to the system. The aim of the research is also to study the transient stability of a system having a group of induction motors, an alternator and transformers, following symmetrical and asymmetrical fault disturbances. Moreover, the project aims to develop a means of improving the quality of the protection performance prediction by supplying the necessary information needed by system protection engineers for selecting proper circuit-breakers and more accurate relays setting.

1.4 Approaches in Research.

From the review given in 1.2, one may deduce that there are two main approaches used to analyse machine performance. The first

method has been developed and adapted for hand calculations and based on the approximated operational equations that can be solved in a closed form. The second method utilises the basic differential equations of the machine representing instantaneous values of flux linkages, voltages, currents, torques and speed; such a representation is sometimes referred to as a three-phase co-ordinate frame of reference. This method was first published by R.H. Park in 1933 [45], and from that time it has been developed and used extensively on analogue computers [1,2]. Both approaches have their advantages and disadvantages. The first, has the advantage of speed of solution enabling large systems to be examined. The second has the advantage of detailed analysis, allowing examination of machines and control loop design. Conversely, the main disadvantage of the operational equations is loss of accuracy of solution, while the chief disadvantage of the second approach is the large number of equations that need to be solved, besides the need for a large computer store and long computation time.

In the last two decades, the most dramatic change in computer science has resulted in modern computers being built. They are extremely fast with large storage capacity, such facilities counteract the disadvantages that accompanied the three phase co-ordinate method of machines representation. As the aim of this research seeks to find a much better representation and understanding of

load behaviour in power systems, and in particular for accuracy in the solution of the transient variables produced by the induction machines; a phase co-ordinate frame of reference has been adopted to simulate the components of the system under investigation. Solutions are obtained by means of a numerical integration routine using the 4th order Runge-Kutta algorithm as modified by Gill [43] and also a Predictor-Corrector routine [42].

1.5 Research Layout

Chapter 2 of this thesis gives a literature survey of load and machine behaviour in power systems. It includes a review of the conventional methods of load and machine representation for transient stability studies. The chapter also gives a detailed analysis of the induction motor and a comparison between the synchronous and asynchronous machine. The effects of the inertia, associated with both primemovers and motor mechanical loads, on the machine behaviour has also been discussed.

Chapter 3 is devoted to study the transient performance of a large induction motor. The equations representing the machine operation in a three phase co-ordinate frame of reference is used. Simultaneous and sequential switching at different points on the voltage wave cycle were carried out to see how the switching angle

effects the starting current and torque. Symmetrical and asymmetrical faults on machine terminals has been applied to assess the fault current infeed from the induction machine.

In chapter 4 the simulation is extended to include the delta-star transformer that is often required to connect the machine to the system. A technique using matrix algebra is developed applying a general rule to study different kinds of faults on both sides of the transformer.

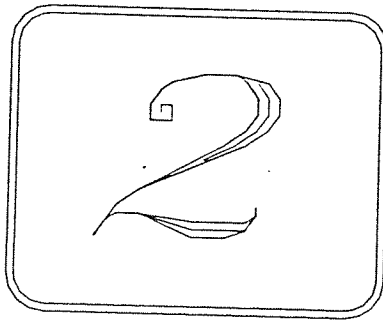
Chapter 5 deals with transient stability studies of a system consisting of a group of induction motors, a large generator, transformers and an infinite bus-bar. The technique developed in chapter 4 is applied to study faults at different points in the system.

In chapter 6, a study was carried out to investigate the possibility of using integrating routines, other than the Runge-Kutta methods, that permit the use of a larger step length and give an acceptable level of accuracy in the solution. The study was aiming towards reducing the long computation time obtained by using the Runge-Kutta-Gill routine that was used in the earlier chapters of this thesis. The outcome from the investigations were used to study faults and transient stability of an isolated system having

a comparable size of motors loading compared to the size of the synchronous generator energising the system.

Finally, the conclusions with the achievements of the project and suggestions for further work are given in chapter 7.

CHAPTER
TWO



LITERATURE SURVEY

CHAPTER II

LITERATURE SURVEY

2.1 Introduction

This chapter reviews the literature which currently describes loads and machines in power systems. The chapter includes the approaches that have been, and are being, used to represent loads and machines for the purpose of transient analysis. Factors that determine system fault levels and choice of circuit-breakers for system protection has also been discussed. Methods used to assess system stability following a disturbance have also been reviewed. The chapter also compares synchronous and induction machines from a design and operation aspect. It also includes the effects of, both prime movers and mechanical load inertia on the performance of synchronous generators and drive motors.

2.2 Types of Load and their

Effects on Power Systems

In power systems, the composition of loads can be broadly divided between industrial and domestic consumers. Statistical studies in industrial countries will show that the proportion of industrial load increases from about one third of total consumption at peak

loads to about one half of total consumption at minimum loads [59]. A very important difference between the two types of consumer is the high proportion of induction motors used by industrial consumers (60% approximately), whereas, domestic consumption consists largely of lighting and heating. The pattern of load distribution between industrial and domestic users has its influence on the design and operation of power systems. Perhaps, load behaviour needs more analysis than any other factor, when considering system transient behaviour. For example, when and what type of load will be switched to the system? Is the system ready to meet that load demand?. How will the overall load behave following switching of large loads or development of fault conditions?. Does the load contribute to the system fault levels?. The answer to such questions may be classified from two points of view :

- (i) economical aspects,
- and (ii) system behaviour.

The first aspect does not fall within the scope of this work. The second aspect is discussed in the following paragraph.

2.2.1 Electric Characteristics of Loads in Steady-State

... load of

The behaviour of loads in power systems are generally determined by the variation of the active and reactive power consumed by the load at various voltages. Such behaviour is of importance when considering the manner of load representation for the purpose of load flow or stability studies. Also; the power-voltage characteristic is taken as a base to classify loads in power systems. Besides transmission losses, the load may take the form of one or a combination of the following :

- (i) static load (lighting and heating),
- (ii) synchronous motors,
- and (iii) induction motors.

Lighting loads are usually considered independent of frequency, they consume no reactive power, and the power consumed by this type of load is often approximated to be proportional to
 $(\text{voltage})^{1.6}$. Heating elements are found to maintain constant resistance independent of voltage variation and the power consumed varies with the square of the voltage. Generally for static loads, there is a limit to the amount of power which the system can

possibly supply without the possibility of instability or loss of synchronism [44].

The voltage characteristic of synchronous motors can be categorised into two parts, first; the power consumed is approximately constant and independent of voltage variation, while in the second part, and for a given excitation, the reactive power taken is found to be changing in a leading direction with voltage reduction. Unlike the static load, systems having a considerable number of synchronous motors, besides imposing a power limit they can also become unstable and lose synchronism.

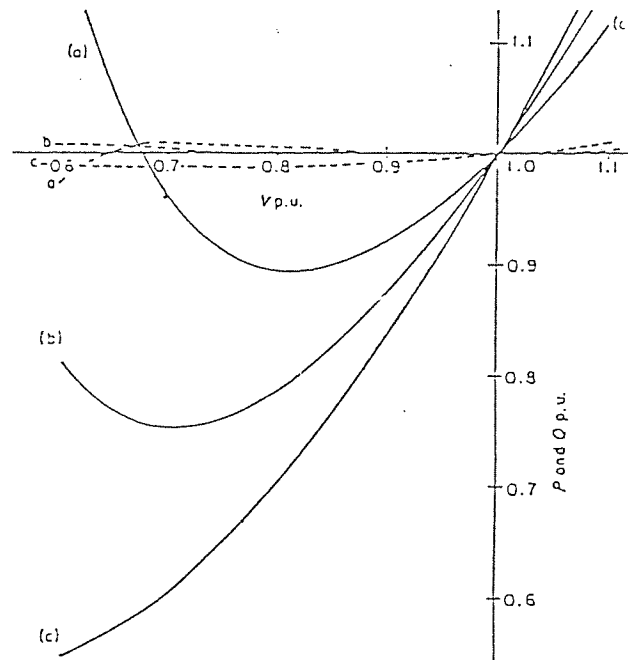


Fig. 2.1

For induction motors, graphs similar to that of figure (2.1) which relates the active and the reactive power to the voltage driving

the motor can be developed using the simplified equivalent circuit. In such an approach, the mechanical power can either be assumed constant or calculated with the torque made proportional to speed or (speed)². Beside the power-voltage characteristic, analysis of power-slip curves can show that there is a critical voltage at a corresponding critical slip beyond which the motor becomes unstable and stalls. This critical point occurs when

$$\frac{dP}{ds} = 0, \text{ where, 'P' is the power and 's' is the slip.}$$

As the induction motor represents the core of this research, more details about the induction machine behaviour will be considered later in this chapter.

When the load is a combination of the load described, the power-voltage characteristic can be approximated by the type of load which predominates.

In practical situations, voltage changes are often accompanied by frequency changes and the question of considering the load frequency characteristic will then be raised. However, information regarding the characteristics of composite loads with frequency are scarce, and in most cases, the effects of small frequency changes, allowed by regulations, on the active and reactive power are usually neglected in calculations.

2.3 Induction-Motors in Power Systems

It has been mentioned in this chapter that industrial loads form a considerable percentage of induction motor load. This is especially true with industries' such as petroleum refineries and chemical and nuclear plants, which are rather complex, expensive and inevitably run continuously. Their maintenance is expensive due to the loss of the product during shut down and the cost of restarting the process. It is most important that under normal operating conditions they must be kept running. In case of a complete supply failure where shut down is unavoidable, considerable damage to the plant may result, unless a local stand-by generator is available. In the event of a short circuit which results in voltage reduction, non-vital motors are usually isolated by tripping on under-voltage protection. Motors such as feed pumps, heater pumps, fan and blowers which have vital operating functions usually remain connected to the system for as long as possible. If the supply is restored quickly, or switched to a local generator, these motors will accelerate and prevent any damage to the plant. However, the acceleration period is normally accompanied by large currents drawn by each machine, which if not limited, they can cause normal over-load trips to operate. It is therefore essential that acceleration of motors maintaining essential supplies, which can be quite large, be as quick as possible with-out overloading. Because the majority of large

motors, in such plants, drive pumps and compressors, low starting torque motors can then be used. Such motors are built with relatively high resistance rotor circuits that give a speed-torque characteristic with reasonable starting torque and comparatively high torque near normal operating speed. This torque-speed characteristic satisfies the operating condition required by these motors following the restoration of the supply. Moreover; a relatively high resistance rotor circuit has the advantage of reducing the effective rotor time constant which improves the rate of decay of the d.c component in the stator fault current fed by the motor, and thus results in a shorter time to a current zero. In addition; a rotor with a relatively high resistance has a higher reliability factor i.e a greater drop in speed is possible following a fault, which is not accompanied by an excessive drop in torque at the upper speed range.

Indeed, it is not always acceptable to have induction motors with relatively high resistance rotor circuits, since this leads to a lower full load power factor, efficiency and pull-out torque, thus as a consequence it is not possible to generalise.

2.4 Transient behaviour of the Induction Motor

Under normal steady-state operating conditions, a flux is set up in the rotor circuit. Because the rotor is a closed circuit of finite resistance, the flux linkage can not change instantaneously to zero in the event of a fault or by isolation of the motor from the supply. In such events, an e.m.f will be induced in the stator circuit due to the fact that the rotor flux is rotating relative to the stator. In the event of a fault, a current will flow from the machine in any closed path of the stator circuit. Such a current and the rotor flux will decay according to a time constant determined by the rotor circuit. Since the stator windings have a finite value of resistance, the flow of current will be associated with power consumption in form of heat and during this period, the motor behaves as a generator with the difference that there is no power input to the shaft. Power consumed in form of heat in the stator circuit will then be at the expense of stored kinetic energy which is accompanied by drop in speed.

Under open-circuit conditions only comparatively high resistance paths exist in the iron of the stator, which acts as a sink for the dissipation of the stored kinetic energy.

2.5 System Fault Levels

In power system engineering, the importance of determining a fault level for assessing the severity of a fault in a network is well known. During a short-circuit, the voltages of the non-faulty bus-bars will fall and their deviation from the nominal value will give an indication of the quality of the network. Also, the network, in the vicinity of the fault, will be subjected to enormous stresses. As a quantitative measure, the fault level (or sometimes called 'Short Circuit Capacity "SCC" ') is used as a measure of the network strength and the short circuit stress. Such a measure is estimated by the pre-fault voltage and the post fault current at the location of the fault. The importance of defining such a measure is in determining devices such as circuit breakers required to deal with the fault.

2.6 Selection of Make-Break Devices.

The selection of proper switch gear for a given location in an electrical power network requires special consideration when choosing its make and break ratings. Such considerations are usually quoted in symmetrical and asymmetrical terms. In symmetrical terms, the duty of the circuit breakers is specified by the r.m.s value of the alternating component of the current with out any reference to the 'd.c' component. On the other hand, when the

... of the
circuit breaker rating is expressed in asymmetrical terms, the r.m.s value of the rated current contains both 'a.c' and 'd.c' components. This is given by the following relationship :

$$I_{asy} = \sqrt{I_{a.c}^2 + I_{d.c}^2} \quad \dots\dots\dots 2.1$$

The make duty is usually expressed in asymmetrical amperes. It is defined as the peak value of current against which the circuit breaker mechanism must close.

The following paragraphs draw comparisons between the practice recommended by:

- a) The British Standards
- b) The International Electrotechnical Commission 'IEC'
- c) The American Specifications.

a) The British Standards

The British Standards BS5311, 1976 [10], specifies for the switch gear break capability a value of d.c. component, at contact separation, that depends upon the method of the circuit-breaker tripping i.e if the circuit-breaker can trip the short circuit without an aid from any form of auxiliary power then the percentage d.c. component shall corresponds to a time interval equal to

the minimum opening time of the circuit-breaker, however, if the circuit-breaker is intended to be tripped by a form of auxiliary power then the percentage d.c. component shall correspond to a time interval equal to a minimum opening time of the circuit-breaker plus one-half cycle of rated frequency. Minimum opening time of a circuit-breaker is the shortest opening time obtainable under any service conditions, whether in a breaking operation or a make-break operating cycle.

The specification quotes percentage values of the d.c. component which depend on the time interval and are based on a standard value of a reactance to resistance ratio (X/R) equal to 14. Also the specification assumes a curve which relates the percentage d.c. component to time interval, based on negligible decrement of the a.c. component of the short-circuit current and on an exponential decay of the d.c. component to an 80% value in 10 milliseconds i.e. a time constant of approximately 0.04 seconds.

The specification quoted above, relates the make-current rating to the symmetrical break current capacity by a factor of 2.55 ($\sqrt{2} \times 2 \times 0.9$).

b) The IEC Specifications.

The IEC specifications publication 56, 1971 specifies for breaking capacity a curve of asymmetry based on a 'd.c' time constant of approximately 0.04 seconds, effectively this means a time of 0.08 seconds which coincides, for many circuit breakers, with the minimum time for contact separation. Similar to the British Standards, the IEC relates the switch gear make capacity to break current capacity by an arbitrary constant of 2.55.

c) The American Specifications

In the American practice [15,16,17,26] and for the breaking capacity, the effect of the 'd.c' component is considered only for the first eight cycles i.e for the first 0.133 seconds. They follow a slightly different procedure from the British Standards and the IEC Specifications in calculating the peak current for the making capacity. The peak current is expressed in terms of an asymmetrical r.m.s current and being made equal to or greater than 1.6 times the symmetrical r.m.s current rating i.e a 'd.c' component of 1.25 times the r.m.s 'a.c' component. Following the same arguments the corresponding r.m.s asymmetrical make duties in the

British Standard & the IEC would be 1.51 times the symmetrical
 r.m.s current rating. $(\sqrt{I_{a.c.}^2 + (\sqrt{2} \times 0.8) \times I_{a.c.}^2})$.

2.7 Induction-Motor Loads and
 their Effects on the Choice of the
 Make-Break Devices.

When a circuit breaker is to be installed to serve in a location having a large induction motor loading, the trend of neglecting the effects of the motors in determining the circuit breaker make and break ratings can no longer be accepted. The main reason arises from the fact that a large induction motor can make an appreciable contribution to the circuit breaker make duty, another reason is the large make-duty/break-duty ratio which can result from tripping part of the motor load following a fault. Although Huening in 1955 [29], Catenacci and Formica in 1958 [14], have suggested methods for calculating the effects of induction motors on switch gear duty, their proposals have rarely been used in practice and the calculation of such vital protective devices have continued to be estimated entirely on the fault level due to synchronous machines alone. In 1969 Cooper and Maclean [11] were the first to appreciate the contribution of the induction motor to the fault level and hence in the calculation of the switch gear

duty. They proposed a simplified approach in establishing calculations for both make and break duties, based upon analysing test results of the r.m.s symmetrical component of fault line currents. Two time constants were suggested T'_d and T_a to calculate the peaks of the current at any instant using :

$$I = \frac{\sqrt{2} E}{X_{sT}} (\exp(-t/T'_d) + \exp(-t/T_a)) \text{ ----- 2.2}$$

X_{sT} is the full voltage motor leakage reactance.

They recommended the following for the make and break rating selection :

- a) to use the sub-transient reactance as found from the short circuit test (if not, then the full voltage leakage reactance is used instead) for the 'a.c' component with all motors connected to determine the make duty rating,
- b) for the break duty, a decrement should be allowed for motors losing their supply, with all other motors in the system ignored.

2.8 Stability of Power Systems
Containing Synchronous and
Induction Machines.

The problem of stability in power systems has been the object of thorough investigation since the second decade of this century. Different types of stability studies have been considered and of these, two major classification areas are generally accepted. These are steady-state and the transient stability studies. The former is concerned with the operation of power systems under all normal steady-state conditions, this being taken to include the effects of governors, automatic voltage regulators, load fluctuations, while the latter, is said to exist in power systems, after an occurrence of a disturbance. It was first thought that, stability is only of importance between large synchronous machines. However, as systems continued to have large concentrations of induction motor loads, closely connected to equally large concentrations of generators, as in the case of nuclear power plants, it has been realised [29,32,51] that not only do large induction motors contribute to system fault current, but also the maintenance of stability is of equal importance between synchronous and induction machines. For such a system, and during the remainder of the fault period, the synchronous machines swing to an increasing angle while the induction motors drop in speed.

Following the fault clearance, the stability of the system depends upon whether the synchronous machines remain in synchronism and whether all the induction motors recover to the original speed just below synchronism. Staats [57] presented a comparison study, of system stability, based on the equivalent circuits of synchronous and induction machines.

2.9 Prediction of Stability in Power Systems.

Conventional methods, based on assumptions simplifying the dynamic performance equations, have been used to assess the steady-state and transient stability of power systems ranging from two machine to multi-machine systems. Simple approaches, solving for the power-angle equation graphically, or using hand calculations by solving for the swing curve using a step-by-step technique, have been implemented for two machine systems. Because of the extreme complexity of rapidly growing electric power systems, there was continuing pressure for the development of powerful methods for predicting power system dynamic performance. The following paragraphs discuss some of the methods in use.

2.9.1 Step-by-Step Methods.

The simple method of the 'equal-area' criterion, which can be applied satisfactorily to determine the stability of two machine system, fails for multi-machine systems. The differential equations describing the multi-machine systems are non-linear, thus; their solution in a closed form is not possible, and numerical integration methods are then an alternative. In such techniques, the solution advances in a discrete fashion by using a suitable step length of the independent variable. In [34], two methods are described.

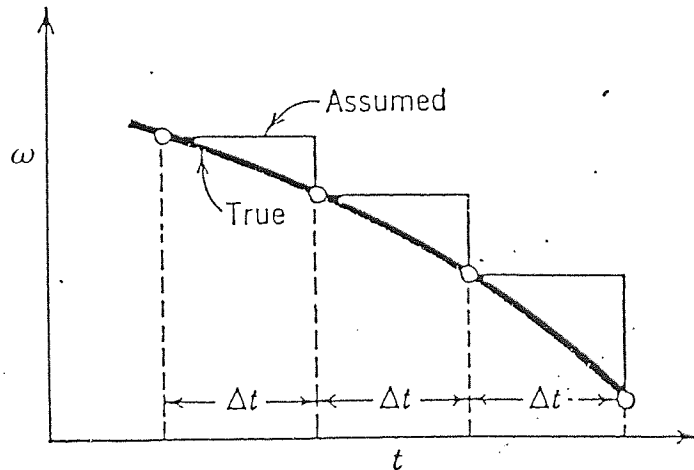


Fig. 2.2

The first is based on an assumption of a constant accelerating power through-out a time interval ' Δt ' and the next value is computed from the beginning of the interval (see fig. 2.2). The

solution is usually determined for the speed ' ω ' and the angular displacement ' δ '. The drawback of this method is a considerable cumulative error. The second method is based on the assumption that the accelerating power is constant from the middle of the interval being considered (see fig. 2.3). Such an assumption is found to yield a more accurate result than the previous method with an advantage of a longer step length which reduces the time and number of calculations.

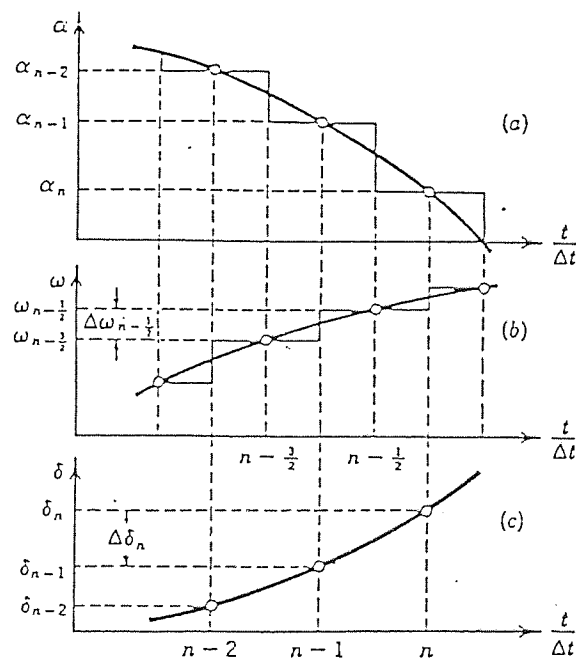


Fig. 2.3

2.9.2 Application of Lyapunovs'

Direct Method

The numerical methods described in section "2.9.1" require the explicit solution of the system differential equations during and

after the disturbance. The concept of the stored kinetic energy together with a Lyapunov function and a defined initial condition can be used to define a region of asymptotic stability [4,24]. The method basically rests upon plotting the dynamic equation of a two machine system in a phase plane that relates the angular velocity ' ω ' to the angular displacement ' δ '. The trajectory in the ω - δ plane can then be modified by moving the ' ω ' axis to a stable equilibrium point δ' , such that the velocity $\omega = d\delta/dt$ has a maximum positive or negative value when the displacement is zero at $\delta = \delta'$. Such changes reduce the system to an equivalent simple spring mass system. If the system angle δ exceeds δ_{\max} the spring

reverses its force and causes the velocity to increase rather than decrease and the machine loses synchronism. The direct method of 'Lyapunov' is applied by choosing a (V) function which is valid in a region over which the restoring force is positive. For a two machine system the function takes the following form

$$V(x) = 1/2 \omega^2 + \left(\int_0^x [-P_i + P_m \sin(x + \delta')] dx \right) / M \quad \text{----- 2.3}$$

with

$$x[-P_i + P_m \sin(x + \delta')] = 0, \quad x=0$$

$$x[-P_i + P_m \sin(x + \delta')] > 0, \quad 0 < x < (\delta - \delta')$$

$$0 > x > -(\delta' + \pi)$$

The method described above is applicable with some limitation to systems having more than two machines [24]. In 1970, a new stability measure for a multi-machine systems was introduced [58]. It is based on the condition that if the initial state of post disturbance is inside the surface $V = V_{\max}$ then, the system trajectory will tend to a stable equilibrium state as time approaches infinity. On the other hand, if this initial state is external to $V = V_{\max}$ then, no conclusion about stability is possible. The paper proposed a measure for relative transient stability given by,

$$\xi = 1 - (V_{sw} / V_{\max}) \quad \text{----- 2.4}$$

where V_{sw} is a 'Lyapunov' function for post disturbance evaluated at some time t_{sw} .

The measure ' ξ ' has some desirable properties, in that it is normalised, monotonic, easily calculated by a digital computer, and falls within an acceptable range of values regardless of system complexity. Moreover, it takes into account the effect of some parameter variations upon system transient stability, such as damping, inertia and other control system variables which are neglected in the method given by [4,24].

Although both of the described methods can assess system stability without solving for system differential equations, they just consider load representation, including the induction motor, by an equivalent static impedance.

2.9.3 Network Analysers and Analogue

Computers.

The automation methods for solving problems associated with electrical power systems were approached as early as 1930. A-C Network Analysers (A.C.N.A) were established as a direct analogy of electrical power networks. A main disadvantage of A.C.N.A was the inadequate representation of synchronous machines which increased the difficulty of carrying out transient stability studies. However, the stability problem was solved with the aid of a semi-automatic computer described by Mortlock [40]. In 1961, Miles [41] developed a method of stability analysis for a multi-machine system using analogue and digital means. His studies included factors such as flux variation and effects of regulators and governors. Dinely [19] carried out a transient stability analysis of a system having a synchronous generator connected to an infinite bus-bar via a double circuit transmission line, by combining an analogue computer and A.C.N.A. He used the analogue computer to represent the synchronous machine while the A.C.N.A was used to represent the transmission network. Balanced and

unbalanced faults with an automatic voltage regulator and speed governor were included in his studies.

2.9.4 Digital Computers.

Different papers have been published describing the use of digital computers in analysis of power systems and their drive equipment [3,8,27,54]. Bennet and others [8], described the use of a high speed digital computer for the solution of the stability problem. At that time, he succeeded in displaying the swing curves by using the continuous recording facility provided by a direct analogue computer. One disadvantage of his approach is the long computing time taken to obtain the equivalent network of the system under analysis. In 1965, Humpage and Scott [27] carried out a comprehensive series of experiments, incorporated with several different predictor-corrector methods, in studying transient stability of a power system. Their aim was to investigate the feasibility of using longer step length than that used in single step methods such as Runge-Kutta routines. Although, the predictor-corrector methods were found to have the advantage of using a longer step length that leads to economy in computation time with the possibility of controlling the error at each step, they have the disadvantage of requiring special auxiliary routines in the presence of a discontinuity, such as the opening of a

circuit breaker. No advantage in computer storage has been claimed over single step methods.

2.10 Representation of Machines for Transient Analysis

The degree of the accuracy required in the solution obtained from analysing machines for transient behaviour depends upon the simplifications made in the equations modelling the machine. The progress that has been made in the means of the analysis has always been accompanied by reviewing the assumptions which simplify the model. Different models have been, and are being, used [28,34,45,54] and each was justified according to the method used in the analysis. The following two paragraphs review the models used in representing synchronous and induction machines.

2.10.1 Synchronous machines

The simplest representation [28] was based upon the following assumptions:

- a) Transformer voltages in the stator equations are neglected.
- b) Speed is assumed constant except in the equation of motion.

- c) Damper windings and saturation are neglected.
- d) Mean flux linkages are assumed to be constant.
- e) Saliency is neglected ($x_q = x_d'$)

The above assumptions enable the representation of the synchronous machine by a constant voltage behind a transient reactance. Such a representation has been used in studying transient stability by both point-by-point and A.C.N.A. [34]. With the available facilities of the analogue computers, a much better representation is introduced by excluding assumption (d), the model thus takes into the account the variation in flux linkages [19]. As a further step, Cooper [12] simulated the performance of the synchronous machine including the effect of saturation.

Another representation was introduced by re-arranging Park's equations to eliminate the damper winding currents which removes some of the transformer voltages from the stator equations. Such a representation gives a solution free from the synchronous frequency component in the stator currents (i_d & i_q). The advantage of this model is a considerable reduction in the computational efforts which were demanded by the original model.

The above models, originated from the untransformed equations of machines, which express the phase variables in a 'd,q' frame of

reference. It appears that, these were the only approaches available at that time and there was a lack of a sophistication associated with some of the calculations. A 'd,q' frame of reference produces differential equations with constant coefficients (assumption b). By neglecting assumption (a) a considerable number of calculations can be introduced. Moreover, the model fails to handle asymmetrical faults and a further transformation is needed. The ' α, β ' frame of reference, which is a solution of the problem of the asymmetry in the analysis, suffers from the non-linearity that is introduced by taking the speed variation into account. In addition, both 'd,q' and ' α, β ' frames of reference require reference back to phase quantities in studies where circuit breaker operations need to be included in the analysis.

The advent of modern computers enable the solutions of non-linear differential equations which simulate the machine performance in a three phase co-ordinate frame of reference [5,54]. The model is versatile and has the following merits:

- a) more accurate representation due to inclusion of two or more rotor circuits,
- b) a uniform approach to study both symmetrical and asymmetrical faults,
- c) retention of the physical identity of the machine

under analysis,
and d) parameters need no transformation.

More recently, improved models [13,21,35] together with new approaches [20,55] to determine the electromagnetic parameters have been developed, overcoming the limitations that have been experienced with the conventional models. The model developed by reference [35] accommodated up to two damper circuits in addition to the field windings in the 'd' axis and up to three damper circuits in the 'q' axis. It has the advantage of including mutual inductances between the 'd' axis stator, field and rotor body circuit as well as saturation in the 'q' axis.

2.10.2 Induction Machines

In past analysis, induction machines were often represented by constant impedances or as a constant load on the supply. However, in the case of large induction motors, such simple forms of representation were found to be inadequate, and the steady-state equivalent circuit was often used. In 1938 Stanley [53] analysed the induction machine using a set of linear transformations to refer the phase variables into a set of orthogonal co-ordinate axes which were stationary with respect to the stator. In 1954 Lyon [39] derived expressions for analysing the induction machine

transient behaviour in terms of the roots of the characteristic equations. Kelly [37] derived a mathematical model, for the induction motor, which expresses the input impedance and the output torque as functions of speed. He used two representations for the analysis, one for 0-95% speed and another for speed above 95%. Hughes and Aldered [25] investigated some variable speed transient conditions on an analogue computer using a 'd,q' representation. Smith and Sriharan in 1966 [50] used a digital computer to solve the basic differential equations, with a 'd,q' frame of reference, for the numerical determination of the overall transient performance. Analysis using a dynamic phase co-ordinate method has been used [47] to predict the dynamic characteristics, of a large induction motor, including the effect of saturation and inertia, with particular emphasis on non-simultaneous breaker operation, system fault conditions and plugging.

2.11 Comparison between Synchronous and Induction Machines

In spite of the vast differences in the methods used for studying, analysing and designing synchronous and induction machines, the two types are very similar. The similarity arises from the fact that both machines consist of three phase primary windings embodied in the stationary member and a secondary system of windings on the rotating member. The difference between the two machines is

established in the type and the way at which the secondary windings are arranged.

In a synchronous machine, an independent d.c source, or a derived rectified signal, excites the field winding in the secondary circuit. Such excitation sets up a flux and if the machine is motoring, the flux will cause the rotor (the secondary member) to rotate in synchronism with the rotating field set up by the three phases that energise the windings in the primary member, therefore in this mode of operation the speed is fixed by the frequency of the supply and the fundamental mechanical relationship is between torque and load angle.

In case of the induction machine there is no field winding to be excited from an external d.c. source, however, the rotor speed differs from the synchronously rotating flux by the slip. Such a difference in the speed maintains flux cutting and thus the induced currents in the secondary circuit interact with the primary currents and produce the torque which maintains motion. In this mode of operation, the slip is load dependent and the fundamental mechanical relationship is between torque and slip.

Another aspect which could be a subject of comparison between the two types of machines, are the damper circuits. In a synchronous machine the damper winding, whether it be a special winding or

simply the iron of the rotor, can be directly compared with the secondary winding of the induction machine which is either of a wound rotor type or in a form of a cage where the bars are short circuited at both ends. The synchronous machine differs in the respect that apart from the asymmetry due to the field winding, there is also appreciable saliency due to the poles and asymmetry in the damper windings.

2.12 Effect of Saturation on Machine Performance.

Both torque and generated voltage in all machines depends on rates of change of flux linkage with the windings of the machine. For accurate analysis, under both transient and steady-state, the effect of saturation should thus be taken into the account. Two forms of saturation can occur in machines and may be of importance in power system analysis. These are :

- a) saturation of the leakage reactance,
- and b) saturation of the main magnetic circuit.

The first is a function of the machine current, it is less important in steady-state, its effect appears only when the current

exceeds about three per unit. In most analysis, the leakage reactance is taken as a constant value based upon a 50% voltage short circuit test.

Saturation of the main magnetic path can be detected by examining the curve of the open circuit output voltage against field current. It limits the internal voltage and effectively reduces the direct and quadrature reactances [38]. In analysis, one method of including the effects of saturation in the main magnetic path is based upon selecting a constant value of a magnetising reactance which depends on the slope of the saturation curve, the variation in such a value due to saturation is then catered for by defining a saturation factor from the open circuit curve such that, at rated speed and rated output voltage the field voltage and current are one per unit.

Induction motors are rarely subjected to excessive voltages and they have no internal excitation, thus saturation is rarely important.

2.13 Effect of Inertia on Machine Performance

In any rotating machine, the transient performance is much affected by the inertia of the machine. On examining the equations of motion of synchronous or induction machines, it should be noted

that the rate of change of speed is inversely proportional to the machine inertia constant. In case of induction machines, and because of the diversity in design of such machines and their coupled loads, it is not possible to state any average or typical electrical and mechanical constants as in the case of synchronous machines. Moreover; the inertia of the loads, that are usually associated with induction motors, have a considerable variation from one load to another, for example; certain types of fan have a large moment of inertia which has the effect of a relatively small drop in speed during a fault, while other loads, like pumps and compressors may have quite small inertias that could result in a considerable drop in speed in the event of faults.

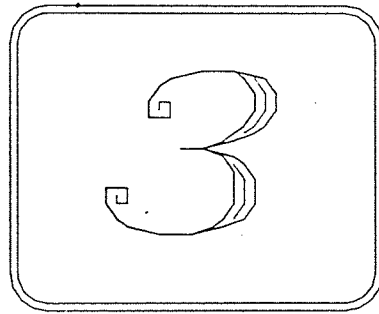
2.14 Conclusion

Analysis of power systems for the purpose of stability studies, or for determining the circuit breaker ratings was first introduced by ignoring the induction motors loading contributions. Later, and for the purpose of selecting the make-break devices, induction motor representation was introduced by using test results of fault currents fed by this type of load. For stability studies, steady state equivalent circuits of induction motors were introduced to approximate representation.

In locations with a large concentration of induction motor loading, closely connected to an equally large concentration of generators, a more reliable analysis has become necessary. This is because large induction motors have an appreciable effect on system behaviour during switching or following a disturbance and thus, the need to find such contributions based upon the dynamic behaviour of the induction motor has become unavoidable. Analysis requires representation which is much more accurate and flexible in performing calculations involve switching and symmetrical and asymmetrical fault studies. Such studies supply the information usually required at design stages as well as selecting proper make-break ratings of circuit breakers, not only for those associated with protecting the induction motors, but also for other auxiliary drive equipment, such as three-phase transformers, in the vicinity where the motors are connected.

In addition, the analysis could provide important information concerning the design and setting of the auxiliary protection devices i.e current transformers and relays.

*CHAPTER
THREE*



*TRANSIENT PERFORMANCE
OF INDUCTION MOTORS*

CHAPTER III

TRANSIENT PERFORMANCE OF LARGE INDUCTION MOTORS

3.1 Introduction

This chapter describes the method of simulation of the transient performance of large induction motors fed from infinite bus-bar systems. The chapter derives a mathematical model using a three phase variable representation. Algorithms and a computer program flow chart are given to describe the steps of solution. In particular, the program analyses the following :

- a) Induction motor starting with simultaneous and sequential switch closure.
- b) Symmetrical and asymmetrical faults.
- c) Fault, and clearance of fault after a specified time interval.

Discussion of the results and conclusions are given at the end of the chapter.

3.2 Differential Equations of Induction

Machines in Three-Phase Frame of Reference

3.2.1 General

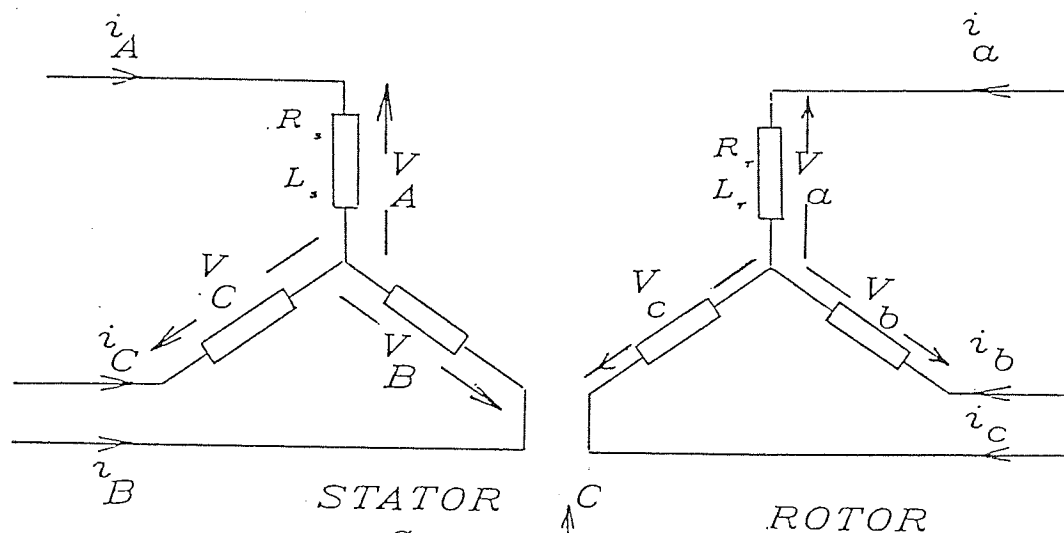


FIG. 3.1

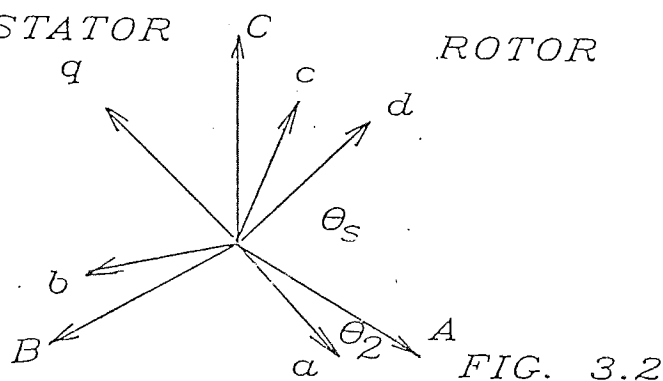


FIG. 3.2

Figure 3.1 shows the current convention for an idealised induction machine. The axis of the stator and rotor circuits are designated by the letters A,B,C and a,b,c respectively. The relation between the two axes can be investigated by referring to fig. 3.2. At instant 't' say, let ' θ ' be the angle the 'a' axis makes

with respect to the phase 'A' stator axis. The rotor angular velocity is then given by :

$$\omega_r = \frac{d\theta}{dt} \dots\dots\dots 3.1$$

If ' ω ' is the stator electrical angular velocity then the rotor slip is given by :

$$s = 1 - \omega_r / \omega \dots\dots\dots 3.2$$

and the rotor slip frequency is

$$\omega_r = s \omega \dots\dots\dots 3.3$$

3.2.2 Assumptions and Limitations

The following assumptions are proposed in deriving the dynamic equations of the induction motor performance.

- a) The induction motor is simulated as a set of linear coupled circuits.
- b) Space m.m.f and flux waves are assumed to be sinusoidally spaced in the machine air-gap.
- c) Saturation, hysteresis and eddy currents are

neglected.

- d) The coefficient of mutual inductance depends on the cosine of the electrical angle between the axes of the stator and rotor circuits.

3.2.3 E.M.F Equations

Applying Faraday's and Ohm's law, and assuming that the rotor circuit is closed, then each winding's voltage depends upon six currents, for example; the j^{th} winding's voltage can be expressed as follows :

$$e_j = R_{jj} i_j + \bar{p} \lambda_j \dots\dots\dots 3.4$$

where,

$$\bar{p} \lambda_j = \sum_{k=1}^6 \bar{p} \cdot L_{jk} i_k \dots\dots\dots 3.5$$

λ is flux linkage

and ' \bar{p} ' is a per unit differential operator.

To generalise equation 3.4, ' j ' takes values from 1 to 6, thus creating a voltage vector $\{e\}$, a current vector $\{i\}$ and a resistance and inductance matrix $[R]$ & $[L]$ having an order of 6x6. The digits from 1 to 3 are then used for the stator circuit and those from 4 to 6 for the rotor circuit. As the inductance matrix is of

major importance for the prediction of the entire performance of the induction machine, it is worth detailed consideration before discussing further analysis.

3.2.4 The Inductance Matrix

To simplify the analyses, the 6x6 inductance matrix can be partitioned as follows :

j\k	1	2	3	4	5	6
1	stator induc			stator/rotor		
2	-tance matrix			mutual indu-		
3				ctance matrix		
4	rotor/stator			rotor induc-		
5	mutual indu-			tance matrix		
6	ctance matrix					

a) Stator Inductance Matrix

If the rotor circuit is considered to be on open-circuit and the windings resistance neglected, then the induced voltages in the stator winding are :

$$e_1 = pL_{11} i_1 + pL_{12} i_2 + pL_{13} i_3$$

$$e_2 = p_{21} \bar{i}_1 + p_{22} \bar{i}_2 + p_{23} \bar{i}_3 \quad \dots \dots \dots (3.4)$$

$$e_3 = p_{31} \bar{i}_1 + p_{32} \bar{i}_2 + p_{33} \bar{i}_3$$

In matrix form the above set of equations become

$$\{e\}_{3 \times 1} = [p]_{s \times 3} [L] [i]_{3 \times 1} \quad \dots \dots \dots 3.5$$

Test results [30] established two important facts about this sub-matrix :

- i) the three self inductances of the identical stator windings are equal,
- ii) as a result of the smooth air-gap, none of the nine elements are rotor position dependent unless the slot ripple needs to be taken into account.

It follows from (ii) that the co-efficients of this matrix are not time dependent and can be treated as constants with respect to the operator ' \bar{p} '. Thus equation 3.5 becomes;

$$\{e\}_{3 \times 1} = [L]_{s \times 3} \bar{p} \cdot \{i\}_{3 \times 1} \quad \dots \dots \dots 3.6$$

one last fact about this sub-matrix is that, the values of the off diagonal elements (L_{jk}, L_{kj}) are equal and negative.

b) Rotor Inductance Matrix

The same arguments, that apply for the stator matrix, also apply to the rotor matrix, which results in the following :

$$[L]_r = \begin{bmatrix} L_{44} & L_{45} & L_{46} \\ L_{54} & L_{55} & L_{56} \\ L_{64} & L_{65} & L_{66} \end{bmatrix}$$

b) The Stator/Rotor & Rotor/Stator

Sub-matrices

These sub-matrices can be considered as the keystone of induction machine representation. The elements of the sub-matrices vary with rotor position thus, the e.m.f equations become time varying and hence non-linear. Indeed, the effect occurs when the rotor windings are short-circuited and therefore, additional components of induced voltage are created and must be added to those produced by the self inductances. At rotor position say ' θ '₂, the voltage added to the jth stator winding of equation 3.5 is

$$\sum_{k=4}^6 \bar{p}_{j,k} M_{j,k} \cos(\theta + \delta_{j,k}) \cdot i_k \dots\dots\dots 3.7$$

where,

$$\delta_{j,k} = \delta_{j+1,k+1} = \delta_{j+2,k+2} = 0$$

$$\delta_{j,k+1} = \delta_{j+1,k} = 2\pi/3$$

$$\delta_{j,k+2} = \delta_{j+2,k} = -2\pi/3$$

and that added to the jth rotor windings is

$$\sum_{k=1}^3 \bar{p}_{j,k} M_{j,k} \cos(\theta + \alpha_{j,k}) \cdot i_k \dots\dots\dots 3.8$$

where $\alpha_{j,k}$ is the transpose of $\delta_{j,k}$

On summing up the four sub-matrices discussed above the general symmetrical matrix of the induction motor can be obtained.

3.2.4 Equations of Motion

Because of the dependency of some elements of the inductance matrix [L] upon the rotor position, equation (3.4) is non linear. A numerical solution is possible in conjunction with a knowledge

of the rotor position at any instant. The rotor position can be determined by integrating the equation of motion which relates the inertia of the machine and any connected load, to the net accelerating torque i.e integration of

$$\frac{d\omega}{dt} = \frac{(T_e - T_m - T_l)}{J} \dots\dots\dots 3.9$$

gives the rotor speed ' ω_2 ', and integration of

$$\frac{d\theta}{dt} = \omega_2 \dots\dots\dots 3.10$$

gives the rotor position θ_2 .

The mechanical torque is approximated as a function of rotor speed and estimated by

$$T_m = A.(1 + Bs + Cs^2) \dots\dots\dots 3.11$$

where A, B & C are constant co-efficients & 's' is slip.

The electrical torque ' T_e ' is computed from :

$$T_e = \frac{1}{2} \cdot \{i\}^t [G(\theta)] \{i\} \dots\dots\dots 3.12$$

where,

$$[G(\theta)] = \frac{d[L(\theta)]}{d\theta} \dots\dots\dots 3.13$$

3.3 Determination of Machine

parameters by test

The envelope of the wave form of the short circuit current of the induction machine can be analysed mathematically by two exponential decay functions [31]. From this analysis, four parameters are usually defined, these are transient and sub-transient reactances and time constants. Tests similar to those applied to synchronous machines can be used to evaluate these parameters [6,31]. The tests are:

- a) short-circuit tests
- and b) stand-still tests

The former tests determine the transient and the sub-transient parameters and can be performed in two ways :

by a,

- a) direct short-circuit test
- or an b) indirect short-circuit test.

In the direct short-circuit test, the stator terminals are suddenly short circuited while they are connected to the supply.

In the indirect short-circuit test, the stator terminals are disconnected first before they are short circuited. In both tests, the calculations are simplified by assuming the speed remains constant [6,50] and solutions to the equations can be obtained by using the ' Laplace transform '. Once the transient and sub-transient parameters are obtained, the time constants are calculated by knowing the stator and rotor resistances from test or design data.

The stand-still test determines the machine impedances needed for the starting characteristics. The stand-still test is usually performed by applying a reduced voltage with the rotor locked.

3.4 System Circuit and Data

The motor, under analysis, is assumed to be of a squirrel cage type and has its stator circuit connected in star with no neutral. Such a connection eliminates the zero sequence currents and thus simplifies the inductance matrix by setting the off diagonal elements of the stator and rotor matrices to zero i.e,

$$[L] = \begin{array}{c} \begin{array}{c} | & L & \emptyset & \emptyset & | \\ & \text{ss} & & & \\ \emptyset & & L & \emptyset & \\ & & & \text{ss} & \\ \emptyset & \emptyset & \emptyset & L & | \\ & & & & \text{ss} \end{array} \\ \text{s} \end{array} \qquad \begin{array}{c} \begin{array}{c} | & L & \emptyset & \emptyset & | \\ & \text{rr} & & & \\ \emptyset & & L & \emptyset & \\ & & & \text{rr} & \\ \emptyset & \emptyset & \emptyset & L & | \\ & & & & \text{rr} \end{array} \\ \text{r} \end{array}$$

where L_{ss} and L_{rr} are the apparent three phase self inductances of the stator and rotor circuits respectively. They are calculated from a knowledge of the stator and rotor leakage reactance and the magnetising reactance. i.e

$$L_{ss} = L_{sl} + L_m \quad \& \quad L_{rr} = L_{rl} + L_m$$

The mutual inductance matrices (the upper right and lower left 3x3 matrices), which result from partitioning the main inductance matrix, are a function of rotor position with 'M' (equations 3.7 & 3.8) determined by :

$$M = \frac{2}{3} L_m \quad \dots\dots\dots 3.14$$

where L_{sl} , L_{rl} are the per unit stator and rotor leakage reactance & L_m is the per unit magnetising reactance.

From the above, and for analysis that does not involve zero sequence currents, the three quantities L_{sl} , L_{rl} and L_m plus the stator and rotor resistances r_s & r_r define completely the parameters of the induction motor.

For more general cases, however, two more parameters are needed. These are the mutual inductance between stator phases and the mutual inductance between the rotor phases.

Table 3.1, shown below, gives the parameters of a 12.6 MVA, 11kv induction motor for which the analysis are carried out. The data was obtained from tests described in section 3.3 and supplied by CEGB.

symbol	Description	value	unit
S	Rating	12.6	MVA
V	Voltage	11.0	kv
L _s	Stator leakage react.	0.1055	p.u
L _r	Rotor leakage react.	0.0684	p.u
L _m	Magnetising reactance	3.9800	p.u
r _s	Stator resistance	0.00414	p.u
r (st) r	Rotor resist.(start.)	0.0324	p.u
r (ru) r	Rotor resist.(running)	0.0108	p.u
H	Inertia constant	2.8500	sec.

Table 3.1

3.5 Algorithms and the Numerical

Solution

Unlike other frames of reference for 'a.c' machine representation, the modelling of induction machines using a three phase co-ordinate method requires particular attention in selecting the integration algorithm for solution. A variety of algorithms exist, such as Runge-Kutta, Predictor-corrector and trapezoidal methods. Between these, experimentation will show that the Runge-Kutta method is the most satisfactory and moreover, it has the merit of self starting. One main disadvantage of the Runge-Kutta method, when used to solve system equations involving induction machines, is the small step length required for numerical stability which increases the time of computation considerably.

For the purpose of investigating the transient current, torque and other variables, equation (3.4) has to be solved in discrete time for the flux linkage derivative vector after substituting the induced voltage vector {e} by the supply vector {v}, i.e at step 'n', the flux linkage derivative for circuit 'j' say, is given by;

$$\left(\frac{d\lambda}{dt} \right)_{jn} = v_j - \sum_{k=1}^6 [R]_{jk} \{i\}_k \dots\dots\dots 3.15$$

the flux linkage at step 'n+1' is then given by:

$$\begin{pmatrix} \lambda \\ j \end{pmatrix}_{n+1} = \begin{pmatrix} \lambda \\ j \end{pmatrix}_n + (\bar{p} \lambda)_{j n} \dots\dots\dots 3.16$$

and the current is computed from:

$$i_j = \sum_{k=1}^6 [L]_{kj}^{-1} \cdot \lambda_k \dots\dots\dots 3.17$$

3.6 Program Flow Chart

The program for the solution can be explained with aid of the flow chart shown by fig. (3.3). The steps of the solution are as follows:

- 1) Read machine parameters, bus-bar voltage, initial time, step-length and limit of integration.
- 2) At time 't' build-up the voltage vector.
- 3) Build-up the resistance and inductance matrix.
- 4) Using Runge-Kutta method as modified by Gill, calculate the flux-linkage vector (eqn. 3.15).
- 5) Up-date the flux-linkage vector (eqn.3.16).
- 6) Using the flux-linkage vector and the inverse of the inductance matrix find the current vector (eqn. 3.17).
- 7) Using equation (3.12), calculate the electrical

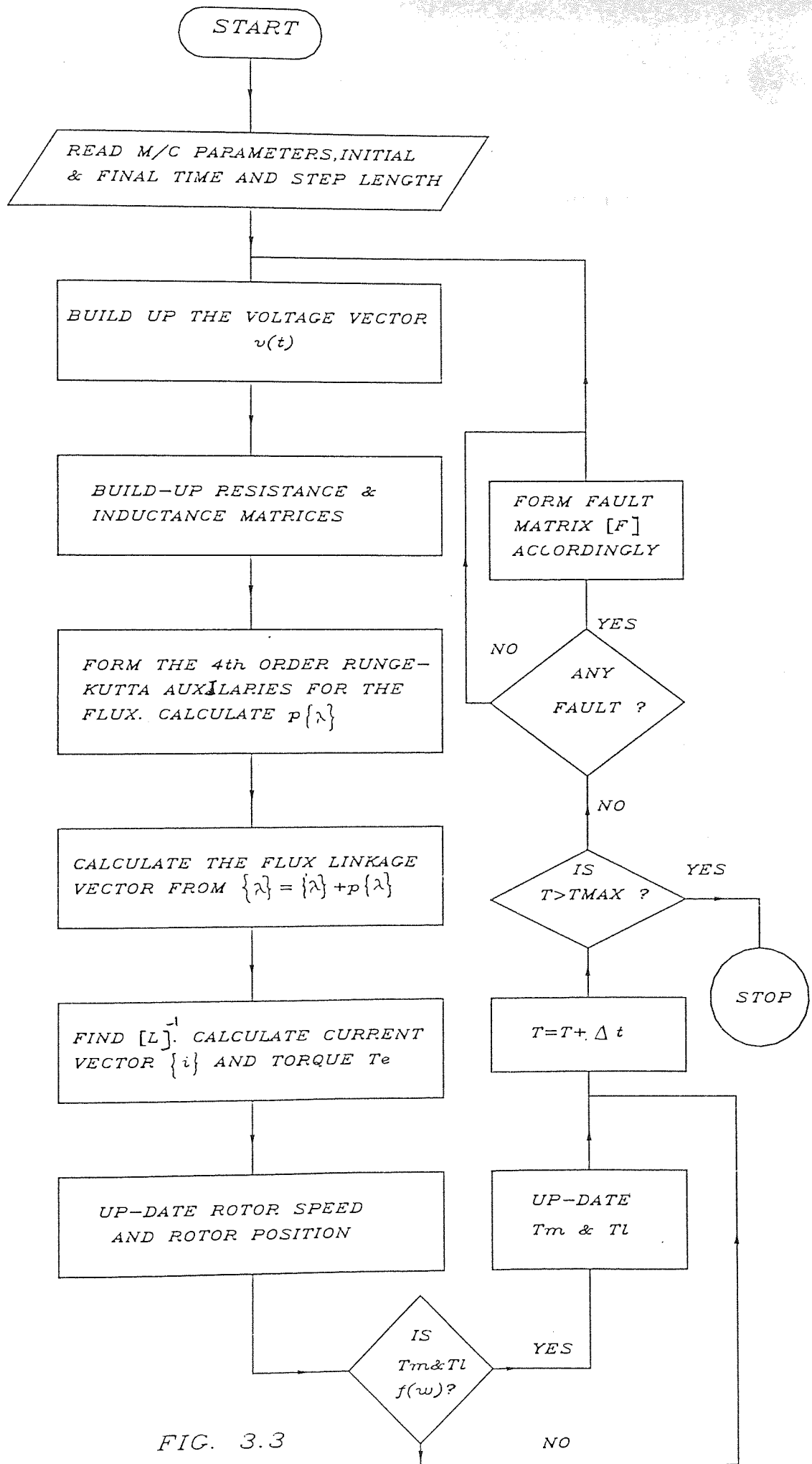


FIG. 3.3

torque and up-date rotor speed and position
(eqns.3.9 & 3.10).

- 8) Modify the mechanical and loss torque if they are speed dependent.
- 9) Up-date time for next step.
- 10) Check the operation condition for faults.

Step 2 to 10 are repeated until the limit of integration is achieved.

3.7 Transient Analysis

In the following paragraphs, studies are described which were used to investigate the behaviour of the induction motor following switching to an infinite source and following faults at the stator terminals.

3.7.1 Switching.

Switching studies at different points on the voltage wave form were carried-out by introducing an angle ' γ ' in the elements of the voltage vector i.e :

$$v_A = V_m \sin(\omega t + \gamma)$$

$$v_B = V_m \sin((\omega t - 2\pi/3) + \gamma) \quad \dots\dots 3.18$$

$$v_C = V_m \sin((\omega t + 2\pi/3) + \gamma)$$

Simulation methods were developed for two different types of switching. These are :

a) Simultaneous Switching

Simultaneous switching at $\gamma = 0$ or $\pi/2$ was investigated with the machine running both on light load and fully loaded. Wave forms of the stator and rotor current (phase A & a) were plotted (figs. 3.4,3.5 & 3.6,3.7). Also, torque/time and torque/slip characteristics (figs. 3.8,3.9 & 3.10) and speed/time curve (figs. 3.11 ,3.12) were developed from these studies.

b) Sequential Switching

Sequential switching was simulated by closing all the three phases at equal magnitude on the voltage wave forms for example, sequential switching at $\gamma = \pi/2$ was simulated by closing phase 'A' at 'peak' value followed by phase 'B' at 1/3 cycle later and phase 'C' at 1/3 cycle after phase 'B'. Results similar to those obtained in simultaneous switching studies were also

produced here i.e figs. (3.13, 3.14) show the stator and rotor currents with the motor running on light load. Also, and for the same condition of loading, torque/slip characteristics are shown in fig. (3.15) and finally, the speed/time curve is given by fig. (3.16).

The graphs are arranged as shown for easy comparison between the two methods of switching.

3.7.2 Faults Analysis

Symmetrical and asymmetrical fault analysis was implemented by invoking a fault matrix [F] at the specified time of fault application. This 3x3 matrix modifies the elements of the voltage vector according to constraints derived from the type of the fault, as explained in the following sections :

a) Single phase-to-earth fault (phase A)

To simulate a single phase-to-earth fault on phase 'A' say, the element of phase 'A' voltage, v_A , is to be eliminated from the voltage vector {v}. The fault matrix [F] in the following form satisfies this condition when operating upon the voltage vector i.e,

$$[F] = \begin{vmatrix} 0 & 0 & 0 \\ 0 & 1 & 0 \\ 0 & 0 & 1 \end{vmatrix}$$

Figs. (3.17,3.18), (3.19,3.20), (3.21,3.22) & (3.23,3.24) are plots for stator, rotor, torque/time & speed/time curves following a single phase-to-earth fault on phase 'A' with the machine running both on light load and fully loaded.

b) Line-to-Line short circuit (phase B&C)

The constraint for this condition is :

$$e_B = e_C$$

also we have,

$$e_A + e_B + e_C = 0$$

It follows from the two above relations that

$$e_B = e_C = -0.5e_A$$

Hence, the fault matrix for this condition is

$$[F] = \begin{vmatrix} 1 & 0 & 0 \\ -0.5 & 0 & 0 \\ -0.5 & 0 & 0 \end{vmatrix}$$

Figs. (3.25,3.26), (3.27,3.28) are for phases B, C, b& c stator and rotor currents following a short-circuit in phases B&C with the machine unloaded. Fig.(3.29) shows the torque/time curve and finally, fig.(3.30) is the speed/time curve for the first 0.5 sec. following the fault with the machine unloaded and fully loaded respectively.

c) Three phase-to-earth fault

In this case, all the three phase voltages at the motor terminals are suddenly reduced to zero, thus, matrix [F] takes the value,

$$[F] = [0]$$

The results for this study are shown in:

- figs.(3.31,3.32) the stator & rotor current of phase A, a
- fig.(3.33) is the torque/time curve,
- fig.(3.34) is the speed/time curve, and finally;
- fig.(3.35) is the internal induced e.m.f curve

d) Fault application & Clearance
for a Specified Time Interval

A study of the speed recovery following a fault was carried out by applying a temporary solid three phase-to-earth fault (for 0.15 sec.). The result is shown in fig. (3.36)

3.8 Discussion and Conclusions

The work described in this chapter shows how the transient performance of a large induction motor is affected by different switching and fault conditions. The results shown in figs. (3.4, 3.6, 3.9, 3.13 & 3.15) are similar to those obtained by other research workers e.g ref. [47]. Following a switching operation with the rotor speed equal to zero, a high stator current, several times the normal rating, is drawn from the supply. This current remains above the rated value until the rotor speed builds-up and reaches its final sub-synchronous value which depends upon the loading conditions. Also, a pulsating torque having a magnitude several times the normal rated value is developed (figs. 3.8 & 3.9). The time taken by the sustained current and the pulsating torque to fall to an acceptable level depends upon how quickly the rotor speed reaches its final steady state value. The rotor speed (figs. 3.11, 3.12) rises slowly in the first 1.1 sec. (first 350 p.u time) followed by a steady rise in the next 2.5 sec. and

thereafter rises asymptotically to the final steady-state value. The rotor speed depends upon the inertia constant of the motor as well as the rotor circuit parameters. Theoretically, if full power is applied to the motor, then the time required by the rotor to reach the final speed from rest is given by $2H$ (H is the motor inertia constant with any connected load).

A high sub-transient current can be reduced by sequential switching through 90° degrees (compare figs. 3.4 & 3.13). Also, switching using this method minimises the oscillation in the starting torque (figs. 3.8 & 3.15) and reduces the time taken by the rotor to reach the final speed by about 19% (figs. 3.12 & 3.16).

Following application of faults, and due to the trapped flux in the air-gap, the motor supplies a large alternating current into the fault. The wave form of the fault current can be analysed using the following equation which was derived to estimate the fault current of the induction machine [31,33] (neglecting the effect of the deep bar circuit) :

$$i_f(t) = -V_m (B \cos \phi - A \sin \phi) \exp(-t/T) - V_m (1/L' - 1/L_{ss}) \times \cos \theta' \sin(\omega t + \phi - \theta') \exp(-t/T') \quad \dots\dots 3.19$$

where L' , T_a , T' , A , B , θ' are defined in appendix (A1) and φ is a switching angle.

From the above equation, the fault current can be considered to contain:

- a) An asymmetrical component which decays with a time constant T_a and has an initial value depending upon the instantaneous voltage at the instant of fault occurrence.
- b) A periodic component alternates at angular frequency ' ω ' and its magnitude depends on transient and apparent stator reactance L' and L_{ss} as well as on loading angle θ' . This component decays exponentially with a time constant T' .

Since equation 3.17 was derived under a condition of a solid three phase to earth fault, the corresponding result obtained here in this work (fig. 3.31) is checked in the following paragraph.

By substituting the parameters, for the motor, in equation T_a , T' ,

L and L_{ss} (see appendix (A1)), the following values can be

obtained:



$$\begin{aligned}
T_a &= 0.1328 \quad \text{sec.} \\
T' &= 0.0509 \quad \text{sec.} \\
L' &= 0.1727 \quad \text{p.u} \\
L_{ss} &= 4.0855 \quad \text{p.u}
\end{aligned}$$

The initial maximum value of the asymmetrical component from equation 3.19 (neglecting the stator resistance and using $B=1/L'$) is 5.75, and the initial value of the periodic component with the machine unloaded is $5.54\sin\omega t$. By allowing a time of 0.005 sec. to elapse (time of first quarter cycle), then,

$$\begin{aligned}
|i_f(0.005)| &= 5.75\exp(-0.005/0.1328) + 5.54\exp(-0.005/0.0509) \\
&= 5.53 + 5.02 = 10.5
\end{aligned}$$

This value, see fig. (3.31), is confirmed with a discrepancy of 4.8%. The difference between the calculated value using equation 3.19 and the computed value obtained from the study may be due to the assumption made in deriving equation 3.19 that the slip 's' is constant following the fault.

In addition to the loading condition, the first peak is also found to be affected by the type of fault (figs. 3.17, 3.18 & 3.31). The maximum 'd.c' off-set occurs for a three phase-to-earth fault with the machine unloaded and the corresponding phase voltage

passing zero value (fig. 3.31). In the case of asymmetrical faults, and due to rotor speed oscillation, second harmonics are generated in the rotor (figs. 3.19, 3.20 & 3.27, 3.28).

Also, following the occurrence of a fault, a transient torque having a magnitude several times the normal rating is developed (figs. 3.21, 3.22, 3.29 & 3.33). The torque as seen from equation 3.11, is a scalar variable and results from the interaction of the stator and rotor currents, thus, the transient torque reflects the asymmetry in the rotor and the stator current. Also the torque is influenced by a combination of frequencies from the stator and the rotor. As the torque depends on the asymmetry of the current, the magnitude of the first peak is a function of the instantaneous voltage at which the switching or fault occurs. In the case of asymmetrical faults, this torque is smaller in magnitude, pulsates at twice the power frequency, and oscillates around a value determined by the loading condition. In case of a solid three phase-to-earth fault the machine torque falls until the fault is cleared or becomes zero if the fault is sustained.

Under all fault conditions, the rotor speed drops and it may continue to retard or oscillate or even settle at another value of sub-synchronous speed depending upon the type of fault as shown by figs. (3.23, 3.30 & 3.34), one may also observe that, the rate of speed variation is affected by the loading condition.

Following a three phase-to-earth fault, the motor induced e.m.f falls by about 62% as seen by fig. 3.35 and then decays exponentially in the following 400 milliseconds.

As a conclusion, modelling of induction machines in a three phase frame of reference provides enhanced facilities for transient analysis by providing a method for determining the machine variables under circumstances of fault and switching which cannot be achieved by other frames of reference. Switching by different methods, as well as, symmetrical and asymmetrical faults can be investigated without alteration in the model. The studies carried out in this chapter, show that large induction motors are subjected to high sustained currents following switching action. Also, such motors are found to supply large currents to the fault location and thus, their contribution to system fault analysis cannot be ignored.

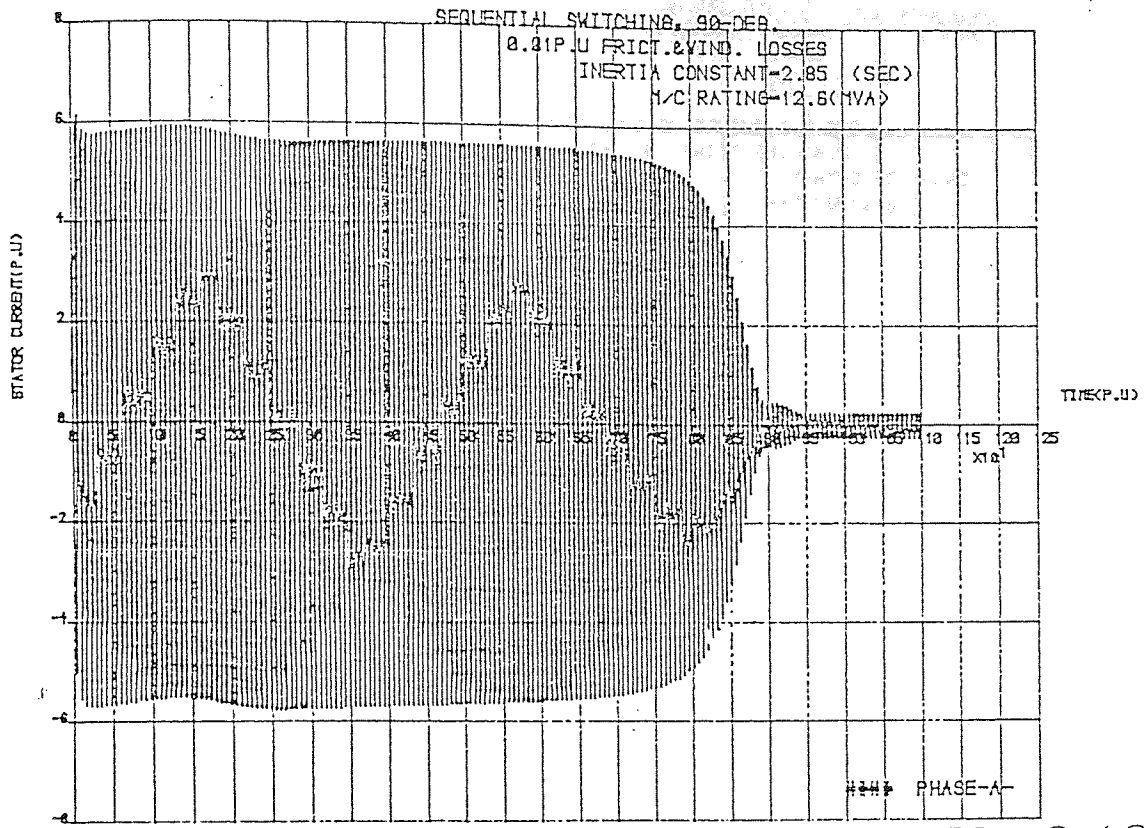


FIG. 3.13

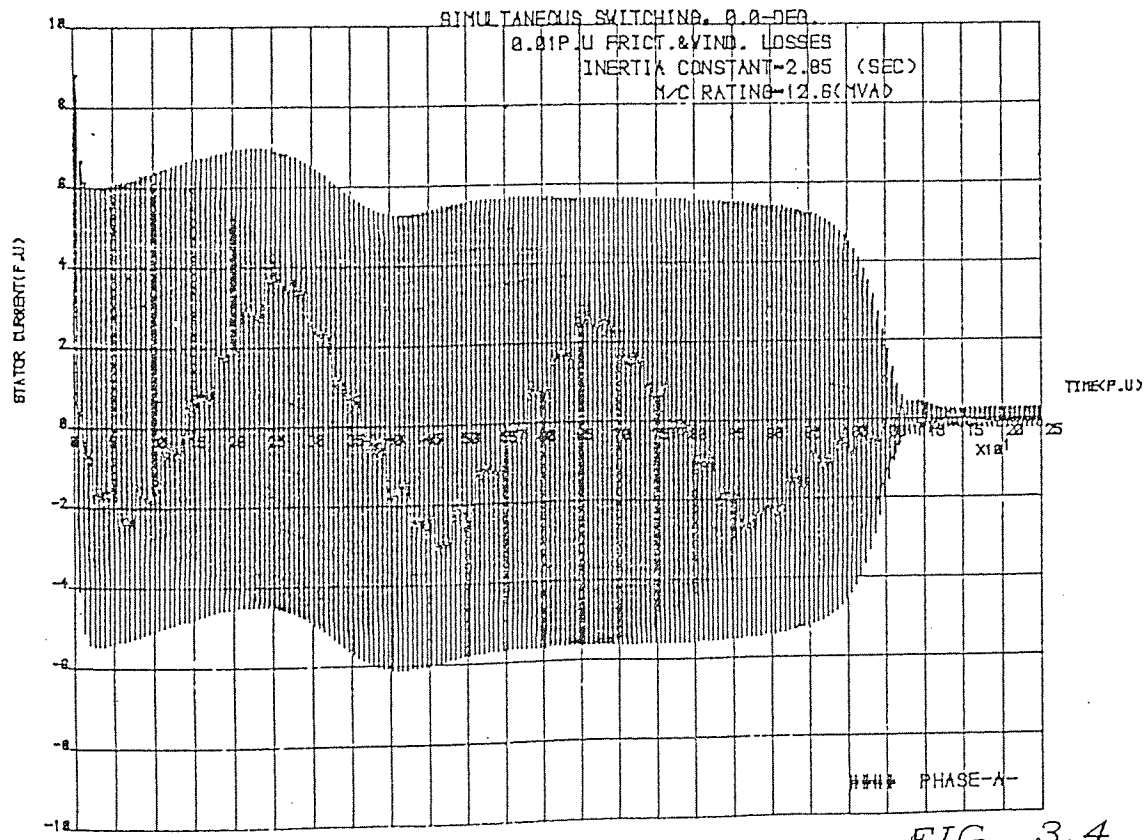
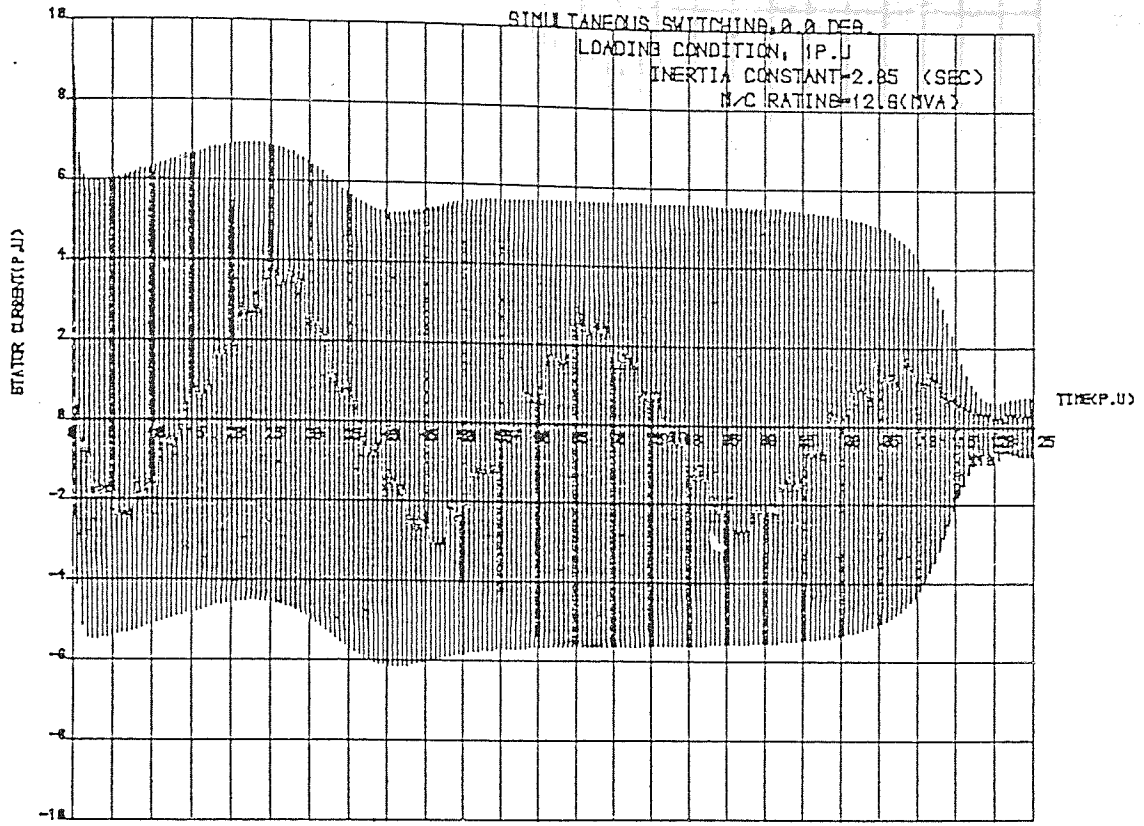
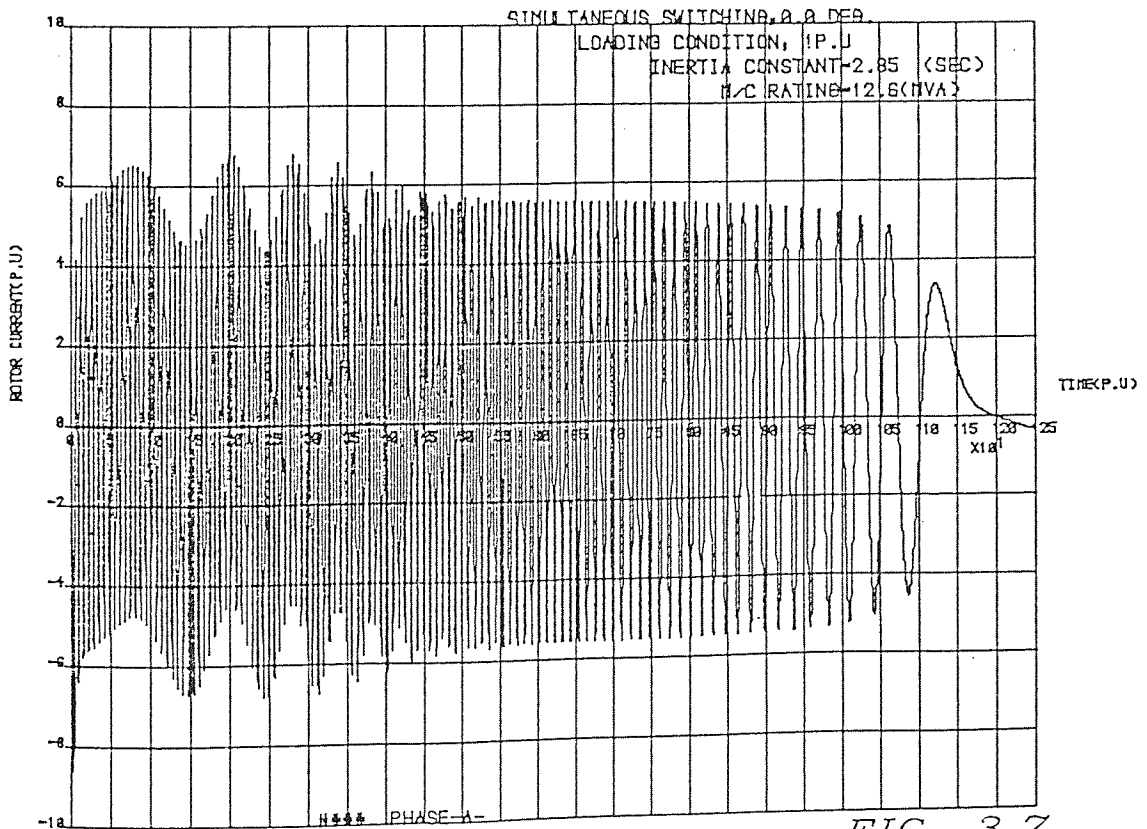


FIG. 3.4



*** PHASE-A-

FIG. 3.5



*** PHASE-A-

FIG. 3.7

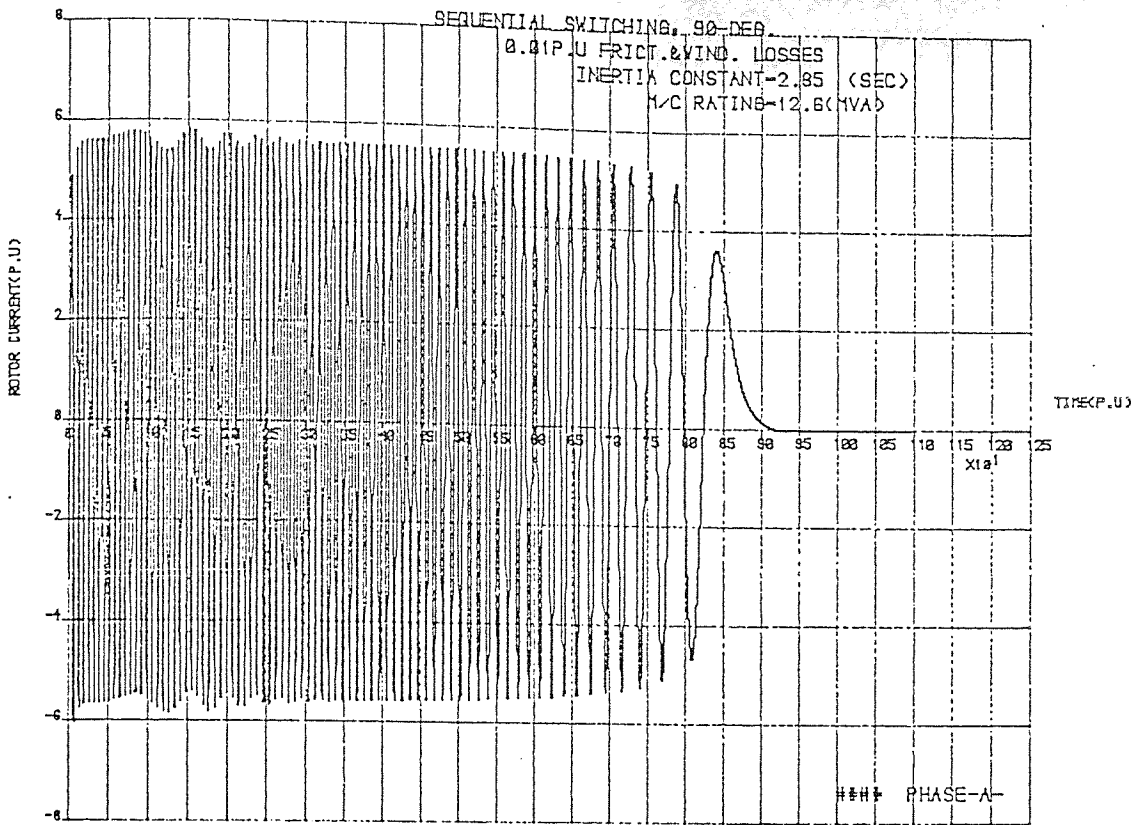


FIG. 3.14

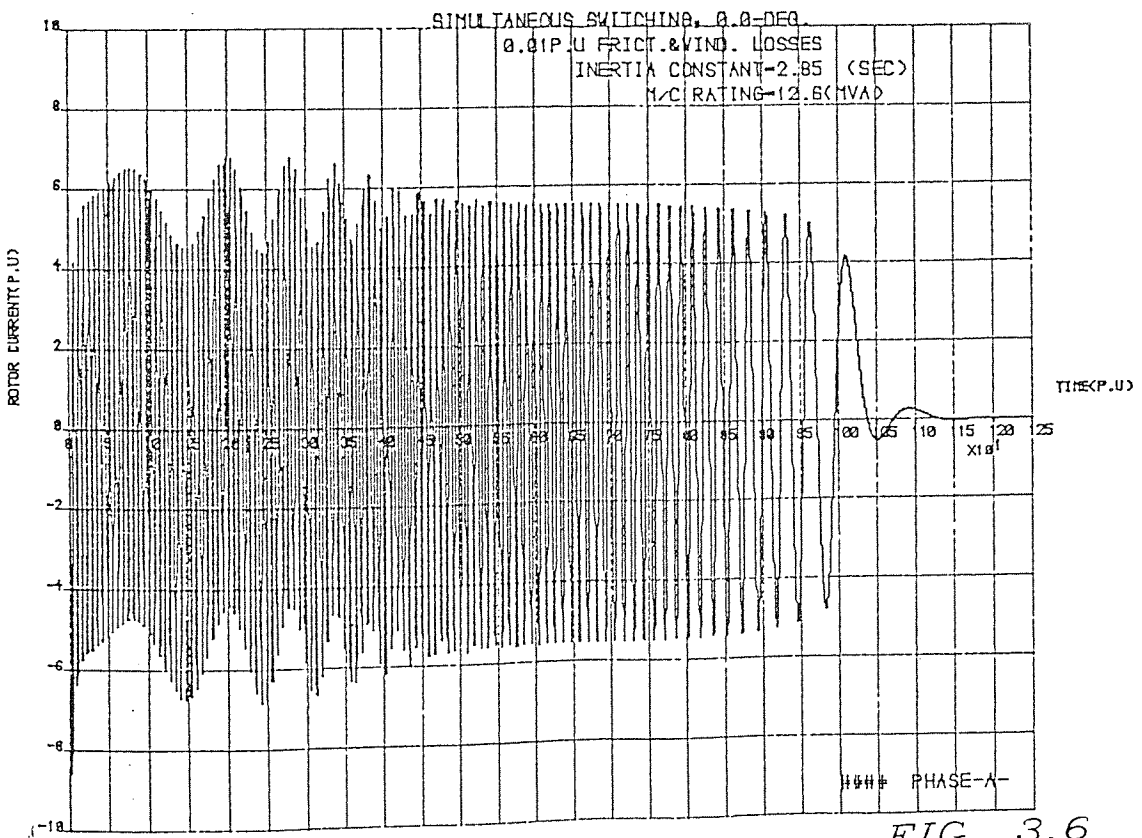


FIG. 3.6

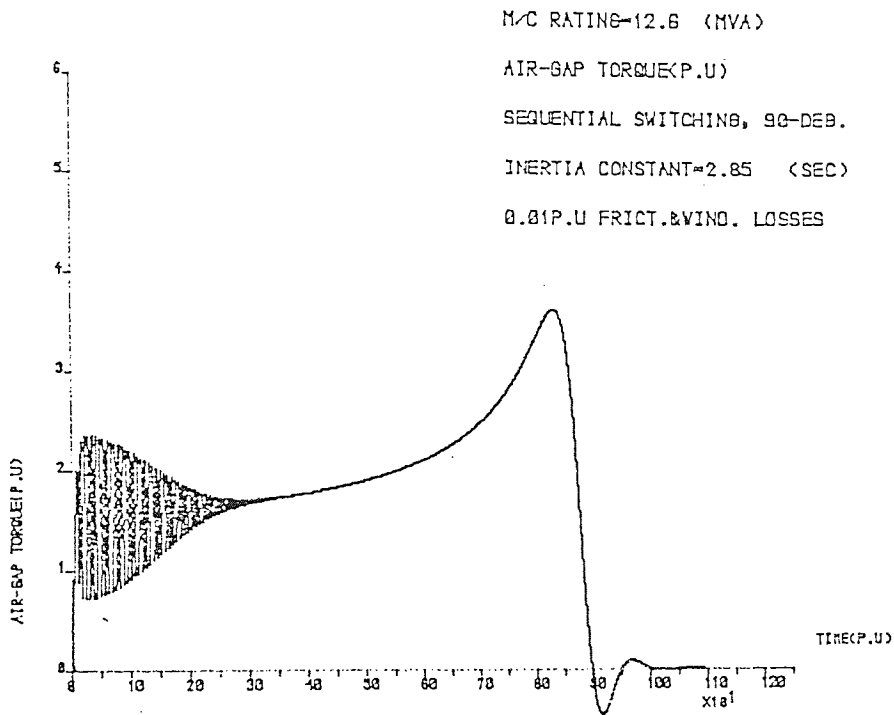


FIG. 3.15

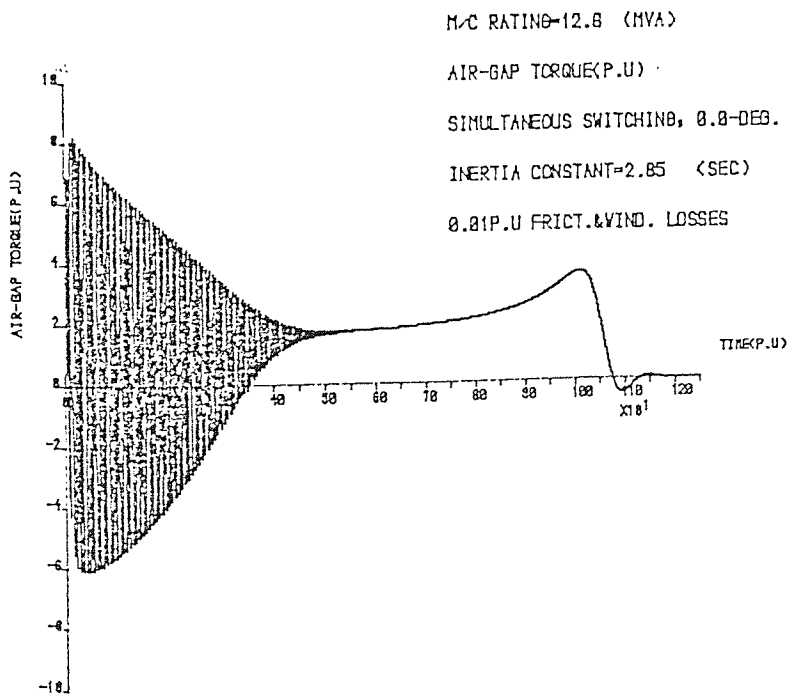


FIG. 3.8

M/C RATING=12.6 (MVA)
 P.U. SLIP-TORQUE CHARACTERISTIC
 SIMULTANEOUS SWITCHING, 0.0 DEG.
 LOADING CONDITION, 1 P.U.
 INERTIA CONSTANT=2.85 (SEC)

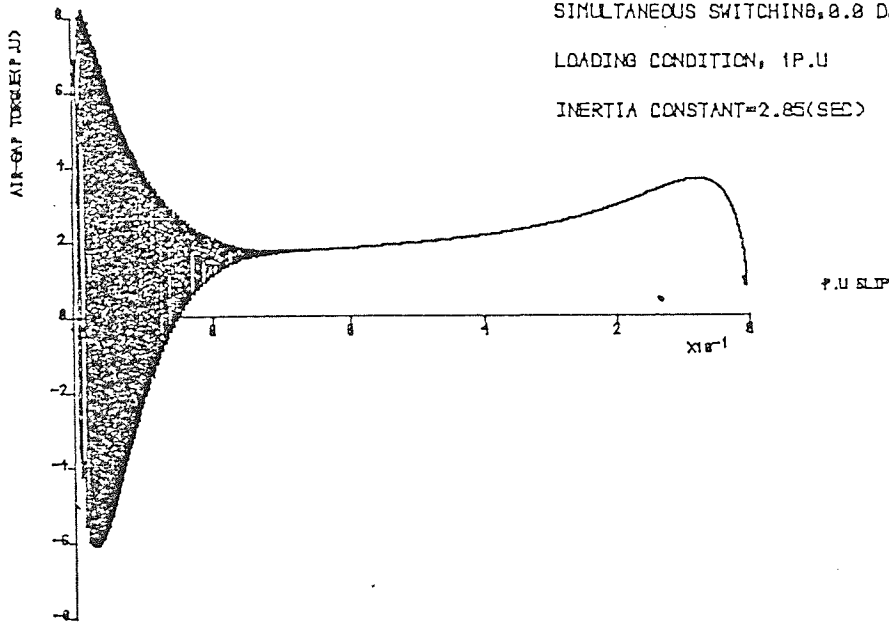


FIG. 3.10

M/C RATING=12.6 (MVA)
 AIR-GAP TORQUE (P.U.)
 SIMULTANEOUS SWITCHING, 0.0 DEG.
 INERTIA CONSTANT=2.85 (SEC)
 LOADING CONDITION, 1 P.U.

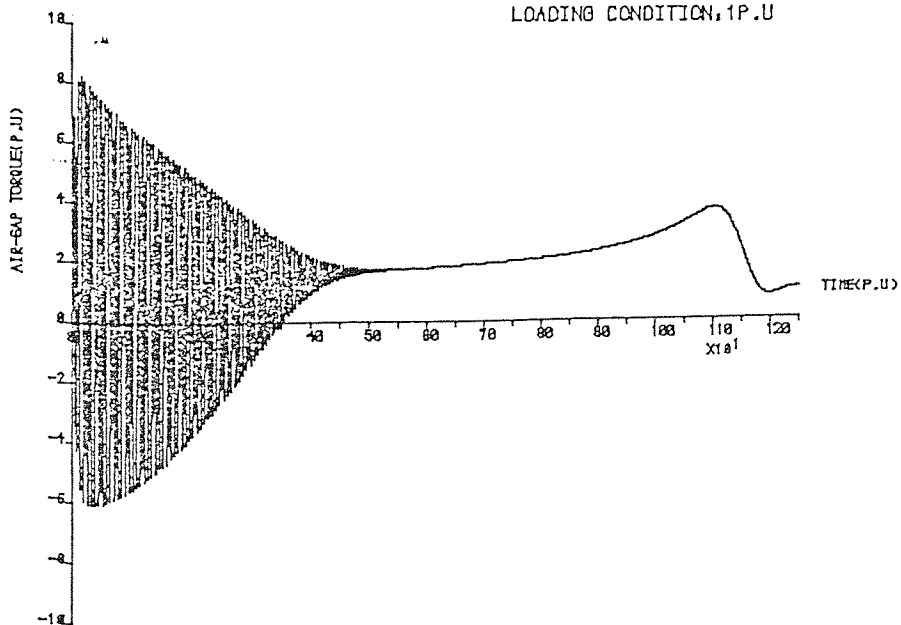


FIG. 3.9

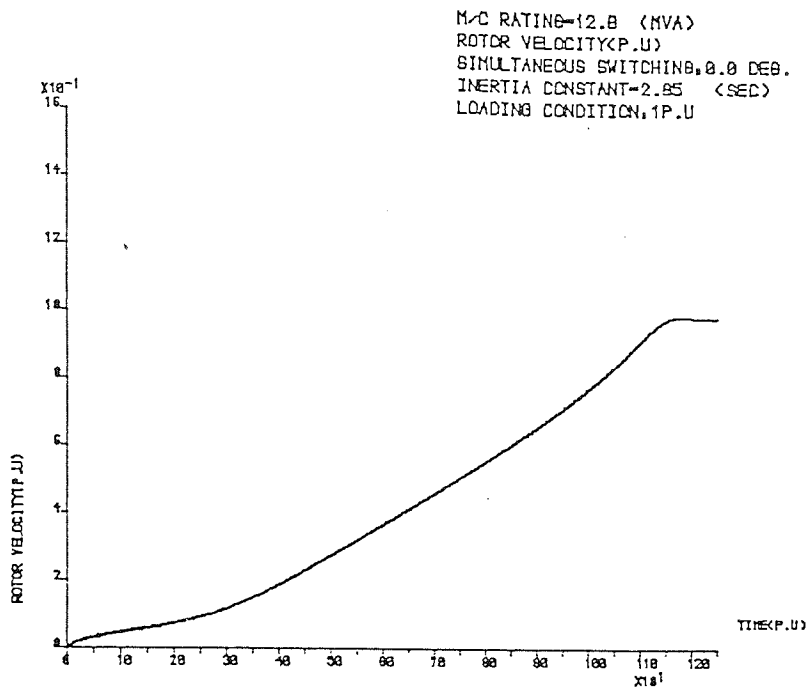


FIG. 3.11

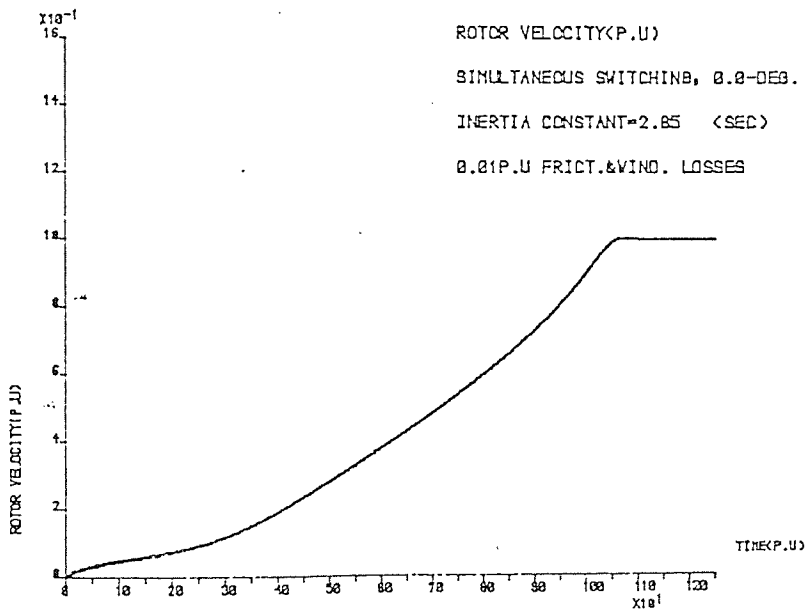
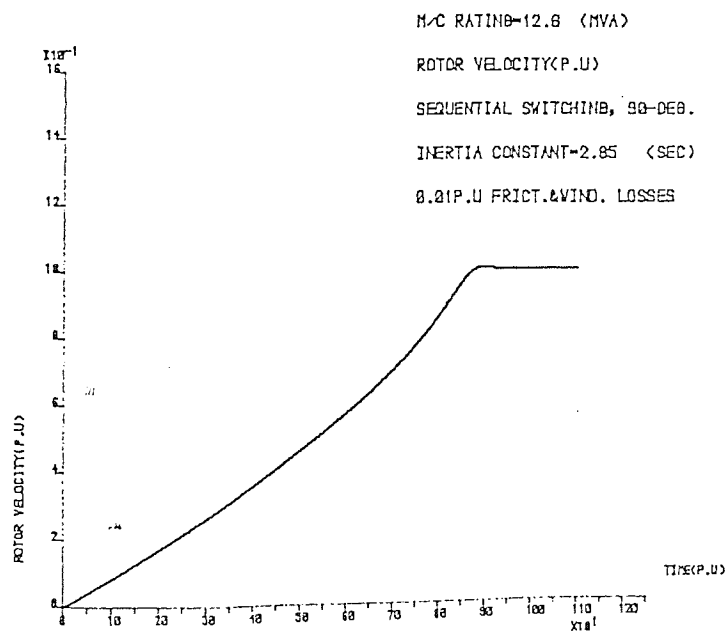


FIG. 3.12



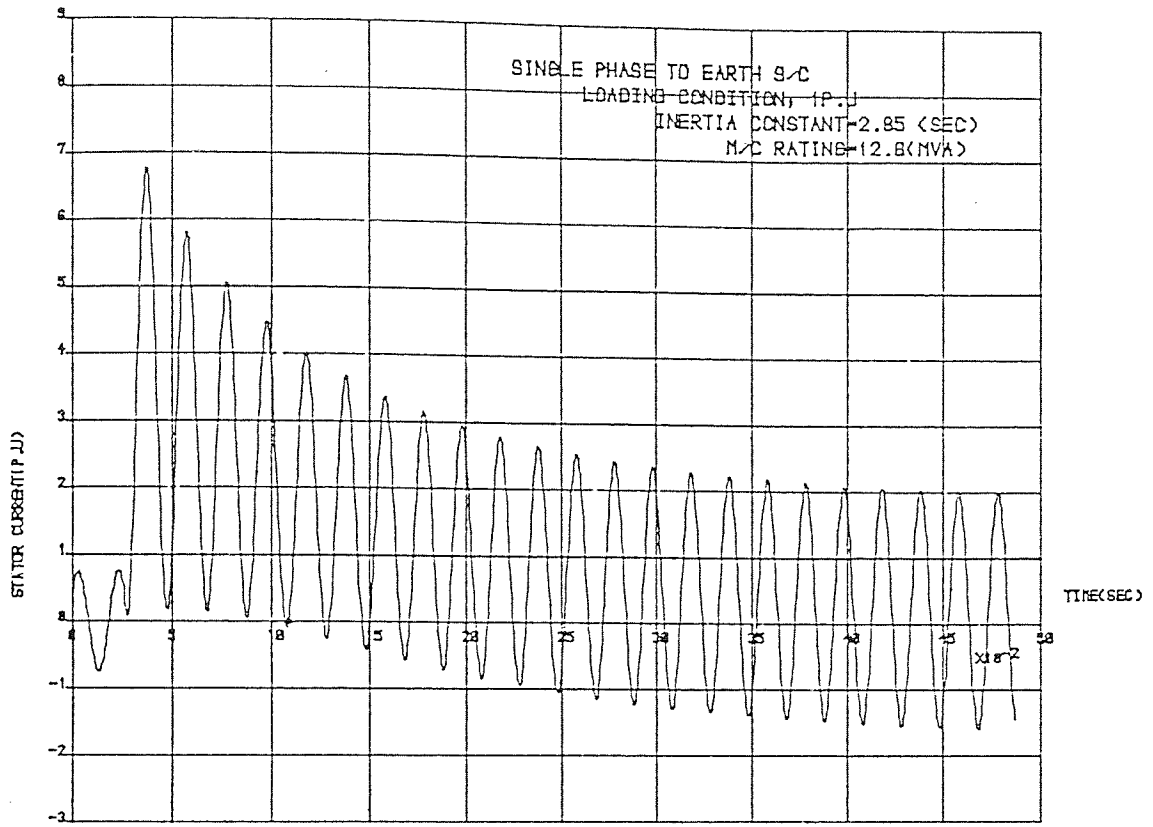


FIG. 3.18

PHASE-A-

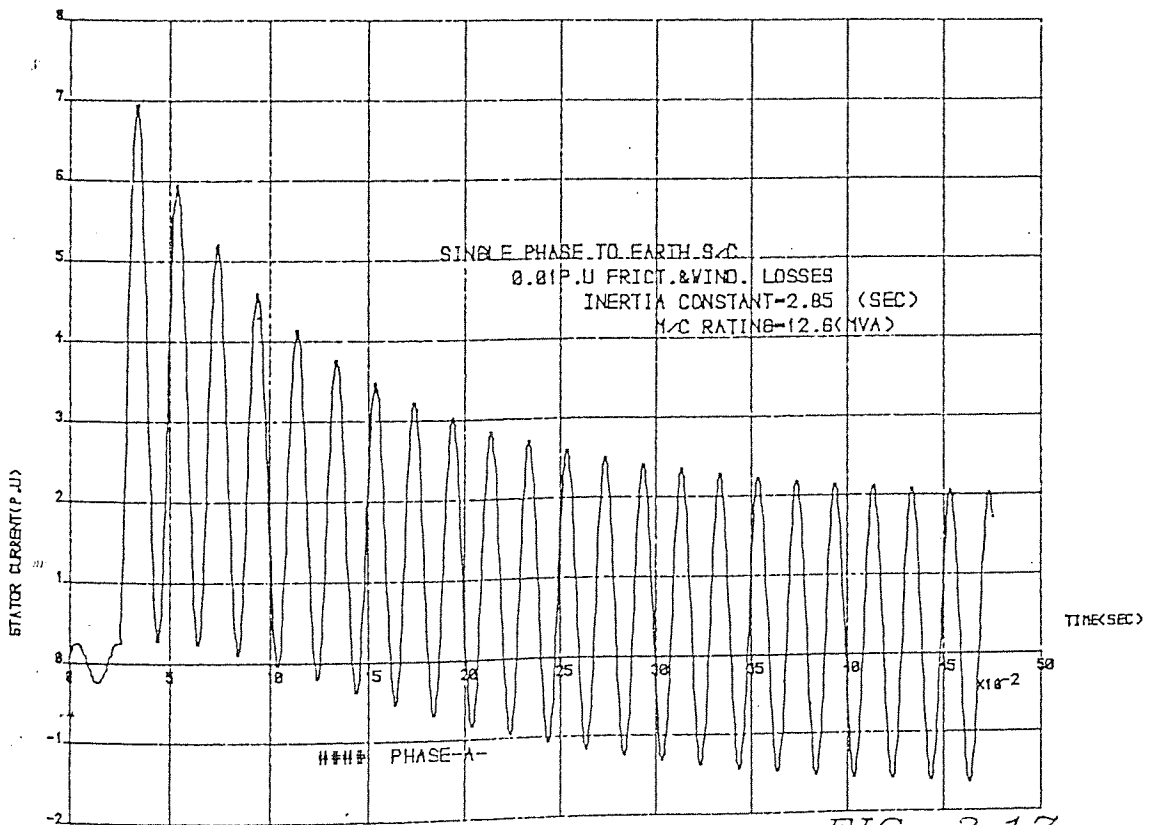


FIG. 3.17

PHASE-A-

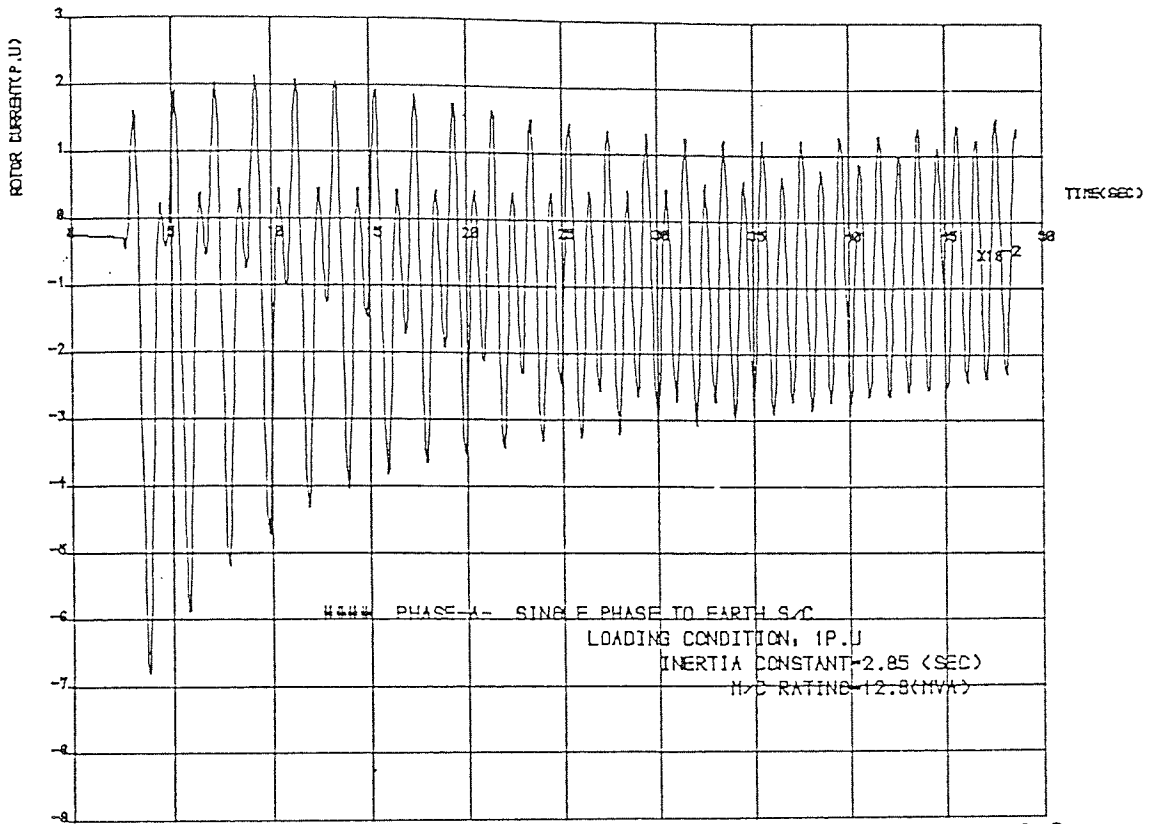


FIG. 3.20

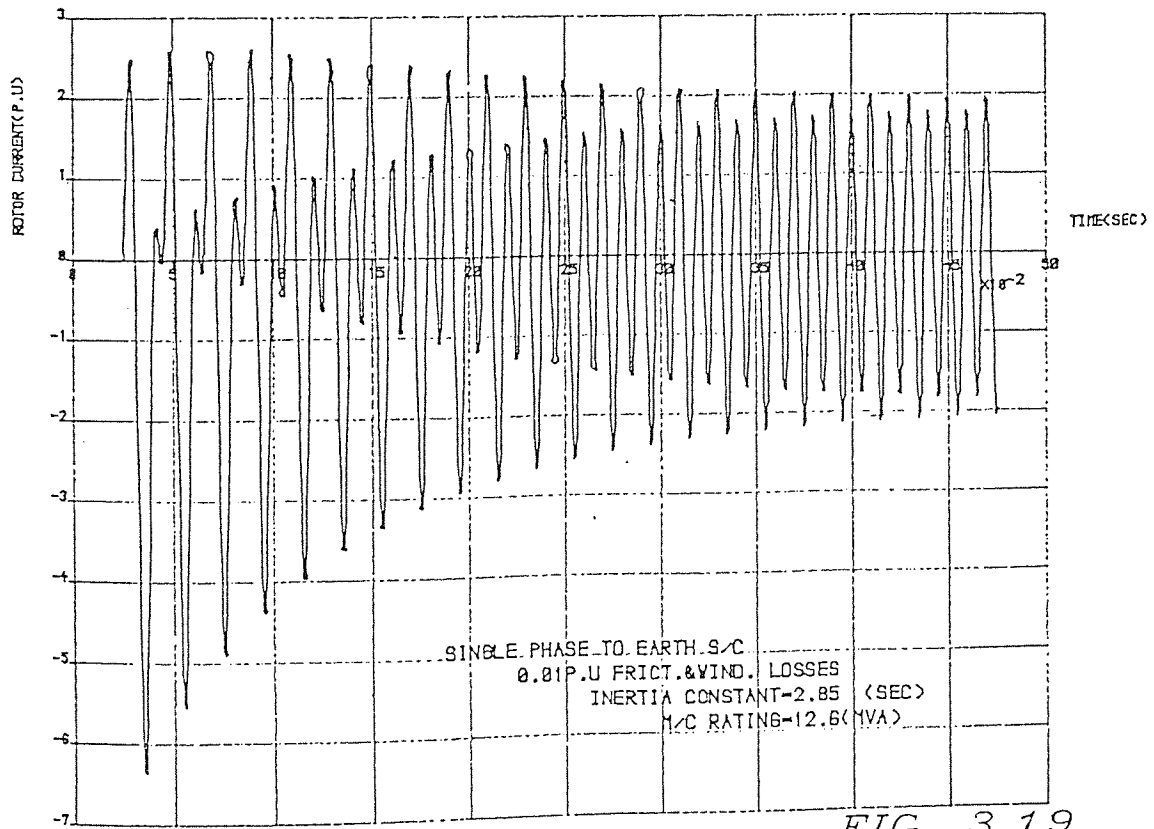


FIG. 3.19

PHASE-A-

M/C RATING=12.8 (MVA)
 AIR-GAP TORQUE(P.U)
 SINGLE PHASE TO EARTH S/C
 INERTIA CONSTANT=2.85 (SEC)
 LOADING CONDITION, 1P.U

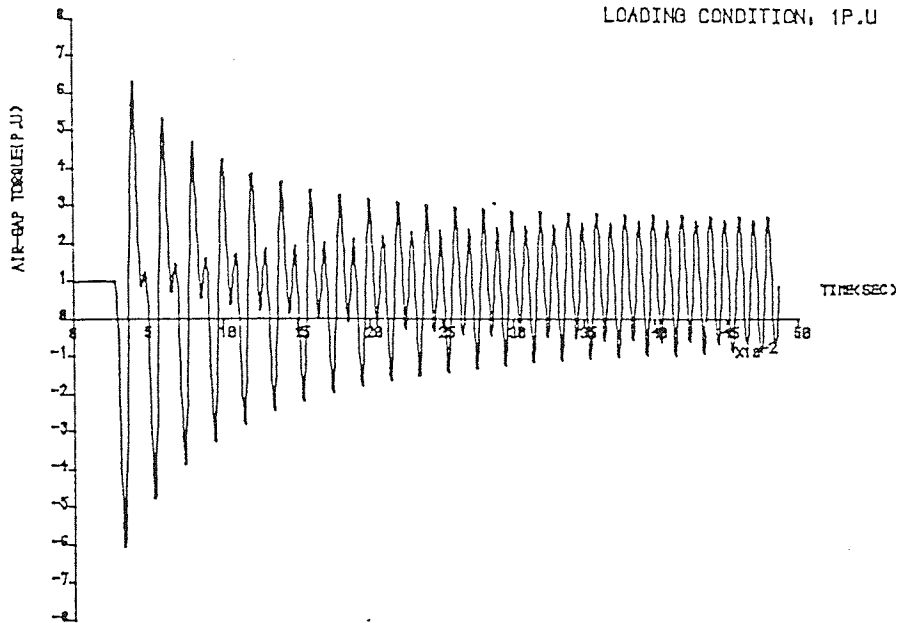


FIG. 3.22

M/C RATING=12.6 (MVA)
 AIR-GAP TORQUE(P.U)
 SINGLE PHASE TO EARTH S/C
 INERTIA CONSTANT=2.85 (SEC)
 0.01P.U FRICT.&WIND. LOSSES

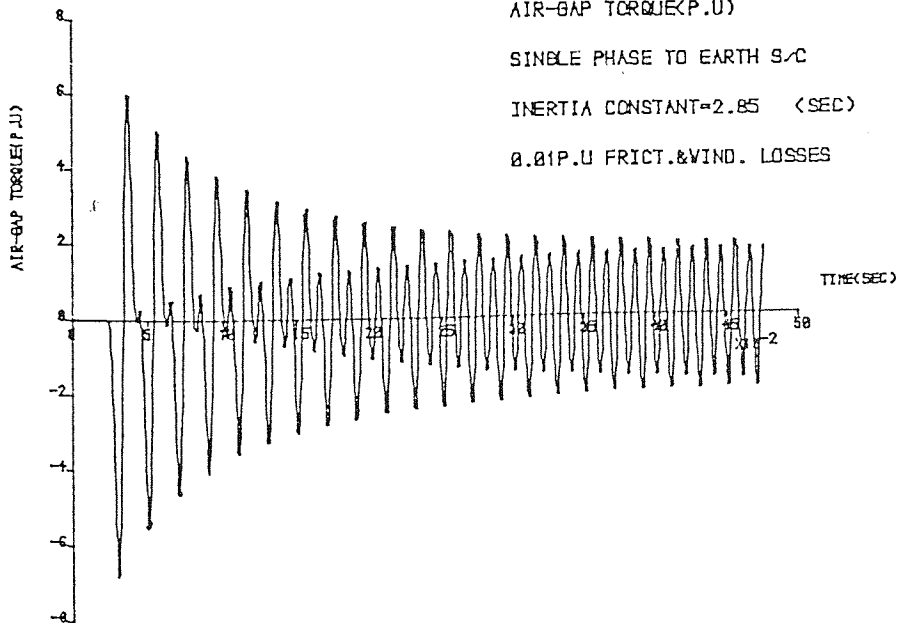


FIG. 3.21

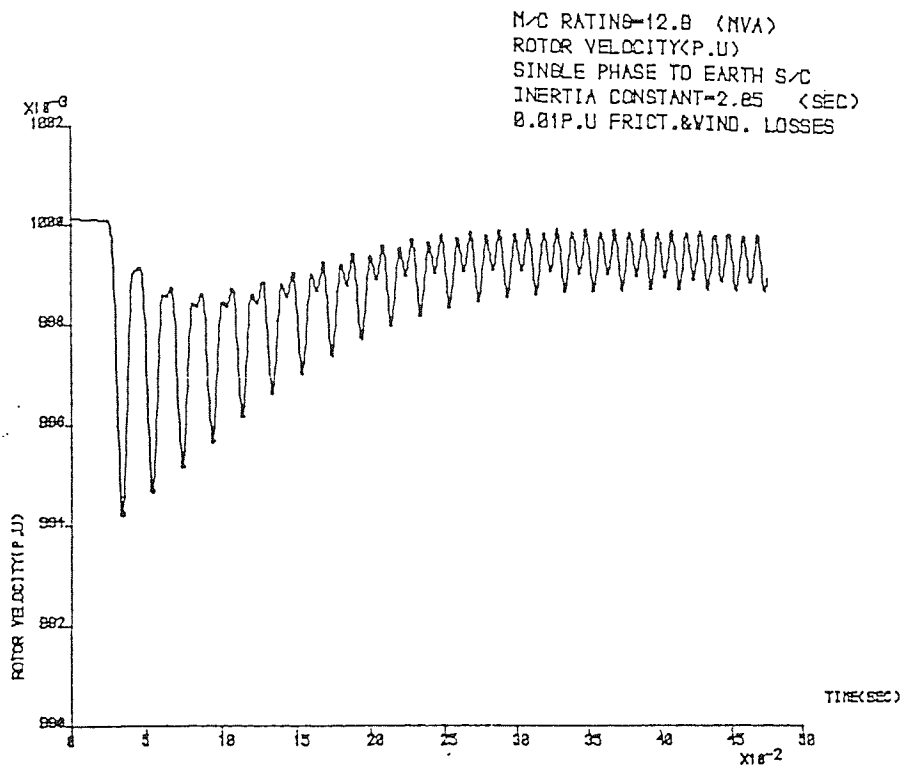


FIG. 3.23

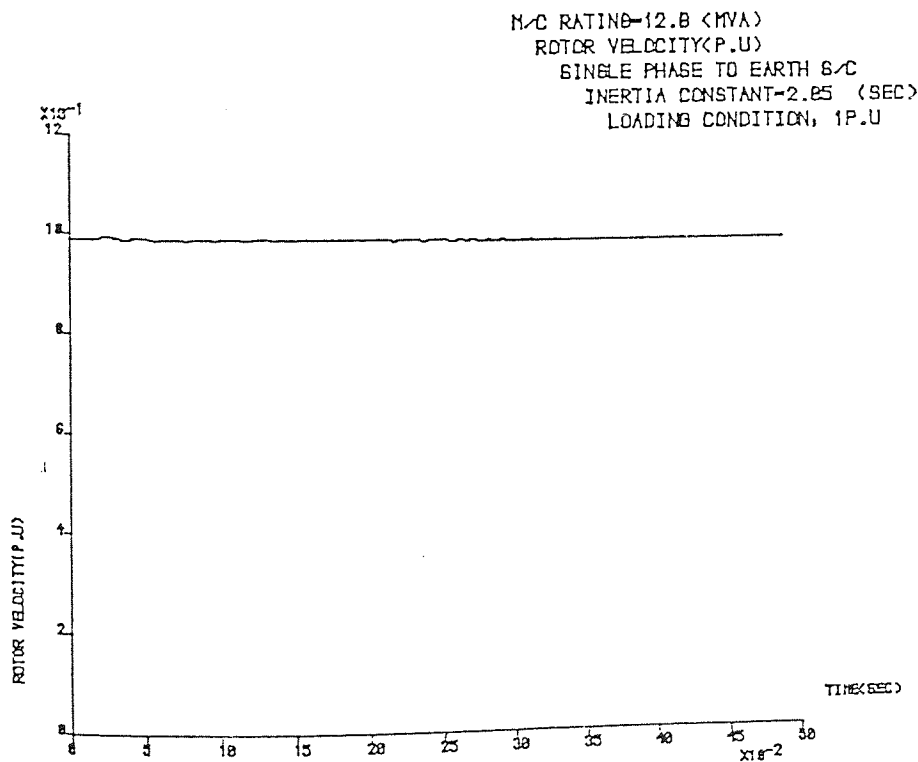


FIG. 3.24

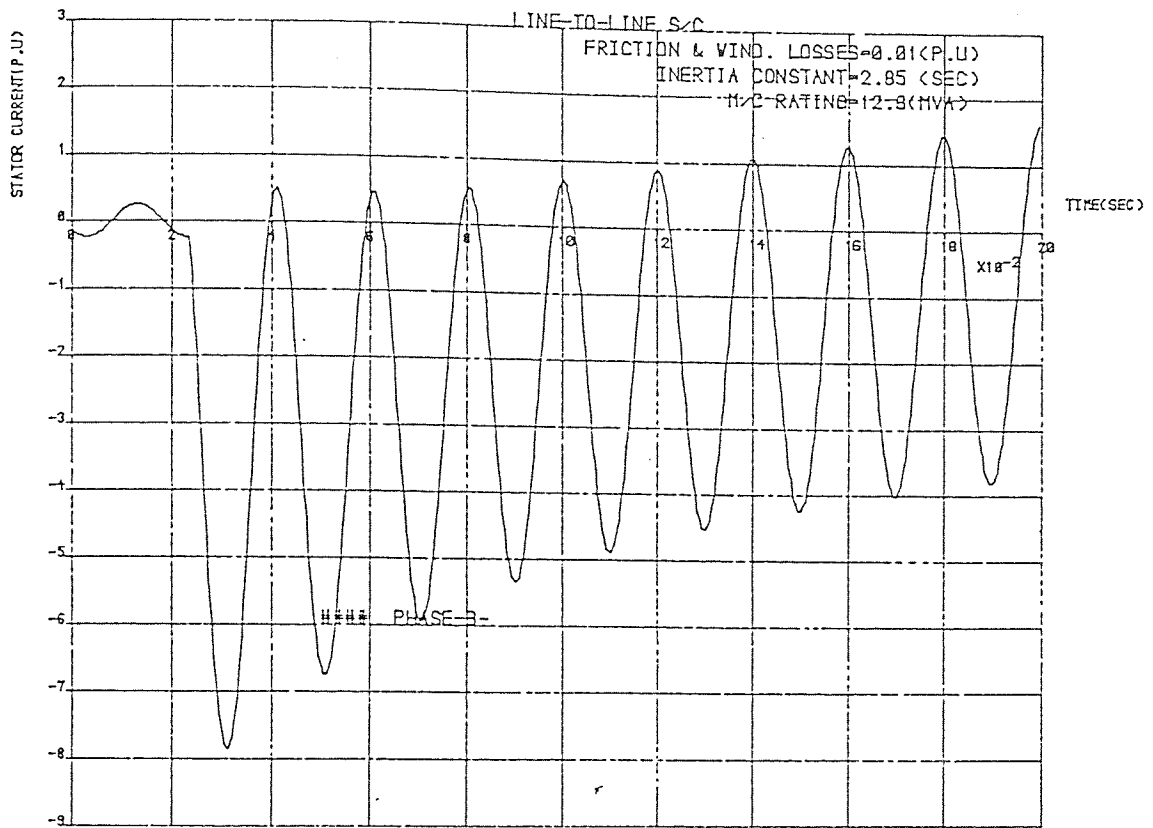


FIG. 3.25

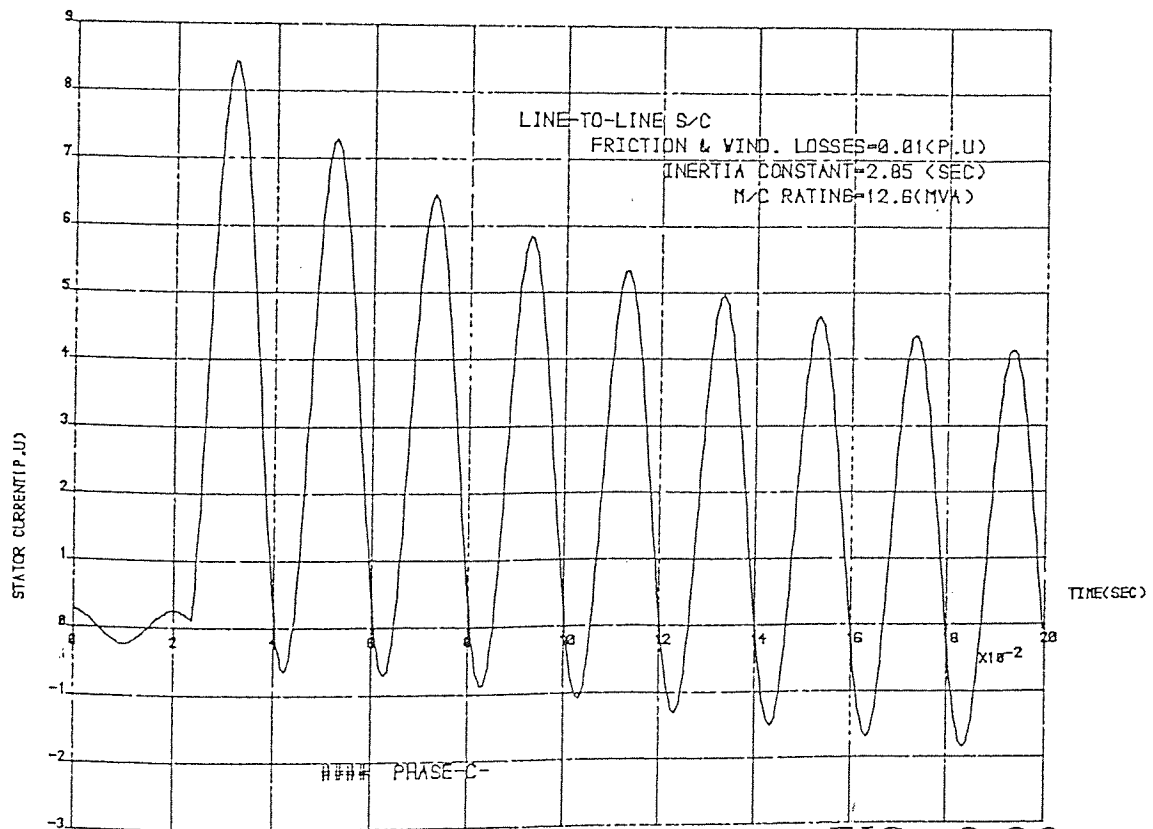


FIG. 3.26

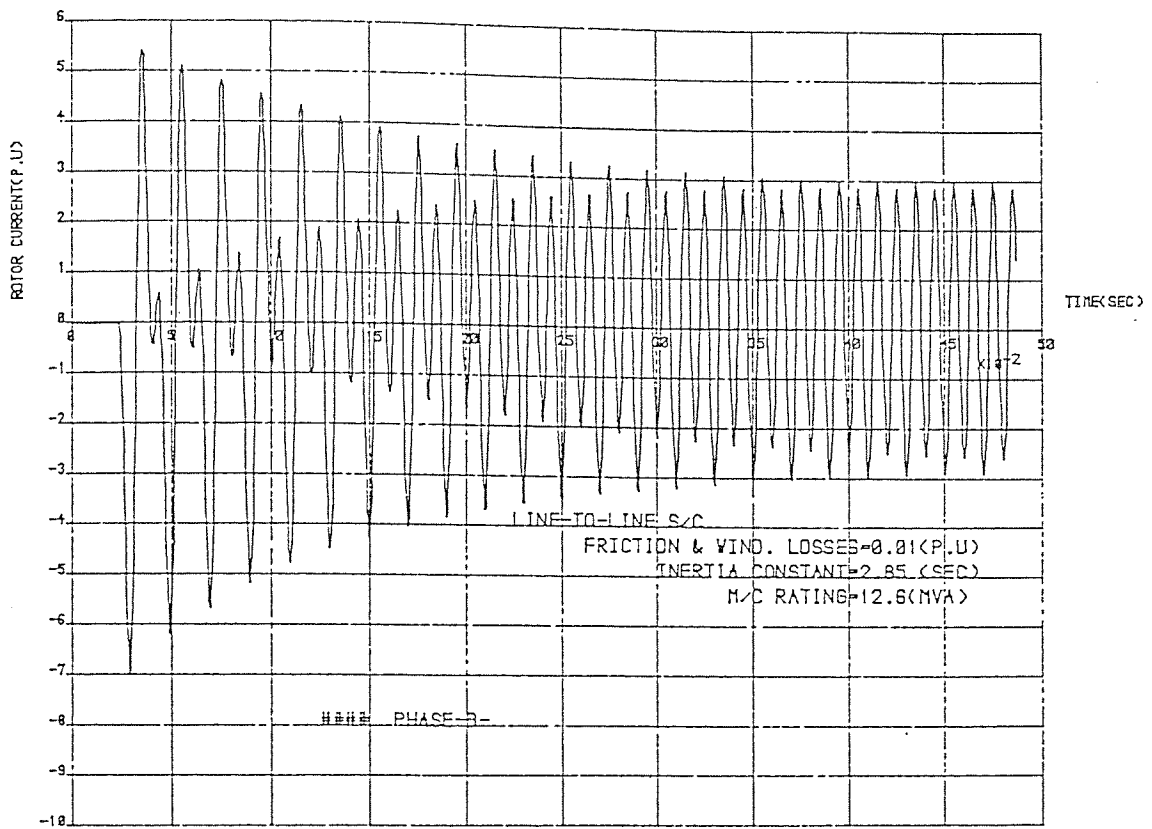


FIG. 3.27

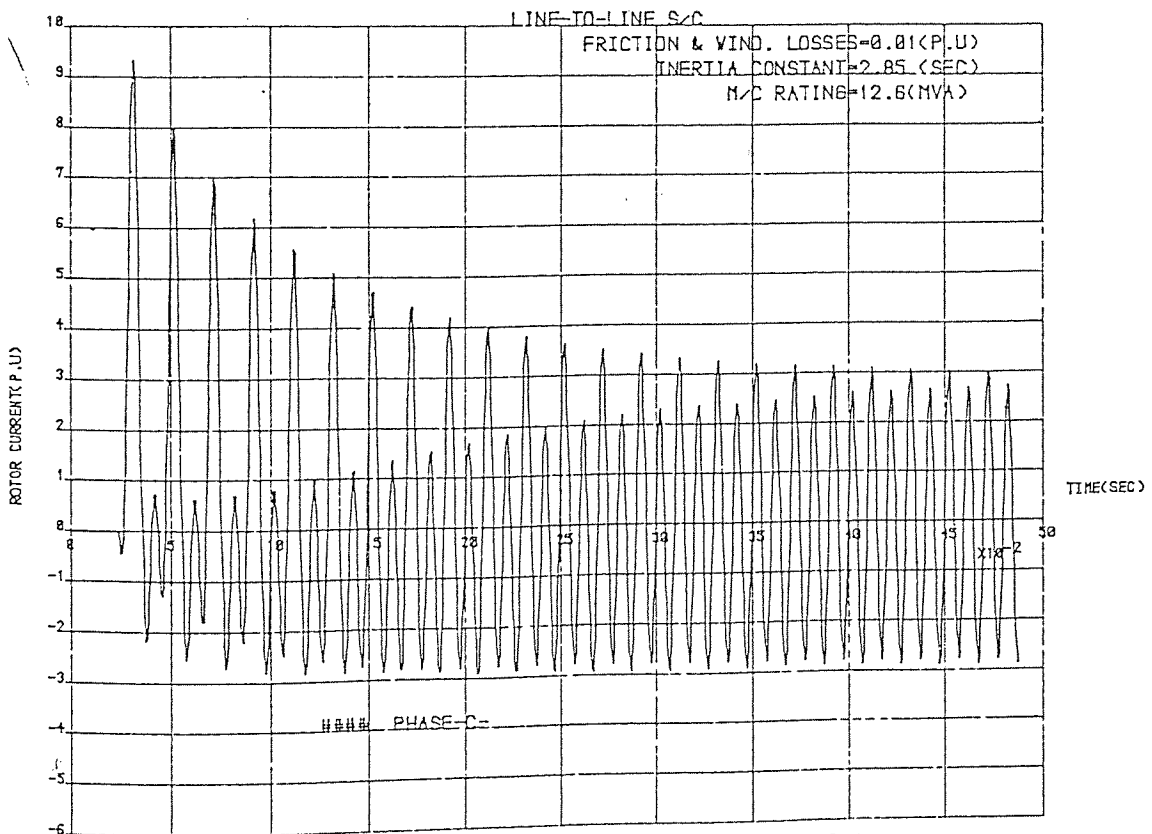


FIG. 3.28

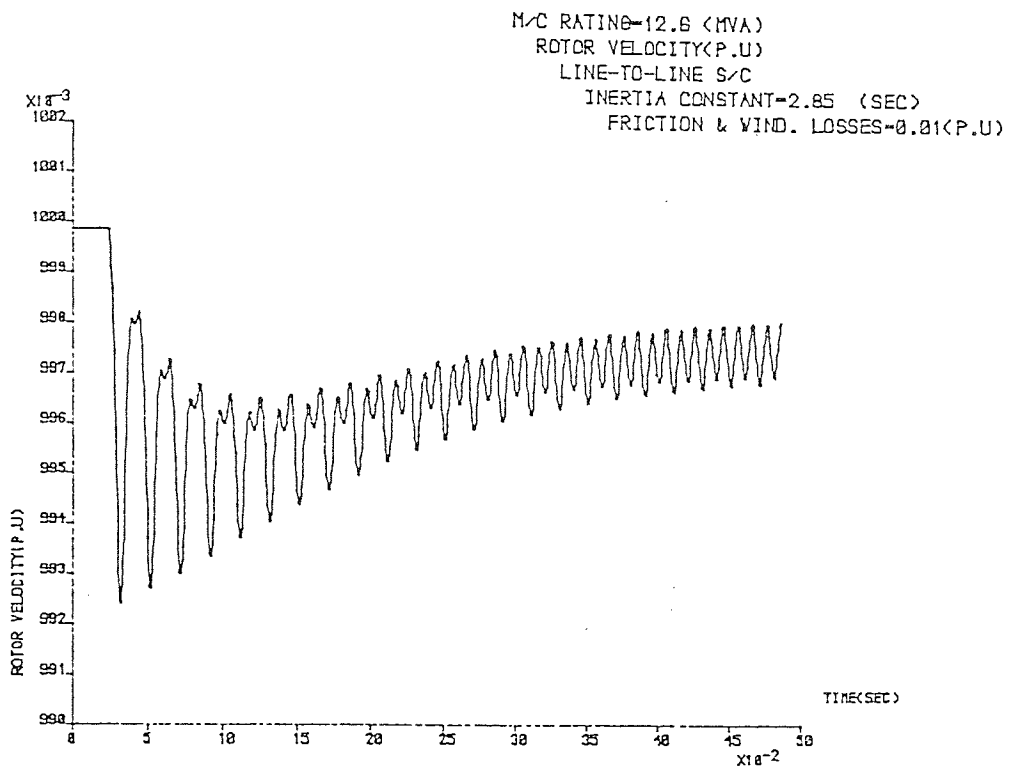


FIG. 3.30

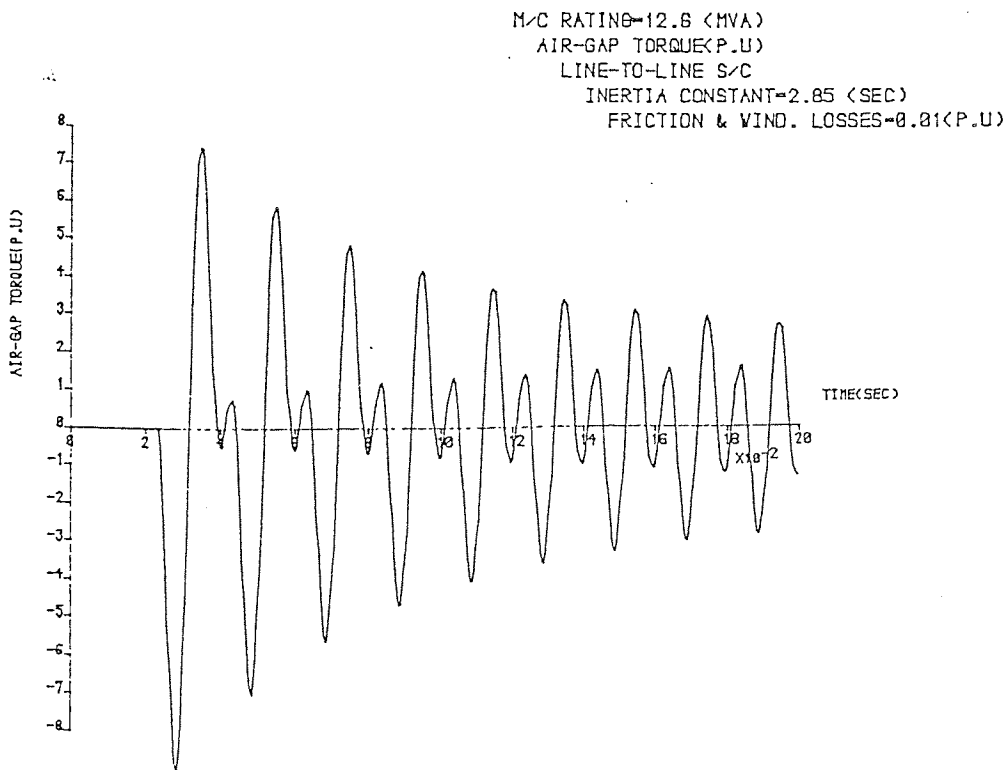


FIG. 3.29

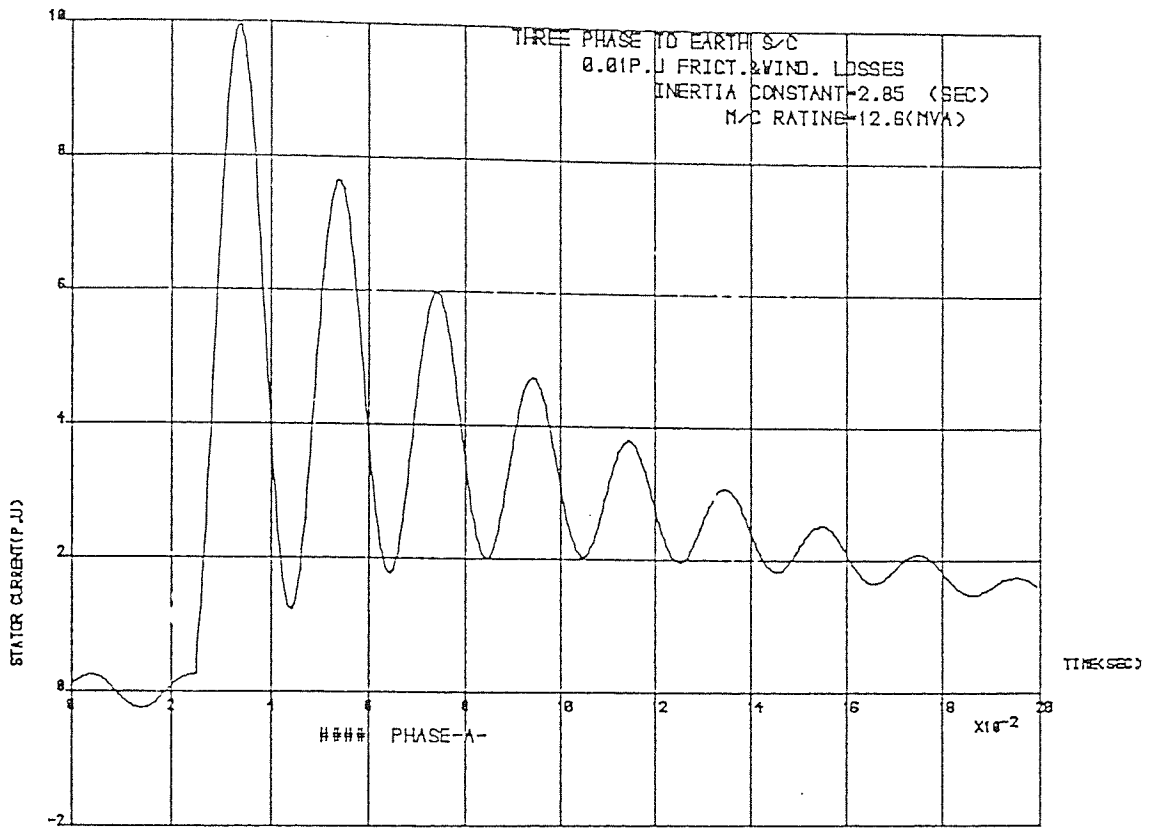


FIG. 3.31

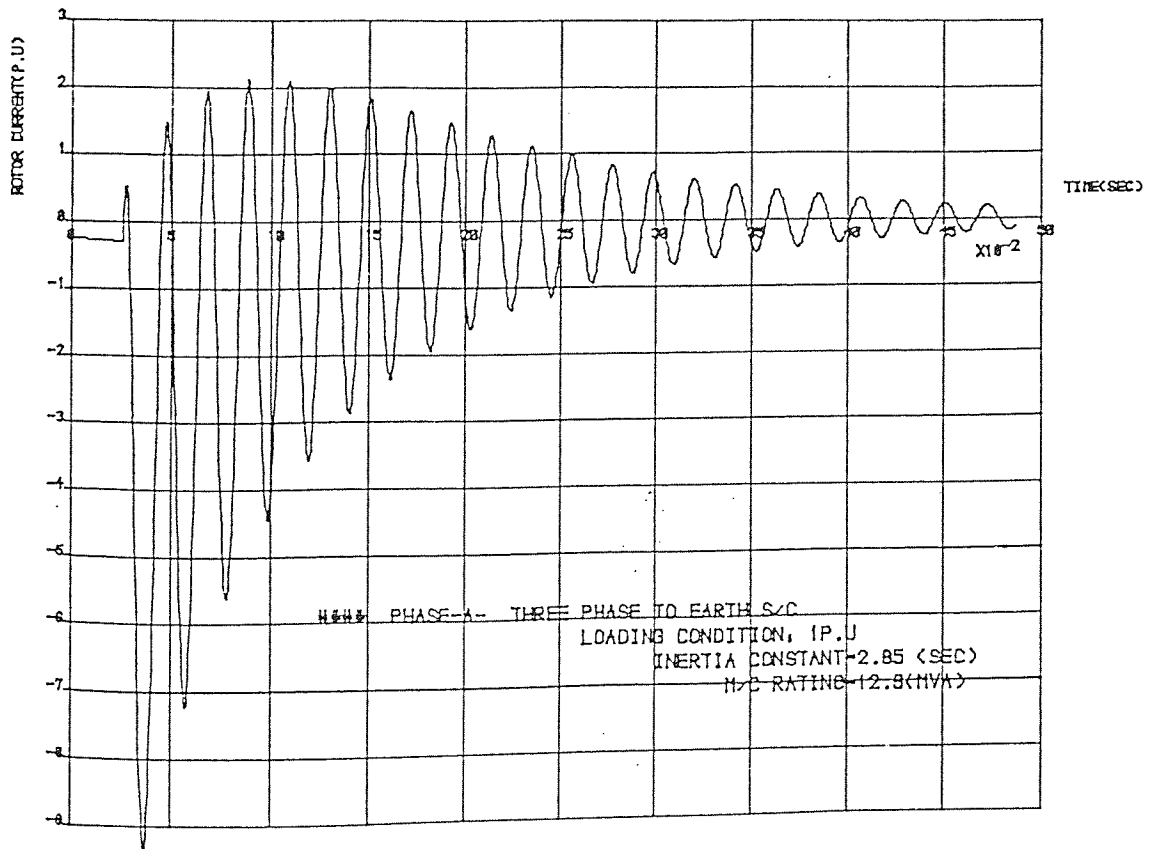


FIG. 3.32

M/C RATING=12.6 (MVA)
 ROTOR VELOCITY(P.U.)
 THREE PHASE TO EARTH S/C
 INERTIA CONSTANT=2.85 (SEC)
 0.81P.U. FRICT.&WIND. LOSSES

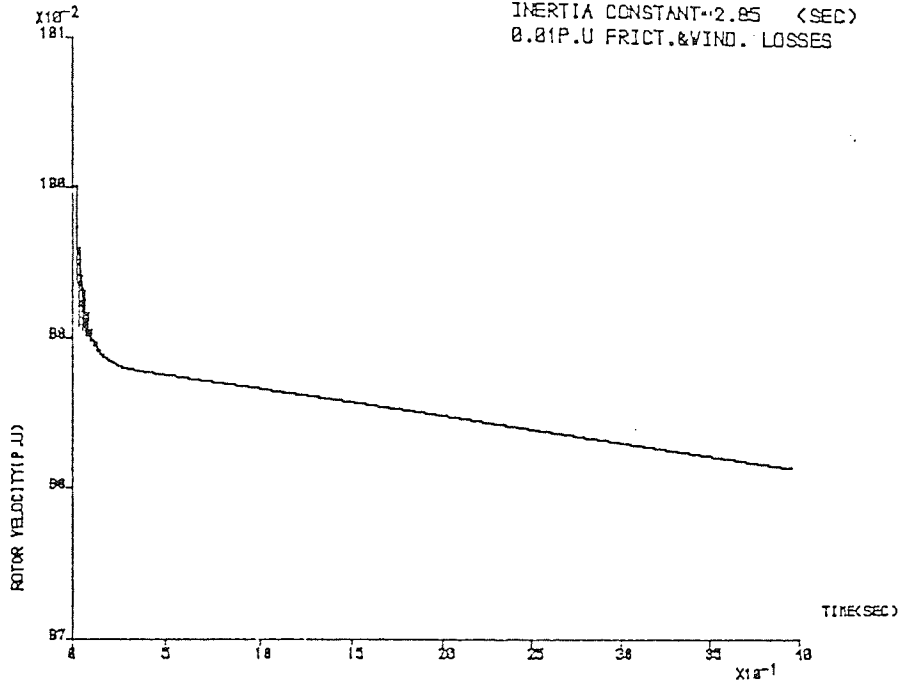


FIG. 3.34

M/C RATING=12.6 (MVA)
 AIR-GAP TORQUE(P.U.)
 THREE PHASE TO EARTH S/C
 INERTIA CONSTANT=2.85 (SEC)
 LOADING CONDITION, 1P.U

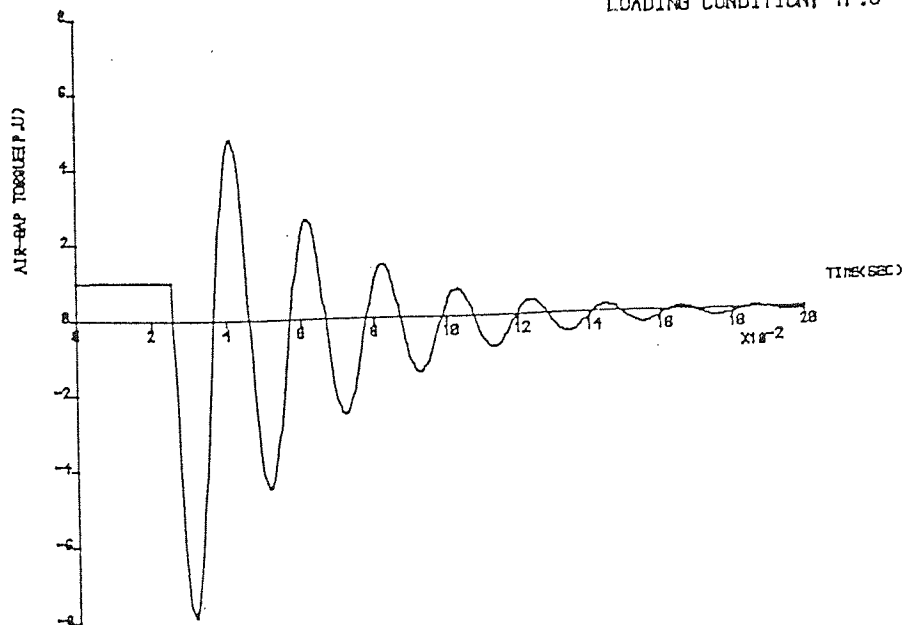
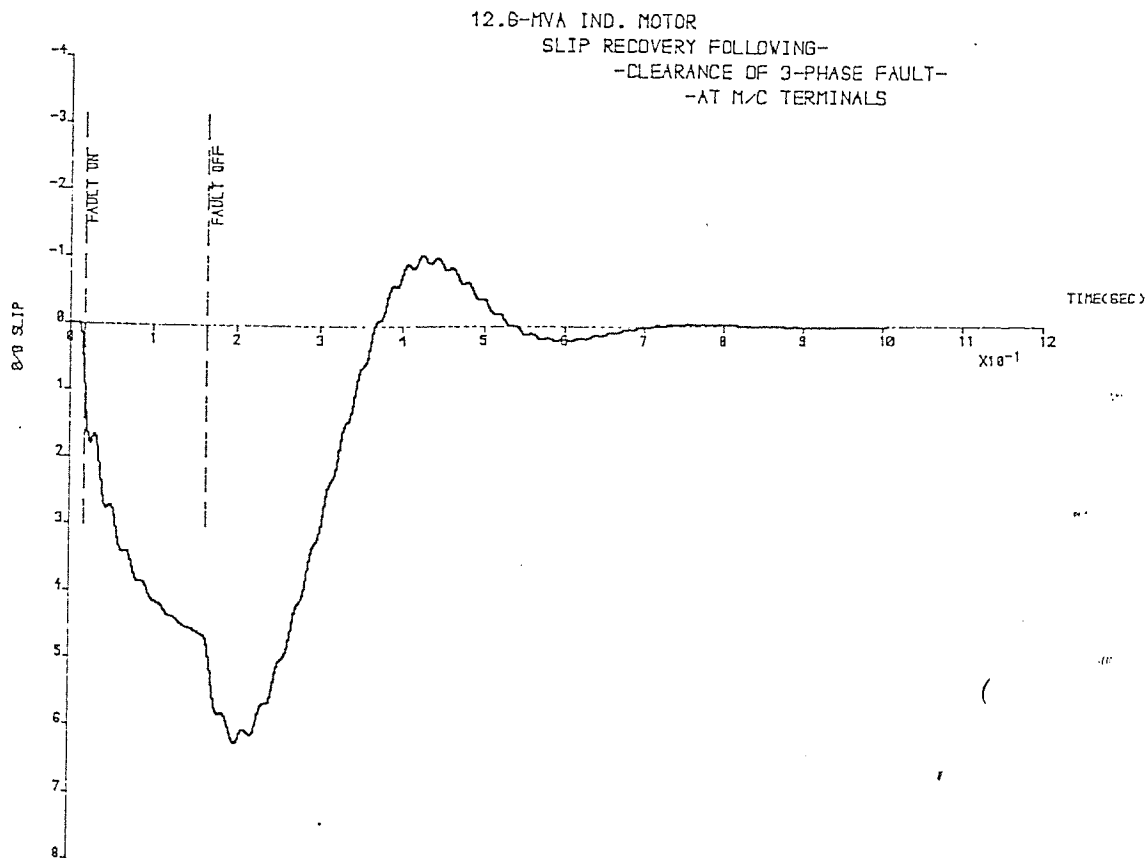
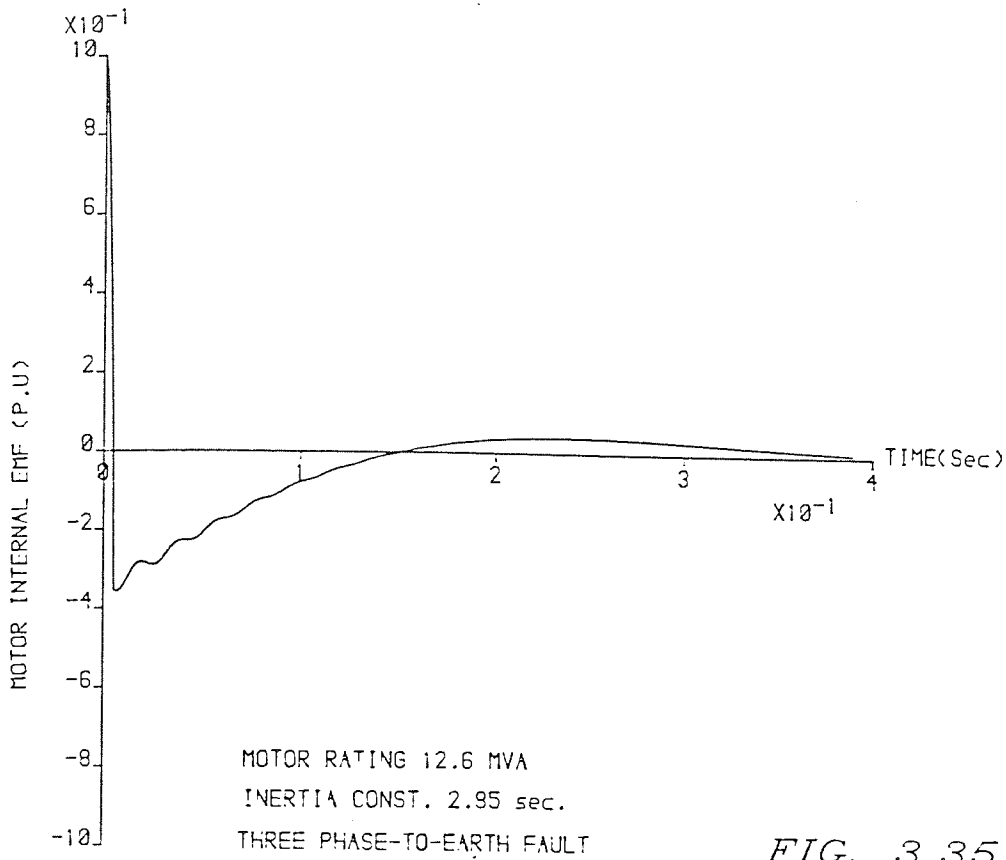
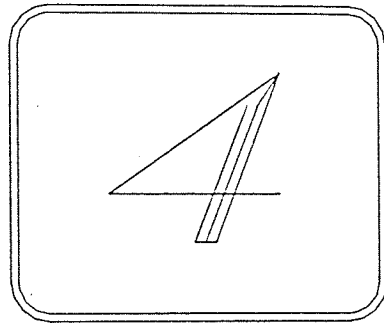


FIG. 3.33



CHAPTER
FOUR



FAULT ANALYSIS OF
INDUCTION MOTORS
FED VIA DELTA/STAR
TRANSFORMERS

CHAPTER IV

FAULT ANALYSIS OF INDUCTION MOTORS FED VIA DELTA/STAR TRANSFORMERS

4.1 Introduction

In industry, large induction motors which drive pumps and fans are most likely to be fed from 3.3 and 11 kv systems. They are usually connected to the distribution systems via delta/star transformers. In such cases, it is of interest to protect both the transformer and the motor from excessive currents that can be produced under abnormal conditions of operation, and thus, fault analysis on both sides of the transformer is essential for the purpose of the protection gear settings. In this chapter, a technique using matrix algebra is developed to analyse symmetric and asymmetric faults on both side of the transformer. The chapter describes the method of analysis together with a numerical solution using a digital computer. The validity of the analysis is confirmed by comparing computed results with those obtained from industry via CEGB.

4.2 Delta/Star Transformers

Fig.(4.1) shows a representation of an ideal transformer. The convention used in the analysis is based on the B.S.S (171). The high voltage windings are designated by capital letters and the low voltage windings by small letters. The connection is of DY1 type (fig. 4.1(a)).

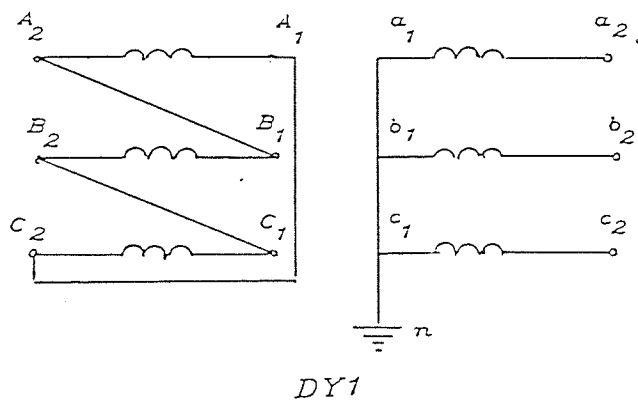


FIG. 4.1(a)

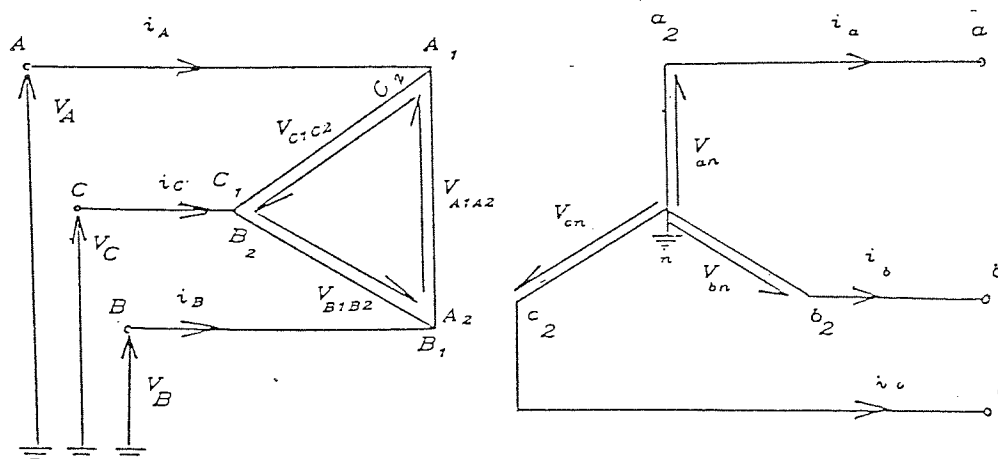


FIG. 4.1(b)

4.2.1 Voltage Analysis

By referring to fig.(4.1(b)) and assuming that the high voltage delta terminals are energised from an infinite bus-bar, then; the induced voltage in the delta windings can be expressed in terms of the infinite bus-bar voltage as :

$$v_{A1A2} = v_A - v_B$$

$$v_{B1B2} = v_B - v_C \quad \} \dots\dots\dots 4.1$$

$$v_{C1C2} = v_C - v_A$$

In a per unit system the base voltage on the star side differs from that at the delta side by a factor of $\sqrt{3}$ i.e the voltage of the star windings of phase 'a' say is given by :

$$v_{an} = (1/\sqrt{3}).v_{A1A2} \quad \dots\dots\dots 4.2$$

Using equations 4.1& 4.2, the voltages at the star secondary terminals in matrix form are,

$$\begin{Bmatrix} v \\ v \\ v \end{Bmatrix}_S = [C] \cdot \begin{Bmatrix} v \\ v \\ v \end{Bmatrix}_D \quad \dots\dots\dots 4.3$$

where [C] is a connection matrix of order 3x3 extracted from combining equations 4.1 & 4.2 i.e.,

$$[C] = \frac{1}{\sqrt{3}} \begin{vmatrix} 1 & -1 & 0 \\ 0 & 1 & -1 \\ -1 & 0 & 1 \end{vmatrix} \quad \dots\dots\dots 4.4$$

The connection matrix inherently includes the transformer phase shift between the delta and star windings. For example; the following analysis shows the angle introduced to the phase voltage under balanced conditions of operation:

$$\begin{aligned} v_a &= \frac{1}{\sqrt{3}} (v_A - v_B) \\ &= \frac{(1/\sqrt{3})V}{m} (\sin \omega t - \sin(\omega t - 2\pi/3)) \\ &= \frac{V}{m} ((\sqrt{3}/2)\sin \omega t + (1/2)\cos \omega t) \\ &= \frac{V}{m} \sin(\omega t + \pi/6) \end{aligned}$$

Thus by comparing phase 'A' voltage (v_A) with (v_a) a phase shift of $\pi/6$ is found to be introduced.

4.2.2 Current Analysis

By using the concept of the ideal transformer, and applying the principle of balancing the ampere-turns in each winding of the transformer, the following relationship in a per unit system can be postulated,

$$i_a = i_{A1A2}$$

$$i_b = i_{B1B2} \quad \} \dots\dots\dots 4.5$$

$$i_c = i_{C1C2}$$

The line current on the delta side can then be found by applying Kirchhoff's current law at each node of the delta windings and taking into the account the $\sqrt{3}$ factor discussed previously. i.e.,

$$i_A = (i_{A1A2} - i_{C1C2}) / \sqrt{3}$$

$$i_B = (i_{B1B2} - i_{A1A2}) / \sqrt{3} \quad \} \dots\dots\dots 4.6$$

$$i_C = (i_{C1C2} - i_{B1B2}) / \sqrt{3}$$

By substituting equation 4.5 in equation 4.6, the following equation in matrix form can be obtained:

$$\begin{matrix} \{i\} \\ D \end{matrix} = [C] \begin{matrix} t \\ \{i\} \\ S \end{matrix} \quad \dots\dots\dots 4.7$$

4.3 Induction Motor Equations

in term of Currents

The induction motor e.m.f relationship derived in chapter III (equation 3.4) is valid when used to predict the induction motor performance with the machine fed directly from infinite bus-bar systems. When the induction motor is to be included in a study of the complete system, modification of equation (3.4) to solve for the current vector, rather than the flux linkage vector, is then necessary. This is because each individual machine in the system has its own flux linkage distribution. As mentioned in chapter 2, the effect of saturations in induction motors is rarely an important to be part of system analysis, then a linear relationship between the machine inductance and flux can be assumed without introducing much error in the analysis. Therefore, and according to this assumption, the flux linkage vector $\{ \lambda \}$ can be substituted for an expression defined in

terms of the machine inductance matrix and the current vector
i.e for equation (3.4), this becomes:

$$\{e\}_m = [r]_m \{i\}_m + \overline{p} [L(\theta)]_2 \{i\}_m \dots\dots\dots 4.8$$

where suffix 'm' stands for motor.

For further simplifications, since the stator and rotor sub-
matrices are independent of rotor position, the inductance
matrix can be considered as a sum of two inductance matrices
thus,

$$[L(\theta)]_2 = \begin{vmatrix} L_{ss} & \emptyset \\ \emptyset & L_{rr} \end{vmatrix} + \begin{vmatrix} \emptyset & L_{sr}(\theta) \\ L_{rs}(\theta) & \emptyset \end{vmatrix} \dots\dots\dots 4.9$$

By substituting equation (4.9) in equation (4.8), the following
equation can be obtained after performing the differentiation,

$$\{e\}_m = [r]_m \{i\}_m + [\Lambda(\theta)]_2 \{i\}_m + [L(\theta)]_2 \overline{p} \{i\}_m \dots\dots\dots 4.10$$

where,

$$[\Lambda(\theta)] = \bar{p} \cdot \begin{vmatrix} \emptyset & L(\theta) \\ L(\theta) & \emptyset \end{vmatrix} \dots\dots\dots 4.11$$

$\begin{matrix} \text{sr } 2 \\ \text{rs } 2 \end{matrix}$

In the numerical solution θ is determined implicitly as a function of time, therefore, the independent variable of the operator ' \bar{p} ' in equation (4.11) is changed from 't' to ' θ ' i.e equation (4.11) becomes,

$$[\Lambda(\theta)] = [G(\theta)] \frac{d\theta}{dt}$$

$$= \omega [G(\theta)] = (1-s)[G(\theta)] \dots\dots 4.12$$

where 's' is the slip and matrix $[G(\theta)]$ is as defined in chapter III.

The final form of equation 4.10 after substituting equation 4.12 is as follow;

$$\{e\}_m = [L(\theta)]_2 \bar{p} \cdot \{i\}_m + [(1-s)[G(\theta)] + [r]]_m \{i\}_m \dots\dots 4.13$$

In analysing equation 4.13, one may realise that, the term $(1-s)[G(\theta)]$ is resistive and of negative sign. This fictitious machine parameter contributes cumulatively to the voltage at the motor terminal.

4.4 Transformation of Parameters
from h.v Delta side to l.v Star
side.

Since the impedances of the h.v delta winding link with both line currents and voltages, then their transformation may be obtained as follows:

if $\{v\}$ is the voltage drop vector associated with an impedance Z

'Z' on the delta side and given by,

$$\begin{matrix} \{v\} \\ Z D \end{matrix} = [Z] \begin{matrix} \{i\} \\ D \end{matrix} \quad \dots\dots 4.14$$

then its equivalent voltage on the secondary side is,

$$\begin{matrix} \{v\} \\ Z S \end{matrix} = [Z] \begin{matrix} \{i\} \\ eq S \end{matrix} \quad \dots\dots 4.15$$

$$= [C] \begin{matrix} \{v\} \\ Z D \end{matrix} = [C][Z] \begin{matrix} \{i\} \\ D \end{matrix} \quad \dots\dots 4.16$$

on substituting the value of $\{i\}_D$ from equation (4.7) in equation (4.16), the following result is obtained,

$$\begin{Bmatrix} v \\ z \\ s \end{Bmatrix} = [C][Z][C]^t \begin{Bmatrix} i \\ s \end{Bmatrix} \quad \dots\dots\dots 4.17$$

By comparing equations (4.15) & (4.17) the equivalent impedance is:

$$[z]_{eq} = [C][z][C]^t \quad \dots\dots\dots 4.18$$

4.5 System Modelling

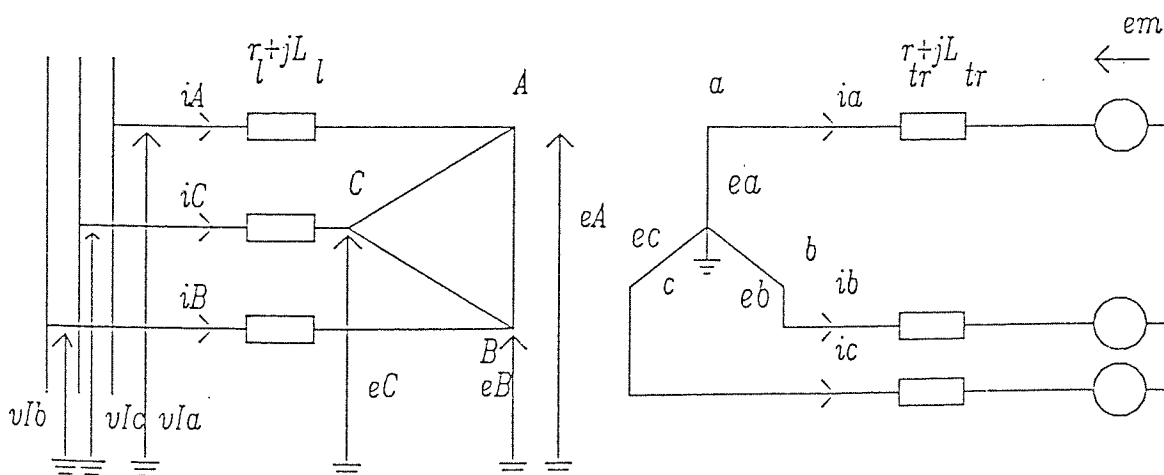


Fig. 4.2

Fig. (4.2) depicts a three phase schematic diagram of an induction motor fed from an infinite bus-bar via a delta/star

transformer. The motor is of the same rating and parameters as that used in the previous chapter. The transformer rating is 32 MVA and has a per-unit inductance and resistance of 0.0998 & 0.000024. The line impedance is $(0.00096 + j0.0026)$ ohms.

The following paragraph deals with the mathematical analysis of the system.

4.5.1 Mathematical Analysis

By following the notation given in fig. (4.2) and noting the definition of matrices in appendix (A1), the following instantaneous relationships can be derived.

On the delta side

$$\{e_{A,B,C}\} = \{v_{Iabc}\} - \left[[r] + [L] \frac{d}{dt} \right] \{i_{A,B,C}\} \quad \dots 4.19$$

where :

$\{e_{A,B,C}\}$ & $\{v_{Iabc}\}$ are the vectors of the node voltages of the

transformer delta connection and the infinite bus-bar voltages respectively.

$[r_l]$ & $[L_l]$ are the line resistance and inductance matrices.

On the star side, in order to relate the variables of the six coupled circuits representing the induction motor to the variables on the secondary side, the latter must be modified by the $[U]$ matrix (defined in appendix (A1)) i.e

$$[U]\{e_{abc}\} = \{e_m\} + [[U][r_{tr}] + [L_{tr}]^p].[U]^t.\{i_{abc}\} \dots 4.20$$

where vector $\{e_m\}$ is the motor induced e.m.f given by

equation(4.13) and $[r_{tr}]$ & $[L_{tr}]$ are the transformer resistance

and inductance matrices of order $[3 \times 3]$

Equations (4.19) & (4.20) are equal provided the former is modified by matrices $[U]$ and $[C]$, thus,

$$N[C]_{rt}\{v_{Iabc}\} = N[C]_{rt}[[r_l] + [L_l]^p].[C]_{rt}^t.\{i_{abc}\}$$

$$= \{e_m\} + [[U][r_{tr}] + [L_{tr}]^p].[U]^t.\{i_{abc}\} \dots 4.21$$

where $[C]_{rt} = [U][C]$ and $N = 1/n$ (n is the transformer tap position).

Finally by substituting equation (3.13) in equation (4.21), rearranging and making use of the fact that,

$$[U]\{i_{abc}\}_{3 \times 1} = \{i_m\}_{3 \times 1} = \{i\} \quad \dots\dots\dots 4.22$$

the following equation of the current derivative vector can be obtained,

$$\bar{p}\{i\} = [A]^{-1} \{[B]\{v_{Iabc}\} - [D]\{i\}\} \quad \dots\dots 4.23$$

where,

$$[A] = [L(\theta)]_2 + N^2 [C]_{rt} [L]_1 [C]_{rt}^t + [U][L]_{tr} [U]^t \dots 4.24$$

$$[B] = N[C]_{rt} \quad \dots 4.25$$

&

$$[D] = [r]_m + (1-s)[G(\theta)]_2 + N^2 [C]_{rt} [r]_1 [C]_{rt}^t + [U][r]_{tr} [U]^t \quad \dots 4.26$$

4.6 Fault Analysis

Faults on both sides of the transformer can be investigated by extending the concept of the fault matrix $[F]$ used in chapter III. The analysis is carried out by using matrix $[F]$ to operate upon those variables of equation (4.23) which are affected by the fault. The sequence of operation of matrix $[F]$ on the matrices $[A]$, $[B]$ & $[D]$ is important, since it was found [22] to be a means of designating the location of the fault .

4.7 Faults on Motor Terminals

Faults on motor terminals can be established by eliminating elements from the current vector $[U]\{i_{abc}\}$ which are not equal to the corresponding elements in the current vector $\{i_m\}$ (equation 4.22). This can be achieved by operation of matrix $[F]$ upon the elements of matrices $[A]$, $[B]$ & $[D]$ in the order shown below.

4.7.1 Symmetrical Faults

$$[A] = [L(\theta)] + [F][N]^2 [C]_{rt} [L]_l [C]_{rt}^t + [U][L]_{tr} [U]_{tr}^t$$

$$[B] = N[F][C]_{rt}$$

$$\& [D] = [r]_m + (1-s)[G(\theta)] + [F][N]^2 [C]_{rt} [r]_l [C]_{rt}^t + [U][r]_{tr} [U]_{tr}^t$$

4.7.2 Asymmetrical Faults

In the case of asymmetrical faults, where the zero sequence currents flow only in the delta circuit, the delta node voltage vector $\{e_{A,B,C}\}$ (equation 4.19) must be up-dated at each step of

the solution by using:

$$\{e_{A,B,C}\} = \{v_{Ia,b,c}\} - [L]_l \{\Delta i_{ABC} / \Delta t\} - [r]_l \{i_{ABC}\} \dots 4.27$$

where, $\{i_{ABC}\}$ can be evaluated using equation (4.7)

The matrices [A], [B] & [D] will then have the following form,

$$[A] = [L(\theta)]_2 + [F][U][L]_{tr}[U]^t$$

$$[B] = N[F][C]_{rt}$$

$$[D] = [r]_m + (1-s)[G(\theta)]_2 + [F][U][r]_{tr}[U]^t$$

and the voltage vector $\{v_{abc}\}$ in equation (4.23) is then re-

placed by the node voltage vector $\{v_{A,B,C}\}$ found by

equation(4.27).

The fault matrix $[F]$ takes different forms according to the type of fault as shown by table 4.1. The steady-state matrix $[F]=[I]$ is introduced to show that the steady state condition is a particular case.

4.8 Fault on h.v Delta Terminals

The secondary voltage following a fault on the primary delta terminals can be found by the appropriate ordering of the multiplication of matrix $[F]$ upon the constituents of matrices $[A]$, $[B]$ & $[D]$. In the following paragraphs, two examples are chosen arbitrarily to demonstrate the application. The effect on

the secondary voltages that result from a fault on the delta terminals is first investigated and then checked using the proper ordering of multiplication of matrix [F].

a) Single phase-to-earth fault (on terminal 'A')

Consider a single phase to earth fault on terminal 'A' (fig.(b) table 4.2) such that a fault brings node 'A' to zero potential. The voltage induced in the delta windings is then given by,

$$v_{AB} = -e_B, \quad v_{BC} = e_B - e_C \quad \& \quad v_{CA} = e_C$$

and the secondary voltage is then,

$$v_a = (-e_B) / \sqrt{3}, \quad v_b = (e_B - e_C) / \sqrt{3} \quad \& \quad v_c = (e_C) / \sqrt{3}$$

From above, the effect of such a fault on the star side of the transformer is an unbalanced induced voltage in the secondary circuit. This condition is found to be satisfied when matrix [F] operates upon the vector of the delta terminal voltages before the action of the transformer connection matrix [C]_{rt}. i.e the

star voltage vector will be given by,

$$\begin{Bmatrix} v \\ abc \end{Bmatrix} = N \begin{bmatrix} C \\ rt \end{bmatrix} [F] \begin{Bmatrix} e \\ A,B,C \end{Bmatrix} \dots\dots\dots 4.28$$

and hence matrix [B] can be found from,

$$[B] = N \begin{bmatrix} C \\ rt \end{bmatrix} [F]$$

b) line-to-line short circuit (phase B & C)

In this type of fault (fig.(d) table 4.2), the voltage of nodes B & C are equal which results in zero potential induced in limb BC i.e

$$e_B = e_C \dots\dots\dots 4.29$$

also since

$$e_A + e_B + e_C = 0 \dots\dots\dots 4.30$$

thus, by combining equations (4.29) & (4.30), the following results can be obtained:

$$e_C = e_B = -(1/2)e_A$$

and

$$v_{AB} = (3/2)e_A, \quad v_{BC} = 0 \quad \& \quad v_{CA} = -(3/2)e_A$$

and finally the star unbalanced voltage is

$$v_a = (\sqrt{3}/2)e_A, \quad v_b = 0 \quad \& \quad v_c = -(\sqrt{3}/2)e_A$$

The above condition is satisfied by the same order of multiplication of fault matrix [F] as in the case of a single phase-to-earth fault.

The principle is applicable to all types of fault. Table 4.2 shows the elements of matrices [F] & [B], circuit diagrams and the voltage phasor diagram of the secondary star side for different types of fault.

4.9 Open-Circuit Faults

Open-circuit faults on the secondary side are analysed by eliminating rows and columns from matrix [A] corresponding to the faulty lines. Since the star point of the motor is isolated, only single line open-circuit faults will be of interest.

Single line open-circuit faults on phase 'A' say, on the high voltage delta side lead to an unbalanced voltage on the secondary side (fig.(f) table 4.2). Analysis can be performed by applying the constraint,

$$v_{CA} = v_{AB}$$

which results in a node 'A' potential of

$$e_A = (e_B + e_C)/2$$

The voltage induced in the delta winding is then given by:

$$v_{AB} = - (e_B - e_C)/2 = - v_{BC} / 2$$

$$v_{BC} = e_B - e_C \quad \} \dots\dots 4.31$$

$$v_{CA} = - (e_C - e_B)/2 = - v_{BC} / 2$$

equations 4.31 can be satisfied by following the same order of multiplication of matrix [F] as given by equation 4.28.

4.10 Numerical Solution.

The algorithm used to perform the numerical solution was based on the 4th order Runge-Kutta routine as modified by Gill. A step length of 0.1 milliseconds has found necessary to retain the stability of the solution without divergance. Computation was initiated by using values obtained from steady-state analysis.

The location and the type of fault are identified by two variables in the program ('K' stands for the location of the fault and 'M' for the type of the fault) as follow,

- K = 1 represents a fault at the machine terminals
- = 2 represents a fault on the h.v delta terminals.

The values of 'M' from 1 to 6 in a consecutive order stand for steady-state, single phase-to-earth fault, double line-to-ground fault, line-to-line short circuit, three phase-to-earth fault and finally single phase open-circuit fault.

The following points in conjunction with the flow chart of fig.(3.4) describe the steps of the solution.

- 1- Read system data, initial condition, step length and maximum time.
- 2- Check the operation condition for fault, build matrix [F] accordingly.
- 3- Up-date the time and the voltage vector.
- 4- Build-up matrices [A], [B] & [D] according to the fault location.
- 5- Solve for the current vector derivative $\bar{p}\{i\}$ and hence up-date the current vector $\{i\}$.
- 6- Up-date rotor speed and position.

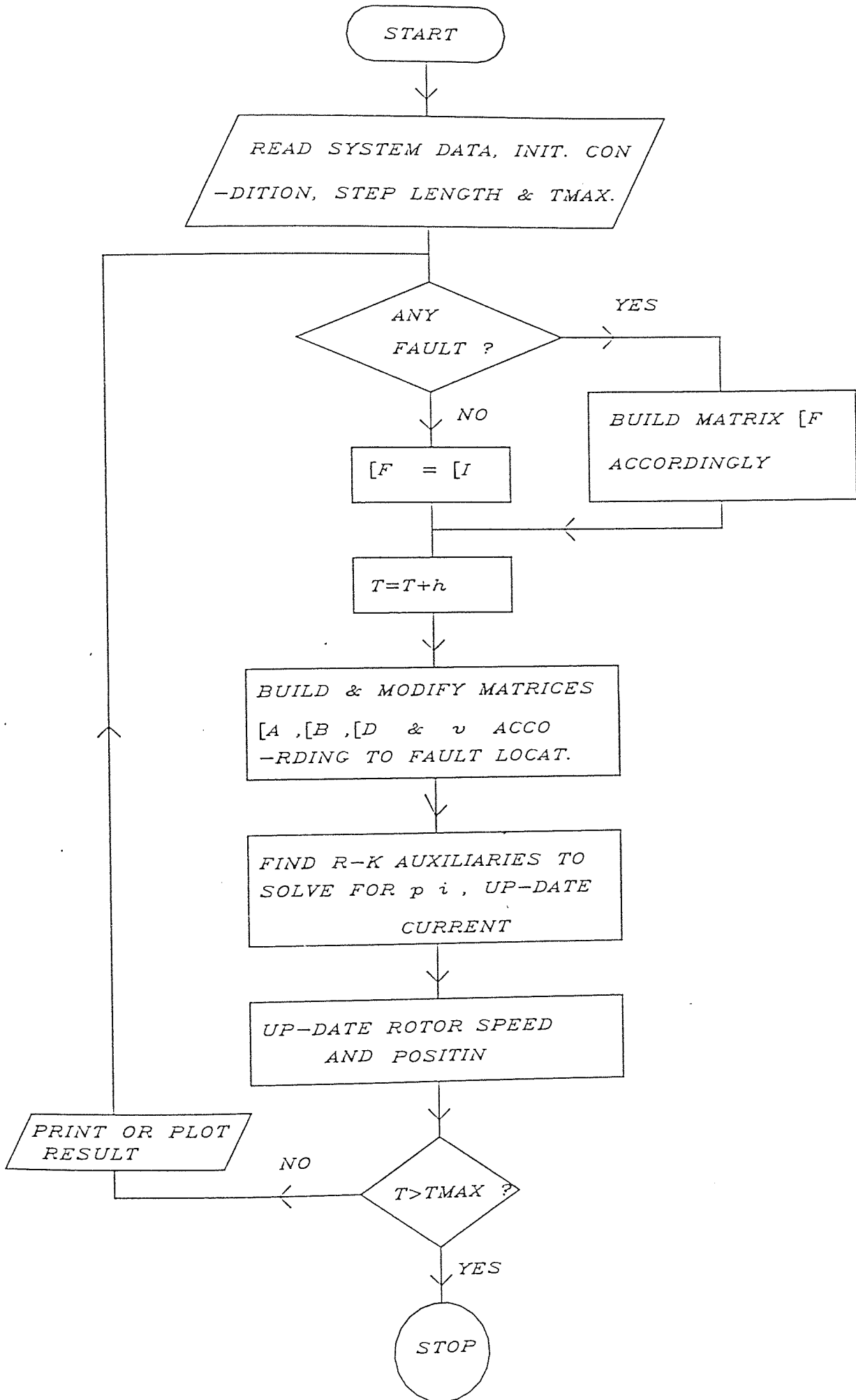


FIG. 4.3

Steps 2 to 6 are repeated until the time chosen to terminate the study has been reached.

4.11 Analysis of the Results

Figs.(4.4& 4.5) show the phase 'a' current wave form obtained with a solid three phase-to-earth fault on the machine terminals and the high voltage delta terminals respectively. Both currents are composed of the power frequency wave form superimposed on a 'd.c' component. The effect of introducing the transformer is to reduce the first current peak by approximately 13.3% with a delay in the first current zero. This is expected since inclusion of the transformer parameters in the motor circuit will result in an increase of the circuit impedance and in a longer overall time constant ($r \ll L$).

$\tau_r \quad \tau_r$

(a case of single phase-to-earth fault) a reduction of 14.3% in the first current peak with a delay of 3.07 msec. in the first current zero can be seen. Similarly, for a double phase-to-earth fault, a reduction of 15% and a delay of 2.03 msec. can be observed for phase 'b' (figs.(4.8)& (4.9)) and 17.7% & 1.54 msec. for phase 'c' (figs. (4.10)& (4.11)). In the case of a line-to-line short circuit (figs. (4.12)& (4.13)) a reduction of 16.67% in the first peak without any significant delay in the

first current zero can be observed. The validity of the results above have been checked by comparing similar results with those obtained by the (C.E.G.B) using other models such as a 'd,q'0' model. Figs. (4.14& 4.15) show the fault current in phases 'b&c' with phase 'a' open circuited at the machine terminals. In this case the two healthy phases are overloaded, and the current in each phase reaches a peak value of 4 p.u in approximately 28 milliseconds after the fault occurrence.

4.12 Conclusions.

In systems where large induction motors are fed from an infinite bus-bar via a delta/star transformer, a single phase-to-earth fault, line-to-line short circuit, double line to ground fault and single line open circuit fault on the h.v delta terminals result in the motor being driven from an unbalanced voltage on the secondary of the transformer, thus asymmetrical currents will flow into the point of fault. The consequence of a three phase-to-earth fault on the machine terminals results in a loss of supply, hence the energy stored in the machine air-gap is dissipated in the form of large currents to the point of fault. The interaction between the induction motor and the transformer can be seen if a similar fault occurs on the h.v delta terminals which results in a low voltage at the motor terminals (<10%). This voltage, which is influenced by the time constant of the

circuit, is induced in the transformer windings by the fault currents.

By using the matrix technique described in this chapter, analysis of all fault conditions can be carried out by simple changes in command structure. The validity of the method used is checked by summing the three phase currents at any instant in the circuit. For asymmetrical faults, as expected, the currents sum to zero on the high voltage delta side due to suppression of the zero sequence component in the delta connection, while they do not sum to zero on the star side of the transformer.

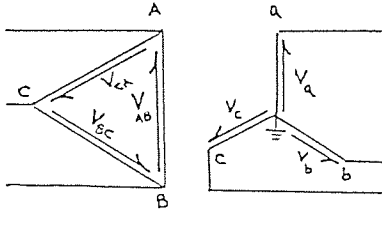
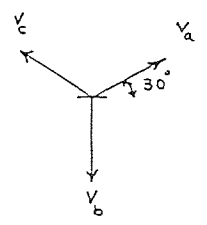
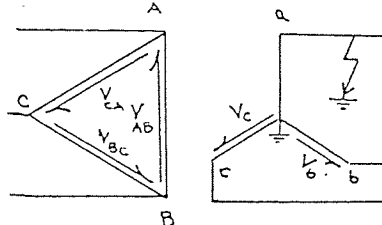

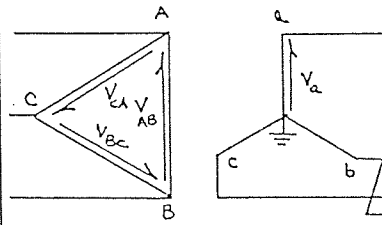
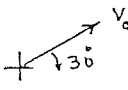
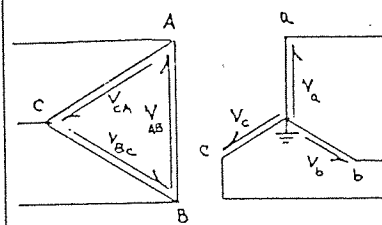
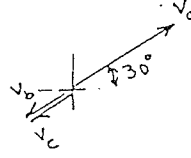
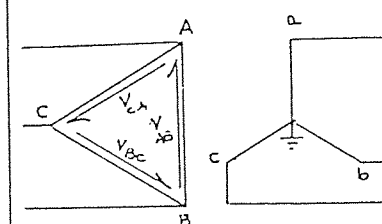
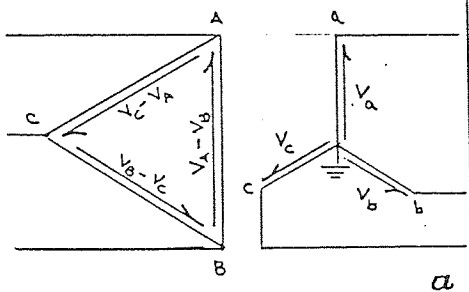
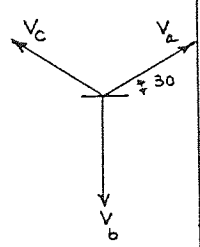
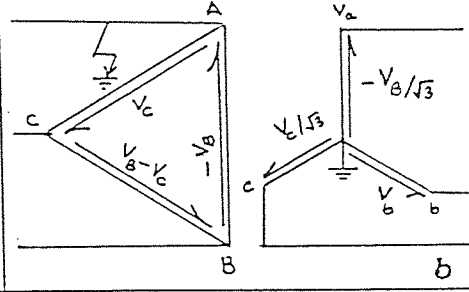
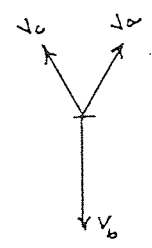
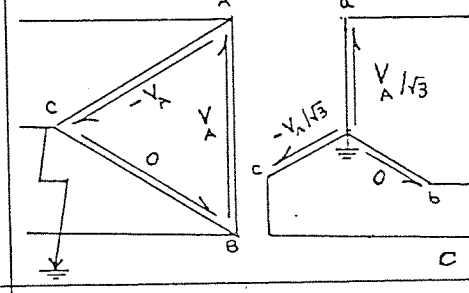
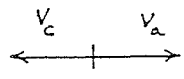
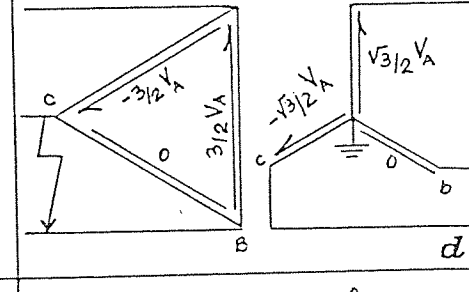
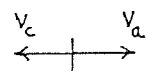
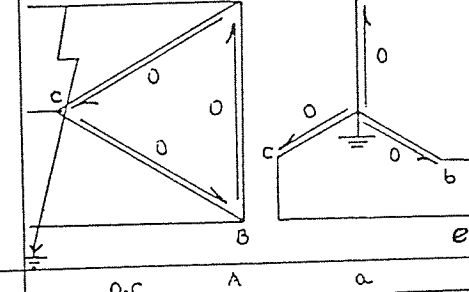

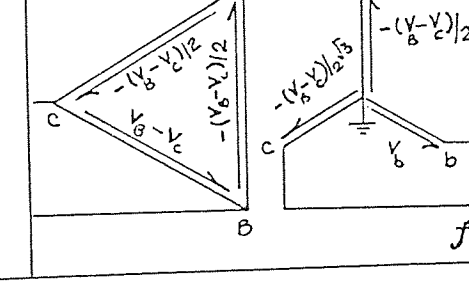
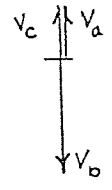
condition of operation	matrix [F]	Circuit diagram	Vector diagram (secondary side)
Steady state	$\begin{bmatrix} 1 & 0 & 0 \\ 0 & 1 & 0 \\ 0 & 0 & 1 \end{bmatrix}$		
Single phase-to-earth fault on phase (a)	$\begin{bmatrix} 0 & 0 & 0 \\ 0 & 1 & 0 \\ 0 & 0 & 1 \end{bmatrix}$		
Double phase to earth fault on phases (b) & (c)	$\begin{bmatrix} 1 & 0 & 0 \\ 0 & 0 & 0 \\ 0 & 0 & 0 \end{bmatrix}$		
Line to line circuit on phases (b) & (c)	$\begin{bmatrix} 1 & 0 & 0 \\ -0.5 & 0 & 0 \\ -0.5 & 0 & 0 \end{bmatrix}$		
Solid three phase to earth fault	$\begin{bmatrix} 0 & 0 & 0 \\ 0 & 0 & 0 \\ 0 & 0 & 0 \end{bmatrix}$		

Table (4.1)

condition of operation	matrix [B] x k *	matrix [F]	Circuit diagram	Vector diagram (secondary side)
steady state	$\begin{vmatrix} 1 & -1 & 0 \\ 0 & 1 & -1 \\ -1 & 0 & 1 \end{vmatrix}$	$\begin{vmatrix} 1 & 0 & 0 \\ 0 & 1 & 0 \\ 0 & 0 & 1 \end{vmatrix}$		
single phase to earth fault on terminal A	$\begin{vmatrix} 0 & -1 & 0 \\ 0 & 1 & -1 \\ 0 & 0 & 1 \end{vmatrix}$	$\begin{vmatrix} 0 & 0 & 0 \\ 0 & 1 & 0 \\ 0 & 0 & 1 \end{vmatrix}$		
double phase to earth fault on terminals B & C	$\begin{vmatrix} 1 & 0 & 0 \\ 0 & 0 & 0 \\ -1 & 0 & 0 \end{vmatrix}$	$\begin{vmatrix} 1 & 0 & 0 \\ 0 & 0 & 0 \\ 0 & 0 & 0 \end{vmatrix}$		
line to line short circuit on B & C	$\begin{vmatrix} 3/2 & 0 & 0 \\ 0 & 0 & 0 \\ -3/2 & 0 & 0 \end{vmatrix}$	$\begin{vmatrix} 1 & 0 & 0 \\ -0.5 & 0 & 0 \\ -0.5 & 0 & 0 \end{vmatrix}$		
solid three phase to earth fault	$\begin{vmatrix} 0 & 0 & 0 \\ 0 & 0 & 0 \\ 0 & 0 & 0 \end{vmatrix}$	$\begin{vmatrix} 0 & 0 & 0 \\ 0 & 0 & 0 \\ 0 & 0 & 0 \end{vmatrix}$		
Open circuit Fault on phase A	$\begin{vmatrix} 0 & -0.5 & 0.5 \\ 0 & 1 & -1 \\ 0 & -0.5 & 0.5 \end{vmatrix}$	$\begin{vmatrix} 0.5 & 0.5 \\ 0 & 1 & 0 \\ 0 & 0 & 1 \end{vmatrix}$		

*k = N/√3
N = Tap position

Table (4.2)

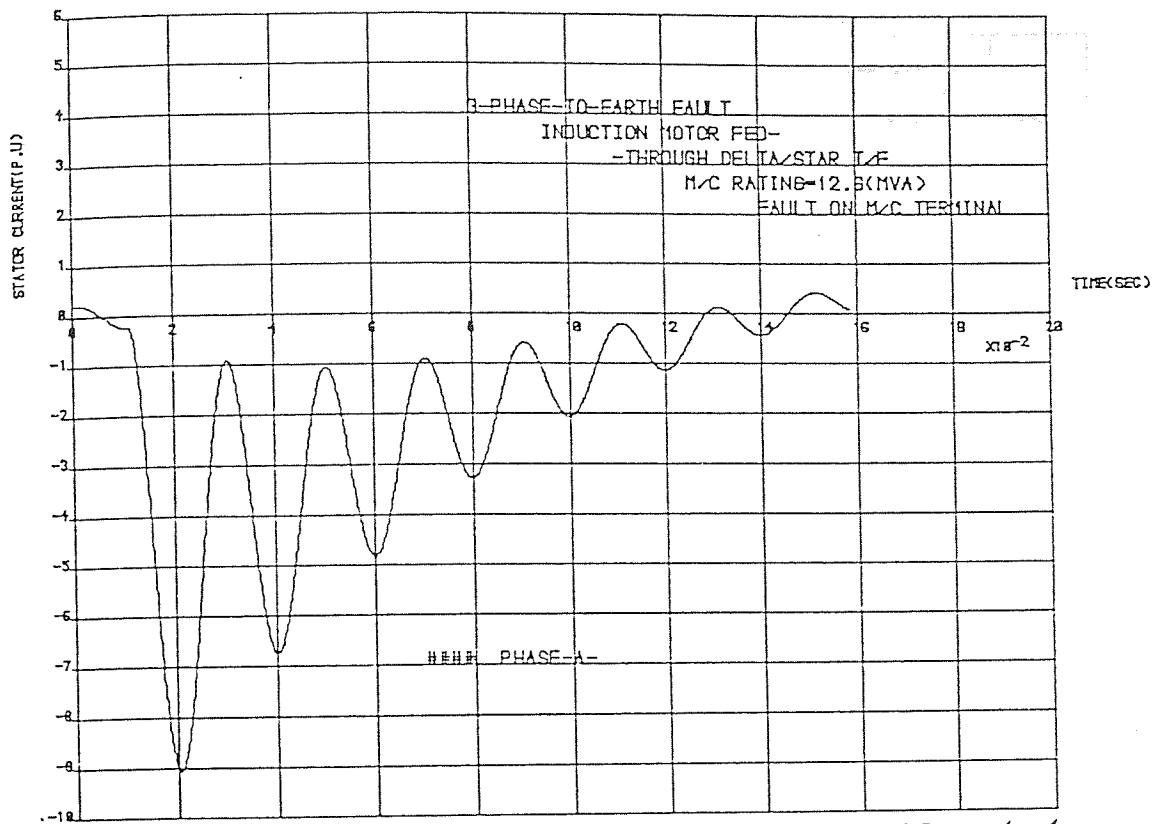


FIG. 4.4

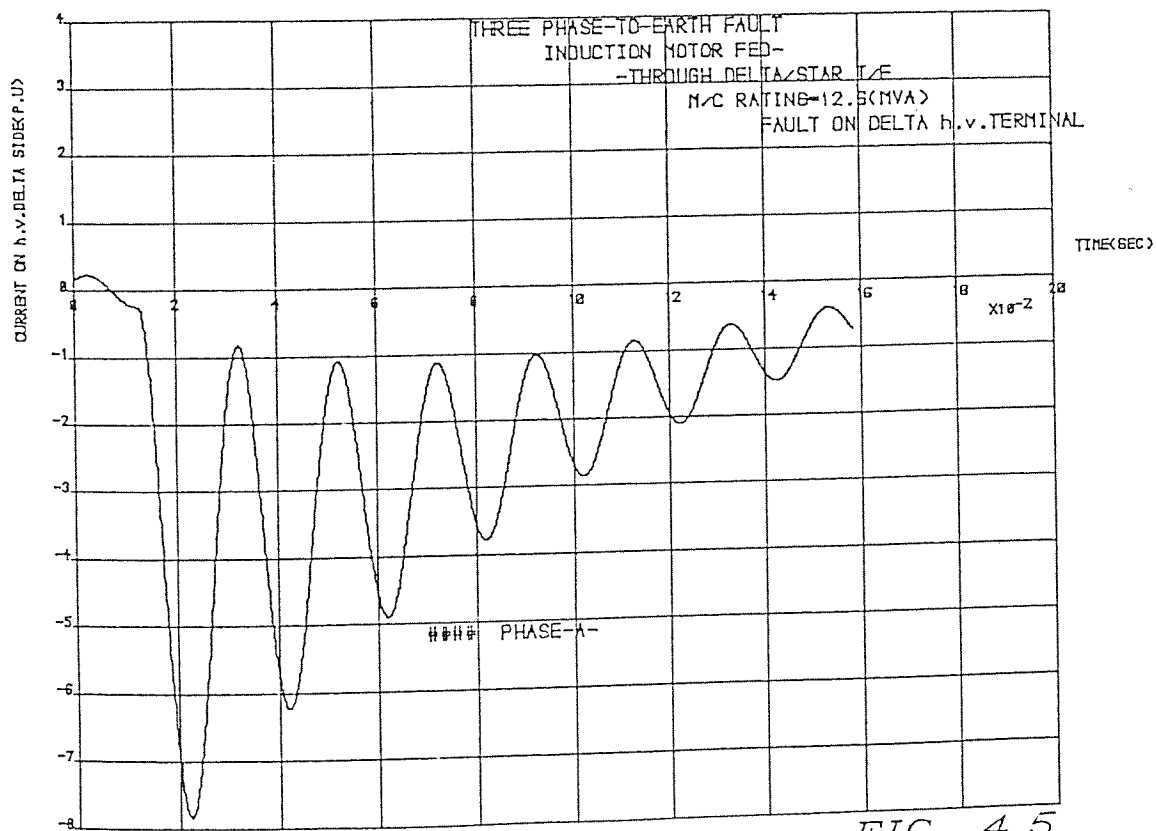


FIG. 4.5

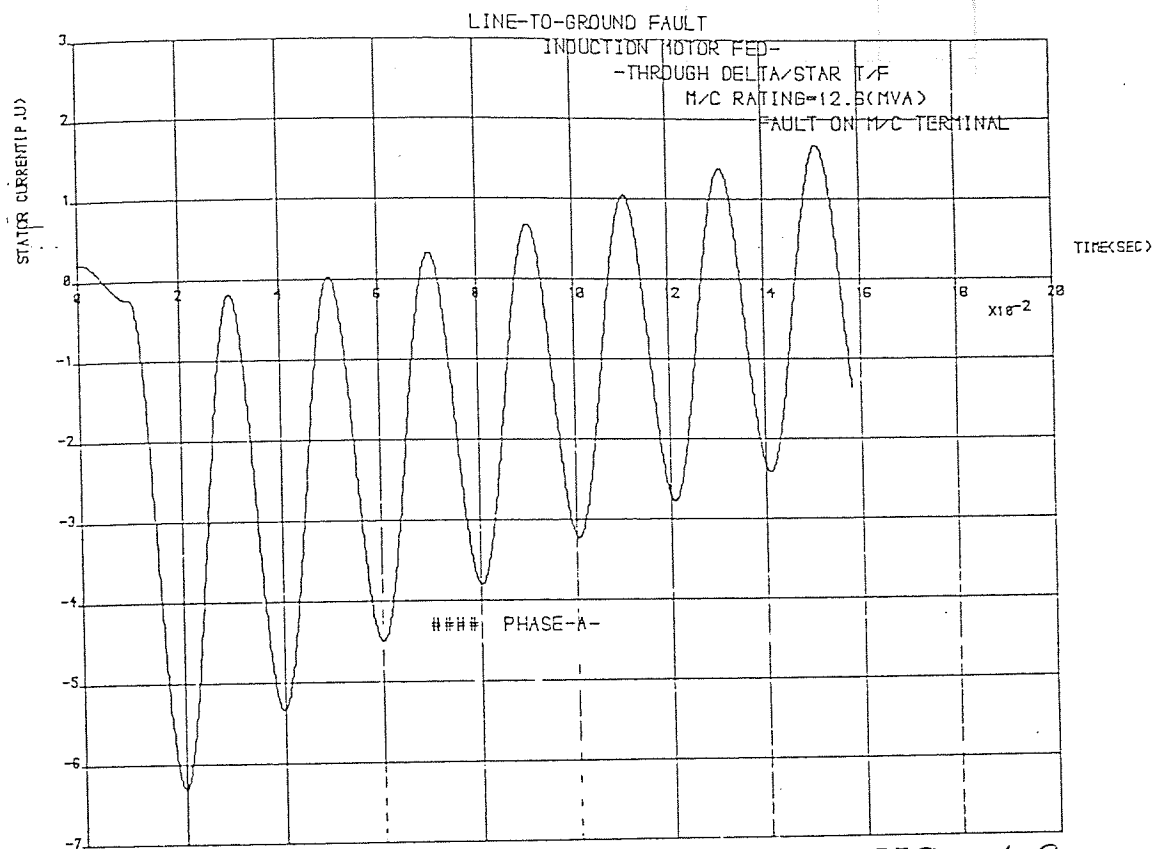


FIG. 4.6

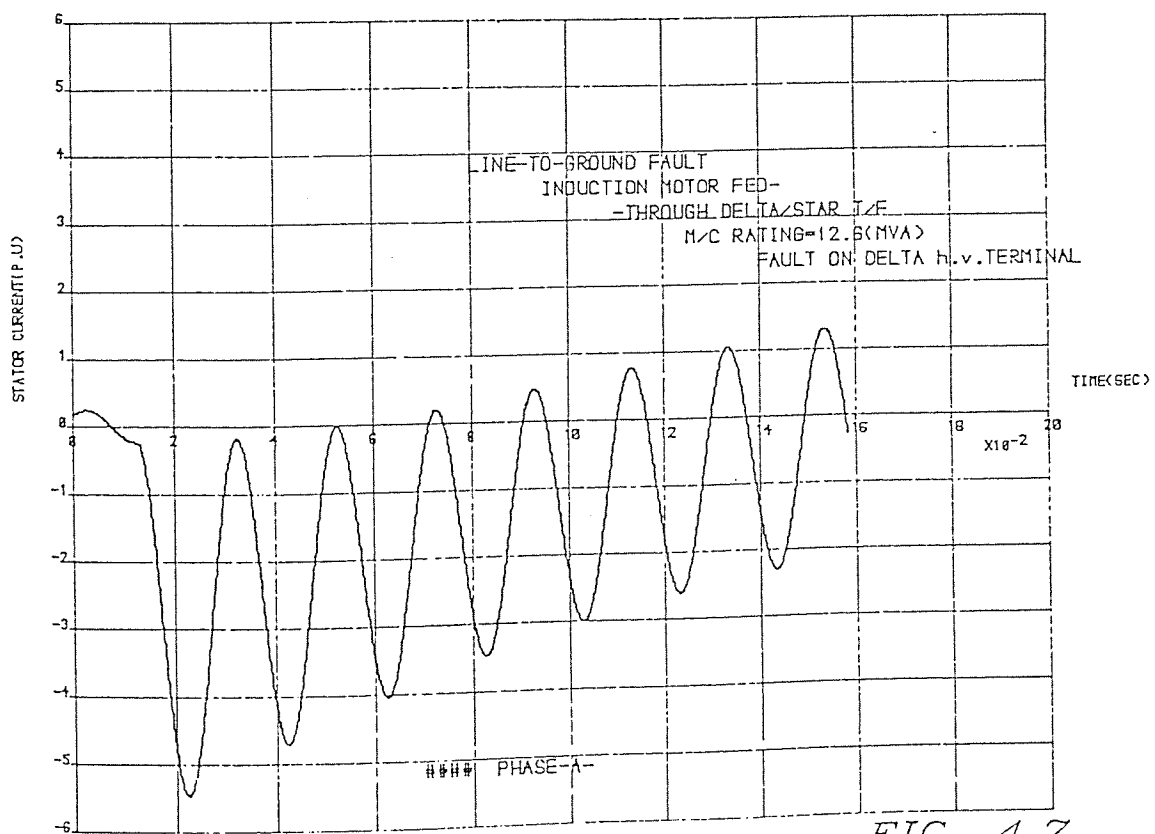


FIG. 4.7

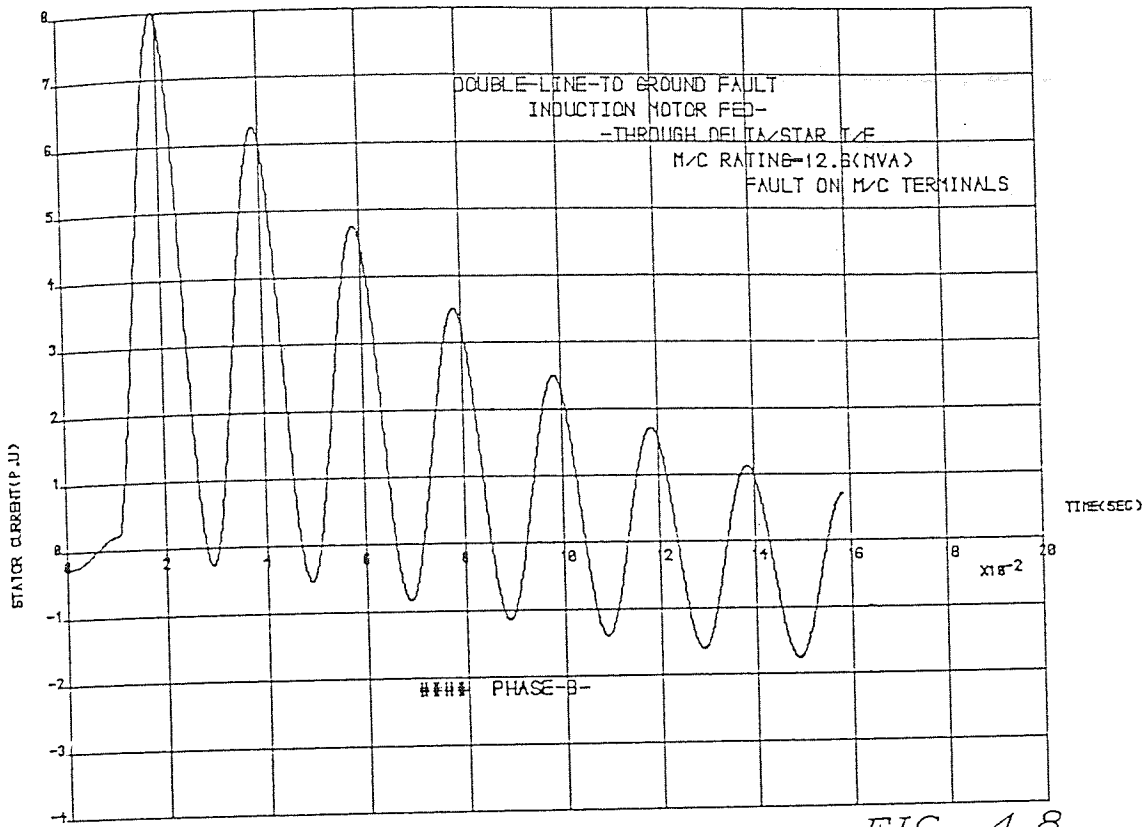


FIG. 4.8

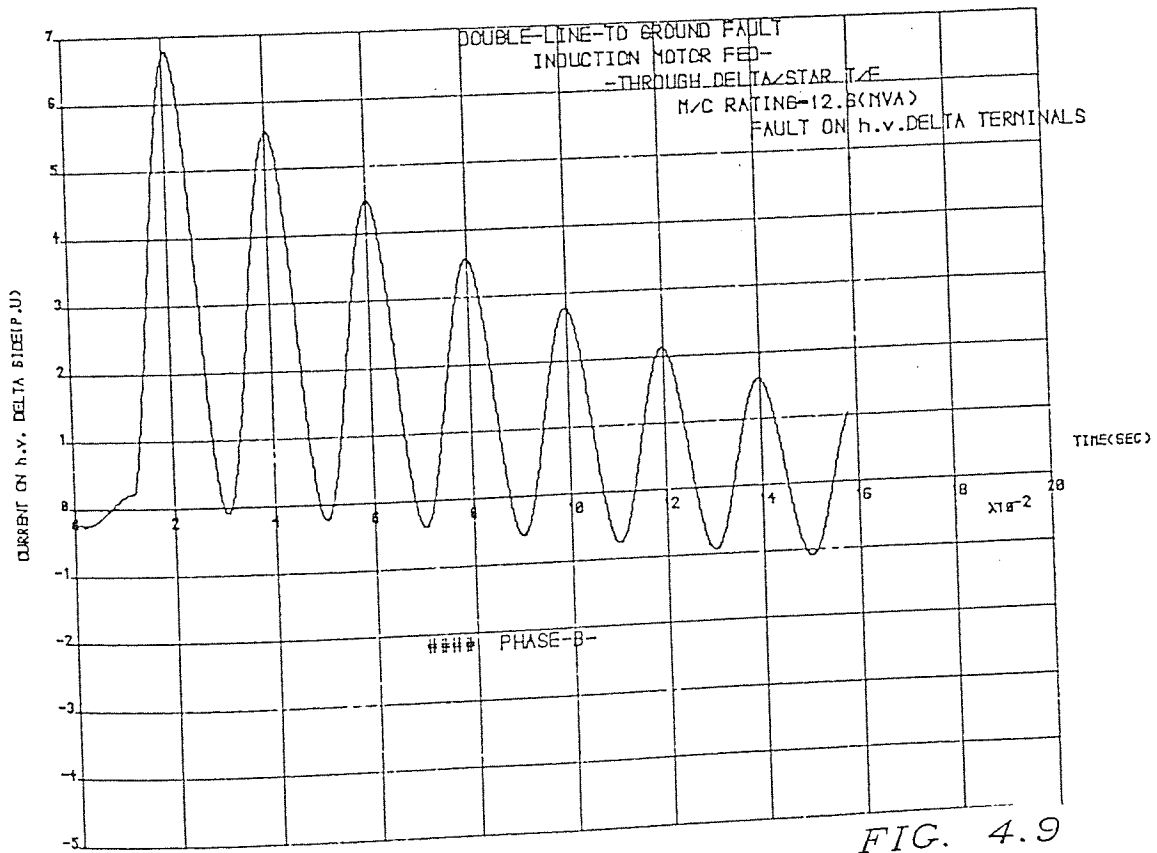


FIG. 4.9

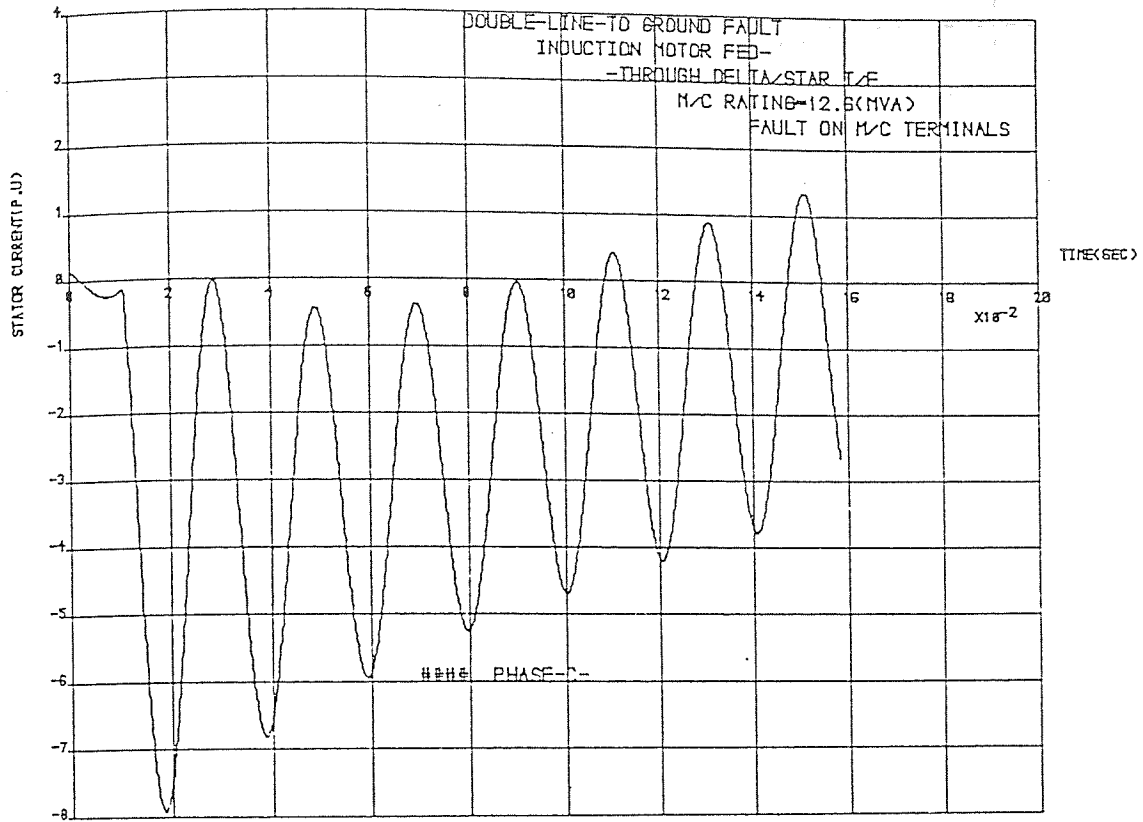


FIG. 4.10

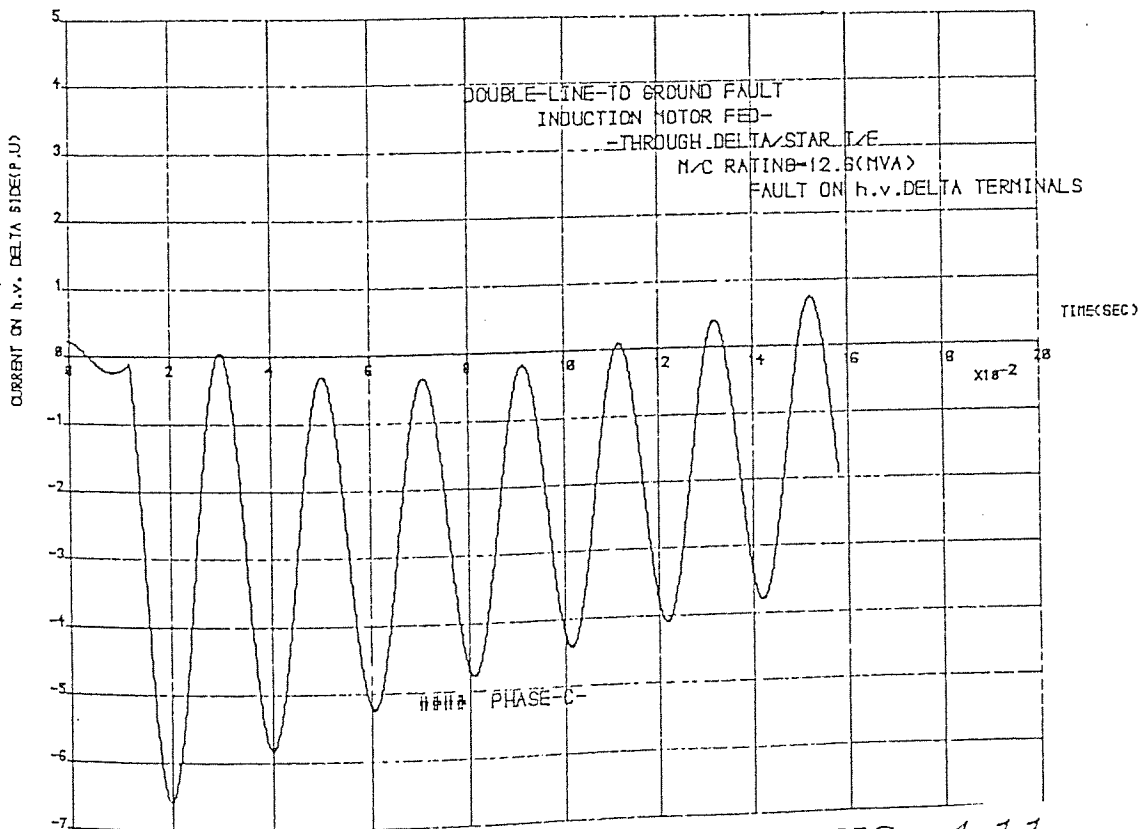


FIG. 4.11

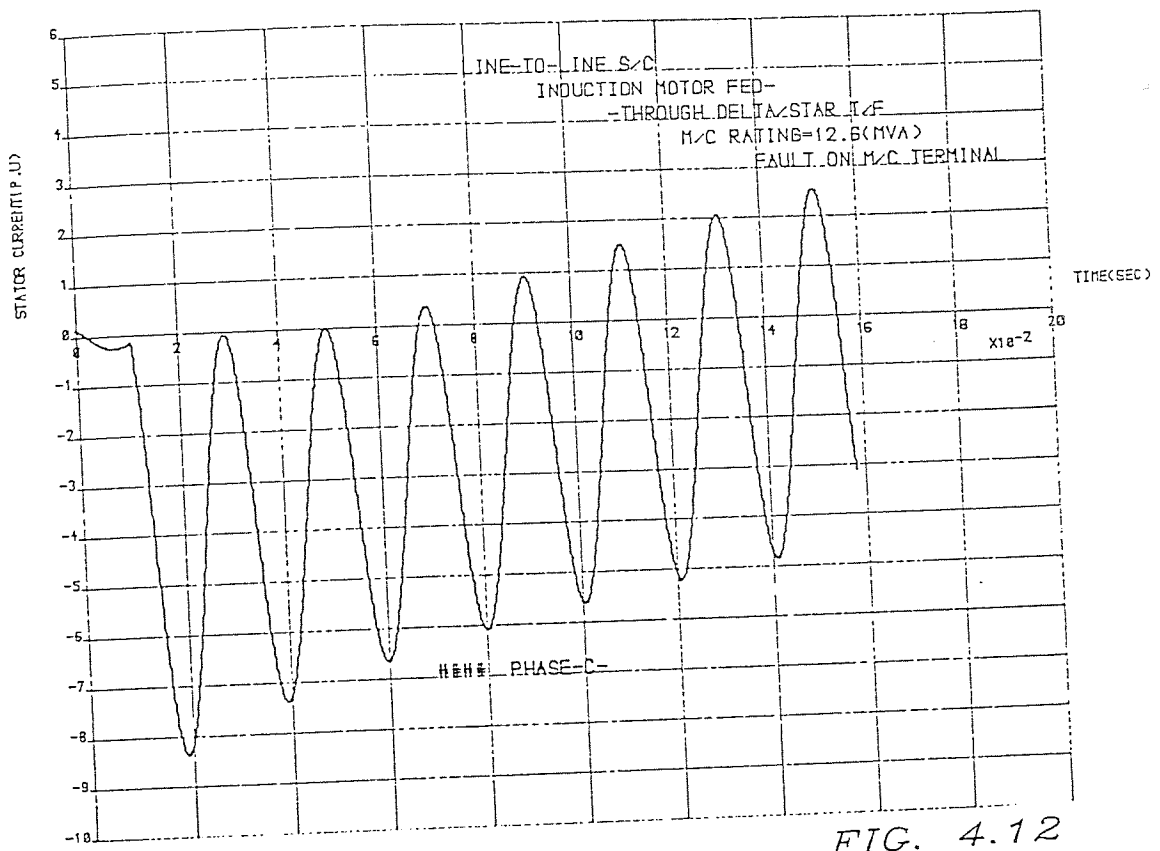


FIG. 4.12

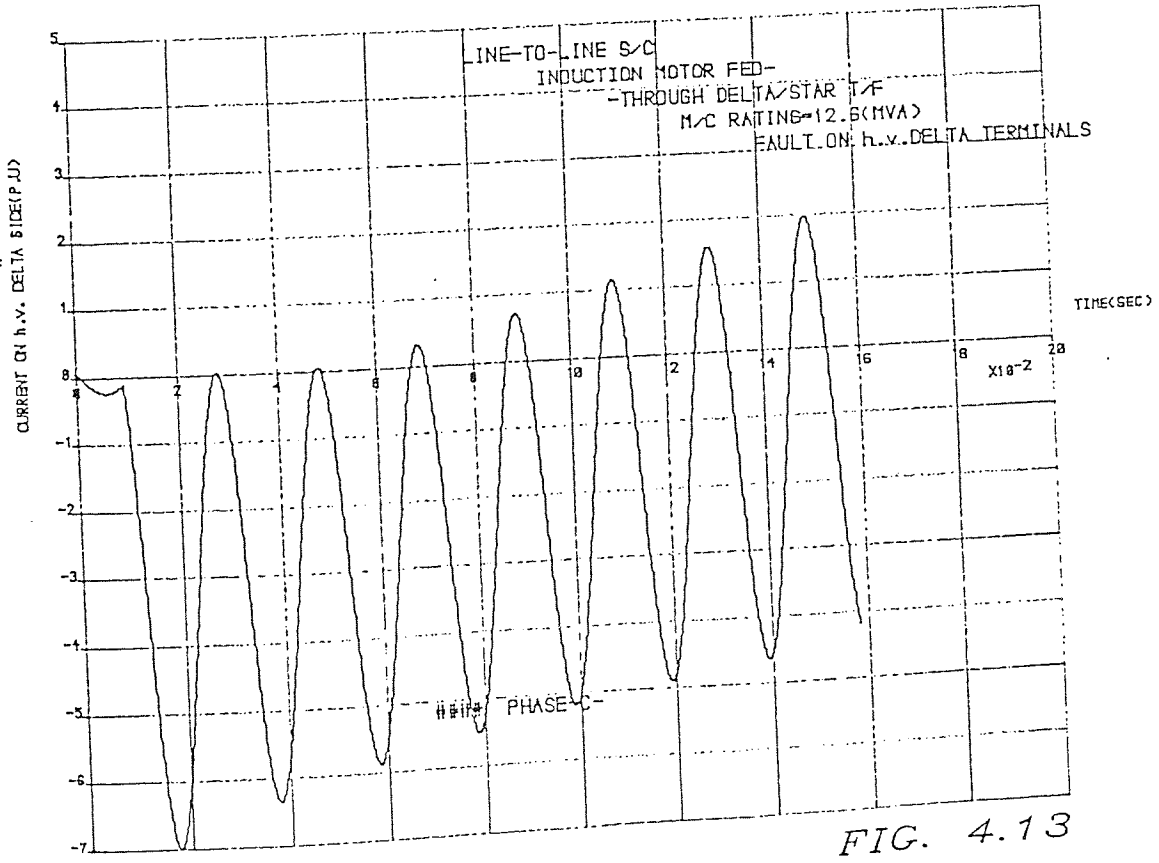


FIG. 4.13

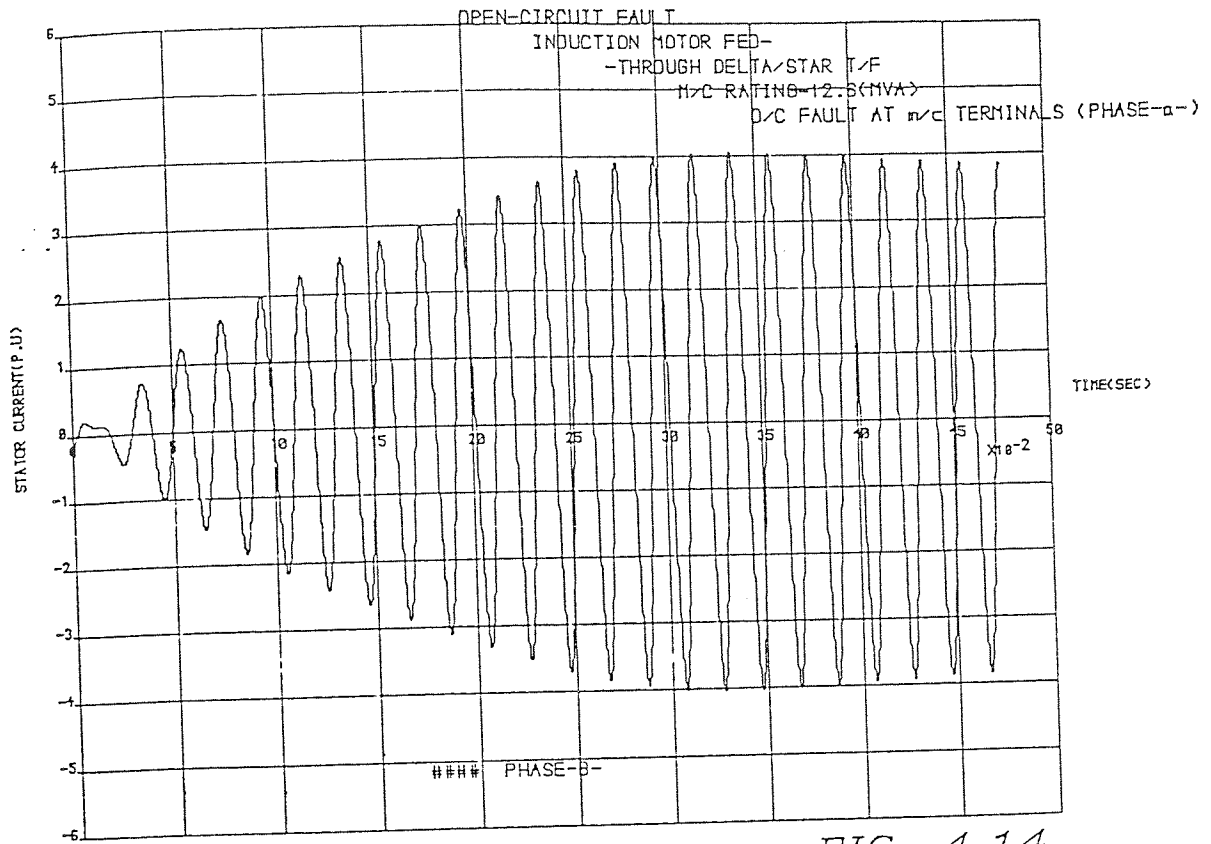


FIG. 4.14

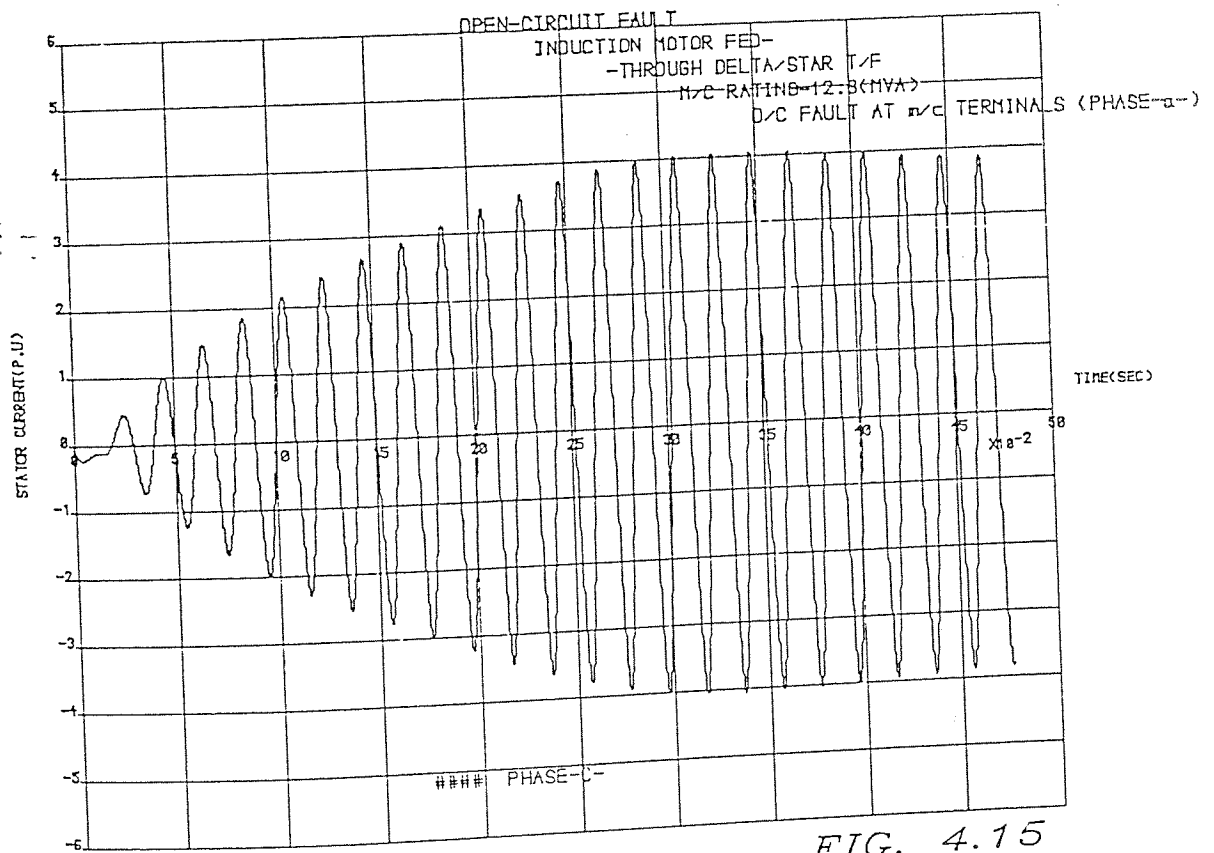
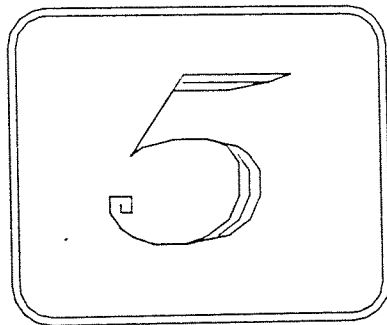


FIG. 4.15

CHAPTER
FIVE



TRANSIENT
STABILITY STUDIES

CHAPTER V
TRANSIENT STABILITY STUDIES

5.1 Introduction

The problems introduced by large induction motors and their effect on the contribution to the system fault current has been considered in the last two chapters. The installation of large numbers of induction motors which are needed by modern industries, and with systems operating fairly close to their power limits, make the inclusion of this type of load necessary for steady-state and transient stability studies. The necessity arises from the fact that such studies form the basis of system design and operation. While previous research work, has represented this type of load, in stability studies, either by motor inertia together with a constant voltage behind a transient reactance [49], or by using a set of equations with a 'd,q' frame of reference, similar to that used for synchronous machines [23]. No complete method based upon the induction motor dynamic behaviour has been considered.

The stability problem is a dynamic problem and requires more elaborate plant component models than those described above. This is especially true when part of the system, under analysis

is heavily loaded with induction motors and thus, their effects cannot be ignored. In this chapter, a mathematical model for the system shown by fig.(5.1) has been developed based upon dynamic phase co-ordinate theory. Transient stability studies were carried out for different types of system fault disturbance at different locations within the system.

5.2 System Description

The system of fig.(5.1) has been adopted in this study for its similarity to those being developed in the industry of electricity generation. Eight induction motors are connected to bus-bar (B1) but only four are shown because each pair of motors perform identical functions. Two machines can therefore be treated as one large machine. They are designated by the following abbreviations according to function,

CWP	cooling water pump
BFP	boiler fan pump
PAF	primary air fan
IDF	induced draft fan

The generator is of 776 MVA rating 23.5 Kv and is connected to the system through the bus-bar (B2). The two three phase transformers are of DY1 connexion and they are connected back to

infinite
bus-bar

bus-bar
(B2)

bus-bar
(B1)

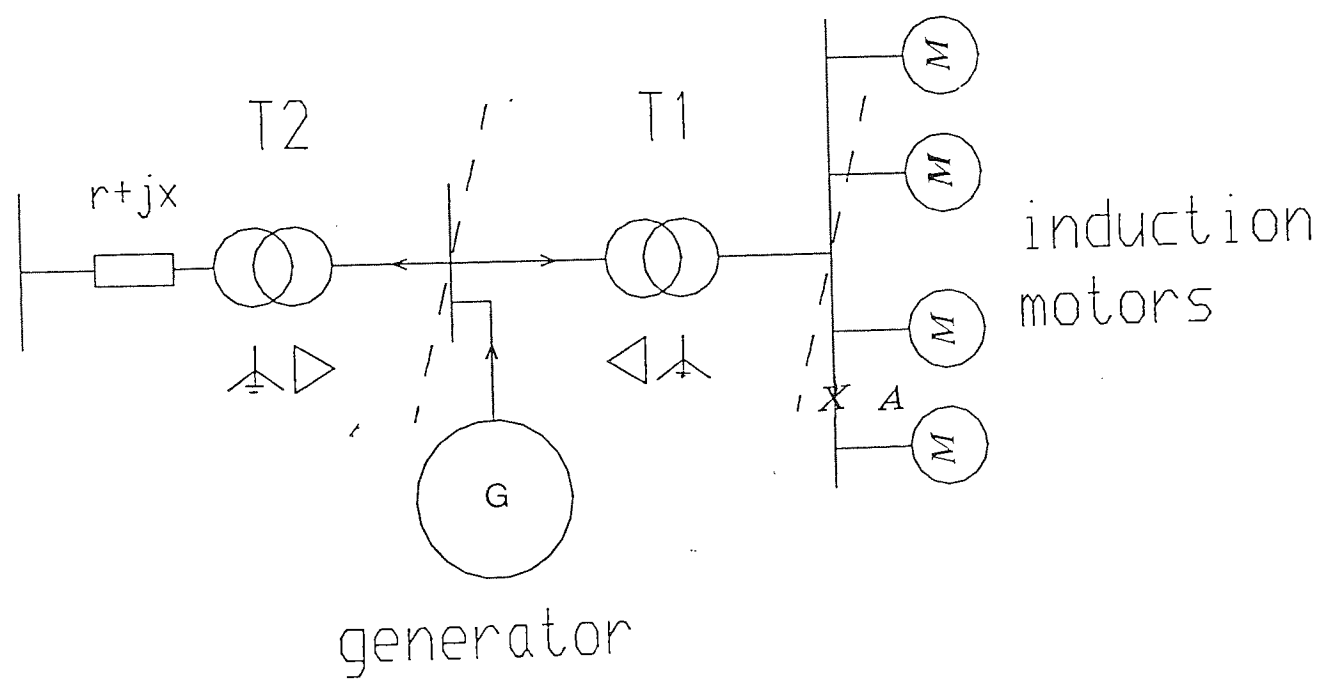


FIG. 5.1

front as shown. A line of impedance ($0.00064 + j0.022$) ohms, connect the system of the generator and motors to an infinite system of 30000 MVA capacity.

Table 5.1 describes the generator data.

Table 5.2 describes the motors and the transformers data.

5.3 Requirements

Discussion with the C.E.G.B pointed the need for a computer package to model the system described and to study the following network conditions of disturbance.

- 1- Faults between phases and to earth at different points throughout the system i.e (on bus-bars B1 & B2)
- 2- Facility to apply faults at any instantaneous voltage or current.
- 3- Facility to clear faults at a current zero.
- 4- Facility, provided by a model, to investigate the interaction between the group of induction motors and the generator following a disturbance at the nodes mentioned above.

Symbol	Description	Value	Unit
S	Rating	776.00	MVA
V	Voltage	23.500	Kv
x_a	Armature reactance	0.1700	p.u
x_d	Direct axis reactance	2.2700	p.u
x_q	Quadrature axis reactance	2.1500	p.u
x'_d	Direct axis transient reactance	0.3200	p.u
x'_q	Quadrature axis transient reactance	2.0000	p.u
x''_d	Direct axis sub-transient reactance	0.2600	p.u
x''_q	Quadrature axis sub-transient reactance	0.2600	p.u
x_0	zero-sequence reactance	0.1933	p.u
T'_d	Direct axis transient short-circuit time constant	0.9500	sec.
T'_q	Quadrature axis transient short-circuit time constant	0.8200	sec.
T''_d & T''_q	Direct & quadrature axis sub-trans. short-circuit time cons.	0.0200	sec.
r_a	Armature resistance	0.0022	p.u
r_0	zero-sequence resistance	0.0019	p.u
H	Inertia constant	3.1600	MJ/MVA

Table 5.1

Symbol	Description	Value				Unit
		Motor name ---->	CWP	BFP	PAF	
S	Rating	3.61	10.4	4.05	4.12	MVA
V	Voltage	11.0	11.0	11.0	11.0	Kv
x _{sl}	Stator leakage reactance	0.1278	0.1395	0.1139	0.1001	p.u
x _{rl}	Rotor leakage reactance	0.1547	0.1046	0.1567	0.1661	p.u
x _m	Magnetising reactance	3.8300	4.4100	3.6000	3.3200	p.u
r _s	Stator resistance	0.0071	0.0047	0.0095	0.0076	p.u
r _r	Rotor resistance	0.0112	0.0084	0.0121	0.0107	p.u
B & C	Mecanical torque co-efficients	-1.7, 0.9	-2, 1	-2, 1	-2, 1	
T _l	Losses torque	0.01	0.01	0.01	0.01	p.u
H	Inertia constant	1.711	1.05	13.0	25.0	MJ/MVA

Symbol	Description	Value		Unit
		Gen. T/F T2	Mot. T/F T1	
S	Rating	800.0	48.0	MVA
V	Voltage	23.5/220.	23.5/11.	Kv
x _T	Reactance	0.1551	0.1350	p.u
r _T	Resistance	0.0039	0.0034	p.u

Table 5.2

5.4 Synchronous Generator Model

The approach used to develop the synchronous generator model in a three phase co-ordinate reference frame is presented in the following paragraphs. In order to include the transient effects more accurately, two windings are assumed on the quadrature axis (see fig. 5.2). Assumptions identical to those made in deriving the induction motor model (paragraph 3.1.2) are also assumed here. Saturation, third and higher order harmonics are ignored in deriving the equations.

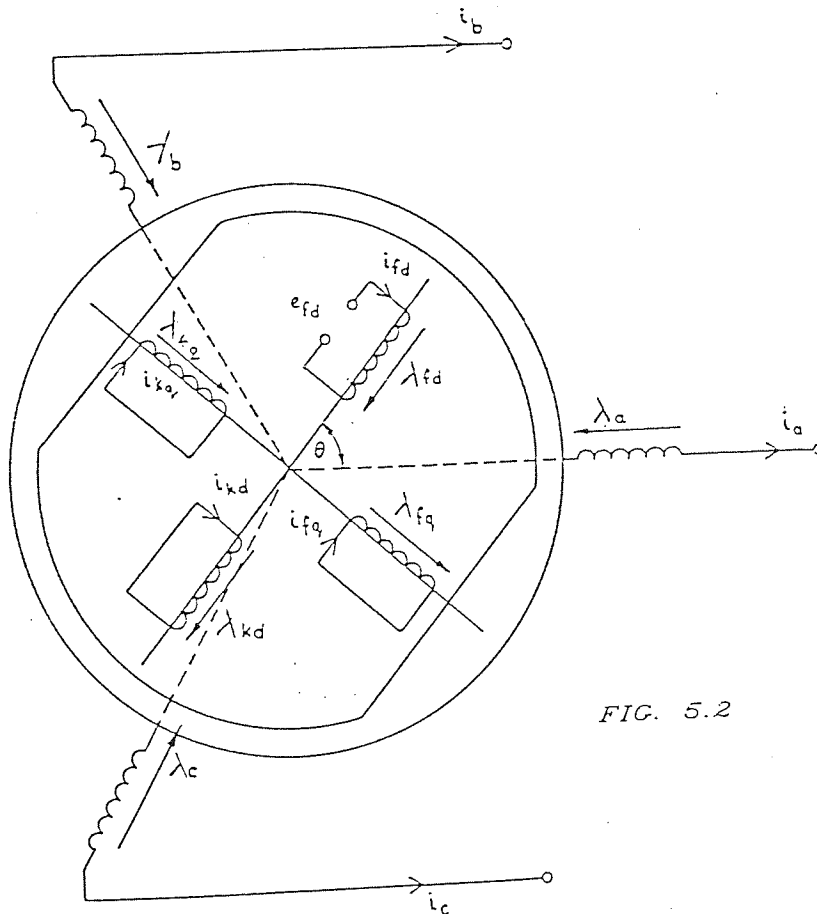


FIG. 5.2

5.4.1 Voltage Equations

When a generator is supplying a load, the three phase induced voltage of the stator windings can be expressed in terms of the instantaneous flux linkage and the other variables of the machine by the following:

$$e_a = \bar{p} \lambda_a - r_a i_a - 3r_o i_o \quad \dots\dots\dots 5.1$$

$$e_b = \bar{p} \lambda_b - r_b i_b - 3r_o i_o \quad \dots\dots\dots 5.2$$

$$e_c = \bar{p} \lambda_c - r_c i_c - 3r_o i_o \quad \dots\dots\dots 5.3$$

where suffices a, b & c stand for the stator phase windings and suffix 'o' is for the zero sequence variable, also

$$3i_o = i_a + i_b + i_c \quad \dots\dots\dots 5.4$$

Similar expressions for the windings on the rotor circuit can be developed i.e,

$$e_{fd} = \bar{p} \lambda_{fd} + r_{fd} i_{fd} \quad \dots\dots\dots 5.6$$

$$\phi = \bar{p} \lambda_{kd} + r_{kd} i_{kd} \quad \dots\dots\dots 5.7$$

$$\phi = \bar{p} \lambda_{fq} + r_{fq} i_{fq} \quad \dots\dots\dots 5.8$$

$$\phi = \bar{p} \lambda_{kq} + r_{kq} i_{kq} \quad \dots\dots\dots 5.9$$

where suffices f, k, d & q stand for field, damper, direct and quadrature.

The instantaneous flux linkage of each of the windings is a function of the current in that winding plus the currents in all other windings. e.g the flux linkage of phase 'a' stator is given by,

$$\lambda_a = L_{aa} i_a + M_{ab} i_b + M_{ac} i_c + M_{afd} i_{fd} + M_{akd} i_{kd} + M_{afq} i_{fq} + M_{akq} i_{kq} \quad \dots\dots\dots 5.10$$

Thus, an inductance matrix linking all the seven windings representing the machine is given by

$$\{\lambda\} = [L]_g \cdot \{i\} \quad \dots\dots\dots 5.11$$

The elements of the inductance matrix are explained later in this chapter.

5.4.2 The Swing Equation

When a disturbance such as a load change, or a fault close to the generator terminals, takes place, the generator performance deviates from the steady-state condition. In such cases, assuming that the turbine governor settings remain unaltered, there will be a deficiency or a surplus of mechanical power input over electrical power output, depending upon the nature of the disturbance. Such unbalance in power causes an oscillation in the rotor angle with respect to the synchronously rotating reference axis. The change in power can be related to the rate of change of the rotor speed by,

$$d\omega/dt = (P_m - P_e)/J \quad \dots\dots\dots 5.12$$

where 'J' is the moment of inertia of all rotating masses referred to the shaft.

In a per unit system, the power and torque are equal, and allowing for the friction and windage losses, the swing equation can be written as :

$$\bar{p}\omega = (T_m - T_e - T_l) / 2\omega H$$

and

$$\bar{p}\theta = \omega \dots\dots\dots 5.13$$

where;

$$H = \frac{J \pi n_o^2}{1800} \text{ is the inertia constant KJ/KVA}$$

$$\bar{p} = p/\omega_o \text{ and } n_o \text{ is the rated shaft speed.}$$

The electrical torque T_e can be estimated from the interaction of the flux linkage components with the current components, i.e. in the 'd,q' frame of reference this is;

$$T_e = \lambda_{dq} i_d - \lambda_{qd} i_q \dots\dots\dots 5.14$$

On using Park's transformations the electrical torque in phase variable form is,

$$T_e = (2/3\sqrt{3}) (\lambda_{abc} (i_a - i_b) + \lambda_{bca} (i_b - i_c) + \lambda_{cab} (i_c - i_a)) \dots\dots\dots 5.15$$

5.4.3 The Elements of the
Generator Inductance Matrix

The elements of the synchronous generator inductance matrix in three phase variables can be fully described by defining nine co-efficients. Part of the elements are rotor position dependent with values that change periodically with time [36]. The elements and their co-efficients are discussed in the following paragraphs.

a) Elements for the Armature

Self Inductance

These are the first three elements in the main diagonal (L_{aa} , L_{bb} & L_{cc}). Such elements vary periodically with period ' π ', being greatest when the direct axis of the field coincides with the axis of the armature phase, and least when the quadrature axis coincides with the field axis. Two co-efficients are needed to define these elements, they are denoted here by L_{AA0} &

L_{AA2} .

The elements are related to these co-efficients by,

$$L_{aa} = (L_{AA0} + L_{AA2} \cos 2\theta)$$

$$L_{bb} = (L_{AA0} + L_{AA2} \cos(2\theta + 2\pi/3)) \quad \dots\dots 5.16$$

$$L_{cc} = (L_{AA0} + L_{AA2} \cos(2\theta - 2\pi/3))$$

where $\theta = \tau - \delta_g$ (δ_g is the load angle)

The parameters L_{AA0} & L_{AA2} can be found from

$$L_{AA0} = (L_d + L_q + L_o) / 3 \quad \dots\dots\dots 5.17$$

$$L_{AA2} = (L_d - L_q) / 3$$

where L_d & L_q are the per unit direct and quadrature reactance.

b) Mutual Inductances between Armature Phases

The mutual inductance between any armature winding and other windings in the armature circuit has also been found to vary periodically with period ' π '. It is a maximum when the direct-axis is mid-way between the axis of one phase and the reverse-axis of the other e.g for phase (b)& (c), phase (a) is on the quadrature axis. Such elements are also defined by two

co-efficients, one is already defined (L_{AA2}), and the other which is denoted by (L_{ABO}), is given by,

$$L_{ABO} = (L_d + L_q - 2L_o) / 6$$

The elements are related to the co-efficients as follows :

$$L_{ab} = L_{ba} = -L_{ABO} + L_{AA2} \cos(2\theta - 2\pi/3)$$

$$L_{bc} = L_{cb} = -L_{ABO} + L_{AA2} \cos 2\theta \quad \} \dots\dots 5.18$$

$$L_{ca} = L_{ac} = -L_{ABO} + L_{AA2} \cos(2\theta + 2\pi/3)$$

In the numerical solution, the presence of the zero sequence reactance is found to be important in determining the elements described above, since without such a parameter an overflow results during the process of matrix inversion.

c) Mutual Inductance between the Stator and Rotor Windings

The mutual inductance between any phase of the stator windings and a field or a damper winding is varying periodically

with period 2π . For a phase winding, the mutual inductance is maximum when the direct-axis coincides with the axis of that phase and it is zero when the phase axis coincides with the quadrature axis, thus the mutual inductance changes sign for every ' π ' turn of the field axis. For phase (a) the elements are,

$$M_{afd} = M_{AFD_0} \cos\theta$$

$$M_{akd} = M_{AKD_0} \cos\theta$$

} 5.19

$$M_{afq} = M_{AFQ_0} \sin\theta$$

$$M_{akq} = M_{AKQ_0} \sin\theta$$

In the above expressions, and for the other two phases, the angle ' θ ' is replaced by ' $\theta - 2\pi/3$ ' & ' $\theta + 2\pi/3$ '.

Since the direct and quadrature damper windings are mounted along the direct and the quadrature axis, then in per unit systems,

$$M_{AKD_0} = M_{AFD_0} = M_{AD_0} \quad \& \quad M_{AKQ_0} = M_{AFQ_0} = M_{AQ_0}$$

Thus, two co-efficients are needed to define the elements for the mutual inductance between the armature windings and the windings mounted on the rotor circuit. They can be found from,

$$M_{ADo} = \frac{2}{3} (L_d - L_a) \quad \dots\dots\dots 5.20$$

$$M_{AQO} = \frac{2}{3} (L_q - L_a)$$

where L_a is the armature reactance

d) Self and Mutual Inductances
for the Rotor Windings

Because of the zero relative speed of the rotor with respect to the machine rotating m.m.f (neglecting speed variation under transient conditions), all the self inductances of the field and damper windings are constant. This defines the last four elements on the main diagonal, of the machine inductance matrix, which are independent of the rotor position. The elements are :

$$L_{ffd} = L_{FDL} + M_{ADo}$$

$$L_{kkd} = L_{KDL} + M_{ADo}$$

} 5.21

$$L_{ffq} = L_{FQL} + M_{AQo}$$

$$L_{kkq} = L_{KQL} + M_{AQo}$$

The above expressions add four new co-efficients to our inductance matrix. These are,

$$L_{FDL} = 2/3 \cdot \left(\frac{(L_{da} - L_{da}^2)}{(L_{dd} - L_{dd}')} \right) - 2/3 \cdot (L_{da} - L_{da})$$

$$L_{KDL} = 2/3 \cdot \left(\frac{(L_{da}' - L_{da})}{(L_{dd}' - L_{dd}'')} \right) + L_{dd} - L_{dd}' - 2/3 \cdot (L_{da} - L_{da})$$

$$L_{FQL} = 2/3 \cdot \left(\frac{(L_{qa} - L_{qa}^2)}{(L_{qq} - L_{qq}')} \right) - 2/3 \cdot (L_{qa} - L_{qa})$$

$$L_{KFL} = 2/3 \cdot \left(\frac{(L_{qa}' - L_{qa})}{(L_{qq}' - L_{qq}'')} \right) + L_{qq} - L_{qq}' - 2/3 \cdot (L_{qa} - L_{qa})$$

The coupling co-efficient between any winding on one axis (d,q) and windings on the other axis (q,d) are zero, thus, only elements for mutual inductance between windings on the same axis exist. In a per-unit system, the mutual inductance between the

direct field and the direct damper winding [48], and that for the quadrature field and the quadrature damper are,

$$\begin{matrix} M & = & M \\ fdk & & ADo \end{matrix} \quad \} \dots\dots\dots 5.23$$

$$\begin{matrix} M & = & M \\ fqk & & AQo \end{matrix}$$

Such parameters have already been defined in (c).

The full derivation of the relationships between the nine coefficients, required to define the synchronous machine inductance matrix in the phase co-ordinate frame, and the parameters in the 'd,q' reference frame is given in appendix (A2).

5.5 Derivation of the System Model.

For the purpose of a simple computer program, the circuit under consideration is partitioned into four main sections. These are,

- a) A group of the eight induction motors fed from bus-bar 'B1'.
- b) The generator connected to the bus-bar 'B2'

- c) The motor-transformer 'T1' connecting bus-bars 'B1' & 'B2'.
- and d) The generator-transformer 'T2' and the line connecting the infinite bus-bar system to bus-bar 'B2'.

The following paragraphs describe the modelling of each section.

5.5.1 Modelling of the Group
of Induction Motors.

Although the computer program has been written to handle any number of induction motors, only four motors out of eight are simulated. Each induction motor is represented, using the three phase co-ordinate model, by a set of differential equations as described in chapter III. The solution for each motor current depends on the current derivative vector, and hence on the other related variables, using the voltage vector of bus-bar 'B1' i.e

$$p\{i\}_m = [L]_m^{-1} \{ \{v\}_{B1} - [(1-s)[G] + [r]]_m \{i\}_m \} \dots 5.24$$

5.5.2 Modelling of the Generator

connected to bus-bar 'B2'.

The generator equation, in terms of the bus-bar voltage vector $\{v_{B2}\}$, can be defined in terms of current derivative

vector as

$$p\{i_g\} = [L_g]^{-1} \{v_{B2}\} + [-p[L_g] + [r_g]]\{i_g\} \quad \dots \quad 5.25$$

where $[L_g]$, $p[L_g]$ & $[r_g]$ are defined in appendix [A2]

The electrical torque T_e required to find the variation in

speed, under transient conditions, is computed using equation (5.15) after the flux linkage vector $\{\lambda_g\}$ has been calculated

from (5.11). Finally, the rotor position for the next step of the solution is found from equation (5.13).

5.5.3 Modelling of the Line and the Generator-Transformer 'T2'

By neglecting the mutual effects between the line phases, and the mutual effects between the transformer windings, the voltage of the bus-bar 'B2', at any instant, is defined by

the voltage of the infinite bus-bar and the drop across the line and the transformer impedance as follows:

Let the current on the high voltage star side of transformer 'T2' be i_{T2} , then the voltage to earth of the star windings

v'_{B2} is

$$\{v'_{B2}\} = N_{T2} \{v_I\} + N_{T2}^2 \{[r]_e + [L]_p\} \{i_{T2}\} \quad \dots\dots 5.26$$

where,

N_{T2} is 1/tap position of transformer T₂

$\{v_I\}$ is the infinite bus-bar voltage vector

$[r]_e$ & $[L]_p$ is the combined resistance and inductance of

the line and transformer 'T2'

from equation (4.3) in chapter IV, the voltage vector $\{v'_{B2}\}$ in

terms of v_{B2} is

$$\{v'_{B2}\} = [C] \{v_{B2}\} \quad \dots\dots 5.27$$

so, substituting equation (5.27) in (5.26) gives

$$[C] \{v_{B2}\} = N_{T2} \{v_I\} + N_{T2}^2 \{[r]_e + [L]_p\} \{i'_{T2}\} \quad \dots\dots 5.28$$

and finally multiplying equation (5.28) by $[C]^t$ to express i' in terms of i gives

terms of i gives

$$[s]_{B2} \{v\}_{T2} = N_{T2} [C]_{T2}^t \{v\}_I + N_{T2}^2 \{ [r]_e + [L]_e p. \} \{i\}_{T2} \dots 5.29$$

where $[s] = [C][C]^t$

Since the solution using a digital computer advances in discrete steps, equation (5.29) takes the following form,

$$[s]_{B2} \{v\}_{T2}^{n+1} = N_{T2} [C]_{T2}^t \{v\}_{I}^{n+1} + N_{T2}^2 \{ [r]_e \{i\}_{T2}^n + [L]_e \{ \Delta i / \Delta t \} \}_{T2}^n$$

..... (5.30)

The current vector $\{i\}_{T2}$ at step 'n' is defined by applying

Kirchhoff's current law at bus-bar 'n' i.e

$$\{i\}_{T2}^n = \{i\}_{B2}^n + \{i'\}_{T1}^n \dots (5.31)$$

where $\{i'\}_{T1} = [C]^t \{i\}_{T1}$

and $\{i_{T1}\}$ is the current through transformer 'T1', defined in the next paragraph.

5.5.4 Modelling of the Motor
-Transformer 'T1'

The voltage of the bus-bar 'B1', required for the solution of the current vector derivative of each motor, can be defined at any step by the knowledge of the voltage at the bus-bar 'B2' at that step and the current drawn by each motor at the previous step i.e the voltage vector $\{v_{B1}\}$ at step 'n+1' is given by,

$$\{v_{B1}\}_{n+1} = N_{T1} [C] \{v_{B2}\}_{n+1} - N_{T1}^2 \{[r_{T1}]\} \{i_{T1}\}_n + [L_{T1}] \{ \Delta i_{T1} / \Delta t \}_n$$

..... (5.32)

where N_{T1} is 1/tap position of transformer T1

$[L_{T1}]$ & $[r_{T1}]$ is the inductance and the resistance matrix of transformer 'T1'

The current vector $\{i_{T1}\}$ is defined by applying Kirchhoff's current law at bus-bar 'B2' i.e

$$[i_{T1}] = 2. \sum_{j=1}^4 [i_{mj}] \cdot B_j \dots\dots\dots (5.33)$$

where B_j is a factor normalising current ' i_m ' to a 776 MVA, 23.5 Kv base.

5.6 Transient Stability Studies

Transient stability studies were carried out by applying a fault for a short duration followed by clearance of the fault. Studies were undertaken for disturbances on bus-bars 'B2' & 'B1'. The following sections give details of the studies.

5.6.1 Disturbance due to Faults

on Generator Bus-Bar 'B2'

Faults on the generator bus-bar 'B2' are applied by introducing the fault matrix [M] on the R.H.S of equation (5.30), i.e

$$[v_{B2}] = N_{T2} [M][C]^T [v_I] + N_{T2}^2 [M][r][i_{T2}] + [L_{T2}] \Delta i_{T2} / \Delta t \dots\dots\dots (5.34)$$

where,

$$[M] = [F][S]^{-1}$$

Under normal operating conditions matrix [M] is a unit matrix. However, under fault conditions, the elements of matrix [M] are determined by the constraints that arise from the type of fault as shown below.

5.6.1.1 Single Phase to Earth
Fault (on phase 'a')

In this case,

$$\begin{pmatrix} v \\ B2 \end{pmatrix} = \begin{pmatrix} 0 \\ a \end{pmatrix}$$

$$\begin{pmatrix} i \\ T2 \end{pmatrix} = \begin{pmatrix} i \\ g \end{pmatrix} + \begin{pmatrix} i \\ T1 \end{pmatrix}$$

$$\begin{pmatrix} i \\ T2 \end{pmatrix} = \begin{pmatrix} i \\ g \end{pmatrix} + \begin{pmatrix} i \\ T1 \end{pmatrix}$$

The elements of matrix [S]⁻¹ is determined by inverting the sub-matrix that results from deleting the row and column corresponding to phase 'a' i.e

$$\frac{1}{3} \begin{vmatrix} s_{22} & s_{23} \\ s_{32} & s_{33} \end{vmatrix} = \frac{1}{3} \begin{vmatrix} 2 & -1 \\ -1 & 2 \end{vmatrix}$$

which results in

$$[S]^{-1} = \begin{vmatrix} 0 & 0 & 0 \\ 0 & 2 & 1 \\ 0 & 1 & 2 \end{vmatrix} \quad [F] = \begin{vmatrix} 0 & 0 & 0 \\ 0 & 1 & 0 \\ 0 & 0 & 1 \end{vmatrix}$$

5.6.1.2 Double Phase to Earth Fault (on phase 'a' & 'b')

in such a case,

$$(v_{B2 a}) = (v_{B2 b}) = 0$$

$$(i_{T2 c}) = (i_{g c}) + (i'_{T1 c})$$

This is satisfied by inverting the element 's' which results

33

from partitioning matrix [S]. This gives,

$$\text{also for this } [S]^{-1} = \begin{vmatrix} -1 & 0 & 0 \\ 0 & 0 & 0 \\ 0 & 0 & 3/2 \end{vmatrix} \quad [F] = \begin{vmatrix} 0 & 0 & 0 \\ 0 & 0 & 0 \\ 0 & 0 & 1 \end{vmatrix}$$

5.6.1.3 Three Phase to Earth Fault

The above conditions are

In this case,

$$(e_{B2 a}) = (e_{B2 b}) = (e_{B2 c}) = 0$$

i.e.,

$$[S]^{-1} = [\emptyset] \quad \& \quad [F] = [\emptyset]$$

5.6.1.4 Line-to-Line Short Circuit

(phase b&c)

In this case ,

$$\begin{pmatrix} e \\ B2 \end{pmatrix}_b = \begin{pmatrix} e \\ B2 \end{pmatrix}_c$$

also we have,

$$\begin{pmatrix} e \\ B2 \end{pmatrix}_a + \begin{pmatrix} e \\ B2 \end{pmatrix}_b + \begin{pmatrix} e \\ B2 \end{pmatrix}_c = 0$$

so from above,

$$\begin{pmatrix} e \\ B2 \end{pmatrix}_b = -1/2 \begin{pmatrix} e \\ B2 \end{pmatrix}_a \quad \& \quad \begin{pmatrix} e \\ B2 \end{pmatrix}_c = -1/2 \begin{pmatrix} e \\ B2 \end{pmatrix}_a$$

also for this case

$$\begin{pmatrix} i \\ T2 \end{pmatrix}_a = \begin{pmatrix} i \\ g \end{pmatrix}_a + \begin{pmatrix} i \\ T1 \end{pmatrix}_a$$

The above conditions are found to be satisfied when

$$[S]^{-1} = \begin{vmatrix} 1 & \emptyset & \emptyset \\ \emptyset & 1 & \emptyset \\ \emptyset & \emptyset & 1 \end{vmatrix} \quad \& \quad [F] = \begin{vmatrix} 1 & \emptyset & \emptyset \\ -0.5 & \emptyset & \emptyset \\ -0.5 & \emptyset & \emptyset \end{vmatrix}$$

5.6.2 Disturbances due to faults on

bus-bar 'B1'

Faults on bus-bar 'B1' can be established by using the fault matrix $[F]$ to eliminate elements of the voltage vector $\{v\}$ in equations 5.24 & 5.32 i.e equation 5.24 which calculates

B1
the motor current derivative vector becomes

$$p\{i\}_m = [L]_m^{-1} \{ [F]\{v\}_{B1} - [(1-s)[G] + [r] \}_m \{i\}_m \} \dots 5.35$$

and equation 5.32 becomes,

and equation 5.32 becomes,

$$[F]\{v\}_{B1} = N_{T1} \{v\}_{B2} - N_{T1} [L]_{T1} p\{i\}_{T1} - N_{T1} [R]_{T1} \{i\}_{T1} \dots 5.36$$

From which the derivative current vector $p\{i\}_{T1}$ is found during

the fault application. The elements of the fault matrix $[F]$ will have the same values for identical types of faults as those discussed in 5.6.1. In this study the fault location is chosen to be at point 'A' on bus-bar 'B1' (see Fig. 5.1).

5.7 Software Development

A computer program was developed to solve the sets of mathematical equations derived above. The program contains four sub-routines (fig. 5.5 to fig. 5.8). Each is solving for a part of the system as partitioned in section 5.5, using the voltage at common bus-bars. The computations are initiated using the values obtained from solving the system in the steady state mode of operation (fig. 5.3). The following steps, with the aid of the flow charts (fig. 5.4), describe the computer program.

- 1) With the knowledge of the voltage at each bus-bar, the fourth order Runge-Kutta evaluations for the voltage vectors can be established.
- 2) The generator current and the rotor position are up-dated using the voltage evaluations of bus-bar 'B2'. These are computed by calling the sub-routine 'SYNG' (fig. 5.5).
- 3) For each motor, the current and the rotor position are up-dated using the voltage evaluations of bus-bar 'B1'. These are carried-out by calling sub-routine 'MOTOR'. The sub-routine is called for as many times as there are number of motors in the system.

- 4) Using the currents obtained in step (3), the currents in transformer 'T1' are found by applying equation (5.33).
- 5) Using the currents obtained in steps (2)& (4), the currents in transformer 'T2' are found by applying equation (5.31).
- 6) Up-date time and the infinite bus-bar voltage.
- 7) By calling sub-routine 'SYSTEM' (fig. 5.7), the voltage evaluations of bus-bar 'B2' are up-dated using the voltage obtained in step (6). Modify the up-dated voltage vector for faults, if any.
- 8) By calling sub-routine 'VOLT', the voltage evaluations of bus-bar 'B1' are up-dated using the voltage obtained in step (7) and the current obtained in step (4). The sub-routine modifies the voltage vector for faults, if any.

Steps (2) to (7) are repeated until the specified time is covered.

	Motors				
	Generator	CMP	BFP	PAF	IDF
slip	0.0000	0.0064	0.0048	0.0071	0.0063
δ	0.3332	0.0668	0.0754	0.0605	0.0536
T_m	0.8500	0.8400	0.8700	0.8480	0.8590

INFINITE
BUS-BAR

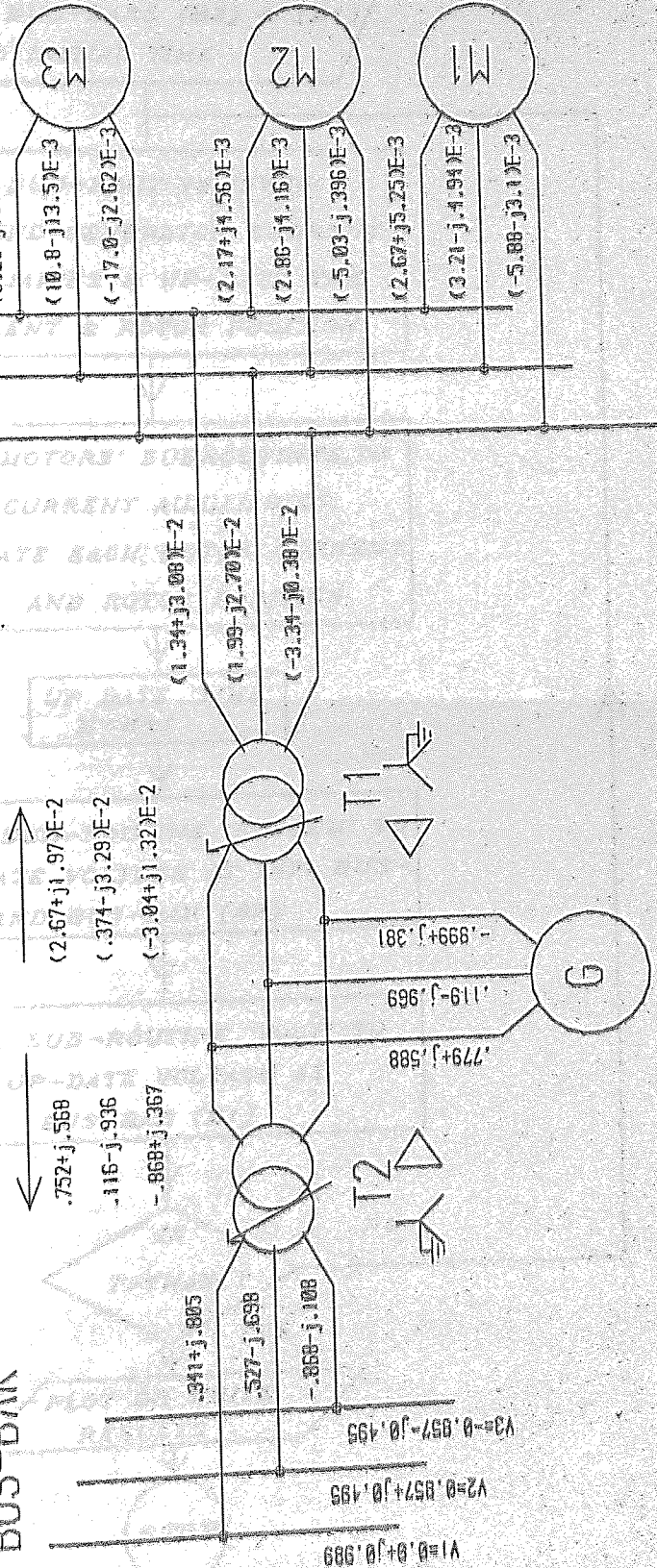


FIG. 5.3

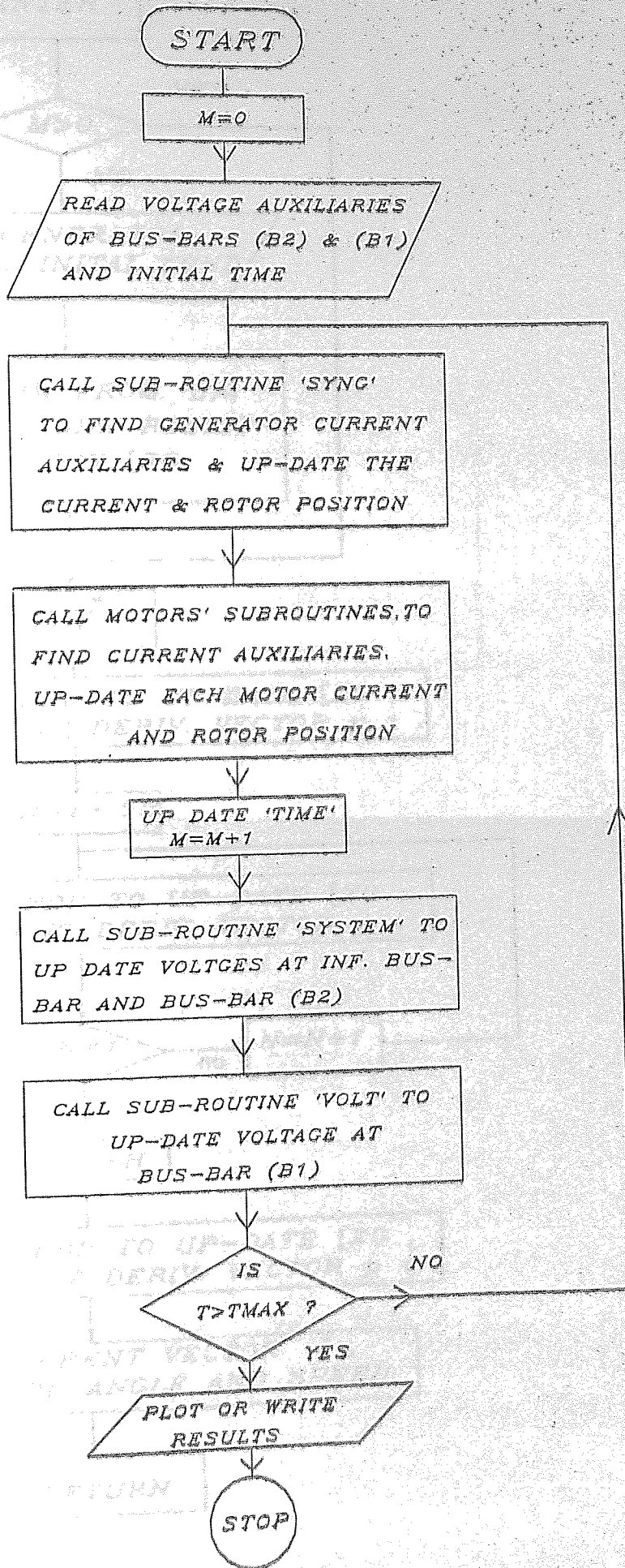
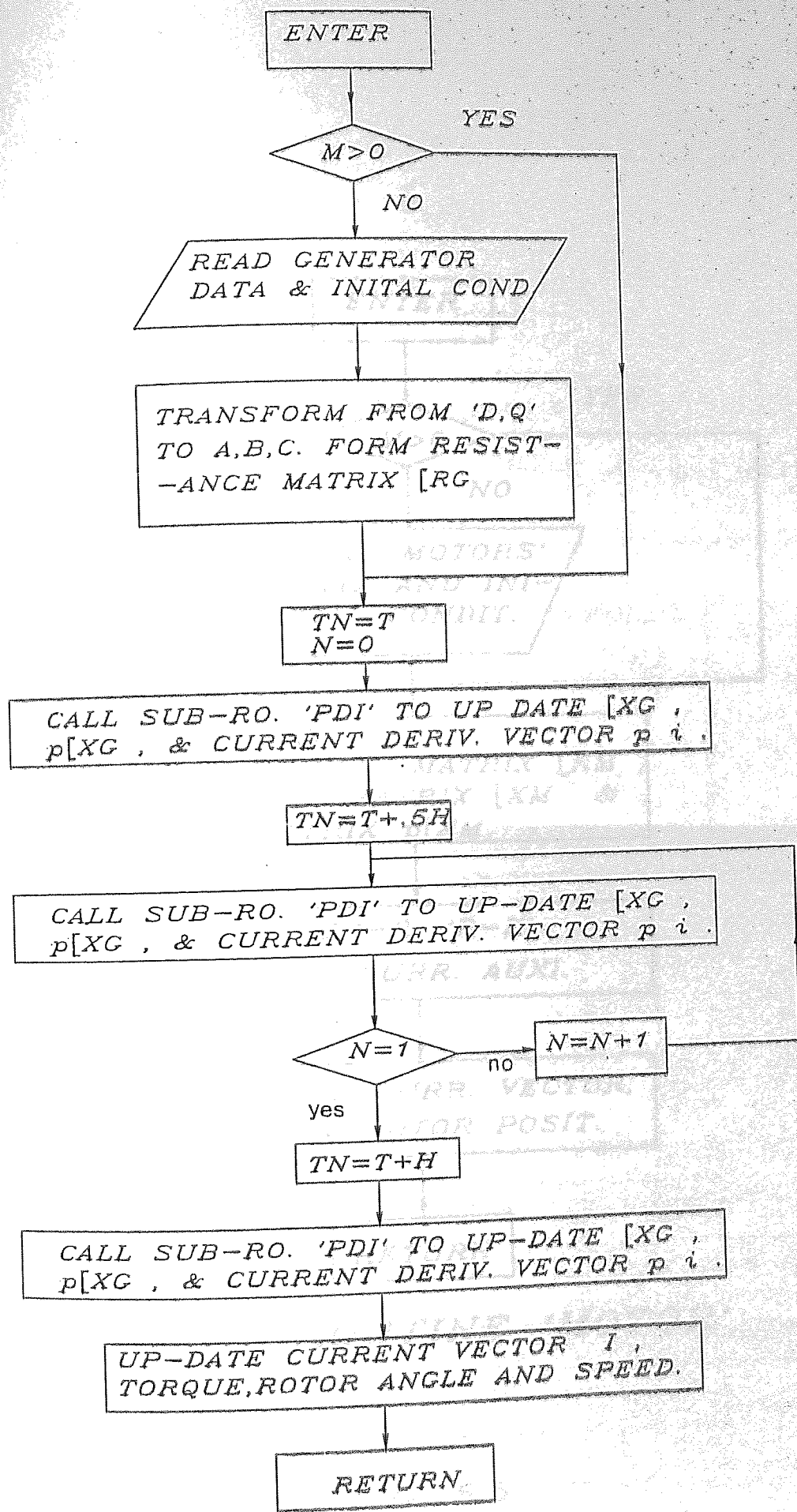
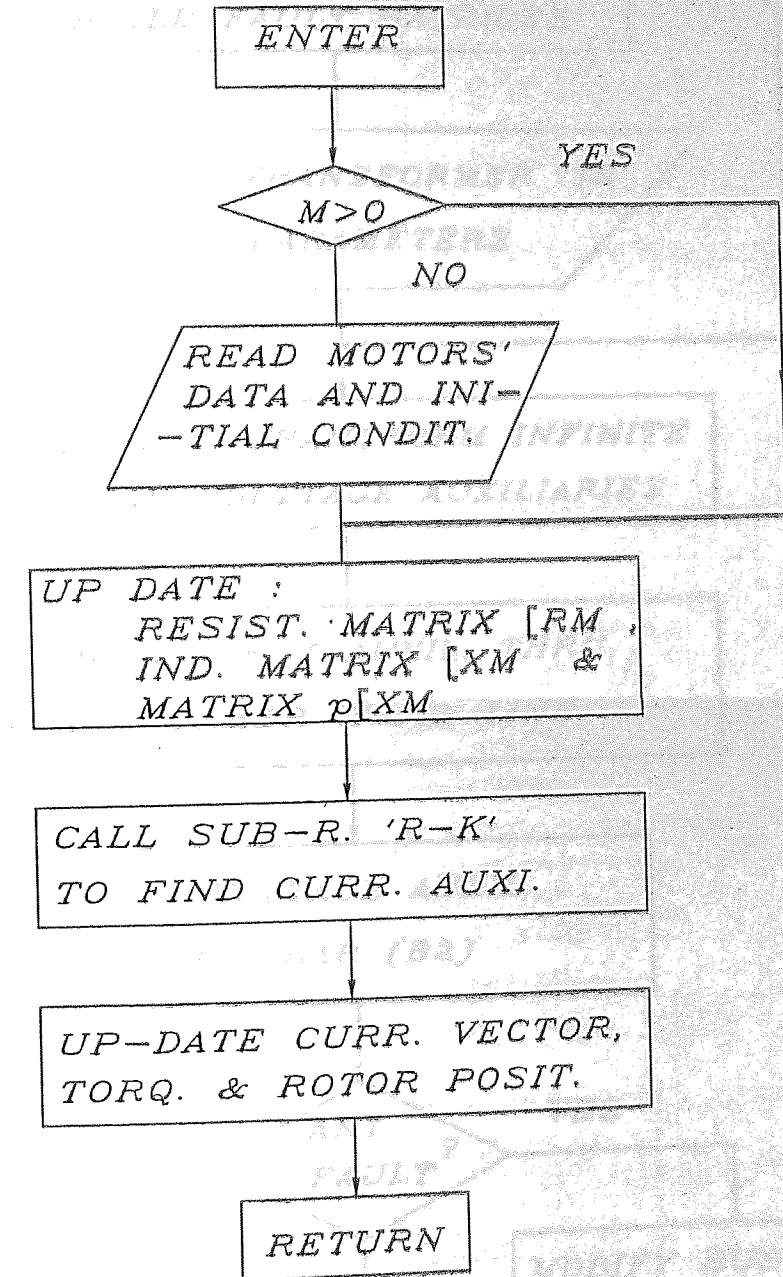


FIG. 5.4



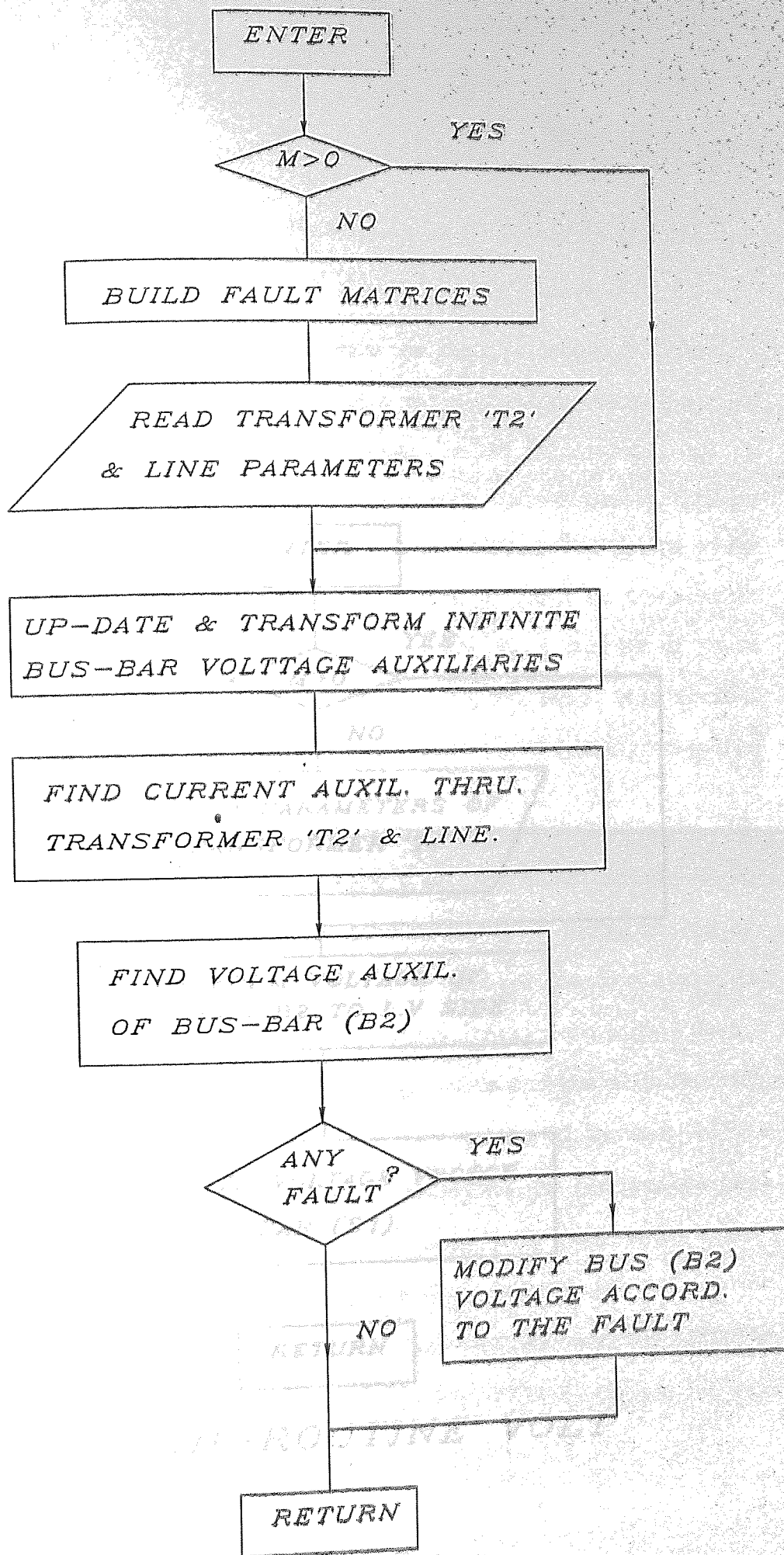
SUB-ROUTINE 'SYNG'

FIG. 5.5



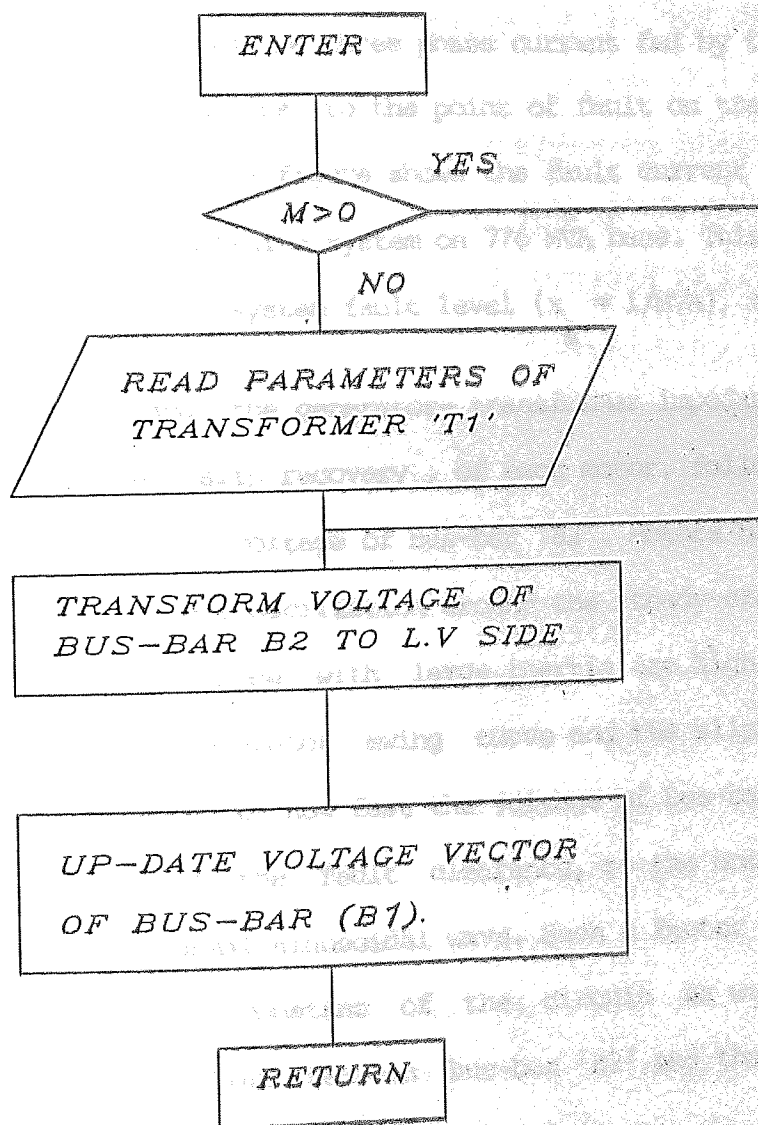
SUB-ROUTINE 'MOTOR'

FIG. 5.6



SUB-ROUTINE SYSTEM

FIG. 5.7



SUB-ROUTINE VOLT

FIG. 5.8

5.8 Results

Figs. 5.9(a), 5.9(b) & 5.9(c) show the results obtained following an application and clearance of a three phase to earth fault on bus-bar 'B2'. The fault duration is 107 milliseconds and is cleared at phase 'a' as the generator current passes through zero. Fig. 5.9(b) shows the three phase current fed by the group of the induction motors to the point of fault on transformer "T1" MVA base. Also the figure shows the fault current of phase 'a' fed from the infinite system on 776 MVA base. This current is limited by the system fault level ($x = 1/\text{MVA}$), together with the line and the generator-transformer impedance. Fig. 5.9(c) shows the slip recovery, of each motor, following the restoration of the voltage of bus-bar 'B2'. Motors having low inertia suffer severe oscillation around the steady-state speed (BFP & CWP) where those with large inertia are highly damped (IDF & PAF). The generator swing curve and the slip recovery curves are influenced by how fast the voltage of bus-bar 'B2' is restored, following the fault clearance, to the nominal peak value and the normal sinusoidal wave. Such a factor is determined by the time constant of the circuit as well as the impedance of the link between bus-bar 'B2' and the infinite system.

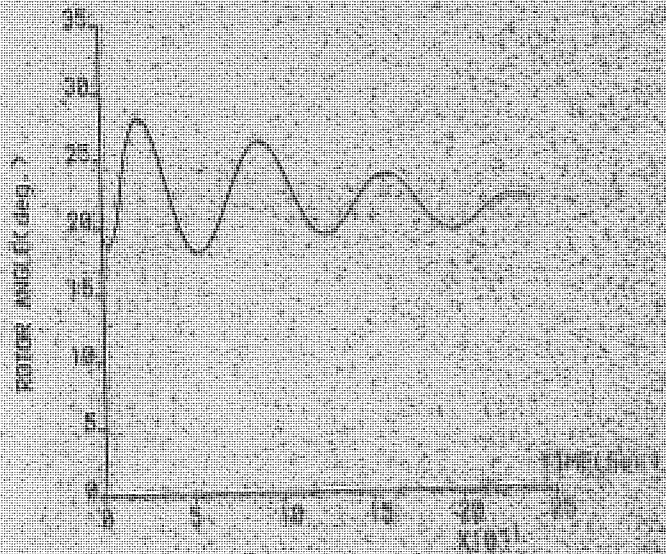
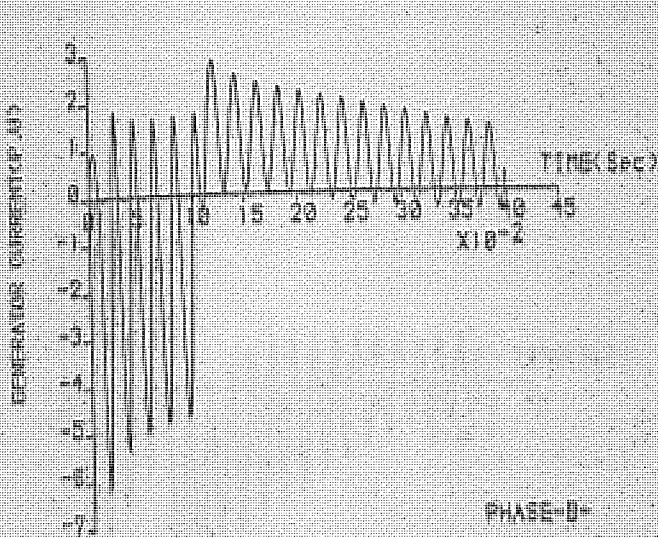
The results of a transient stability study due to a double phase to earth fault on phase 'a' & 'b' are shown by figs. 5.10(a), 5.10(b) & 5.10(c). The effects on the generator rotor angle swing and drop in motor speed, are less severe, when compared to the three phase fault of the same duration. Fig. 5.10(a) shows the maximum swing of the generator rotor angle of less than 25 degrees compared to about 28 degrees for the case of a three phase to earth disturbance. Similar comparisons will show that the motor speed drops below the steady-state value e.g. for motors IDF & PAF, a maximum deviation in slip of 1% & 2.5% respectively, for a two phase-to-earth fault, compared to 1.5% & 2.9% for the case of a three phase to earth fault.

The results obtained from the study of a three phase to earth disturbance on bus-bar 'B1' are shown in figs. 5.11(a), 5.11(b), 5.11(c) & 5.11(d). In this case, during the fault, the generator is affected by the distorted voltage of bus-bar 'B2' that results from the asymmetry of the currents passing through the link connecting bus-bar 'B2' to the infinite system. This condition accelerates the generator rotor and thus, the angle deviates increasingly from the steady-state value. Also during that period the motors feed the fault with a large current (figs. 5.11(b) & 5.11(c)) at the expense of the stored kinetic energy and thus, the motor speeds fall. Following the clearance of the fault, the motors start drawing currents from the system

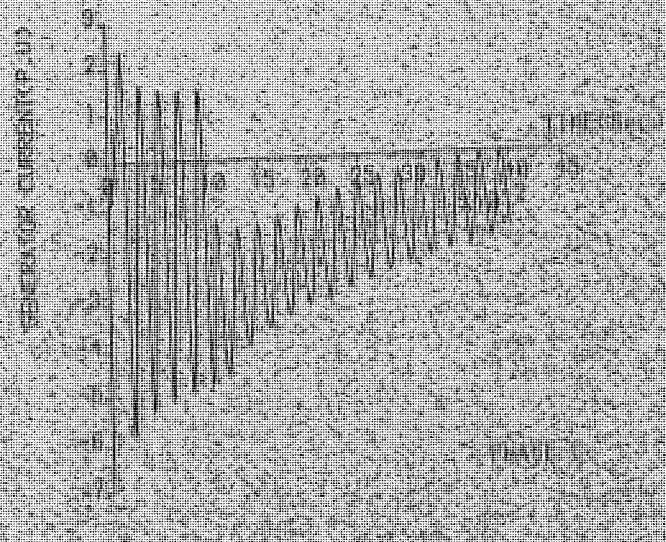
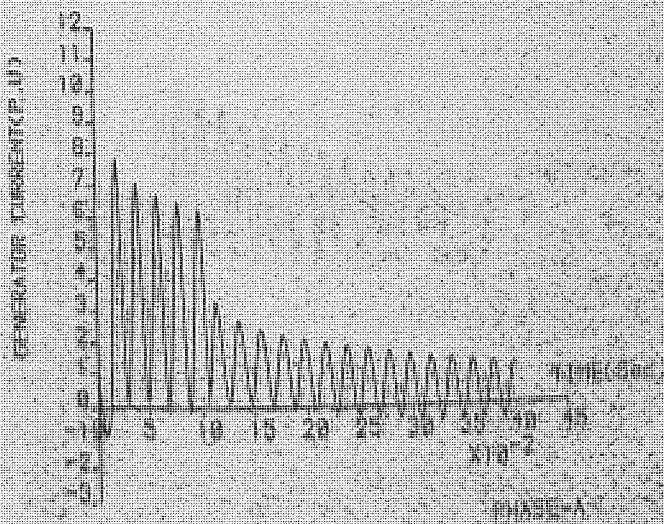
to re-accelerate back to the pre-fault speed, also the generator rotor angle swings back and oscillates until the steady-state mode of operation is restored.

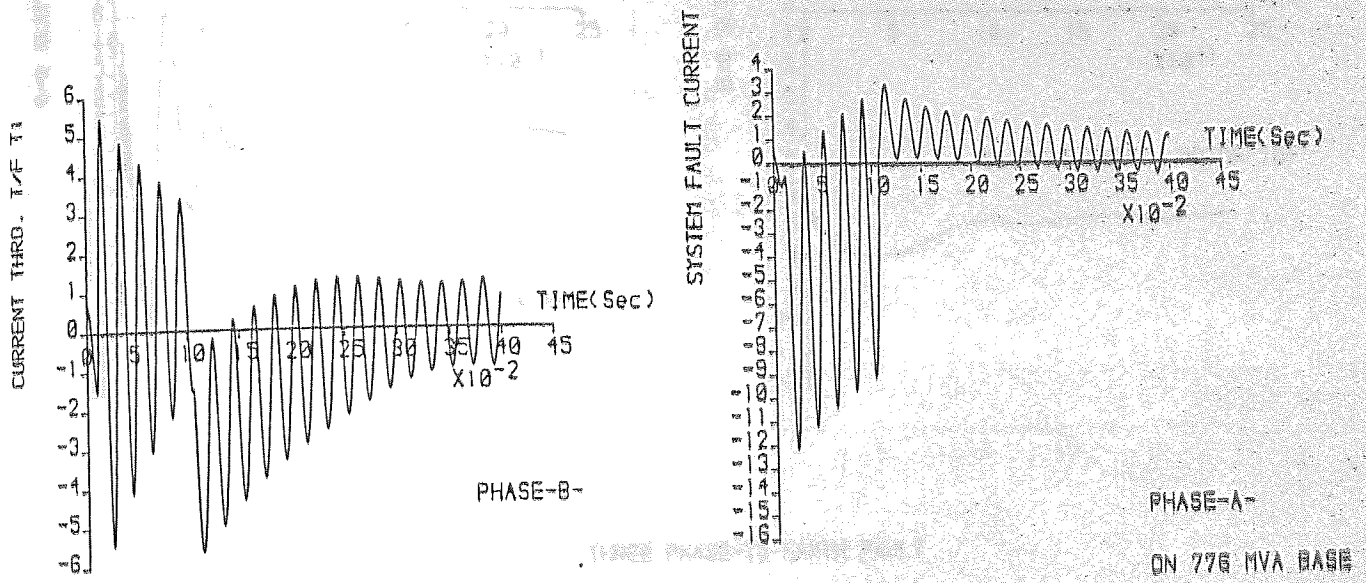
5.9 Conclusions

A computer program to study the transient stability of a system having a large generator and a group of induction motors has been developed. The program allows for the effect of both balanced and unbalanced disturbances to be studied at different locations throughout the system. The program requires 72 minutes of 'CPU' time, using the -HARRIS 5500- computer system, for 2.5 seconds of study. The long computation time arises from the fact that the set of equations representing the induction motors are sensitive to errors arising from the computing routine, as well to the step interval. In this study, a step length of 0.1 milliseconds has found to give satisfactory results. In the next chapter, an improvement in the computing time is achieved by applying a routine other than the Runge-Kutta method to study the isolated system.



THREE PHASE-TO-EARTH FAULT
 FAULT CLEARED AT 0.187 Sec.
 FAULT AT BUS-BARB23
 BASE MVA = 775





THREE PHASE-TO-EARTH FAULT
 FAULT CLEARED AT 0.107 Sec.
 FAULT AT BUS-BAR(B2)
 BASE MVA = 48

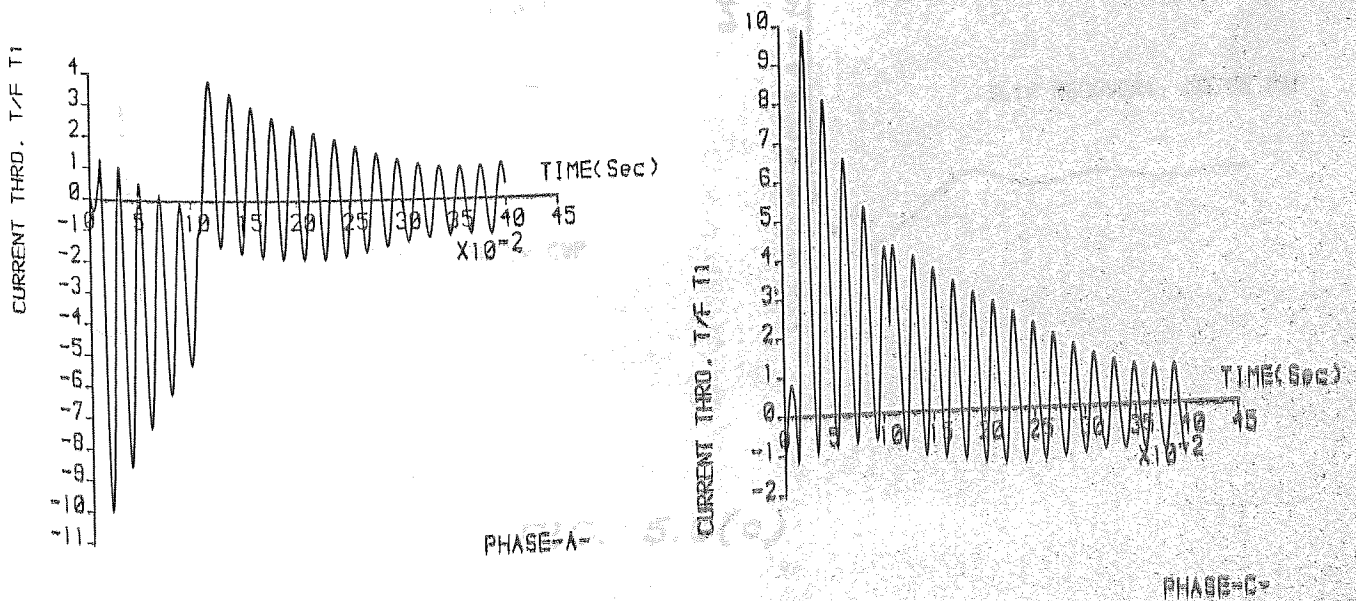
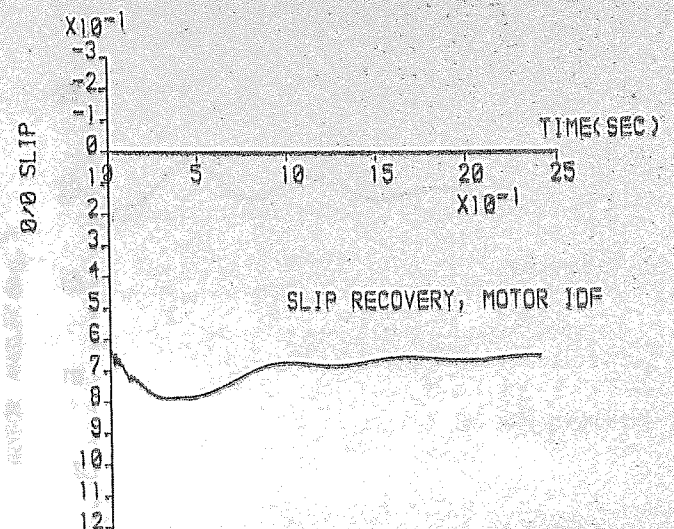
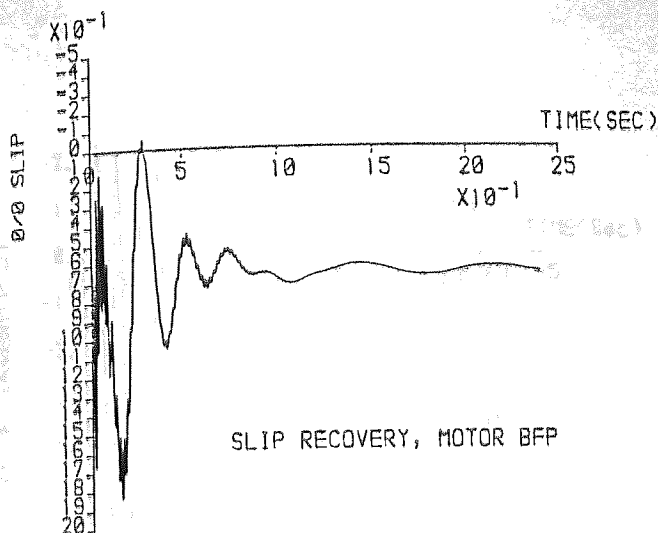


FIG. 5.9(b)



THREE PHASE-TO-EARTH FAULT

FAULT AT BUS-BAR(B2)

FAULT CLEARED AT 0.107 Sec.

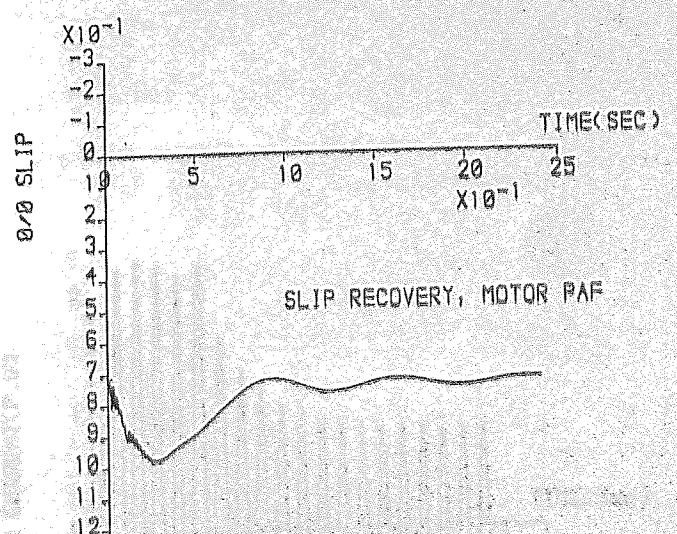
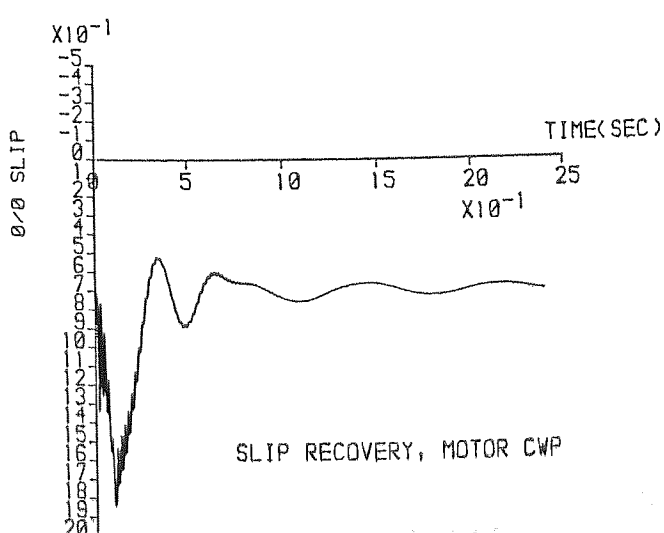
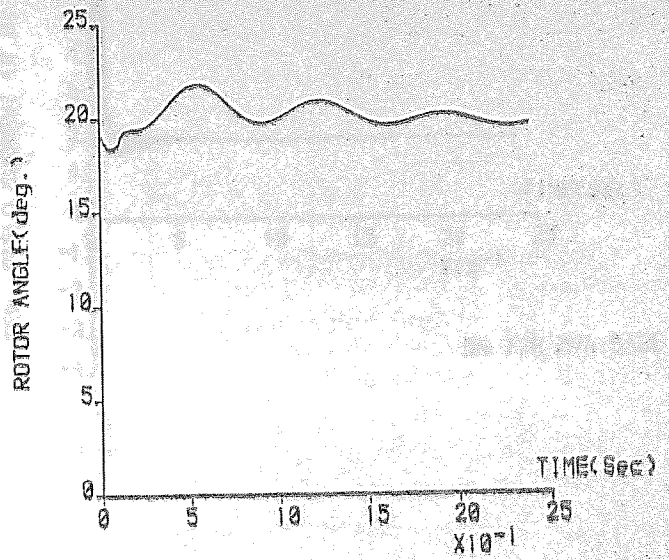
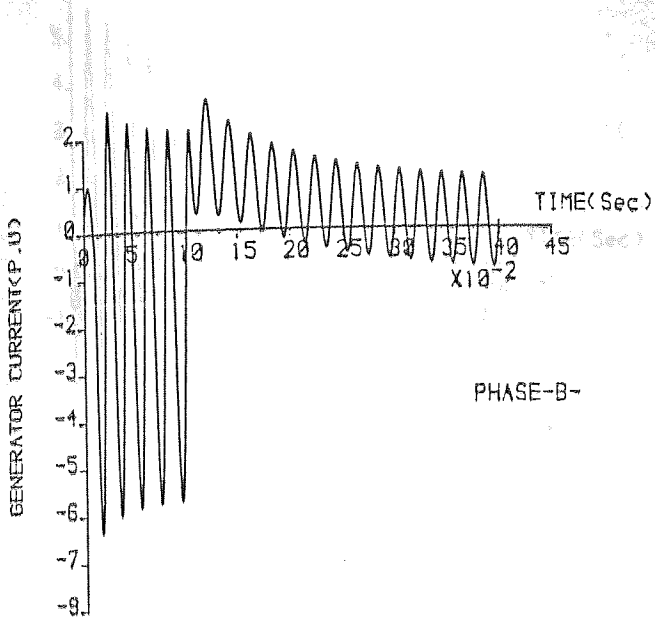


FIG. 5.9(c)



DOUBLE PHASE-TO-EARTH FAULT
 FAULT CLEARED AT 0.107 Sec.
 FAULT AT BUS-BAR(B2)
 BASE MVA = 776

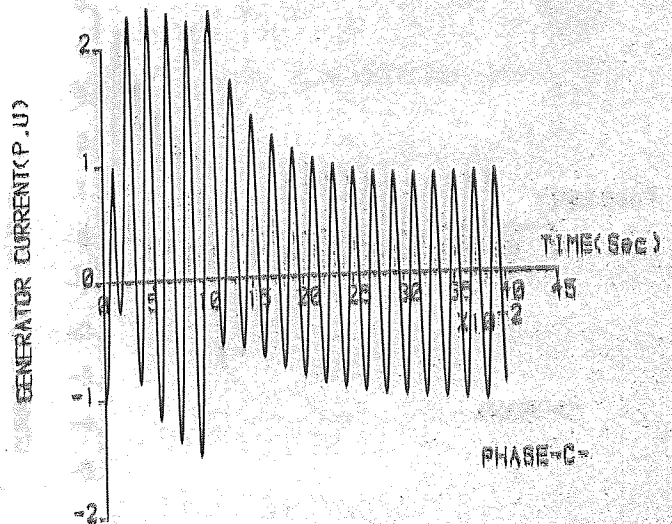
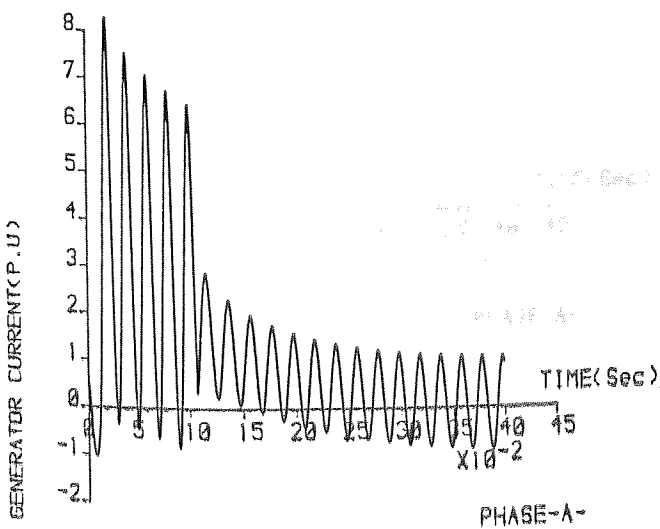
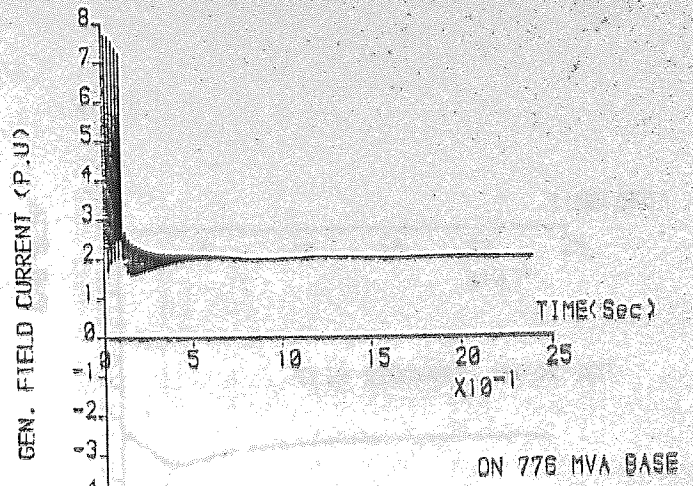
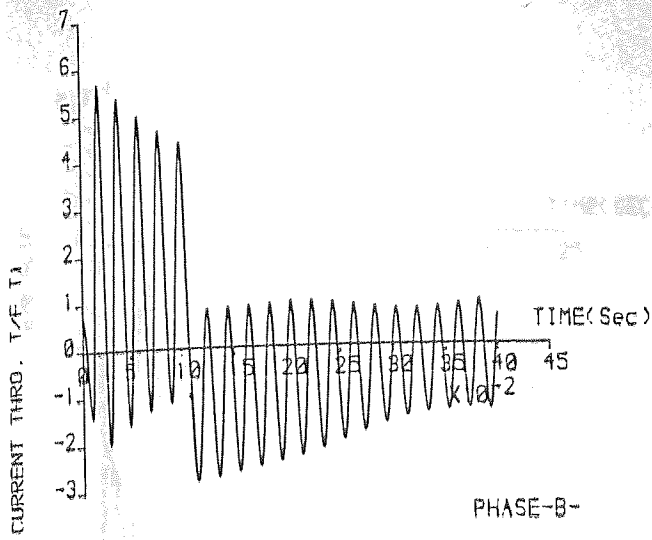


FIG. 5.10(a)



DOUBLE PHASE-TO-EARTH FAULT
 FAULT CLEARED AT 0.107 Sec.
 FAULT AT BUS-BAR(B2)
 BASE MVA = 48

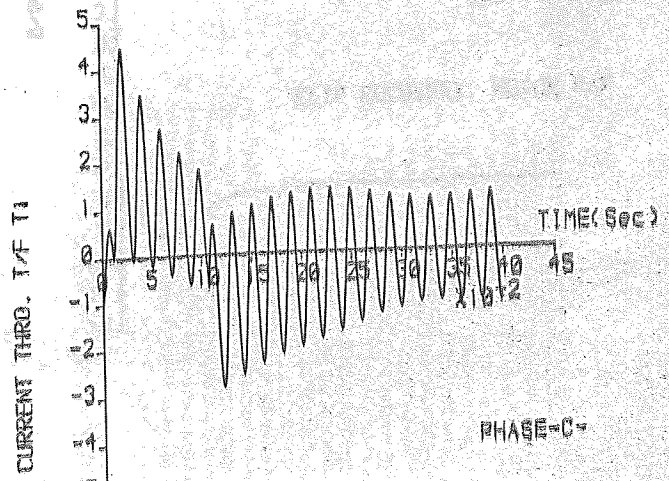
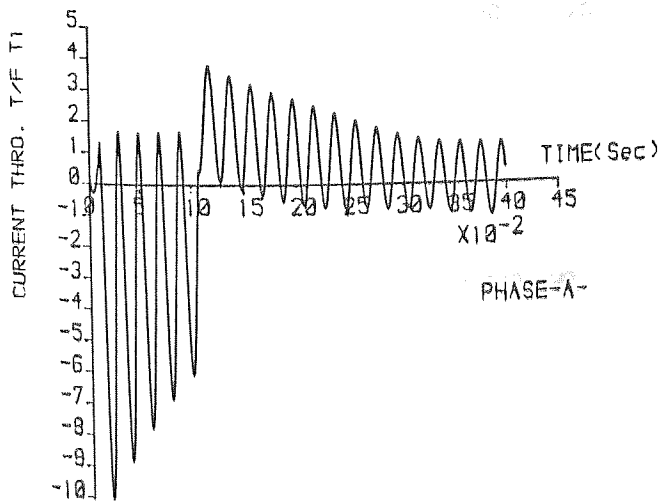
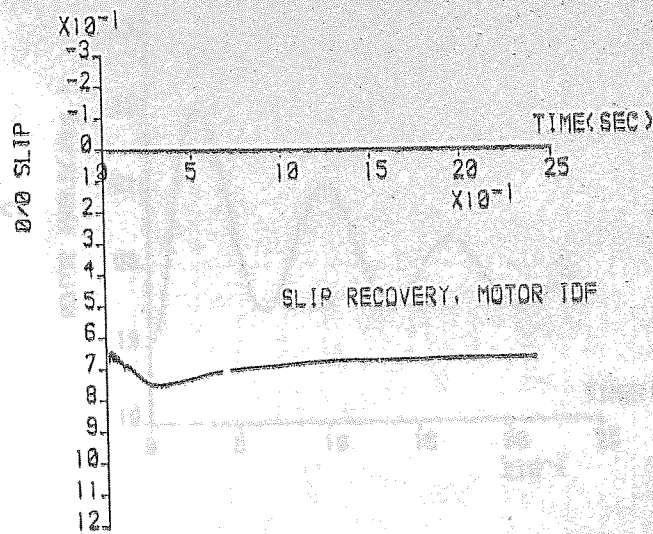
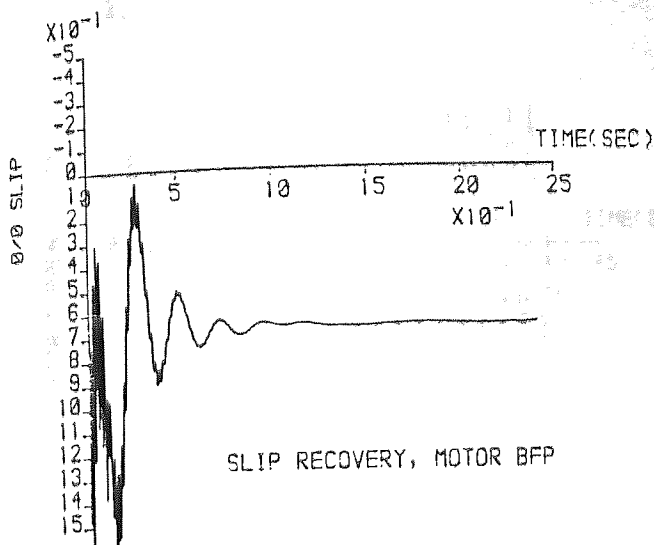


FIG. 5.10(b)



DOUBLE PHASE-TO-EARTH FAULT

FAULT CLEARED AT 0.107 Sec.

FAULT ON BUS-BAR(B2)

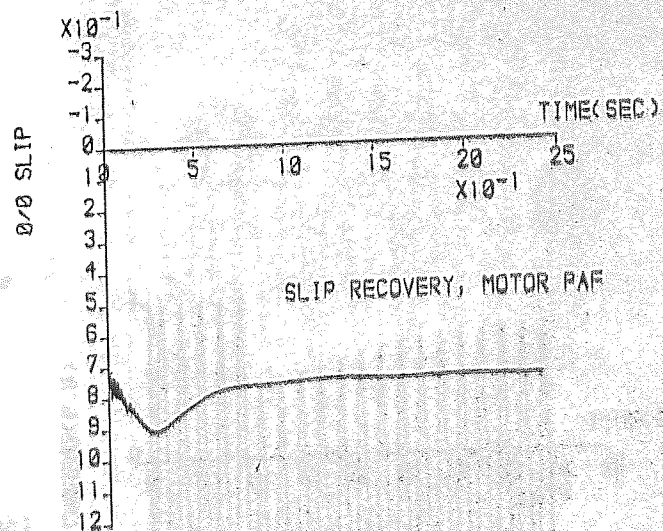
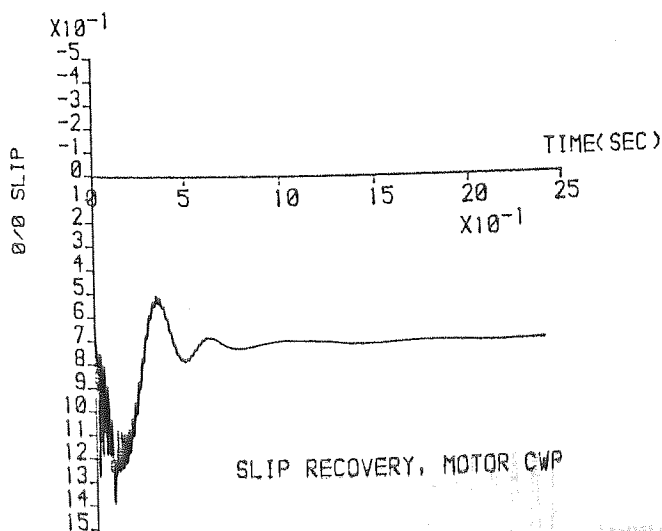
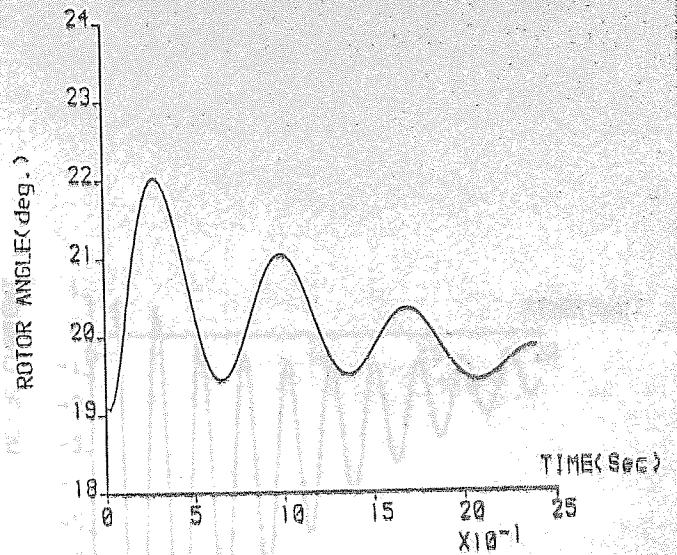
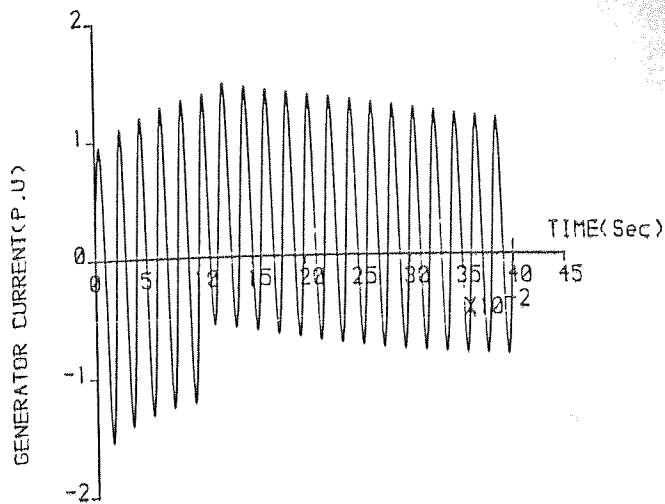


FIG. 5.10(c)



PHASE-B-

THREE PHASE-TO-EARTH FAULT
 FAULT CLEARED AT 0.106 Sec.
 FAULT AT BUS-BAR(B1)
 BASE MVA = 776

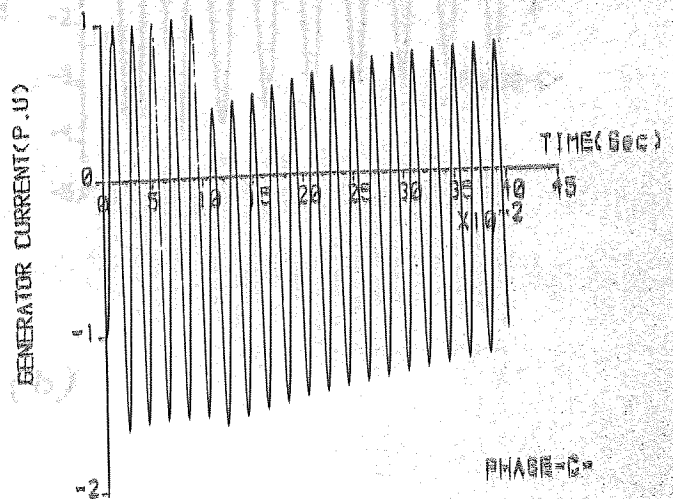
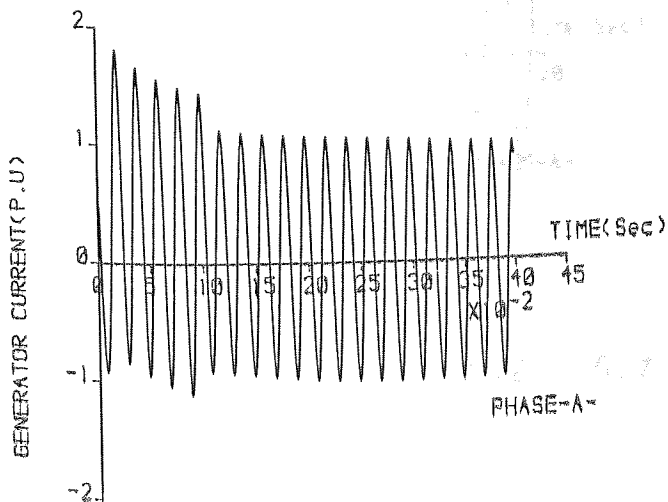
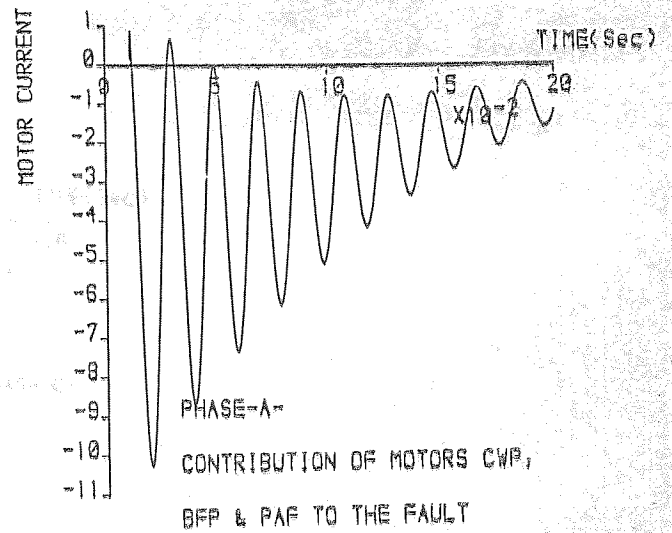
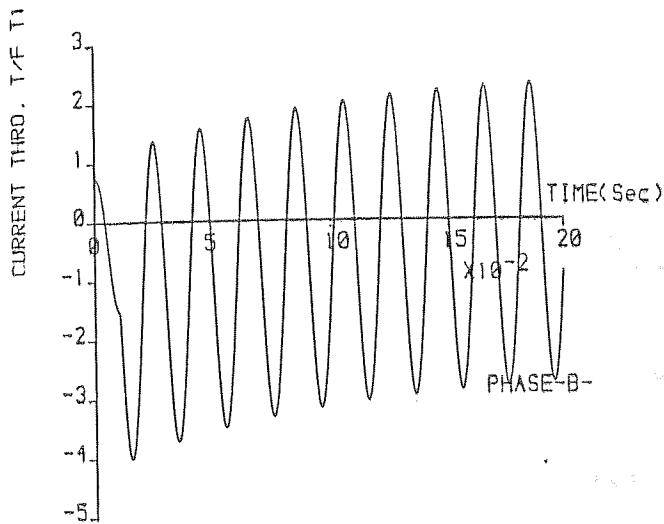


FIG. 5.11 (a)



THREE PHASE-TO-EARTH FAULT
 FAULT AT BUS-BAR(B1)
 CURRENT FED FROM GEN.&SYSTEM

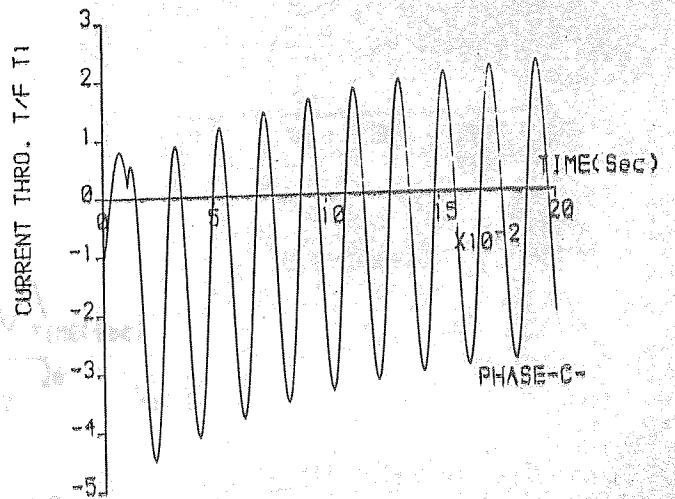
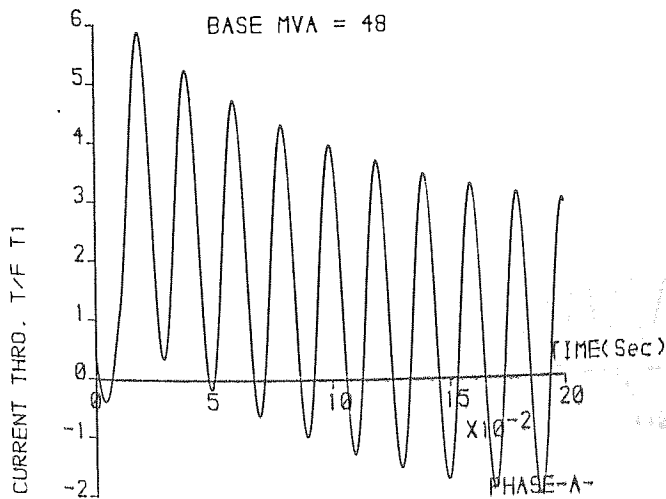
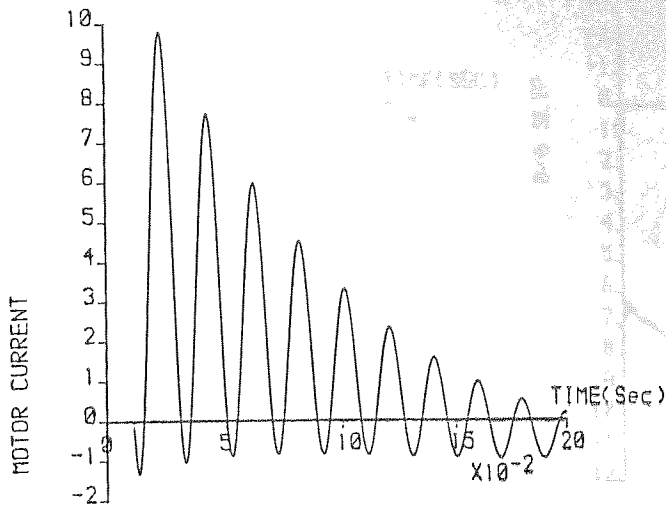


FIG. 5.11(b)



PHASE-C-

THREE PHASE-TO-EARTH FAULT

FAULT AT BUS-BAR(B1)

CONTRIBUTION OF MOTOR CWP

BFP & PAF TO THE FAULT

BASE MVA = 48

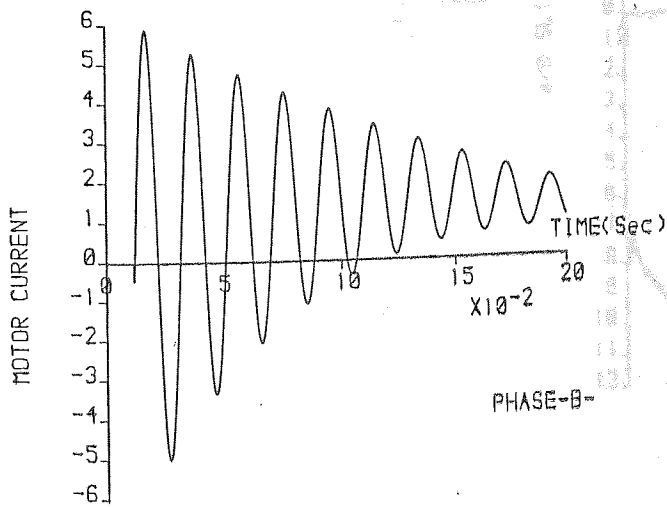


FIG. 5.11(c)

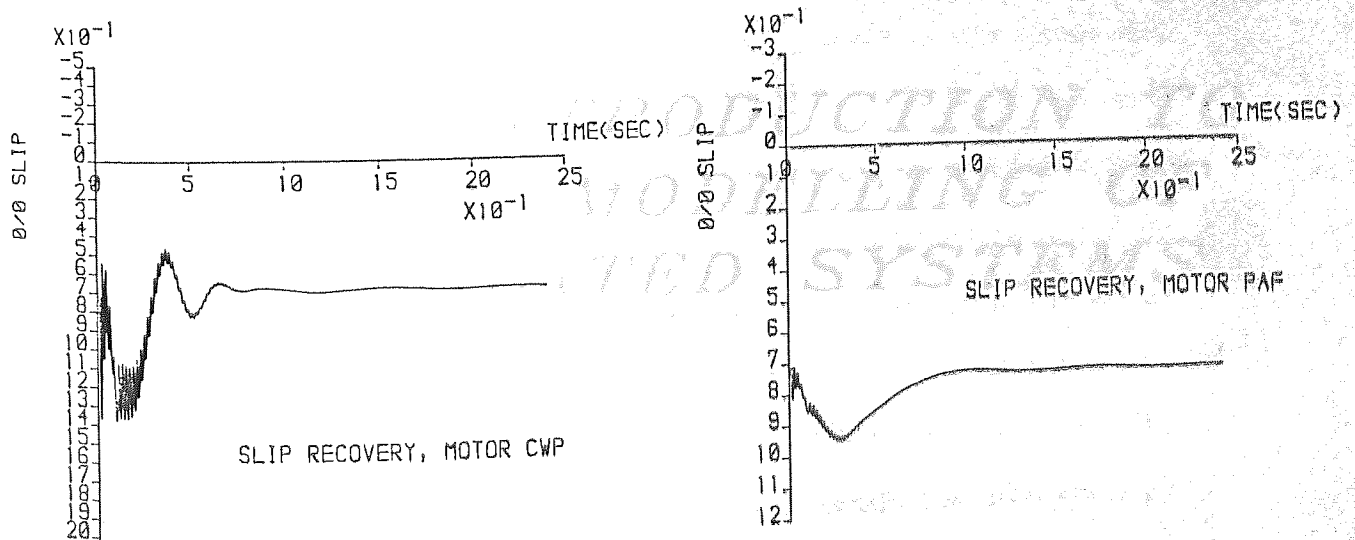
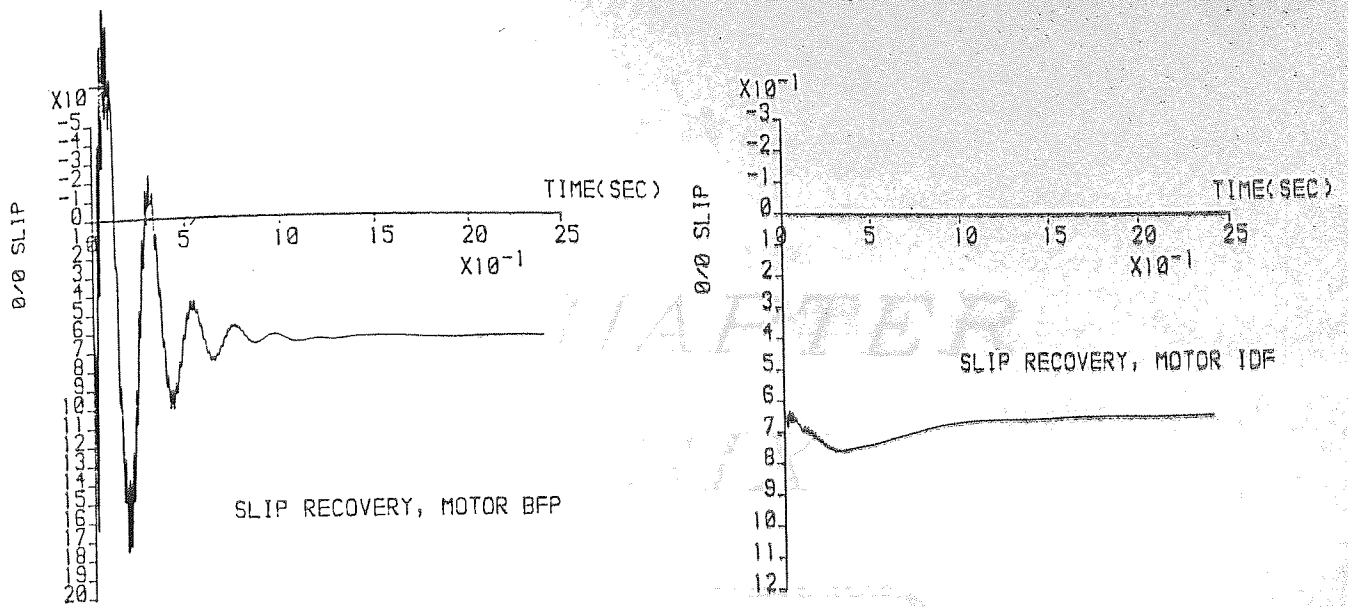
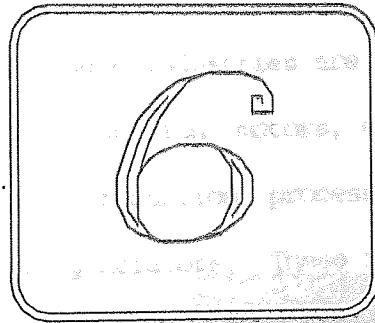


FIG. 5.11(d)

CHAPTER 6

INTRODUCTION TO

CHAPTER SIX



AN INTRODUCTION TO THE MODELLING OF ISOLATED SYSTEMS

The primary objective of this study is to predict fault clearance by using computer software, the study was conducted in a laboratory. Although the inclusion of a fault is important for a complete analysis, the study has been made to

CHAPTER VI

AN INTRODUCTION TO THE MODELLING OF ISOLATED SYSTEMS

6.1 Introduction

In many practical situations, where industries are remote from the national power grid, large induction motors, used for driving pumps and fans required by production processes, are usually energised from large local generators. These isolated systems differ somewhat in their performance from those which are connected to large power systems, which can be modelled using the concept of an infinite bus-bar. This chapter investigates the performance of the isolated system shown in fig. 6.1. In particular, the model is first developed with a main objective of analysing the system for faults to provide information required by system protection engineers. However, as modelling using the phase variable method enhances the ability to predict fault clearance by simply changing a flag in the computer software, the study was extended to include transient stability. Although the inclusion of the generator control systems is important for a complete analysis of the system, little attempt has been made to

GENERATOR

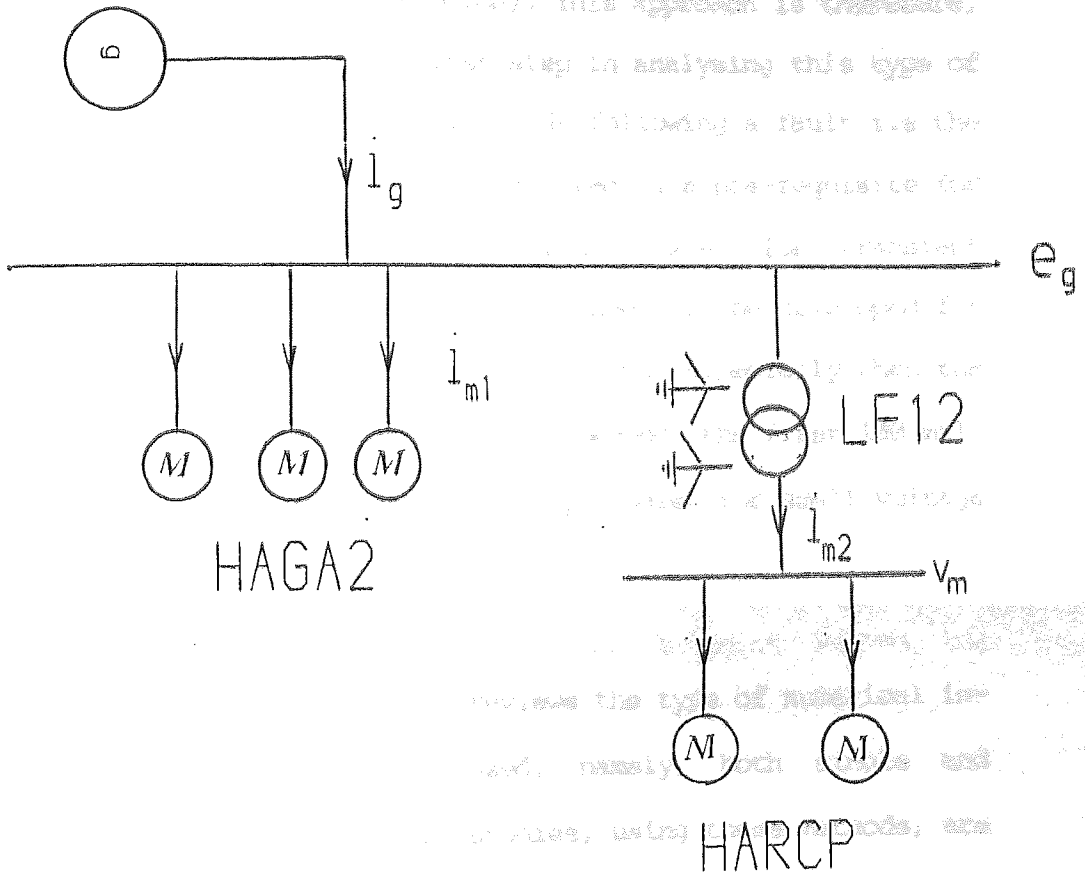


FIG. 6.1

include them in this study (a discussion is given later in the chapter to justify this assumption). This approach is therefore, considered to be only the first step in analysing this type of system up to the first 100 milliseconds following a fault i.e the model developed here can thus be considered as a pre-requisite for investigating the complete isolated system for transient stability. A more sophisticated model needs to be developed for more precise prediction of the system response especially when the simulation time is to be extended beyond the first 100 milliseconds and for transient stability studies for small voltage changes following fault clearance.

The first part of the chapter reviews the type of numerical integration routines that were used, namely, both single and multistep methods. Comparison studies, using these methods, are also presented with the aim of showing how to economize the computation time.

6.2 Integration routines

These are routines used to solve ordinary differential equations. The solution is basically achieved by replacing the differential equation by a difference equation. The routines in use can be broadly divided into two main types. These are:

- a) Multistep techniques in which the values of the previously calculated ordinates are used to calculate the future ordinate.
- b) One step methods, these are routines in which the calculation of the future ordinates do not depend upon the previous ordinates.

... with an error of order

6.2.1 Runge-Kutta methods

These are 'One step methods'. They are techniques which utilize the high order local truncation error of the Taylor methods, while eliminating the computation and the evaluation of the derivative of the function. Different routines have been derived and can be classified according to the order of the truncation error. Among these are, the midpoint method, the modified 'Euler' method and 'Heum' method. They are stated here in the order given above.

... of Runge-Kutta techniques.

$$y_{n+1} = y_n + hf(t_n + 0.5h, y_n + 0.5h(f(t_n, y_n))) \dots 6.1$$

$$y_{n+1} = y_n + 0.5h(f(t_n, y_n) + f(t_{n+1}, hf(t_n, y_n))) \dots 6.2$$

... (y) in case of

... K (n) ...

$$y_{n+1} = y_n + 0.25h(f(t_n, y_n) + 3f(t_n + (2/3)h, y_n + (2/3)hf(t_n, y_n))) \dots\dots\dots 6.3$$

which are classified as Runge-Kutta methods with an error of order two.

In practice the most common Runge-Kutta methods in use are of order four, and they have a local truncation error of order $O(h^4)$. The dependent variable 'y', at any step along the solution, is given by;

$$y_{n+1} = y_n + \delta y \dots\dots\dots 6.4$$

The increment ' δy ' can be estimated using different techniques, some of them are quoted here in the interest of accuracy.

6.2.1.1 Gill process

The increment in the dependent variable (y) is found in this technique by

$$\delta y = K_1/6 + 1/3((1-1/\sqrt{2})K_2 + (1+1/\sqrt{2})K_3) + K_4/6 \dots 6.5$$

where,

$$\begin{aligned}
K_1 &= hf(t, y) & K_2 &= hf(t + 0.5h, y + 0.5K_1) \\
K_3 &= hf(t + 0.5h, y + (-0.5 + 1/\sqrt{2})K_1 + (1 - 1/\sqrt{2})K_2) \\
K_4 &= hf(t + h, y + (-1/\sqrt{2})K_2 + (1 + 1/\sqrt{2})K_3)
\end{aligned}$$

This method has a small round off error and can be economical in storage space, however, these achievements are at the expense of speed.

6.2.1.2 Runge-Kutta 4th order

In early Runge-Kutta fourth order version, using computers with fast high precision arithmetic and adequate storage facilities, the method has been found to give solutions comparable in accuracy with Gills- and in a considerably shorter time. The increment δy can be found, in this method, as follows:

$$\delta y = (K_1 + 2(K_2 + K_3) + K_4) / 6 \quad \dots\dots\dots 6.6$$

where,

$$\begin{aligned}
K_1 &= hf(t, y) & K_2 &= hf(t + 0.5h, y + 0.5K_1) \\
K_3 &= hf(t + 0.5h, y + 0.5K_2) & K_4 &= hf(t + h, y + K_3)
\end{aligned}$$

6.2.1.3 Kutta's three-eighth rule

This method is less accurate when compared to those previously described, the increment can be estimated from,

$$\delta y = (K_1 + 3(K_1 + K_2) + K_4) / 8 \quad \dots\dots\dots 6.7$$

where,

$$K_1 = hf(t, y) \quad , \quad K_2 = hf(t+(h/3), y+(K_1/3))$$

$$K_3 = hf(t+(2/3)h, y-(K_1/3)+K_2)$$

$$K_4 = hf(t+h, y+K_1 - K_2 + K_3)$$

6.1.2.4 Runge-Kutta-Fehlberg

Generally, in the Runge-Kutta methods, estimation of the global error, introduced by the truncation process, is indeterminable. However; using suitable hypotheses on the initial value problem and the difference method, a theorem [9] relating the local truncation error to the global error has been formulated. It essentially states that, " a bound on the local truncation error produces a corresponding bound in the global error". Such a theorem has been used by 'Fehlberg' to control the error by controlling the size of the step length. He produced a technique, in

which the error can be controlled, called the 'Runge-Kutta-Fehlberg' method. The method is mainly used as a Runge-Kutta routine with a local truncation error of order five and is of the form,

$$\bar{y}_{n+1} = y_n + (16/135)K_1 + (6656/12825)K_2 + (28561/56430)K_3 - (9/50)K_4 + (2/55)K_5 + \dots \dots \dots 6.8$$

to estimate the local error in a Runge-Kutta routine of order four, and of the form,

$$y_{n+1} = y_n + (25/216)K_1 + (1408/2565)K_2 + (2197/4104)K_3 - (1/5)K_4 + \dots \dots \dots 6.9$$

The local truncation error is used to define a variable 'q' such that,

$$q = 0.84 (\epsilon h / |\bar{y}_{n+1} - y_{n+1}|)^{0.25} \dots \dots \dots 6.10$$

The value of the variable 'q' determined at the th step is used for two purposes:

- a) To reject the initial choice of the step length 'h' at the n^{th} step if necessary, and repeat the calculation using a step 'qh'.
- b) To predict an appropriate initial choice of 'h' for the 'n+1' step.

The full algorithm is given in references [9,42].

The Runge-Kutta methods claim their superiority from the following advantages:

- 1- No special starting procedure is required.
- 2- A fresh start in each integrating step.
- 3- No estimation is necessary, and hence a straight forward computational procedure is repeated throughout the calculation.
- 4- It integrates with satisfactory accuracy following a discontinuity that occurs at the beginning of a step. For power systems studies, this enables the simulation of switching action including fault clearance and circuit breaker opening effects.

On the other hand, the shortcomings of the method are related to the small step length required which leads to increased computational time. This is especially true when solving system equations

with several exponential terms, some with small indices which tends to increase settling time, or in cases of solving problems involving rapidly decaying transient variables which leads to very small step lengths.

6.2.2 Multistep methods.

These are methods which utilize calculations at more than one previous ordinate to determine the prediction at the next ordinate. They can be classified as:

- either Implicit methods.
- or Explicit methods.

6.2.2.1 The Implicit or closed methods.

In this technique, the dependent variable, at any step of the solution, occurs on both sides of the difference equation and a solution in open form cannot be achieved. The difference equation takes the following form,

$$y_{n+1} = a_{m-1} y_n + a_{m-2} y_{n-1} + \dots + a_0 y_{n+1-m} + h [b_m f(t_{n+1}, y_{n+1}) +$$

$$b_{m-1} f(t_n, y_n) + \dots + b_0 f(t_{n+1-m}, y_{n+1-m})] \dots \dots \dots 6.11$$

The Adams-Moulton technique is an example of the implicit type and there are different versions, e.g. two-step, three-step and four-step. They have a local truncation error of order $(O(h^3))$, $(O(h^4))$ & $(O(h^5))$ respectively. The three-step method and its local truncation error is quoted here;

$$y_{n+1} = y_n + h[9f(t_{n+1}, y_{n+1}) + 19f(t_n, y_n) - 5f(t_{n-1}, y_{n-1}) + f(t_{n-2}, y_{n-2})]/24 \quad \dots\dots\dots 6.12$$

and the error

$$\epsilon = (-19/720)w^{(5)} (\mu)_m^4 h^4$$

The method is known as the fourth-order Adams-Moulton.

6.2.2.2 The Explicit or open methods.

In this technique, the value of 'b' in equation 6.11 is substituted for zero, which results in determining the dependent variable at step n+1 explicitly in terms of the previously determined values. The Adams-Bashforth technique is of the explicit

type, and also exists in different versions i.e two-step, three-step and four-step. The four-step version (known as the fourth order Adams-Bashfourth) is of the form,

$$y_{n+1} = y_n + h[55f(t_n, y_n) - 59f(t_{n-1}, y_{n-1}) + 37f(t_{n-2}, y_{n-2}) - 9f(t_{n-3}, y_{n-3})]/24 \quad \dots\dots 6.13$$

Comparison between an 'm' step Adams-Bashfourth explicit method and 'm-1' step Adams-Moulton implicit method is found [9] to lead to the following facts:

- 1- Both require the same number of the function evaluations per step.
- 2- Both have similar terms in their local truncation errors $(z^{(m+1)} (\mu h)^m)$
- 3- The implicit method was found to have greater stability and smaller rounding off error. This is due to the smaller co-efficients in the terms involving the function 'f' as well as in the local truncation error.

In many applications, multistep methods are not used as described above. However, a first approximation is usually predicted using

the explicit method and an improvement upon the first prediction is made by applying the implicit method. Such a combination is called a Predictor-Corrector method.

6.2.3 Criteria for choice of the step-length.

When an integrating routine is used for solving the differential equations describing a power system, one main approach used to reduce the total computing time is to increase the step length. However; this approach should be governed by the following requirements:

- a) an adequate control of error growth,
- and b) a sufficient number of points for satisfactory solution in graphical form.

In practice, the step-length which satisfies condition (a) above is often determined empirically. For the purpose of selecting a satisfactory maximum step-length, studies are usually carried-out using a range of values of step-length and then comparing the results for the best accuracy which is usually obtained using the smaller step-length.

6.3 Investigations with different integration routines.

As stated before, due to the fast decaying transients introduced by the induction motors, the system equations have to be solved using a small step-length. This leads to an excessive time for computations, which could make the three phase co-ordinate method of system representation unacceptable to some users. This is especially true when the time for study is extended over the first 0.5 seconds. This section is devoted to investigate the possibility of economizing the process of computation by increasing the step-length without introducing much error in the accuracy of the solution.

The study carried out follows the strategy discussed in section 6.2.3 above. The data for motor -HARCP-, given in table 6.3 is used in the study. Computer programs using:

- 1- Runge-Kutta-Gill (equation 6.5)
- 2- Runge-Kutta-Fehlberg (equations 6.8 & 6.9)
- and 3- Predictor-Corrector method (equations 6.12 & 6.13)

were used. These programs solve for the currents following a three phase to earth fault from a steady-state condition. Results obtained using the R-K-F were considered to be the most accurate.

This was taken to be so, because the local truncation error was bounded in the analyses using an accuracy test time 't' advanced by a current step size 'h' only if a Ratio = error[h]/h was not larger than Rmax, otherwise, if Ratio was greater than Rmax, another attempt was made to obtain the dependent variable 'i' such that approximates i(t+h) but with a smaller step size according to equation 6.10. In that way, two parameters 'ScaleMin' & 'ScaleMax' were specified to control the rate at which the step size 'h' was allowed to vary. The values for Rmax, ScaleMin and ScaleMax used

were respectively 10^{-5} , 0.1, 4.0. Also, another variable 'Hmin' was specified such that if the step size becomes too small (less than $Hmin = 10^{-5} (Rmax)^{0.25}$), which indicates apparent singularity near current time 't', then, the program was directed to stop.

The value of the first peak, of the current wave form, obtained using this method is 6.33 p.u (see fig. 6.3) and the CPU time using the - HARRIS H800 - computer system was 1 minute 2.25 seconds for a 0.1 seconds system study. The accuracy of the other two routines, using different step-length, are measured by expressing the first peak of the current wave form relative to that obtained by the R-K-F routine. Also, the improvement, gained by R-K-G & P-C method, in the CPU time using different step-lengths are calculated as a percentage relative to the time taken using the R-K-F routine. Results obtained from these comparisons are tabulated

as shown by table 6.1. In this table, one may observe that the accuracy of the R-K-G and the P-C methods can be higher than 100% with negative gain in the computer CPU time, relative to R-K-F, when the step length is made equal or less than 0.1 seconds. Graphs of current wave forms as well as graphs relating the step-length to the accuracy, and step-length against improvement in computation time were produced for comparison between the three integrating techniques used in the study (figs. 6.2, 6.3, 6.4).

6.4 Outcome of the investigations

From the study described in the preceding paragraph, one may conclude the following;

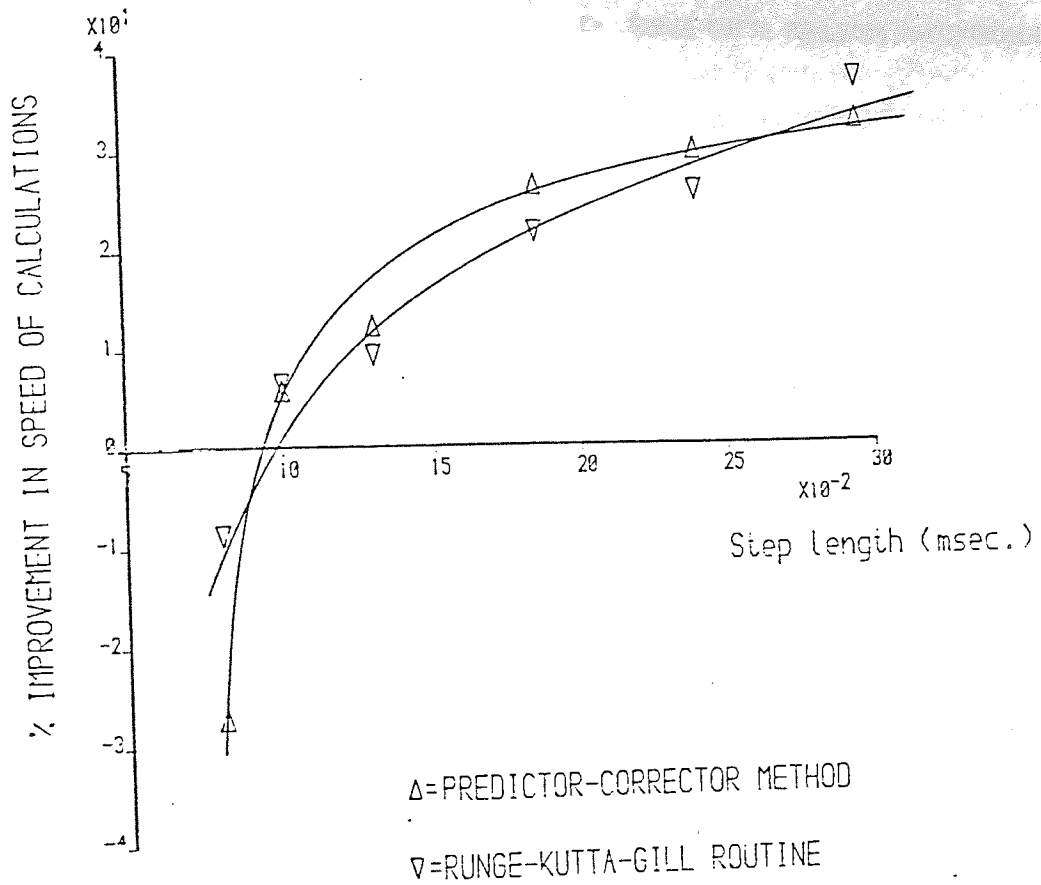
- a) The accuracy obtained from using the R-K-G routine drops significantly as the step length increases (fig. 6.2(b)) which shows that the method is sensitive to the size of the step interval. This proves what has been said previously in this chapter, i.e the method can only work satisfactorily over small ranges of step length, specially when solving system equations involving rapidly decaying transient solutions.

b) The method of the P-C gives a considerable improvement in the speed of the calculation without introducing much loss in the accuracy of the solution (fig. 6.2(b)). The method can be used as an alternative to the R-K-G routine, if the speed of the calculation judged against accuracy, without introducing unacceptable error in the solution.

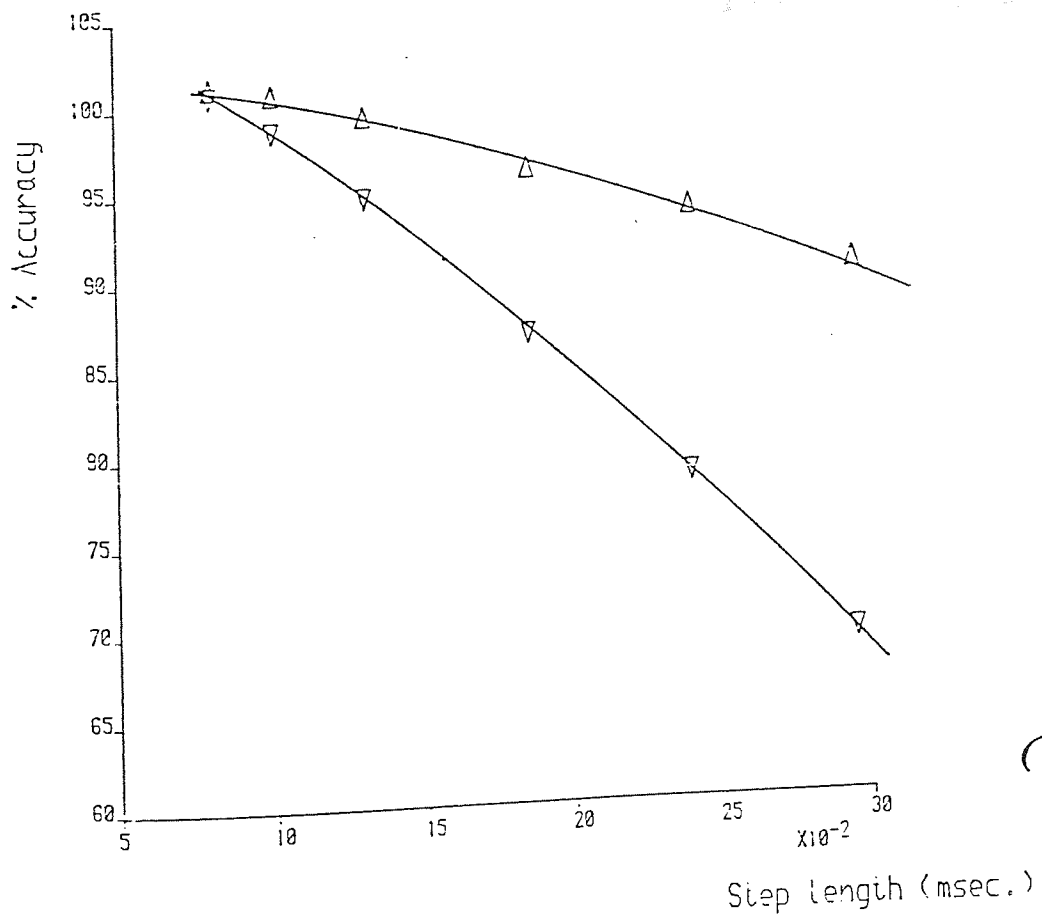
The outcome, as described, of this study, has been utilised to analyse the isolated system of figure 6.1 in the rest of this chapter.

Step-length (msec.)	RUNGE-KUTTA-GILL			PREDICTOR-CORRECTOR		
	Accuracy %	C.P.U (sec)	Gain in C.P.U %	Accuracy %	C.P.U (sec)	Gain in C.P.U %
0.080	100.80	67.70	-8.76	101.30	79.22	-27.26
0.100	98.74	58.25	6.43	100.90	58.66	5.78
0.130	94.90	56.5	9.23	99.60	54.65	12.20
0.185	87.00	48.78	21.63	96.50	45.81	26.41
0.245	78.80	46.23	26.13	94.15	43.59	29.97
0.295	69.40	39.10	37.19	90.8	41.73	32.96

Table 6.1



(a)



(b)

FIG. 6.2

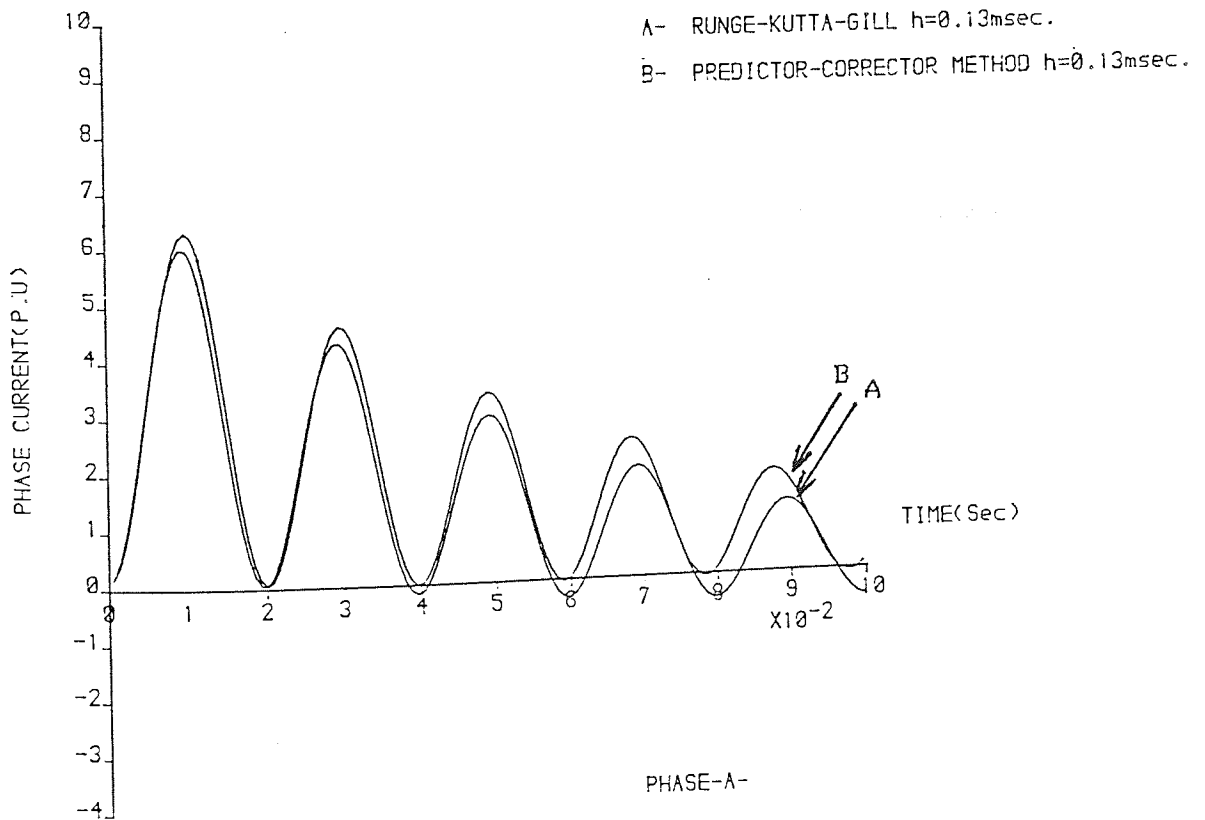
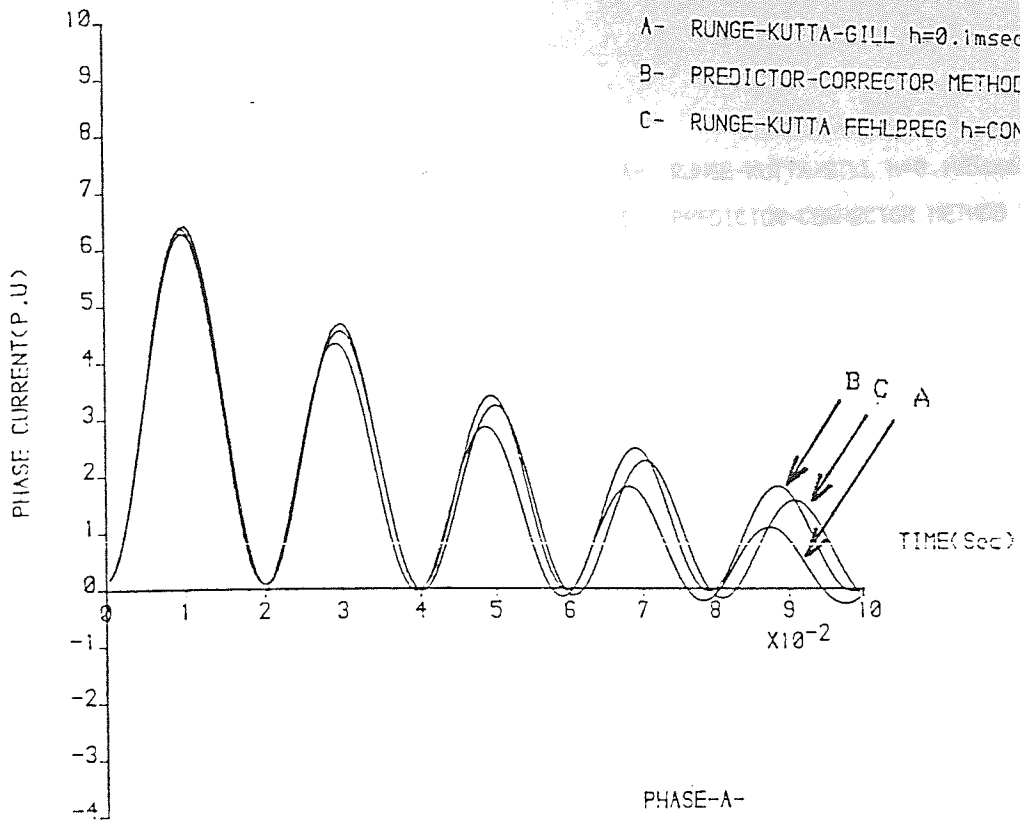
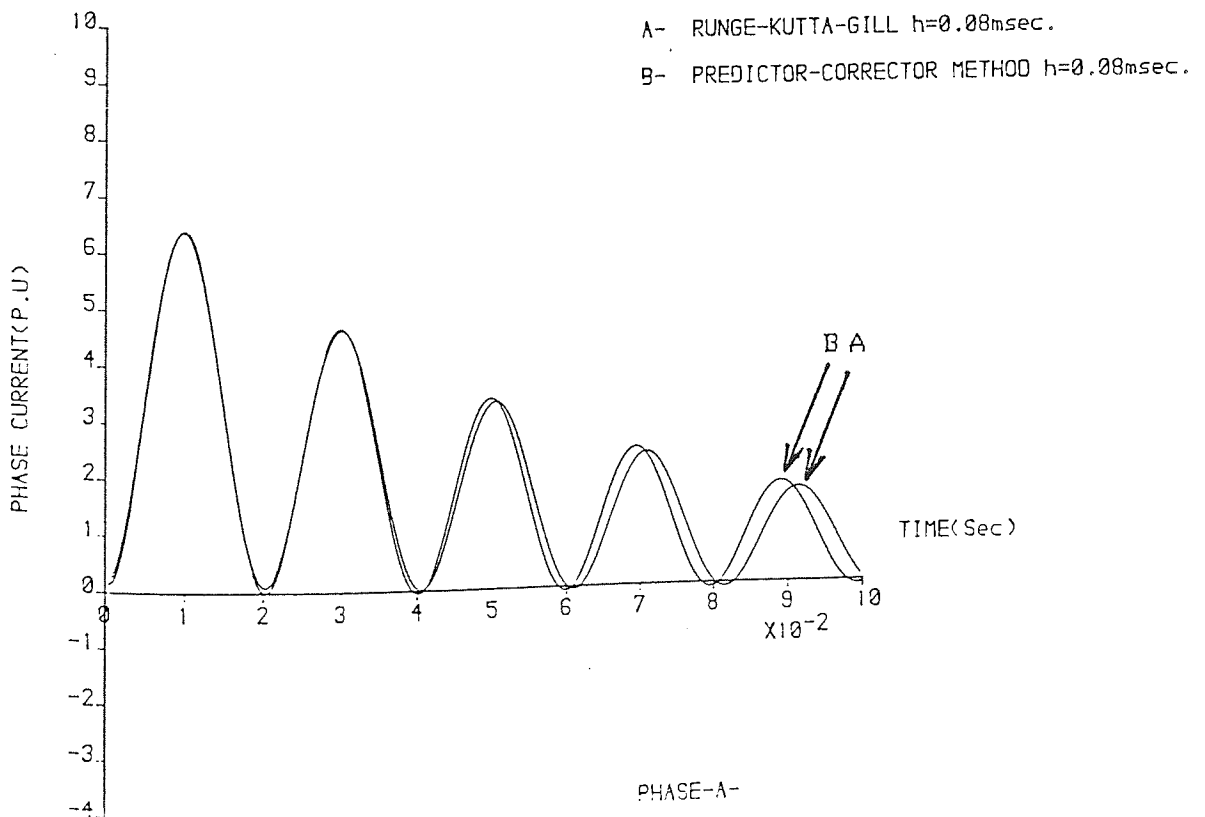
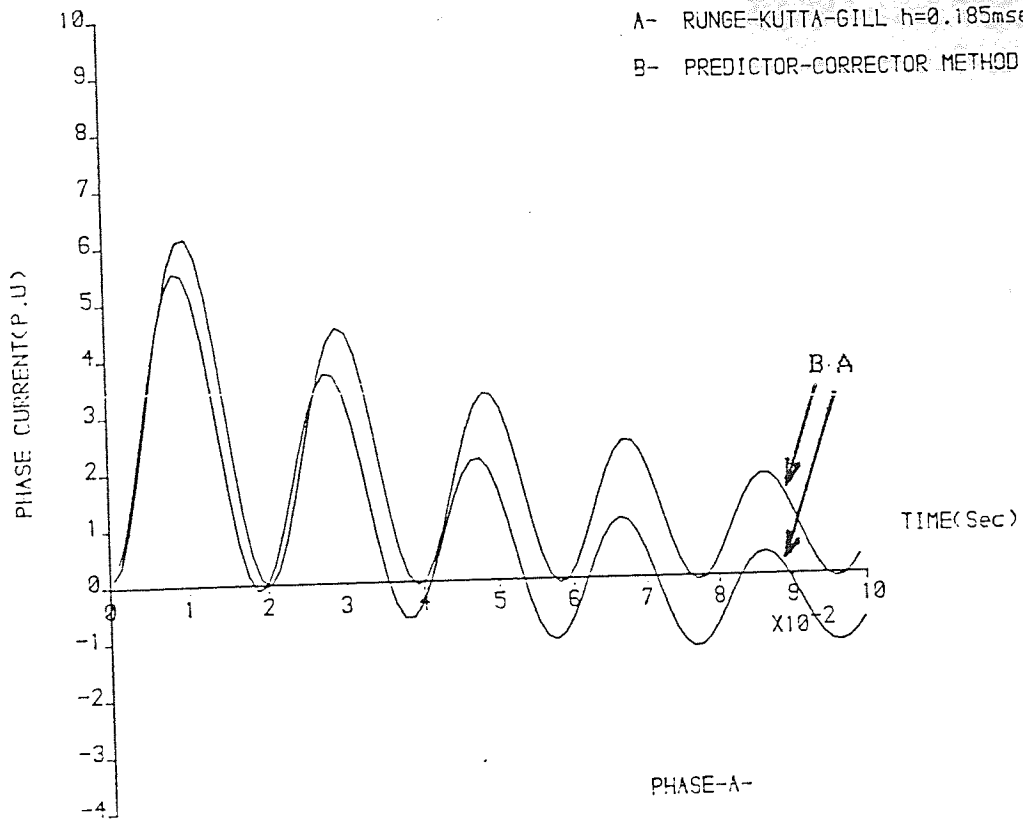


FIG. 6.3



6.5 The system and its equations

Here, in this study, the system (fig. 6.1) is chosen to have an induction motor load comparable in size to the size of the generator in the system. The data for the generator is given in table 6.2 and those for motors and the transformer are given in table 6.3. The initial steady-state condition was established on the assumption that the voltage ' v ' of the bus-bar connected to the driving motors - HARCP - is one per unit. Also, the two motor sets -HAGA2 & HARCP- were assumed to have loads of 75% & 65% of full load at 0.85 & 0.75 power factor respectively. Figure 6.5 shows the system current distribution, based on generator rating under a steady-state mode of operation.

6.5.1 Assumptions & Justification

As mentioned earlier in this chapter, the effects of the automatic voltage regulator (AVR) together with the speed governor were excluded from the model developed to analyse the system. These assumptions are justified for analysing the system for faults during the first 100 milliseconds providing :

Symbol	Description	Value	Unit
S	Rating	24.670	MVA
V	Voltage	11.000	Kv
x_a	Armature reactance	0.120	p.u
x_d	Direct axis reactance	2.220	p.u
x_q	Quadrature axis reactance	2.110	p.u
x'_d	Direct axis transient reactance	0.257	p.u
x'_q	Quadrature axis transient reactance	0.300	p.u
x''_d	Direct axis sub-transient reactance	0.178	p.u
x''_q	Quadrature axis sub-transient reactance	0.178	p.u
x_0	zero-sequence reactance	0.075	p.u
T'_d	Direct axis transient short-circuit time constant	0.800	sec.
T''_d & T''_q	Direct & quadrature axis sub-trans. short-circuit time cons.	0.035	sec.
r_a	Armature resistance	0.003	p.u
H	Inertia constant	3.23	MJ/MVA

Table 6.2

Symbol	Description	Value		Unit
Motor's name ----->		HARCP	HAGA2	
S	Rating	0.702	6.250	MVA
V	Voltage	3.300	11.000	Kv
x _{sl}	Stator leakage reactance	0.182	0.187	p.u
x _{rl}	Rotor leakage reactance	0.091	0.084	p.u
x _m	Magnetising reactance	5.153	5.207	p.u
r _s	Stator resistance	0.014	0.005	p.u
r _r	Rotor resistance	0.013	0.009	p.u
B& C	Mechanical torque co-efficients	-2& 1	-2& 1	
T _l	Losses torque	0.010	0.010	p.u
H	Inertia constant	1.986	2.430	MJ/MVA

Symbol	Description	Value	Unit
Transformer name		LF12 (step down T/F)	
S	Rating	100.000	MVA
V	Voltage	11/3.3	Kv
x _T	Leakage reactance	0.360	p.u on 24.67 MVA
r _T	Resistance	0.018	p.u on 24.67 MVA

Table 6.3

	Generator	Motors	
		HARCP	HAGA2
slip	0.0000	0.0043	0.0038
σ	0.5078	0.0553	0.0716
T	0.3795	0.5000	0.6500

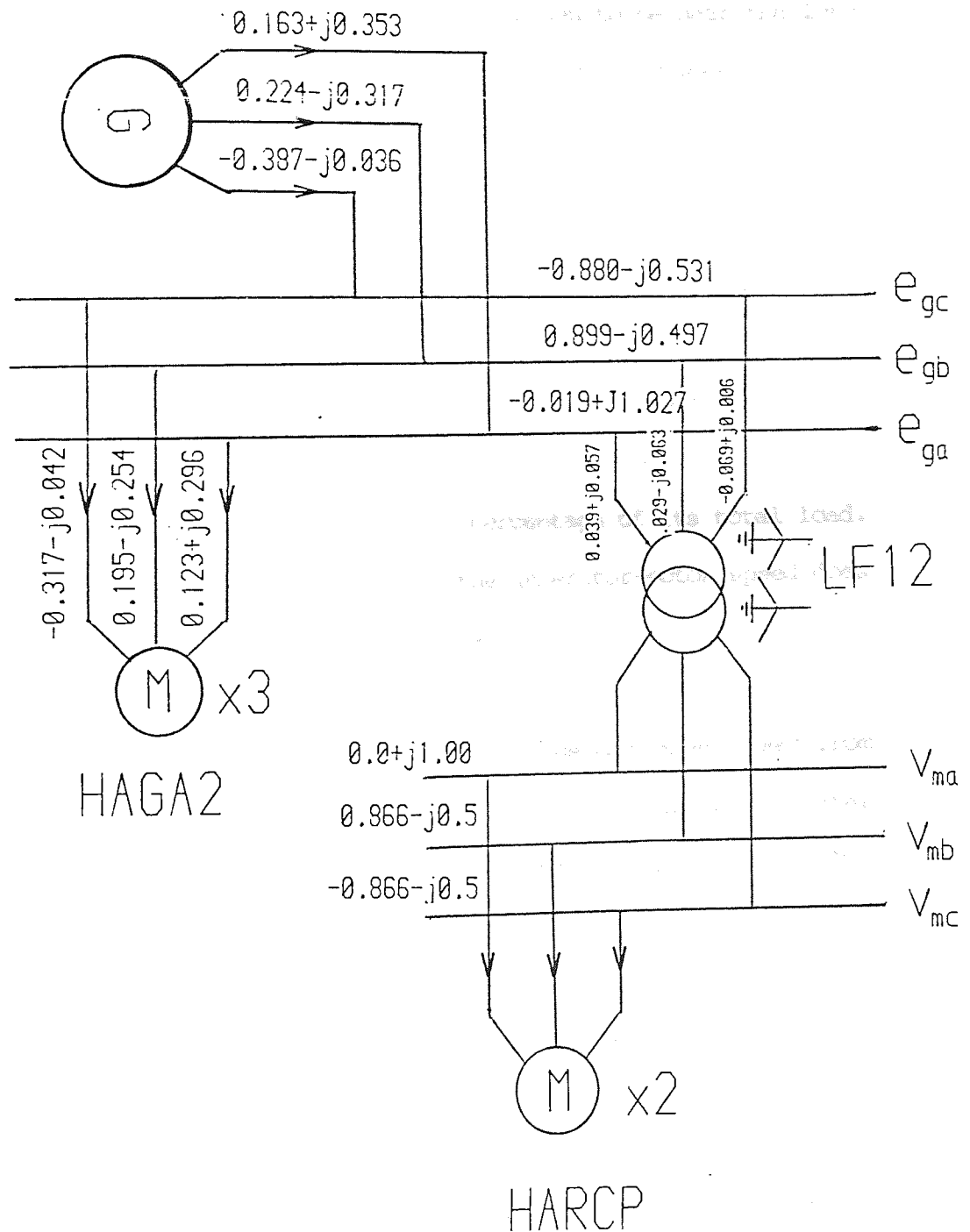


FIG. 6.5

- ... were able to recover to their
- a) The generator, energising the system, has a relatively high inertia constant i.e $H > 3$ MJ/MVA.
 - b) The fault location is chosen to be near the load terminals and will therefore be some distance from the generator terminals.
 - c) The bus-bar connected to the generator terminals takes a high percentage of the total load in the system.

If the above system conditions are to be satisfied, then for a fault on the low voltage bus-bar of the system shown in fig. 6.1, the generator will lose only a small percentage of its total load. Under this condition of operation, the generator-rotor speed does not change significantly (less than 2%).

The impact of the fault on the system voltage can be analysed from two points of view. These are, an effect on the generator bus-bar voltage and a counter effect produced by the action of the AVR .
In more detail :

- a) A fault for a duration of up to 250 milliseconds, applied under conditions a)-c) above, was found to cause a drop in the generator terminal voltage of about 25%. This reduction was found to be acceptable for the motors

in the system as they were able to recover to their prefault steady-state condition without the system going unstable.

- b) In isolated systems, for small variation in the terminal voltage ' δV ', the AVR acts to vary the field voltage in order to correct the deviation in the terminal voltage. However, as most of the AVRs used in these type of systems respond fairly quickly, then for a fault duration of about 250 milliseconds which produces a 25 % variation in the terminal voltage, the field voltage will rise rapidly to twice the rated value and remain fixed until the fault is cleared.

Therefore, from (a) & (b) above, it can be argued that the AVR does not influence the prediction of fault current for the first 200 milliseconds, which is the period when protective devices would operate, although one has to admit that the AVR will improve performance by speeding up the system recovery time once the fault has been cleared. On the other hand if the fault persists, then a field voltage of twice the rated value, set by the action of the AVR, can do little to correct the continually falling generator terminal voltage.

6.5.2 System Mathematical Model

The following paragraph develops the equations that enable the system to be simulated with the induction motors and the synchronous generator. By referring to fig. 6.1, the equation relating the voltage 'v' to motor variables is

$$[U] \{v\}_m = [L]_{m2} \overline{p} \{i\}_{m2} + \overline{p} [L]_{m2} \{i\}_{m2} + [R]_{m2} \{i\}_{m2} \quad \dots 6.15$$

from which the current vector derivative can be found.

The generator bus-bar voltage under steady-state conditions can be defined as,

$$\{e\}_g = \{v\}_m + [L]_t \overline{p} \{i\}_{m2} + [R]_t \{i\}_{m2} \quad \dots 6.16$$

where $[L]_t$ & $[R]_t$ are transformer inductance and resistance matrices.

The generator equations in terms of equation 6.16 can be written as,

$$[U] \begin{Bmatrix} v \\ m \end{Bmatrix} + [L]_t \bar{p} + [R]_t \begin{Bmatrix} i \\ m2 \end{Bmatrix} = [L]_g \bar{p} \begin{Bmatrix} i \\ g \end{Bmatrix} + \bar{p} [L]_g \begin{Bmatrix} i \\ g \end{Bmatrix} - [R]_g \begin{Bmatrix} i \\ g \end{Bmatrix}$$

..... 6.17

and from which the generator current derivative vector is

$$\bar{p} \begin{Bmatrix} i \\ g \end{Bmatrix} = [L]_g^{-1} \{ [U] \begin{Bmatrix} v \\ m \end{Bmatrix} + [-\bar{p} [L]_g] + [R]_g \begin{Bmatrix} i \\ g \end{Bmatrix} \}$$

$$[U] \{ [L]_t \bar{p} + [R]_t \begin{Bmatrix} i \\ m2 \end{Bmatrix} \} \quad \text{..... 6.18}$$

The current derivative vector of the set of motors -HAGA2- is solved in terms of the voltage 'e' i.e

$$\bar{p} \begin{Bmatrix} i \\ ml \end{Bmatrix} = [L]_{ml}^{-1} \{ [U] \begin{Bmatrix} e \\ g \end{Bmatrix} - [\bar{p} [L]_{ml}] + [R]_{ml} \begin{Bmatrix} i \\ ml \end{Bmatrix} \} \quad \text{..... 6.19}$$

where the voltage vector $\begin{Bmatrix} e \\ g \end{Bmatrix}$ is found from;

$$\begin{Bmatrix} e \\ g \end{Bmatrix}_{3 \times 1} = [L]_{g \ 3 \times 6} \bar{p} \begin{Bmatrix} i \\ g \end{Bmatrix} + \bar{p} [L]_{g \ 3 \times 6} \begin{Bmatrix} i \\ g \end{Bmatrix} - [R]_{g \ 3 \times 6} \begin{Bmatrix} i \\ g \end{Bmatrix} \quad \text{...6.20}$$

However, when a three phase to earth fault takes place on the low-voltage bus-bar, the current through the transformer -LF12- (the

fault current) is found by applying Kirchoff's current law at the high-voltage bus-bar i.e at any instant,

$$\{i\}_g = \{i\}_{ml} \cdot B + \{i\}_t$$

(under steady-state $\{i\}_t = \{i\}_{m2}$)

so

$$\{i\}_f = \{i\}_t = \{i\}_g - \{i\}_{ml} \cdot B \quad \dots\dots\dots 6.21$$

where 'B' is a factor normalising the current of motor HAGA2 to 24.67 MVA.

By substituting equation 6.21 in equation 6.16 and using the result to find the generator current derivative vector, the following can be obtained;

$$\bar{p}\{i\}_g = [L_g - L_t]^{-1} \{[F][U]\{v\}_m + [-p[L_g] + [R_g] + [R_t]\}\bar{p}\{i\}_g -$$

$$[[R_t] + [L_t] \bar{p}]\{i\}_{ml} \} \quad \dots\dots\dots 6.22$$

6.6 Faults and transient stability studies.

The following studies were carried out,

- a) A solid three-phase-to-earth sustained fault on the low voltage side of the transformer - LF12.
- b) A transient stability study, due to a three-phase-to-earth disturbance on the low voltage side of transformer - LF12.

6.6.1 A sustained solid three phase-to-earth fault.

The object of this study was to investigate two factors:

- a) Since the size of the induction motors -HAGA2- are comparable to the generator size (6.25MVx3), the contribution of these motors to a fault on the system should be included when selecting the settings of protective gear.
- b) Analysis is also needed for investigating the performance of these machines when fault clearance is delayed. Also, this study is necessary in order to

investigate the behaviour of different relays used to protect the system components.

Two studies were carried out :

1) A study which completely neglected the effect of the AVR.

2) A study in which the action of the AVR was approximated by a linear increase in the field voltage according to the relation $v_f = v_{fo} + kt$ (see

fig. 6.13). The constant 'k' was calculated based upon the fact that the maximum field voltage, of twice the rated value, is reached in 300 milliseconds from the initial value ' v_{fo} '.

The second study was carried out to provide results, for comparison with those obtained by a model which neglects the effect of the AVR.

The studies were carried out by eliminating the elements of the voltage vector $\{v\}_m$ in equation 6.22. Equation 6.20 was used to

find vector $\{e\}_g$ required for the solution of equation 6.19.

Both studies were used to predict the variables for the first 3.25 seconds following the fault application. The P-C method was used, with a step length of 0.24 milliseconds, and the CPU time using the -HARRIS H800- computer system was found to be 19 minutes.

6.6.2 A transient stability study.

The study was implemented by applying and clearing a three-phase-to-earth fault at the low voltage bus-bar. The duration of the fault was 0.241 seconds. The study of the isolated system differs from those of similar systems, connected to an infinite source, in that, the voltage of the faulted bus-bar, following the fault clearance, is determined by the voltage at the generator terminals and the drop across the transformer -LF12-, due to the current drawn by motor -HARCP- .

The same set of equations, that have been used in the study described in section 6.6.1, were also used here during the application of the fault, i.e equations 6.15, 6.20, 6.21 & 6.22. However; following the clearance of the fault, the voltage vector $\{v\}_m$ was made a function of the voltage vector $\{e\}_g$ and was determined using equation 6.16, the set of equations used were 6.15, 6.19, 6.20 & 6.21.

The results obtained from this study are given by figs.(6.13-6.16)

6.7 Discussion

Figure 6.6(a) shows the generator terminal voltage following a three phase-to-earth fault at the low voltage side of transformer -LF12-, obtained by a model that neglects the action of the AVR. The terminal voltage is depressed to about 80% at the instant following the fault application, and continued to fall until it reached a value of approximately 25% after 3.2 seconds. During that time, the power output from the generator fell to a value less than that developed by the turbine ($T = \text{constant}$ determined from analysing the system under a steady-state mode of operation). The unbalance in the net power resulting from the fault, caused the machine to accelerate as seen by the increase in the generator rotor angle (fig. 6.9(a)). Under this mode of operation, a large transient current is fed to the fault. Also, on the occurrence of the fault, the currents which flow in the generator stator windings induce proportional currents in the rotor windings as seen by the increase in the field current in fig.(6.8(b)). This high current in the field winding, which results initially from constant air-gap flux, falls slowly towards its initial value as the other system variables gradually decay to their short-circuit steady-state values. Also, under this mode of operation, the group of motors -HAGA2- contribute (about 25% of the fault current) to the first peak of the total fault current (see fig. 6.8(a)). The

motors were also found to be driven by a low distorted voltage which led to a loss in the machine stored kinetic energy and resulted in a reverse of the direction of power flow. This was indicated by the drop in the speed fig. (6.9(b)).

By introducing an approximation to include the effect of the AVR in the system model, enables comparison between the two cases i.e a case where the field voltage is fixed at the steady-state level and a case where the field voltage is allowed to increase under influence from the AVR, see figs. figs. 6.6 (a), 6.8(b) with figs. 6.10(a) & 6.10(b) respectively. The effect of the AVR was to prevent the generator terminal voltage from falling below 0.56 p.u. Also, one may observe that, once the steady-state short circuit condition is established, the field current remains constant by the action of the AVR at about 3 p.u. (based upon 0.65 loading)

For the case of fault clearance after 0.24 seconds, with the assumption of neglecting the effects of the controlling devices, and with making the voltage at the low voltage side of the transformer equal to a function of the generator terminal voltage and the current drawn by motors -HARCP-, the generator speed started to decelerate. In other words, clearing the fault 0.24 seconds after its application restores the power transmission capability of the generator which in turn has the effect of balancing the

power output against the power input. As a result, the system gradually settles, after a few swings of the generator rotor angle, to its original prefault steady-state condition (see fig. 6.14(a)). This is clearly shown by the slow change in the rotor angle, that was accompanied by a slow growth in the generator terminal voltage figs. (6.12(a) & 6.13(a)) [$P = \frac{VE}{X} \sin \delta$, P, E & X are constant while V increases and δ decreases).

Figure 6.14(b) shows the percentage slip-time characteristic of motor -HAGA2-. For the purpose of the analyses, this characteristic can be divided into two parts i.e, a part following the fault application and a part corresponding to the post fault clearance. The first part expresses the slip variation with the motor being driven from the distorted voltage 'e', followed by a steep drop in the speed afterwards.

Following the fault clearance, the motor starts to draw energy from the supply to compensate for the loss in the stored kinetic energy. This was indicated by the high currents that are associated with the large air-gap torque developed. Since the machine was not fully loaded and had a relatively low inertia, the rotor overspeed, lasted for about 130 milliseconds, giving a value above synchronous speed as shown in fig. (6.14(b)), before it settled at the sub-synchronous initial value. Again, one may observe from the results obtained that the motor variables passed

through a state of a gradual and steady rise towards the value of the pre-fault steady-state condition of operation (figs. 6.12(b) & 6.14(b)). Indeed, such behaviour shows the interaction between the motors and the generator, since the transient performance of the generator has been influenced by the motors performance.

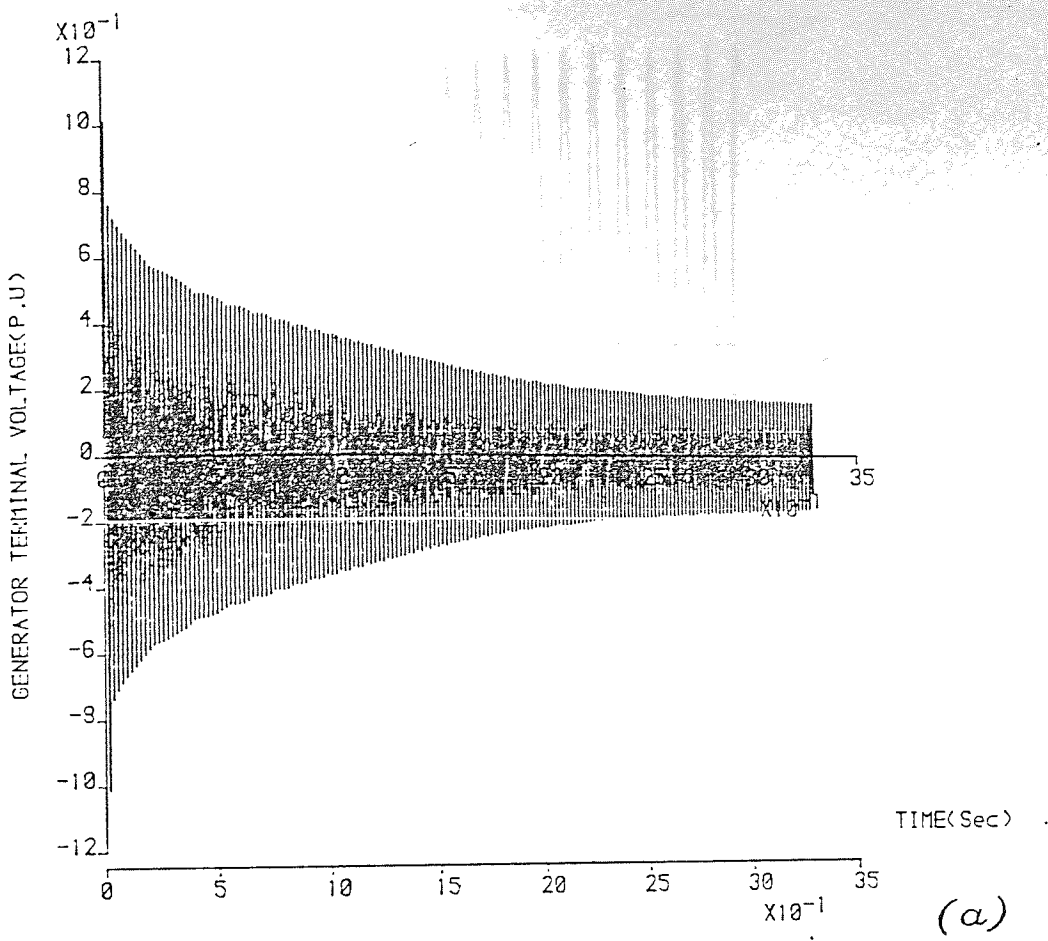
6.8 Conclusions.

In solving systems equations, containing rapidly changing variables, a Predictor-Corrector method was found to give an improvement in the speed of calculations compared to the Runge-Kutta routines, together with an acceptable level in the accuracy of the solution. The method may be used in situations where system studies require the simulation time to be extended over the first 100 milliseconds i.e between 1 to 5 seconds. The method described in this chapter was used to analyse an isolated system for a sustained three phase-to-earth fault and to study transient stability with the assumptions that the generator input power and the field voltage are kept constant during the transient period.

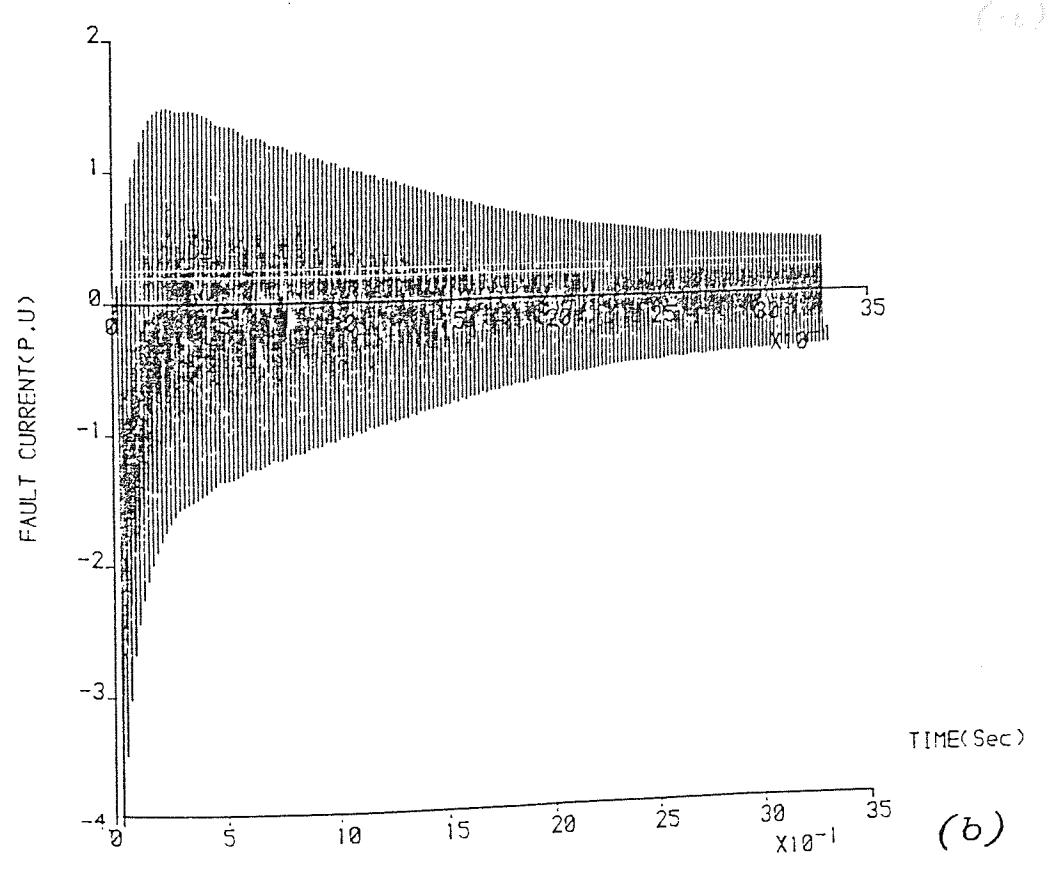
In the case of a three phase-to-earth fault at the low voltage side of the transformer, the generator terminal voltage falls suddenly to approximately 80 percent. Under this condition, the induction motors, connected to the generator terminals, suffer a drop in speed and consequently a loss in the stored kinetic

energy. The losses result from the release of the trapped magnetic energy in the machine air-gap, leading to the high currents that contribute (approximately 25 %) to the total fault current.

Following the clearance of the fault, the motors consume energy from the generator in a process of speed recovery. This situation is accompanied by a phase of operation, where both the motors and the generator, are operating in an oscillatory mode before being restored to the state of the prefault condition of operation.

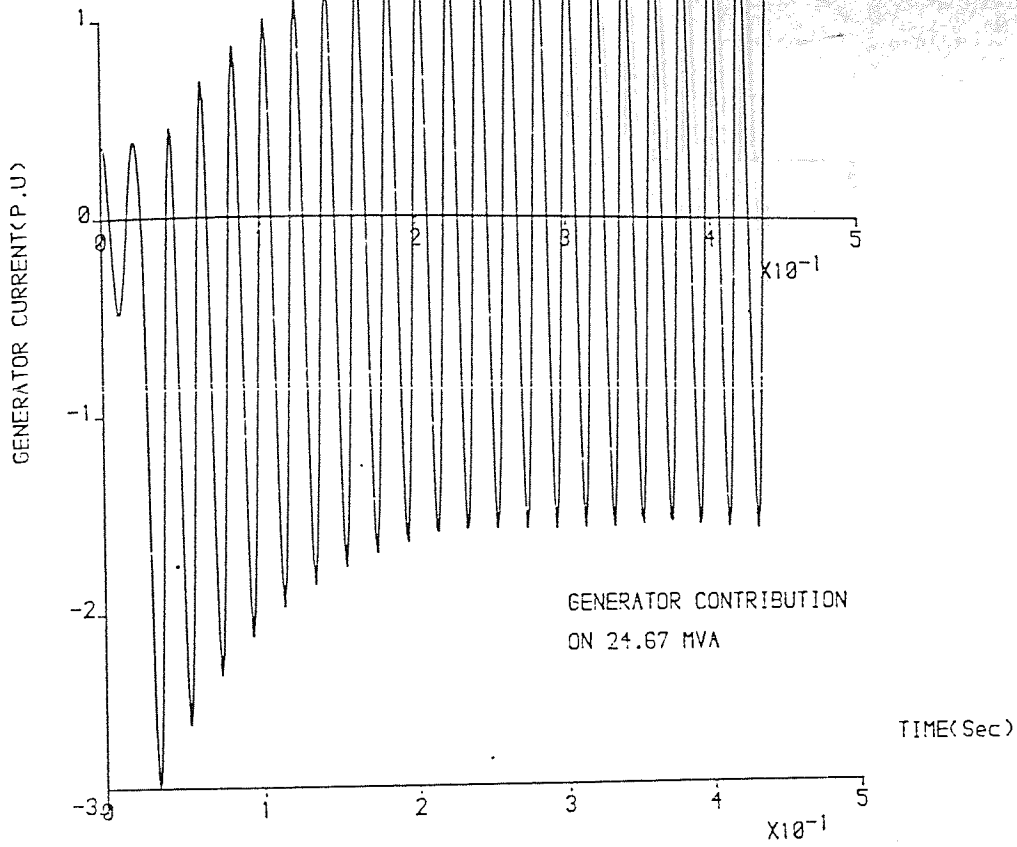


(a)

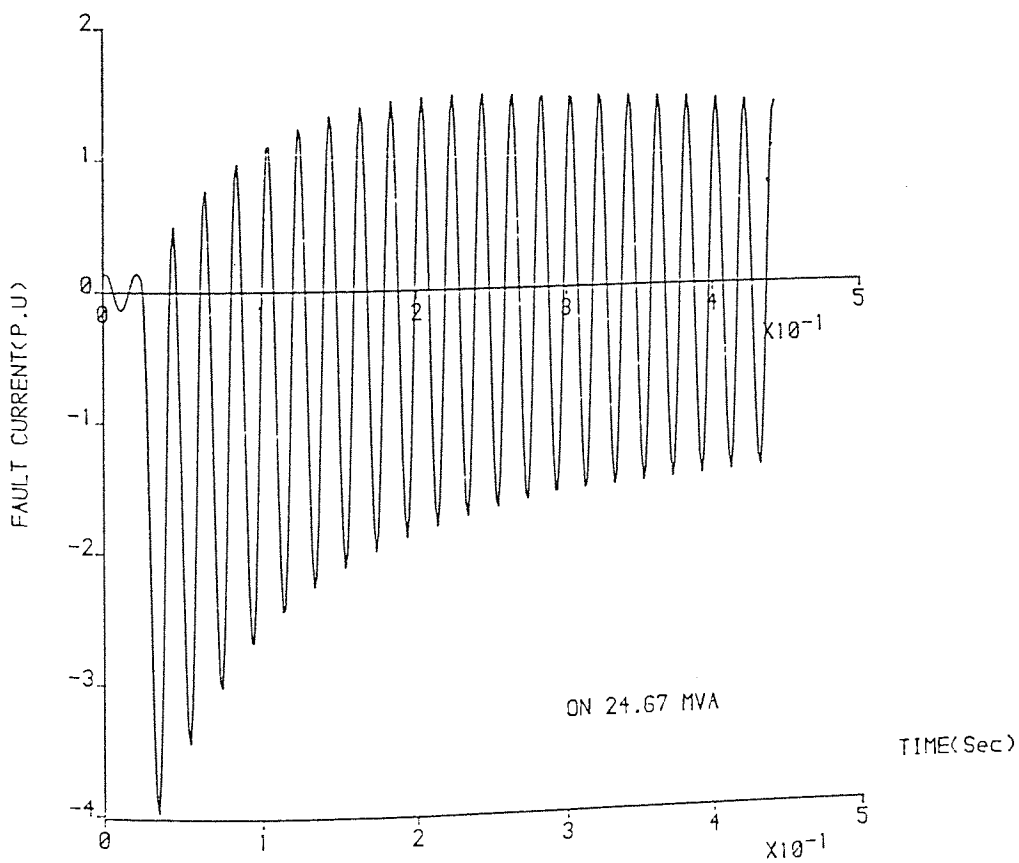


(b)

FIG. 6.6



(a)



(b)

FIG. 6.7

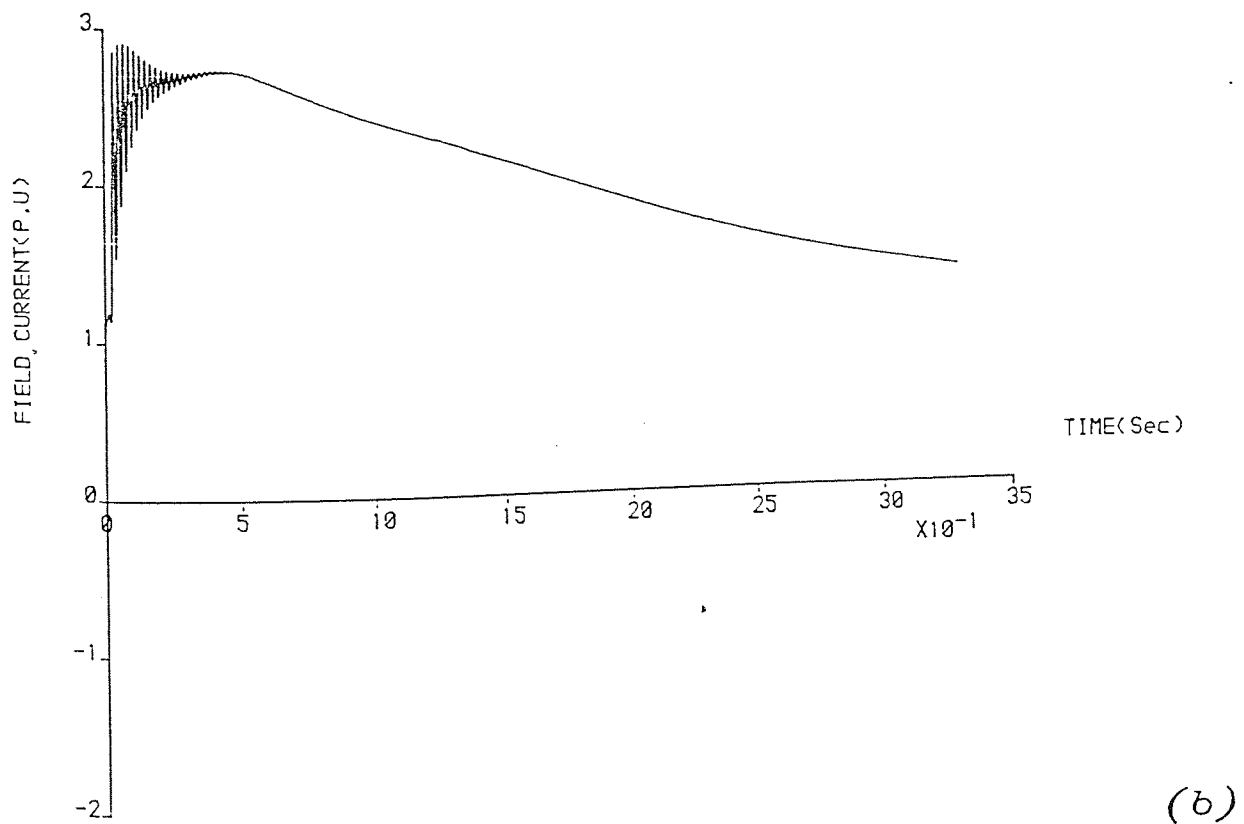
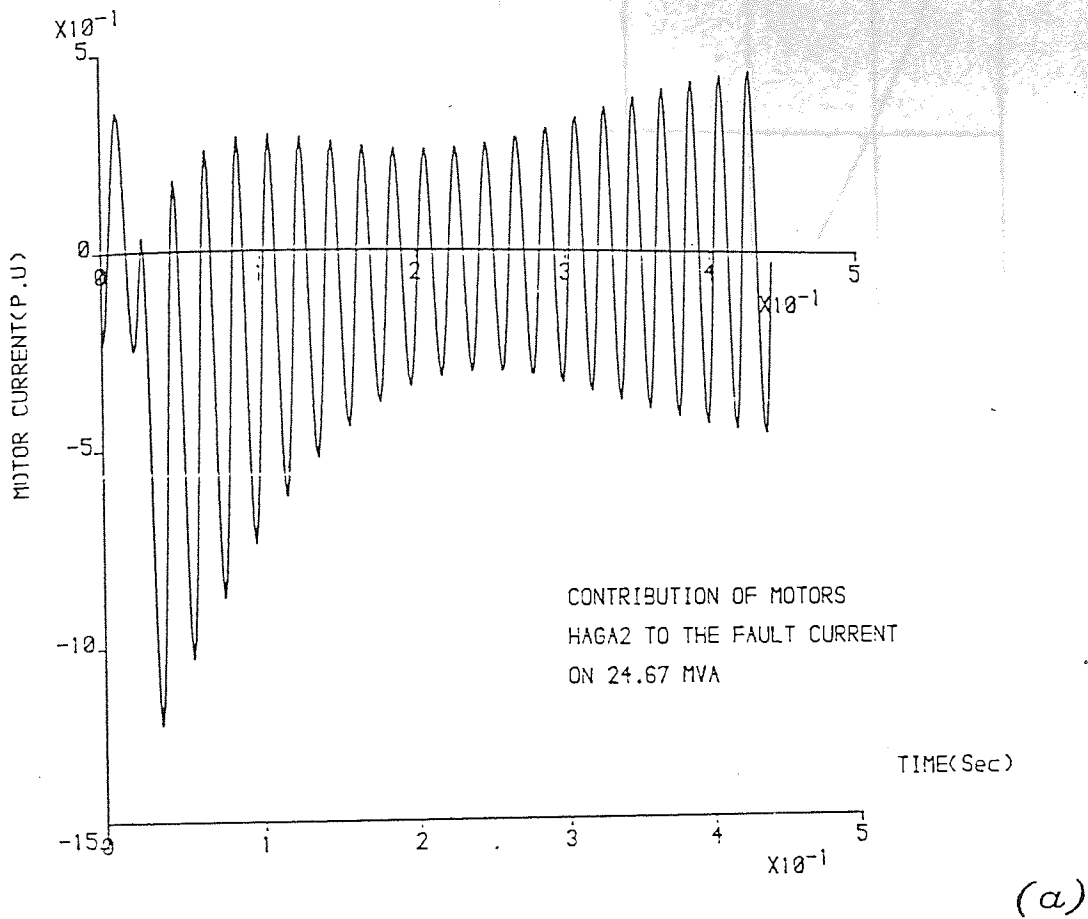
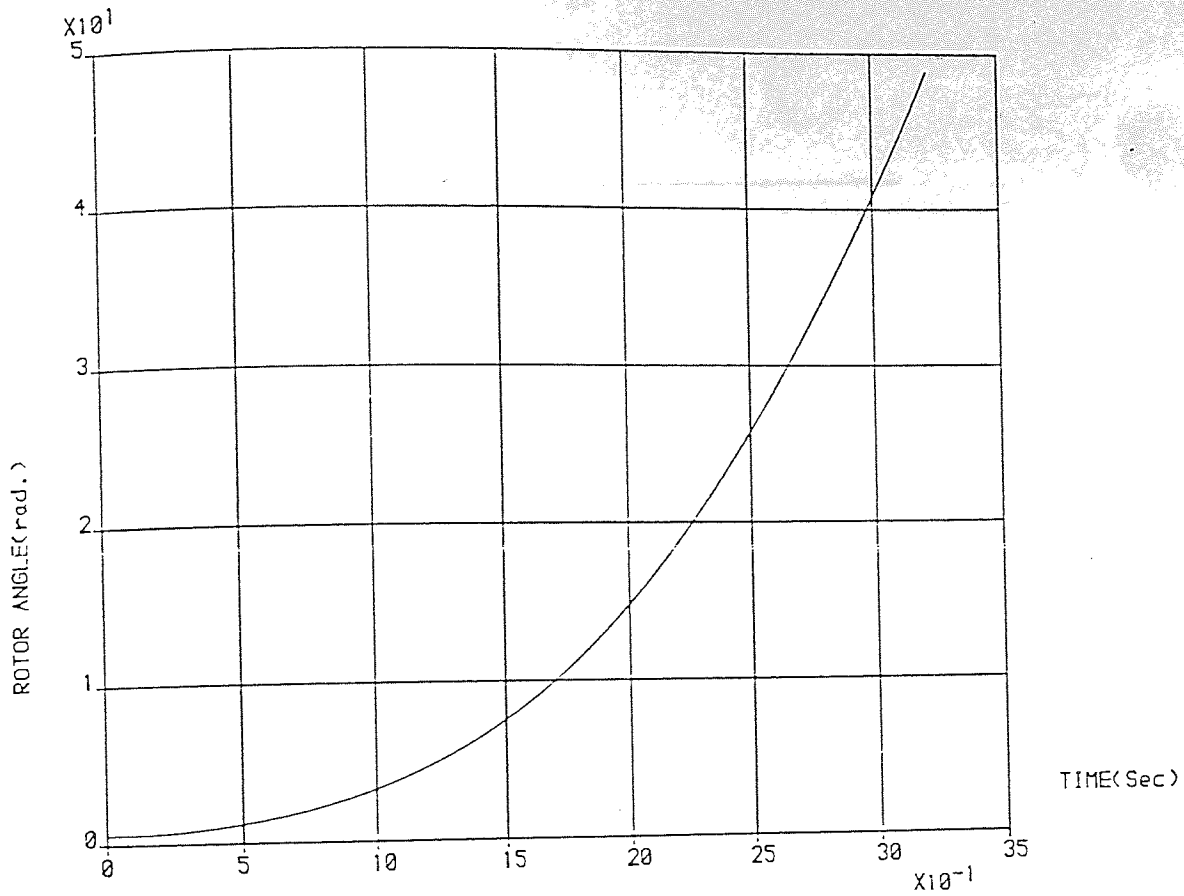
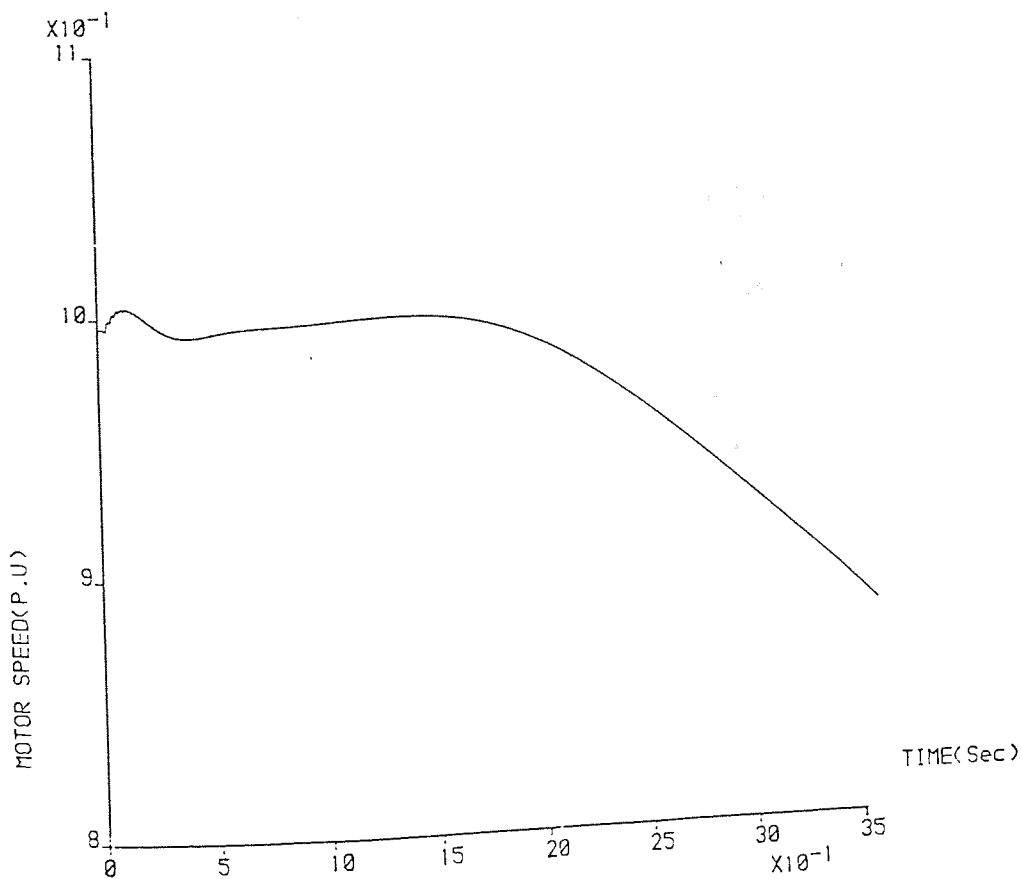


FIG. 6.8



(a)



(b)

FIG. 6.9

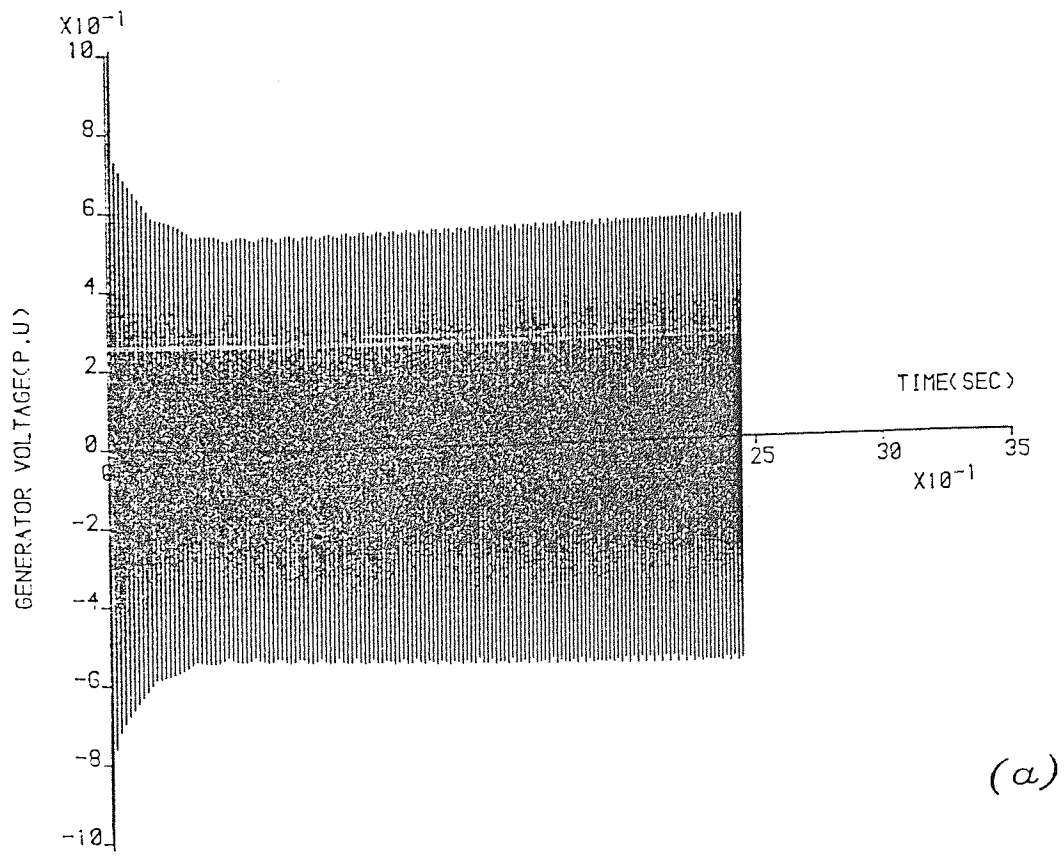
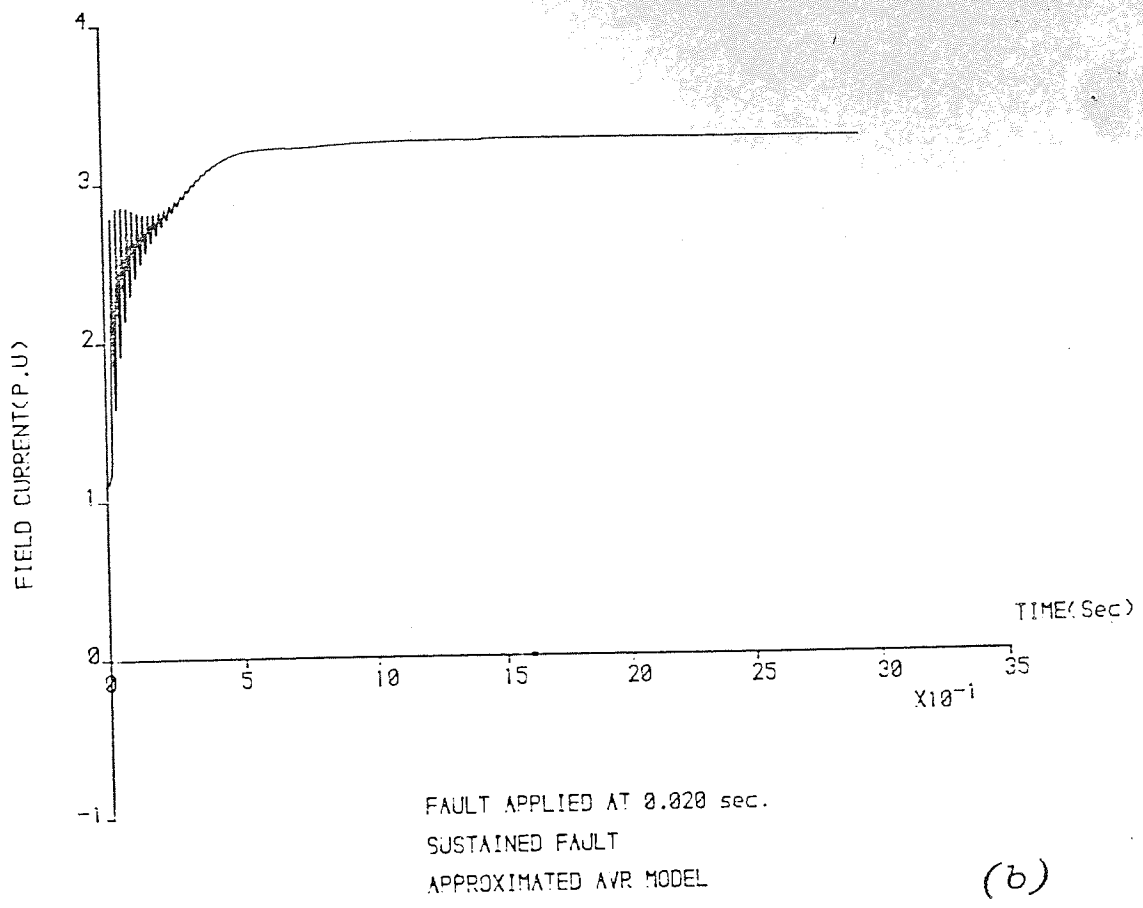
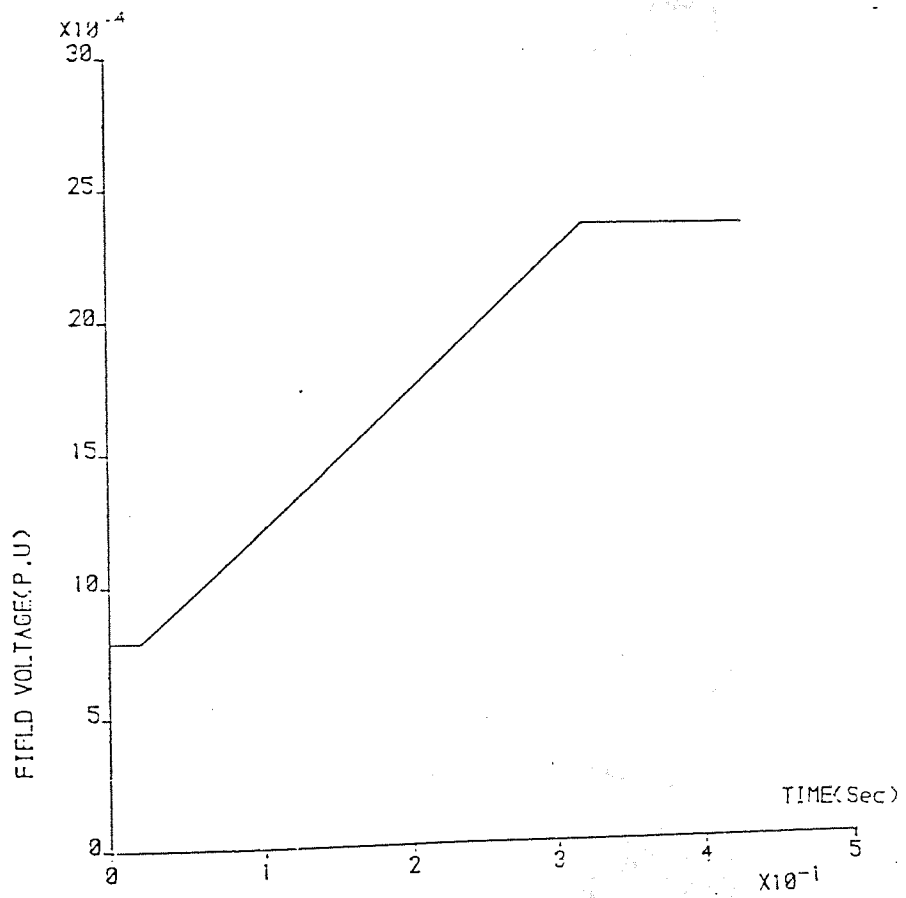


FIG. 6.10



FAULT APPLIED AT 0.020 sec.
 SUSTAINED FAULT
 APPROXIMATED AVR MODEL

FIG. 6.11

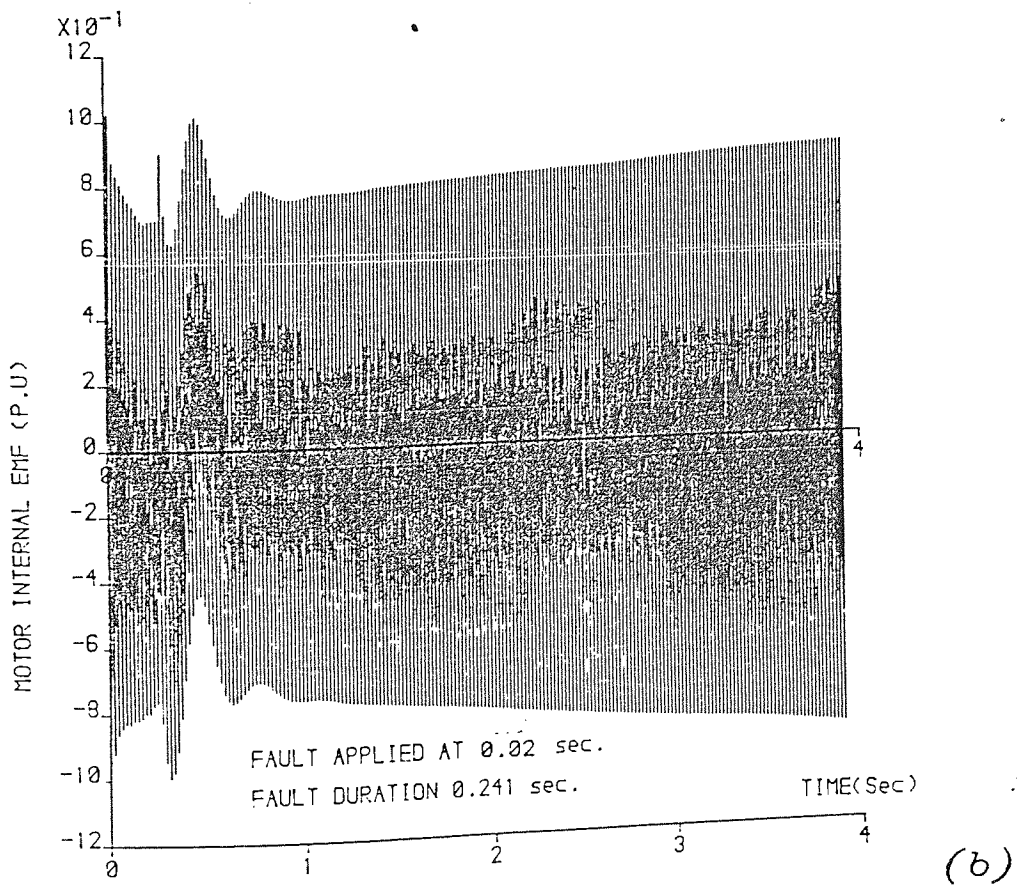
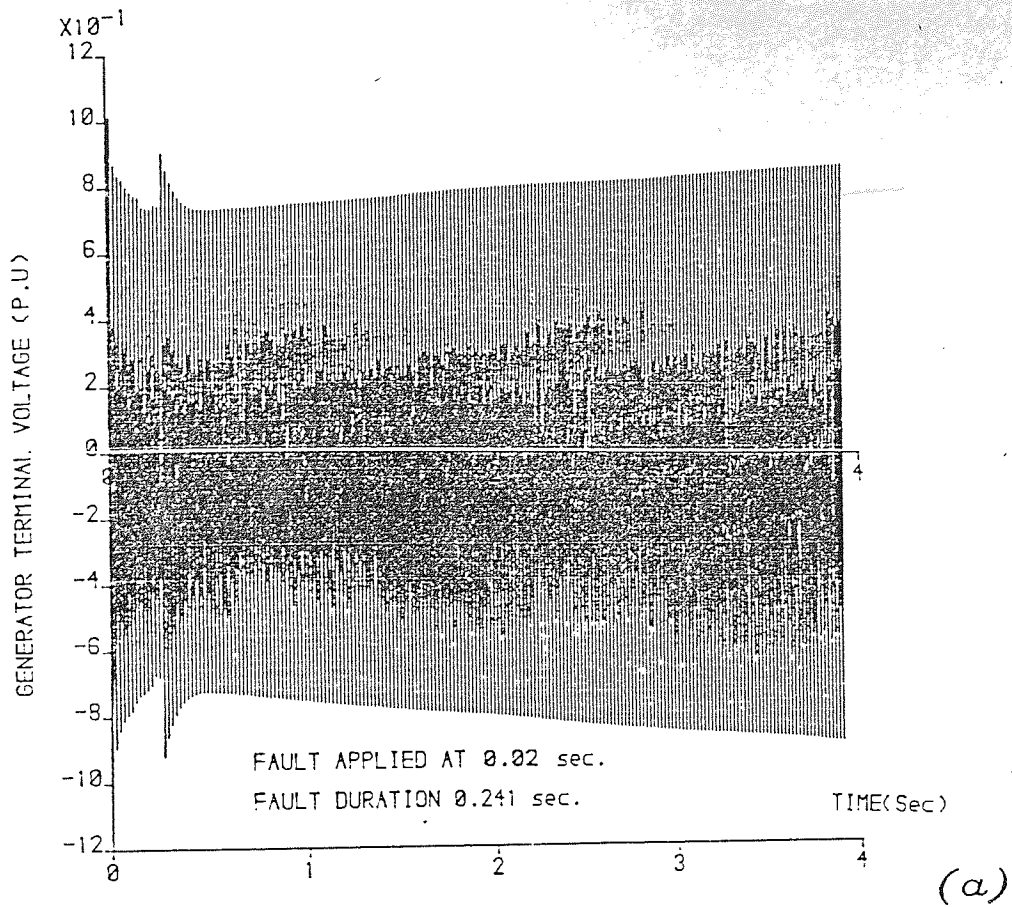


FIG. 6.12

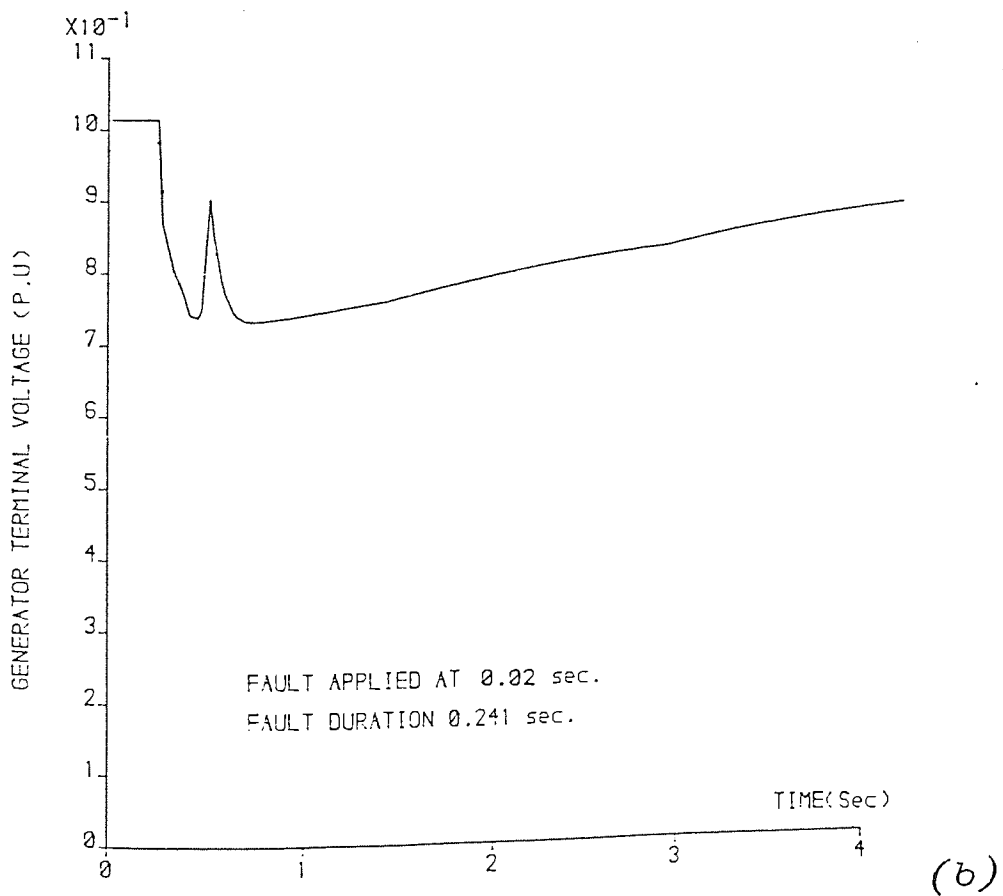
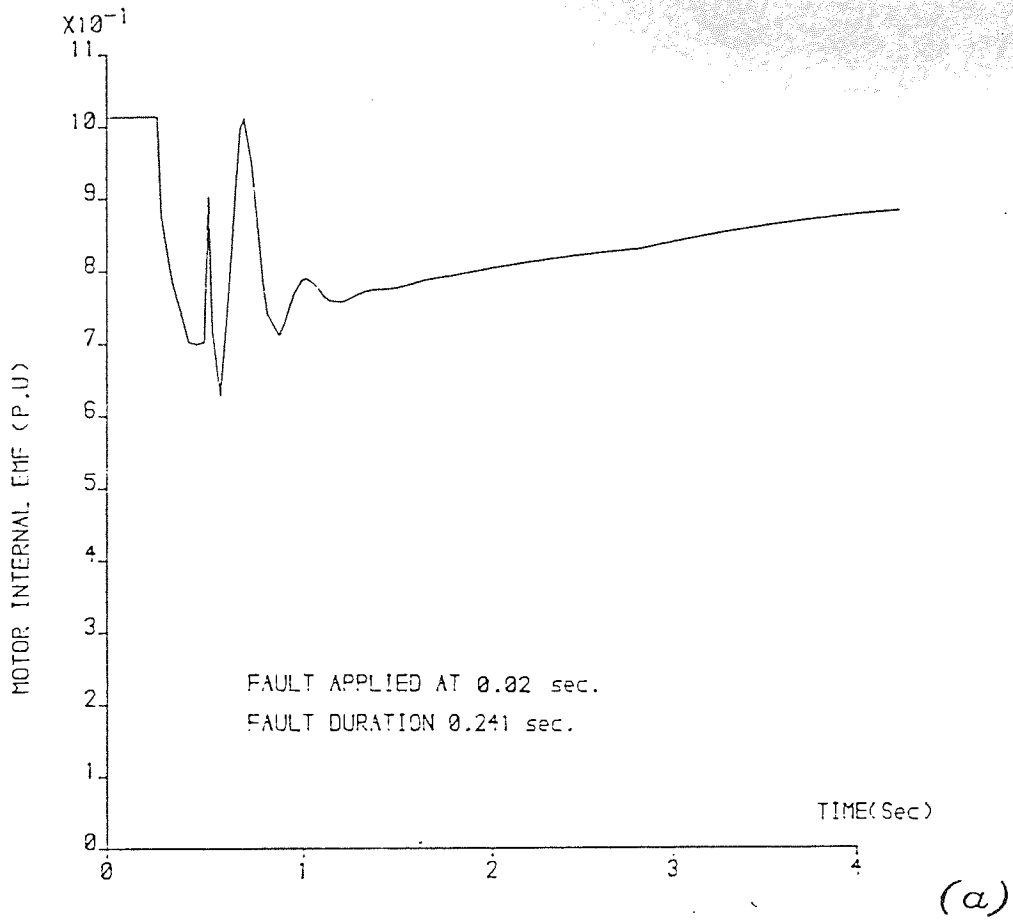


FIG. 6.13

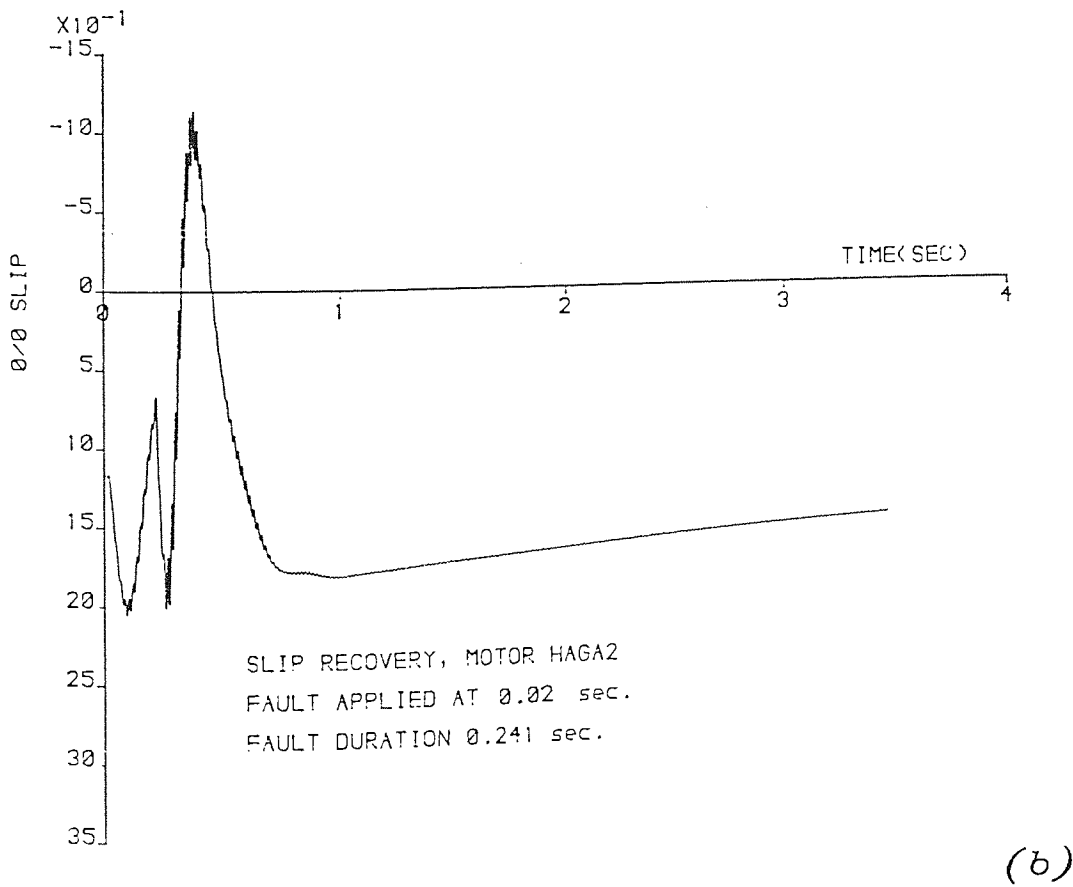
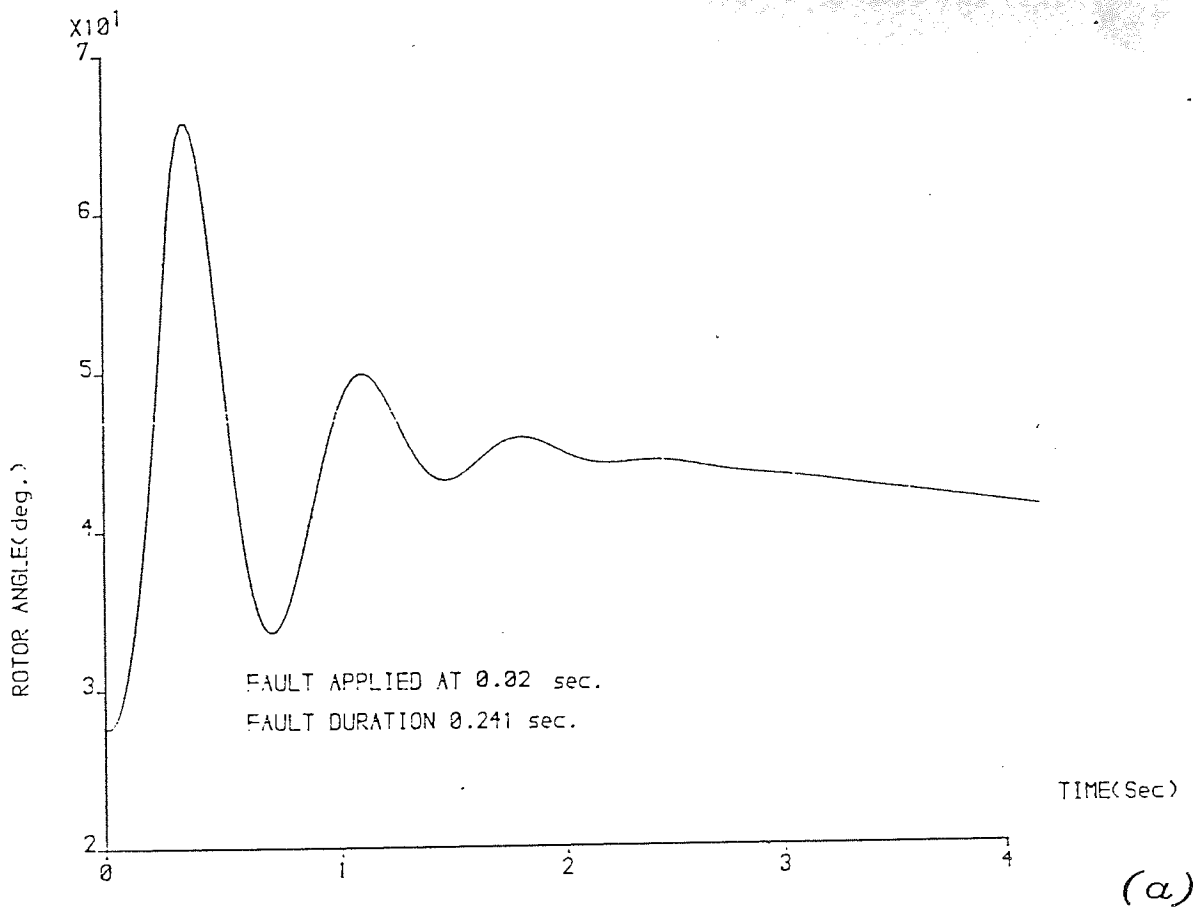


FIG. 6.14

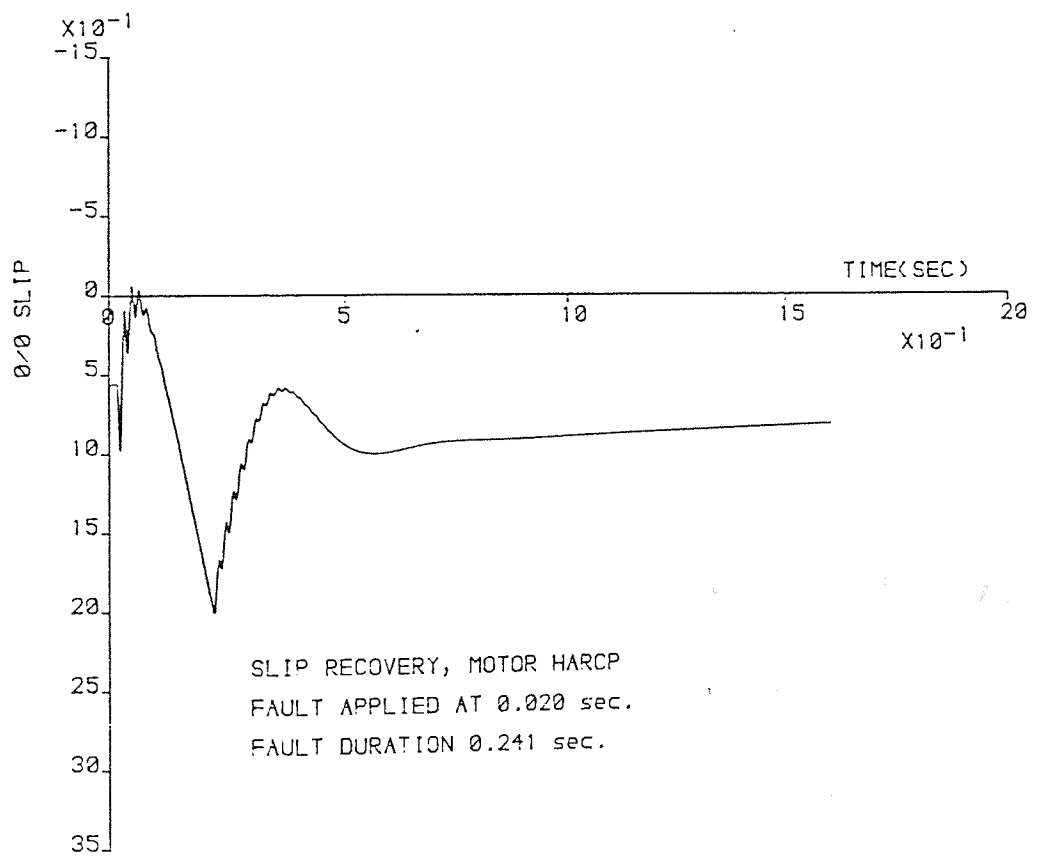
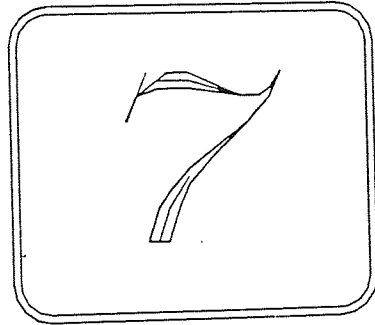


FIG. 6.15

*CHAPTER
SEVEN*



*CONCLUSIONS AND
SUGGESTIONS FOR
FURTHER WORK*

CHAPTER VII

CONCLUSIONS AND SUGGESTIONS

FOR FURTHER RESEARCH

7.1 CONCLUSIONS

It has been pointed out in the first two chapters of this thesis that, the effects of induction motor loads have been treated simply in the past by using equivalent circuits for transient analysis of power systems. The equivalent circuits were based upon parameters derived under transient operating conditions of the induction machine. Also, for the purpose of circuit-breaker selection, the induction motor effects were either neglected or included by using test results obtained from actual induction motor loads operating under system fault conditions. Although some useful simulation studies have been carried out, based upon the dynamic behaviour of induction machines, none of them has been extended to include the transient effects of large induction motors on the whole system.

The research carried out in this thesis contributes to the field of power system engineering by enabling the following :

1- A technique, using dynamic phase co-ordinate theory and matrix algebra, has been developed to include the transient analysis of the induction motor as part of the auxiliary drive equipment for a power system. The technique enables the inclusion of the delta/star transformer which connects large motors to the supply systems. The method developed is capable of handling different kinds of faults (symmetrical and asymmetrical) on both sides of the transformer connecting the motor to the supply source. Such studies can be carried out by simply changing a directing command in the computer software. Analysis cannot be achieved by other methods, such as 'd,q,0' representation, without a further transformation in the reference frame.

2- The analysis showed that the fault current supplied by the induction motor has a high asymmetry factor (the ratio of the asymmetrical current to the symmetrical current). This is because of the high X/R ratio (typically, 25 for 12.6 MVA induction motor). Therefore; this suggests that the current methods of switchgear specification, which assume a small direct current component based on an X/R ratio of 14, at the time of contact separation, may be inappropriate if the effects of induction motor loads are to be considered in selecting circuit-breaker ratings.

- 3- The analysis provides useful information to system protection engineers to enable better selection of the make-break devices, by taking into account the effect of the large sustained switching current and the contribution of the induction motor to system fault levels. Also, the analysis could provide a useful guide for setting the relevant protective gear devices such as relays and choosing appropriate current transformers.

- 4- Based upon the technique described, a computer package has been developed to study the transient stability of a system with a large synchronous generator, two three-phase transformers and a group of induction motors. The package differs from those which have been developed in the past in that, it uses a more elaborate model, for induction machine representation, which more nearly meets the dynamic nature of the stability problem occurring in practice. Moreover; the package has an advantage of initiating system disturbances due to different types of fault at different locations through out the system.

- 5- The extensive studies carried out in chapter III, investigate the process of switching-on large induction motors at different points on the voltage wave cycle and show that, smoother starting of induction motors can be obtained, by switching the motor phases sequentially through the peak point of the voltage

wave cycle. Switching using this method was found to have the following advantages :

- a) Minimisation of the sub-transient component in the starting current.
- b) Reduction of the severe oscillation in the starting torque to an acceptable level.
- c) Shorter run-up time.

Although, this method of switching is not in use at the present time, the principle could be applicable in the age of the microprocessor. Starting could be achieved by using a device which has the ability to measure the point in the voltage cycle when the phase arm of a circuit breaker makes contact.

6- One of the objectives of this research was to minimise the excessive computation time required for a detailed analysis of a complete system when using the phase co-ordinate method. To achieve this objective, investigations using different integrating routines, with different step lengths were used. The study showed that, when solving system equations containing variables that decay rapidly, as in the case of induction motors, the Predictor-Corrector methods can be an alternative to the Runge-Kutta routines if reduced accuracy is acceptable. Compared to a Runge-Kutta routine, in which the local

truncation error is controlled by automatically controlling the size of the step length, a less than 10% reduction in accuracy results in more than a 30 percent saving in computation time.

7- The research was extended to include an investigation of system behaviour, using a simplified model of an isolated system in which the effects of the prime mover speed control and the voltage regulator are neglected and having an induction motor load of the same order of the generator energising the system. From the investigations the following conclusions and observations should be noted :

A solid three phase-to-earth fault on the main out going feeder can cause the voltage at the generator terminals to suddenly drop to approximately 80 percent. In this case the group of induction motors (with a total rating equivalent to 75 % of the generator rating) connected to the generator terminals can contribute an additional 25 % to the fault current at the instant of the fault application. If the fault persists, (with the effects of the prime mover speed governor and the voltage regulator not introduced) the generator terminal voltage will continue to fall to 25 %. This situation leads to a deficiency of power delivered by the generator to the group of induction motors connected to the system. As a result, the motors will

use the stored kinetic energy to maintain the load and their speeds will fall.

If fault clearance is achieved within the first 0.25 seconds, the terminal voltage will start to pick-up slowly (since no AVR is included) and energy can be returned to the motors. This process is found to be accompanied by a phase of speed oscillation in the motors and a swing in angle of the generator followed by a gradual and steady recovery to the pre-fault condition of operation.

The validity of the study carried out without including the system control devices, was based upon the facts that :

a) the location of the fault at some distance from the generator terminals together with the size of the load connected to the generator-bus and the relatively high inertia of the generator, introduce only a small variation in the rotor speed in the event of a fault. This enables the effect of the speed governor to be neglected.

b) The drop in the voltage at the generator bus-bar, for the duration of the fault, was not of critical importance in maintaining system stability following

the fault clearance. In addition, this drop in terminal voltage is sufficient to set the rated field voltage 'v_f' via AVR action, rapidly to its upper

limit of 2v_f and enables comparison of practical fault

studies. In this study where the objective is to estimate peak fault currents for protection settings it appears that there is little difference in the predicted peak fault currents with and without AVR control provided the conditions described in (a) above are relevant.

Although the above conditions enable analysis of the isolated system, the study has the limitation of not including effects, that would be introduced by the control systems which are important in relation to stability and the prediction of small changes in terminal voltage. For example; what will be the effect of control action on the corrected terminal voltage and on system stability ?. What control action is required to enable system recovery in optimum time ?. These questions can only be answered by proper modelling of the controlling devices, based upon a knowledge of the parameters of generator control systems.

In addition to what has been achieved by the research, one may observe that modelling of system components using three phase variables together with applying the concept of a transformer connection matrix provide enhanced facilities for analysing systems under different conditions of operation, as well as the flexibility in changing circuit configurations without much change in the computer software, for example, the motor-transformer 'T1' in the circuit of fig. 5.1 can be excluded from the circuit by simply replacing the off-diagonal elements in the transformer connection matrix [C] by zero, i.e. converting the connection matrix into a unit matrix. Such changes in the circuit could be useful in simulating the introduction of a stand-by generator which is usually used to supply power to keep vitally important machines running in the event of a fault on the main incoming feeder.

7.2 Suggestion for further research.

The following areas, which have emerged from the present work, could be subjects for further research :

- 1- In the case of the isolated system, a study including the effects of both the automatic voltage regulator 'AVR' and the speed governor, is required. The study could be useful in investigating how the 'AVR' affects the generator flux

level, which in turn affects the terminal voltage and the system recovery time. Also, for a complete analysis of the isolated system, the effect of the speed governor has to be included for both sustained faults and transient stability studies where analysis is extended beyond the first 100 milliseconds.

2- A study to investigate the implications of the results on the selection and co-ordination of relays and associated devices is needed for both systems studied in chapter V& VI.

3- The inclusion of controlling devices in the system model could be useful in extending the studies to investigate isolation of faulty sections by quick switching. In other words, the model would have the capability of investigating the response of the system and its controlling devices when the load is rearranged transiently.

4- Models could also be developed to include the effects of magnetic saturation on both the generator and the induction motor. Investigations are required to see if there is any variation on machines dynamic performance that may be introduced by such phenomena, and whether these changes have any significant effects on the results obtained.

APPENDICES

Appendix A1

$$[L(\theta)]_m = \begin{bmatrix} L & \emptyset & \emptyset & M \cos\theta & M \cos\theta & M \cos\theta \\ s & & & 1 & 2 & 3 \\ \emptyset & L & \emptyset & M \cos\theta & M \cos\theta & M \cos\theta \\ & s & & 3 & 1 & 2 \\ \emptyset & \emptyset & L & M \cos\theta & M \cos\theta & M \cos\theta \\ & & s & 2 & 3 & 1 \\ M \cos\theta & M \cos\theta & M \cos\theta & L & \emptyset & \emptyset \\ 1 & 3 & 2 & r & & \\ M \cos\theta & M \cos\theta & M \cos\theta & \emptyset & L & \emptyset \\ 2 & 1 & 3 & \emptyset & r & \\ M \cos\theta & M \cos\theta & M \cos\theta & \emptyset & \emptyset & L \\ 3 & 2 & 1 & & & r \end{bmatrix}$$

$$[G(\theta)] = \begin{bmatrix} \emptyset & \emptyset & \emptyset & -M \sin\theta & -M \sin\theta & -M \sin\theta \\ & & & 1 & 2 & 3 \\ \emptyset & \emptyset & \emptyset & -M \sin\theta & -M \sin\theta & -M \sin\theta \\ & & & 3 & 1 & 2 \\ \emptyset & \emptyset & \emptyset & -M \sin\theta & -M \sin\theta & -M \sin\theta \\ & & & 2 & 3 & 1 \\ -M \sin\theta & -M \sin\theta & -M \sin\theta & \emptyset & \emptyset & \emptyset \\ 1 & 3 & 2 & & & \\ -M \sin\theta & -M \sin\theta & -M \sin\theta & \emptyset & \emptyset & \emptyset \\ 2 & 1 & 3 & & & \\ -M \sin\theta & -M \sin\theta & -M \sin\theta & \emptyset & \emptyset & \emptyset \\ 3 & 2 & 1 & & & \end{bmatrix}$$

$$\theta_1 = \theta, \theta_2 = \theta + 2\pi/3, \theta_3 = \theta - 2\pi/3$$

$$[r]_m = \begin{bmatrix} r & \emptyset & \emptyset \\ s & & \\ \emptyset & r & \emptyset & \emptyset \\ & s & & \\ \emptyset & \emptyset & r & \\ & & s & \\ & & & r & \emptyset & \emptyset \\ & & & r & & \\ \emptyset & & & & r & \emptyset \\ & & & & & r \\ & & & & & & r \end{bmatrix}$$

$$[r]_1 = \begin{bmatrix} r & \emptyset & \emptyset \\ 1 & & \\ \emptyset & r & \emptyset \\ & 1 & \\ \emptyset & \emptyset & r \\ & & 1 \end{bmatrix}$$

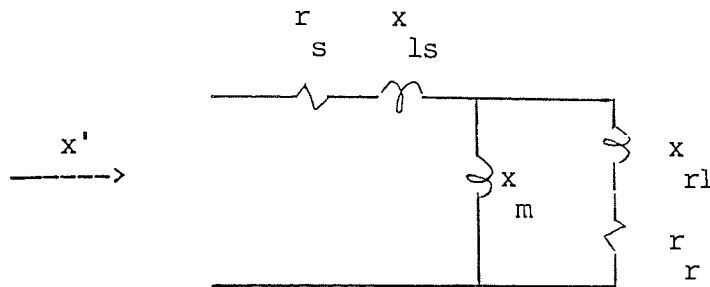
$$[r]_{tr} = \begin{bmatrix} r & \emptyset & \emptyset \\ tr & & \\ \emptyset & r & \emptyset \\ & tr & \\ \emptyset & \emptyset & r \\ & & tr \end{bmatrix}$$

$$[U] = \begin{bmatrix} 1 & \emptyset & \emptyset \\ \emptyset & 1 & \emptyset \\ \emptyset & \emptyset & 1 \\ \emptyset & \emptyset & \emptyset \\ \emptyset & \emptyset & \emptyset \\ \emptyset & \emptyset & \emptyset \end{bmatrix}$$

$$[L]_1 = \begin{bmatrix} L & \emptyset & \emptyset \\ 1 & & \\ \emptyset & L & \emptyset \\ & 1 & \\ \emptyset & \emptyset & L \\ & & 1 \end{bmatrix}$$

$$[C]_{rt} = \begin{bmatrix} 1 & -1 & 0 \\ 0 & 1 & -1 \\ -1 & 0 & 1 \\ 0 & 0 & 0 \\ 0 & 0 & 0 \\ 0 & 0 & 0 \end{bmatrix}$$

$$[L]_{tr} = \begin{bmatrix} L & 0 & 0 \\ tr & L & 0 \\ 0 & 0 & L \\ 0 & 0 & L \\ 0 & 0 & L \\ 0 & 0 & L \end{bmatrix}$$



Neglect the resistance r_s, r_r then,

$$x' = x_{sl} + (x_m \cdot x_{rl}) / (x_{rl} + x_m)$$

in a per unit system $x = L$

therefore,

$$L' = L_{sl} + (L_m \cdot L_{rl}) / (L_{rl} + L_m)$$

The admittance 'Y' of the circuit shown above with the resistances neglected is

$$Y = A + jB \\ = 0 + j1/x'$$

therefore;

$$A = 0, \quad \& \quad B = 1/L'$$

The armature time constant is $T_a = L' / \omega r_s$

and the transient time constant is $T' = L' / \omega r_r$

the load angle $\theta' = \tan^{-1}(\sin \omega t)$

Appendix A2

1) To show that

$$\begin{aligned} L_{AA0} &= (L_d + L_q + L_o)/3 \\ L_{AA2} &= (L_d - L_q)/3 \\ L_{AB0} &= (L_d + L_q - 2L_o)/6 \end{aligned}$$

The flux linkage λ in the three phase variables for the phase stator windings with the rotor open circuit are;

$$\begin{aligned} \lambda_a &= L_{aa} i_a + L_{ab} i_b + L_{ac} i_c \\ \lambda_b &= L_{ba} i_a + L_{bb} i_b + L_{bc} i_c \\ \lambda_c &= L_{ca} i_a + L_{cb} i_b + L_{cc} i_c \end{aligned} \quad \dots A2.1$$

On substituting equations 5.16 & 5.18 in A2.1, the following equation can be obtained

$$\begin{aligned} \lambda_a &= (L_{AA0} + L_{AA2} \cos 2\theta) i_a + (-L_{AB0} + L_{AA2} \cos(2\theta - 2\pi/3)) i_b \\ &\quad + (-L_{AB0} + L_{AA2} \cos(2\theta + 2\pi/3)) i_c \\ \lambda_b &= (-L_{AB0} + L_{AA2} \cos(2\theta - 2\pi/3)) i_a + (L_{AA0} + L_{AA2} \cos(2\theta + 2\pi/3)) i_b \\ &\quad + (-L_{AB0} + L_{AA2} \cos 2\theta) i_c \\ \lambda_c &= (-L_{AB0} + L_{AA2} \cos(2\theta + 2\pi/3)) i_a + (-L_{AB0} + L_{AA2} \cos 2\theta) i_b \\ &\quad + (L_{AA0} + L_{AA2} \cos(2\theta - 2\pi/3)) i_c \quad \dots A2.2 \end{aligned}$$

In 'd,q' frame of reference the flux linkage in terms of λ_a, λ_b & λ_c is

$$\begin{aligned} \lambda_d &= 2/3 (\lambda_a \cos \theta + \lambda_b \cos(\theta - 2\pi/3) + \lambda_c \cos(\theta + 2\pi/3)) \\ \lambda_q &= -2/3 (\lambda_a \sin \theta + \lambda_b \sin(\theta - 2\pi/3) + \lambda_c \sin(\theta + 2\pi/3)) \quad \dots A2.3 \\ \lambda_o &= 1/3 (\lambda_a + \lambda_b + \lambda_c) \quad \dots A2.4 \end{aligned}$$

Similar equations for current in 'd,q' can be written. In substituting A2.2 in A2.3 and performing the trigonometric manipulations the following expressions can be obtained,

$$\lambda_d = (L_{AA0} + L_{AB0} + 3/2L_{AA2})i_d = L_{dd}i_d$$

$$\lambda_q = (L_{AA0} + L_{AB0} - 3/2L_{AA2})i_q = L_{qq}i_q$$

$$\lambda_o = (L_{AA0} - 2L_{AB0})i_o = L_{oo}i_o$$

Therefore

$$L_{dd} = L_{AA0} + L_{AB0} + 3/2L_{AA2} \dots\dots\dots A2.5$$

$$L_{qq} = L_{AA0} + L_{AB0} - 3/2L_{AA2} \dots\dots\dots A2.6$$

$$L_{oo} = L_{AA0} - 2L_{AB0} \dots\dots\dots A2.7$$

By adding A2.5& A2.6

$$L_{dd} + L_{qq} = 2L_{AA0} + 2L_{AB0} \dots\dots\dots A2.8$$

and adding A2.7& A2.8

$$L_{AA0} = (L_{dd} + L_{qq} + L_{oo})/3$$

and by subtracting A2.6 from A2.5

$$L_{AA2} = (L_{dd} - L_{qq})/3$$

and finally, multiplying A2.7 by 2 and subtract the result from A2.8 gives

$$L_{AB0} = (L_{dd} + L_{qq} - 2L_{oo})/6$$

2) To show the relationship

relation of Fig. AA1

$$L_{fdl} = \frac{2}{3} \frac{(L_d - L_a)^2}{(L_d - L'_d)} - \frac{2}{3} (L_d - L_a)$$

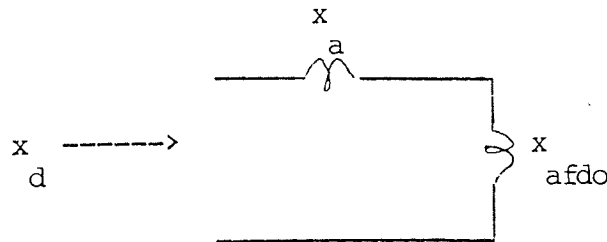


fig. AA1

Figure AA1 represents the equivalent circuit of a generator in direct axis under the steady-state condition with the resistance neglected. The equivalent direct reactance 'x_d' is given by,

$$x_d = x_a + x_{afd0}$$

hence,

$$x_{afd0} = x_d - x_a \quad \dots\dots\dots A2.9$$

In phase values and using the per unit system

$$M_{afd0} = \frac{2}{3} (L_d - L_a)$$

let the equivalent circuit under the transient condition be as shown by fig. AA2

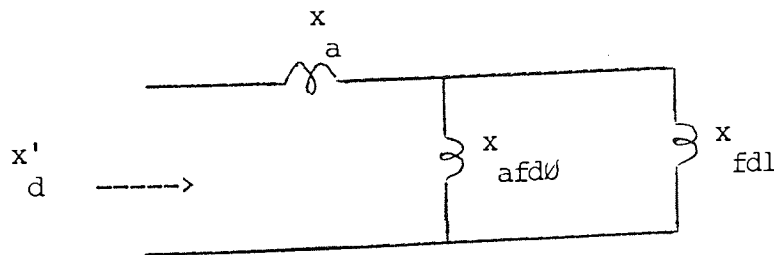


fig. AA2

The leakage field reactance 'x_{fdl}' can be determined from the field winding reactance 'x_{afd0}' and the magnetising reactance 'x_{afd0}' as follows

$$x_{fdl} = x_{fd0} - x_{afd0} \quad \dots\dots\dots A2.10$$

the transient reactance x'_d from the equivalent circuit of fig. AA2 is

$$x'_d = x_a + (x_{afd0} \cdot x_{fdl}) / (x_{afd0} + x_{fdl}) \quad \dots\dots A2.11$$

by substituting the value of x_a from A2.9 & A2.10 in A2.11 then,

$$x'_d = (x_d - x_{afd0}) + (x_{afd0} \cdot (x_{fd0} - x_{afd0})) / (x_{afd0} + (x_{fd0} - x_{afd0}))$$

therefore;

$$x_{fd0} \cdot x'_d = (x_d - x_{afd0})(x_{fd0}) + (x_{afd0} \cdot x_{fd0}) - x_{afd0}^2$$

$$x_{fd0} \cdot x'_d = x_d \cdot x_{fd0} - x_{afd0}^2$$

hence;

$$x_{fd0} = x_{afd0}^2 / (x_d - x'_d) \quad \dots\dots\dots A2.12$$

By substituting A2.12 in A2.10 then

$$x_{fdl} = x_{afd0}^2 / (x_d - x'_d) - x_{afd0} \quad \dots\dots\dots A2.13$$

and finally A2.9 in A2.13

$$x_{fdl} = (x_d - x_a)^2 / (x_d - x'_d) - (x_d - x_a)$$

in a per unit values $x=L$ and transform into the three phase variables the above equation becomes

$$L_{fdl} = 2/3(L_d - L_a)^2 / (L_d - L'_d) - 2/3(L_d - L_a)$$

3-To show the relationship

$$L_{KDL} = 2/3 ((L'_d - L_a)^2 / (L'_d - L''_d) + L_d - L'_d) - 2/3(L_d - L_a)$$

Under the sub-transient condition, the following equivalent circuit is valid

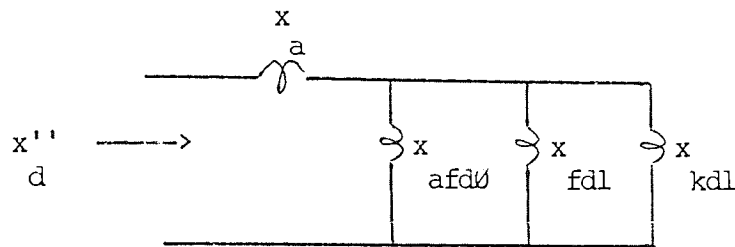


fig. AA3

The equivalent reactance x''_d is thus given by:

$$x''_d = x_a + \frac{((x_{fdl} \cdot x_{kdl}) / (x_{fdl} + x_{kdl})) \cdot x_{afd0}}{((x_{fdl} \cdot x_{kdl}) / (x_{fdl} + x_{kdl})) + x_{afd0}}$$

$$x''_d = x_a + (x_{fdl} \cdot x_{kdl} \cdot x_{afd0}) / (x_{fdl} \cdot x_{kdl} + x_{afd0} \cdot (x_{fdl} + x_{kdl}))$$

by substituting the value of x_{fdl} from A2.10 then

$$x''_d = x_a + \frac{x_{afd0} \cdot x_{kdl} (x_{fd0} - x_{afd0})}{(x_{kdl} - x_{afd0})(x_{fd0} - x_{afd0}) + x_{afd0} \cdot x_{kdl}}$$

therefore,

$$x''_d (x_{kdl} \cdot x_{fd0} + x_{afd0} \cdot x_{fd0} - x_{afd0}^2) = x_a (x_{kdl} \cdot x_{fd0} + x_{afd0} \cdot x_{fd0} - x_{afd0}^2) + x_{afd0} \cdot x_{kdl} \cdot x_{fd0} - x_{afd0}^2 \cdot x_{kdl}$$

and by substituting the value of x_{fd0} from A2.12 the following expression can be obtained

$$\begin{aligned}
& x'' \left(\frac{x^2}{d} \right) / (x - x') + x^3 / (x - x') - x^2 / d \\
&= x \left(\frac{x^2}{a} \right) / (x - x') + x^3 / (x - x') - x^2 / d \\
&+ \frac{x^3}{afd\emptyset} / (x - x') - x^2 / d
\end{aligned}$$

re-arrange,

$$\begin{aligned}
& x \left(x'' \cdot x^2 - x \cdot x^2 - x^3 + x^2 (x - x') \right) \\
&= x^3 - x^2 (x - x') - x'' x^3 + x'' x^2 (x - x')
\end{aligned}$$

and by substituting the value of x on the L.H.S from A2.9 we get

$$\begin{aligned}
& x \left(x'' \cdot x^2 - x' \cdot x^2 \right) = x^3 - x^2 (x - x') + \\
& \quad x'' (-x^3 + x^2 (x - x')) \\
& x \left(x'' - x' \right) = x \cdot x - x (x - x') + x'' (-x^3 + (x - x')) \\
& x \left(x'' - x' \right) = x \cdot x - x (x + x) + x x' - x'' \cdot x + \\
& \quad x'' \cdot x - x'' \cdot x' \\
& = -x^2 + x \cdot x' - x'' \cdot x + x'' \cdot x - x'' \cdot x'
\end{aligned}$$

The R.H.S can be replaced by the following identity

$$- \left(\frac{x' - x}{a} \right)^2 + (x - x')(x' - x'') - x^2 (x' - x'')$$

which leads to

$$x_{kdl} = \frac{(x'_d - x'_a)^2}{(x'_d - x''_d)} + (x_d - x'_d) - x_{afd}$$

$$= \frac{(x'_d - x'_a)^2}{(x'_d - x''_d)} + (x_d - x'_d) - (x_d - x'_a)$$

In the per unit system, and expressing the above relation in the three phase variables we get,

$$L_{kdl} = \frac{2}{3} \left(\frac{(L'_d - L'_a)^2}{(L'_d - L''_d)} + (L_d - L'_d) - \frac{2}{3}(L_d - L'_a) \right)$$

Similar expressions can also be developed for the quadrature axis.

Defination of matrices

$$[L] = \begin{bmatrix} -L_{aa} & -L_{ab} & -L_{ac} & M \cos \theta & M \cos \theta & -M \sin \theta & -M \sin \theta \\ -L_{ba} & -L_{bb} & -L_{bc} & M \cos \theta & M \cos \theta & -M \sin \theta & -M \sin \theta \\ -L_{ca} & -L_{cb} & -L_{cc} & M \cos \theta & M \cos \theta & -M \sin \theta & -M \sin \theta \\ -M \cos \theta & -M \cos \theta & -M \cos \theta & L & M & \emptyset & \emptyset \\ -M \cos \theta & -M \cos \theta & -M \cos \theta & M & L & \emptyset & \emptyset \\ +M \sin \theta & +M \sin \theta & +M \sin \theta & \emptyset & \emptyset & L & M \\ +M \sin \theta & +M \sin \theta & +M \sin \theta & \emptyset & \emptyset & M & L \end{bmatrix}$$

where; $\theta_1 = \theta$, $\theta_2 = \theta - 2\pi/3$, $\theta_3 = \theta + 2\pi/3$

$$[R] = \begin{bmatrix} r_a & \emptyset & \emptyset & \emptyset & \emptyset & \emptyset & \emptyset \\ \emptyset & r_a & \emptyset & \emptyset & \emptyset & \emptyset & \emptyset \\ \emptyset & \emptyset & r_a & \emptyset & \emptyset & \emptyset & \emptyset \\ -r_{fd} & \emptyset & \emptyset & \emptyset & \emptyset & \emptyset & \emptyset \\ -r_{kd} & \emptyset & \emptyset & \emptyset & \emptyset & \emptyset & \emptyset \\ -r_{fq} & \emptyset & \emptyset & \emptyset & \emptyset & \emptyset & \emptyset \\ -r_{kq} & \emptyset & \emptyset & \emptyset & \emptyset & \emptyset & \emptyset \end{bmatrix}$$

where,

$$r_{FD} = L_{ffd} \cdot L'_d / \omega_0^T L_{dd} \quad , \quad r_{FQ} = L_{ffq} \cdot L'_q / \omega_0^T L_{qq}$$

$$r_{KD} = L'_{kd} \cdot L''_d / \omega_0^T L'_{dd} \quad , \quad r_{KQ} = L'_{kq} \cdot L''_q / \omega_0^T L'_{qq}$$

$$L'_{kd} = L_{KDL} + M_{AD\emptyset} L_{FDL} / (M_{AD\emptyset} + L_{FDL})$$

$$L'_{kq} = L_{KQL} + M_{AQ\emptyset} L_{FQL} / (M_{AQ\emptyset} + L_{FQL})$$

Appendix A3

```

C THIS PROGRAM STUDIES THE TRANSIENT STABILITY OF THE SYSTEM
C SHOWN BY FIG. (5.1). THE PROGRAM ALLOWS DISTURBANCES DUE TO
C DIFFERENT TYPES OF FAULTS ON BUS-BARS 'B1' & 'B2'. "MF" IS A
C VARIABLE TO DEFINE THE TYPE OF FAULTS ON BUS-BAR 'B1' AND "KC"
C IS A VARIABLE TO DEFINE THE TYPE OF FAULTS ON BUS-BAR 'B2' e.g,
C MF=4 IS A CASE OF NO FAULT OR STEADY STATE CONDITION
C MF=1 IS A CASE OF A SINGLE PHASE TO EARTH ON BUS-BAR 'B1'
C MF=2 IS A CASE OF A DOUBLE PHASE-TO-EARTH FAULT
C MF=3 IS A CASE OF A THREE PHASE-TO-EARTH FAULT
C THE VALUES GIVEN HERE ARE FOR ANALYSING A CASE OF A DOUBLE
C PHASE-TO-EARTH FAULT ON BUS-BAR 'B2'
C *****
C
C DOUBLE PRECISION H,AUXT1(3),AUXT2(3),AUXT3(3),AUXT4(3),E1(3),
1 E2(3),E3(3),E4(3),CT(3),AUXA1(6),AUXA2(6),AUXA3(6),AUXA4(6),
2 C11(3),T,C22(3),C33(3),C44(3),AUXB1(6),AUXB2(6),AUXB3(6),AUXB4(6)
3 ,AUXC1(6),AUXC2(6),AUXC3(6),AUXC4(6),AUXD1(6),AUXD2(6),
4 AUXD3(6),AUXD4(6),VG1(3),VG2(3),VG3(3),VG4(3),AXG1(3),AXG2(3),
5 AXG3(3),AXG4(3),CU(7),S1,S2,S3,S4,DM(3,3),DMT(3,3),V11(3),V22(3),
6 V33(3),V44(3),CRF(3)
C
C KJ=0
C LK=0
C KK=0
C MF=4
C H=.0314
C T=0.0
C READ THE VALUES FOR VOLTAGE AUXILIARIES OF BUS-BARS 'B1'
C & 'B2'
C *****
C READ(16,1)(E1(I),I=1,3)
C READ(16,1)(E2(I),I=1,3)
C READ(16,1)(E3(I),I=1,3)
C READ(16,1)(E4(I),I=1,3)
C READ(14,1)(VG1(I),I=1,3)
C READ(14,1)(VG2(I),I=1,3)
C READ(14,1)(VG3(I),I=1,3)
C READ(14,1)(VG4(I),I=1,3)
1 FORMAT(3F15.8)
C CALL CONMAT(DM,DMT)
C
9 CALL SYNG(H,T,VG1,VG2,VG3,VG4,AXG1,AXG2,AXG3,AXG4,CU,KK)
CALL CWP(H,C11,AUXA1,AUXA2,AUXA3,AUXA4,E1,E2,E3,E4,CC,S1)
CALL BFP(H,C22,AUXB1,AUXB2,AUXB3,AUXB4,E1,E2,E3,E4,CC,S2)
CALL PAF(H,C33,AUXC1,AUXC2,AUXC3,AUXC4,E1,E2,E3,E4,CC,S3)
CALL IDF(H,C44,AUXD1,AUXD2,AUXD3,AUXD4,E1,E2,E3,E4,CC,S4)
C
C IF(KK.EQ.111)MF=3
C IF(KK.EQ.1060)MF=4
C IF(MF.EQ.4)GOTO 11
C IF(MF.EQ.3)GOTO 22
C IF(MF.EQ.1)GOTO 33

```

```

2AUXC2,AUXC3,AUXC4,AUXD1,AUXD2,AUXD3,AUXD4)
DO 15 I=1,3
15  CRF(I)=C44(I)
    GOTO 44
22  CALL MFAULT3(CT,C11,C22,C33,C44,AUXT1,AUXT2,AUXT3,AUXT4,
1V11,V22,V33,V44,H,CRF)
    GOTO 44
33  CALL MFAULT1(CT,C11,C22,C33,C44,AUXT1,AUXT2,AUXT3,AUXT4,
1AUXA1,AUXA2,AUXA3,AUXA4,AUXB1,AUXB2,AUXB3,AUXB4,AUXC1,CRF,
2AUXC2,AUXC3,AUXC4,AUXD1,AUXD2,AUXD3,AUXD4,V11,V22,V33,V44,H)
44  CONTINUE
    T=T+H
    CALL SYSTEM(AUXT1,AUXT2,AUXT3,AUXT4,AXG1,AXG2,AXG3,AXG4,CT,
1CU,VG1,VG2,VG3,VG4,T,H,KK,DM,DMF)
    CALL VOLT(H,AUXT1,AUXT2,AUXT3,AUXT4,E1,E2,E3,E4,CT,
1VG1,VG2,VG3,VG4,DM,V11,V22,V33,V44,KK,MF)
C
T1000=T/314.16
DO 4 I=1,3
4  CT(I)=CT(I)*(776./48.)
    IF(KK.LT.4000.AND.KJ.EQ.5)WRITE(35,88)T1000,(CT(I),I=1,3)
C  IF(KK.LT.4000.AND.KJ.EQ.5)WRITE(39,88)T1000,(CRF(I),I=1,3)
    IF(LK.EQ.20)WRITE(38,99)T1000,S1,S2,S3,S4
88  FORMAT(2X,4F15.8)
99  FORMAT(2X,5F12.8)
    IF(LK.EQ.20)LK=0
    IF(KJ.EQ.5)KJ=0
    KJ=KJ+1
    KK=KK+1
    LK=LK+1
    IF(KK.GT.25000)GOTO 3
GOTO 9
3  STOP
END
C  SUBROUTINE TO FIND THE GENERATOR-VARIABLES
C  *****
SUBROUTINE SYNG(H,T,VG1,VG2,VG3,VG4,AXG1,AXG2,AXG3,AXG4,CU,KK)
DOUBLE PRECISION CU(7),CUN(7),TN,T,H,PI(7),ANI,
1E,TE1,T1000,XG(7,7),W,F(7),X,SIC1,SIC,TL,RG(7,7),
2XA,X0,XD,XQ,XD1,XQ1,XD11,XQ11,TD1,TQ1,TD11,TQ11,B,XAA0,
3XAB0,TE,TM,XAA2,XAD0,XAQ0,XAFD,XFDL,XKDL,XAFQ,XFQL,XKQL,XKD11,
4RS1,XKQ11,RFD,RFQ,RKD,RKQ,TA,PI1(7),PI2(7),PI3(7),PI4(7),V4,RA,
5R0,HE,XALN0,XAQN0,AIC,TIME,VG1(3),VG2(3),VG3(3),VG4(3),AXG1(3)
6,AXG2(3),AXG3(3),AXG4(3)
C
IF(KK.GT.0)GOTO 15
JJ=0
C  READ GENERATOR DATA AND INITIAL CONDITIONS
C  *****
LL=0
READ(13,1)(CU(I),I=1,6)
READ(13,1)CU(7),E,XA,X0,XD,XQ
READ(13,1)XD1,XQ1,XD11,XQ11,TD1,TQ1
READ(13,1)TD11,TQ11,B,T,H,ANI

```

```

READ(13,2)W,V4,RA,R0,HE,TIME,J1,N
READ(13,1)RS1,TA,TL,AIC,SIC,SIC1
READ(13,3)CI, TM
1  FORMAT(6F10.5)
2  FORMAT(6F10.5,2I4)
3  FORMAT(2F10.5)
C
WRITE(34,1)(CU(I),I=1,6)
WRITE(34,1)CU(7),E,XA,X0,XD,XQ
WRITE(34,1)XD1,XQ1,XD11,XQ11,TD1,TQ1
WRITE(34,1)TD11,TQ11,B,T,H,ANI
WRITE(34,2)W,V4,RA,R0,HE,TIME,J1,N
WRITE(34,1)RS1,TA,TL,AIC,SIC,SIC1
WRITE(34,3)CI, TM
C
TRANSFORMATION FROM D-Q TO A-B-C
*****
XAA0=((XD+XQ-2.*XA)/RS1+2.*XA+X0)/3.
XAB0=((XD+XQ-2.*XA)/RS1+2.*XA-2.*X0)/6.
XAA2=(XD-XQ)/(3.*RS1)
XADN0=B*(XD-XA)
XAD0=XADN0/RS1
XAQN0=B*(XQ-XA)
XAQ0=XAQN0/RS1
XAFD=XADN0*XADN0/((XD-XD1)*B)
XFDL=XAFD-XADN0
XFDL=1.*XFDL
XKDL=B*((XD1-XA)*(XD1-XA)/(XD1-XD11)+XD-XD1)-XADN0
XKDL=1.0*XKDL
XAFQ=XAQN0*XAQN0/((XQ-XQ1)*B)
XFQL=XAFQ-XAQN0
XFQL=1.*XFQL
XKQL=B*((XQ1-XA)*(XQ1-XA)/(XQ1-XQ11)+XQ-XQ1)-XAQN0
XKQL=1.*XKQL
XKD11=XKDL+XADN0*XFDL/XAFD
XKQ11=XKQL+XAQN0*XFQL/XAFQ
RFD=XAFD*XD1/(W*TD1*XD)
RFQ=XAFQ*XQ1/(W*TQ1*XQ)
RKD=XKD11*XD1/(W*TD11*XD1)
RKQ=XKQ11*XQ11/(W*TQ11*XQ1)
WRITE(34,1)XAA0,XAB0,XAA2,XADN0,XAD0,XAQN0
WRITE(34,1)XAQ0,XAFD,XFDL,XKDL,XAFQ,XFQL
WRITE(34,1)XKQL,XKD11,XKQ11,RFD,RFQ,RKD
WRITE(34,6)RKQ
6  FORMAT(F12.7)
C  FORM GENERATOR RESISTANCE MATRIX [R]
C  *****
DO 8 I=1,7
DO 8 J=1,7
8  RG(I,J)=0.0
RG(1,1)=RA+R0
RG(1,2)=R0
RG(1,3)=R0
RG(2,1)=R0
RG(2,2)=RA+R0

```

```

RG(2,3)=RØ
RG(3,1)=RØ
RG(3,2)=RØ
RG(3,3)=RA+RØ
RG(4,4)=-RFD
RG(5,5)=-RKD
RG(6,6)=-RFQ
RG(7,7)=-RKQ
T1ØØØ=T/W
TN=T
NN=Ø
I9=1
DO 9 I=1,7
9 CUN(I)=CU(I)
C
15 TN=T
MM=1
CALL PDI(W,ANI,CUN,PI,TN,XG,RG,HE,NN,X,SIC1,
1V4,XAAØ,XABØ,XAA2,XADØ,XAQØ,XAFD,XFDL,XKDL,XAFQ,XFQL,
2XKQL,XKD11,XKQ11,RFD,RFQ,RKD,RKQ,TIME,MM,VG1,VG2,VG3,VG4)
NN=Ø
DO 2Ø K=1,7
PI1(K)=PI(K)*H
2Ø CUN(K)=CU(K)+PI1(K)*Ø.5
DO 25 I=1,3
25 AXG1(I)=PI1(I)
TN=T+Ø.5*H
MM=2
C
CALL PDI(W,ANI,CUN,PI,TN,XG,RG,HE,NN,X,SIC1,
1V4,XAAØ,XABØ,XAA2,XADØ,XAQØ,XAFD,XFDL,XKDL,XAFQ,XFQL,
2XKQL,XKD11,XKQ11,RFD,RFQ,RKD,RKQ,TIME,MM,VG1,VG2,VG3,VG4)
NN=1
DO 3Ø K=1,7
PI2(K)=PI(K)*H
3Ø CUN(K)=CU(K)+PI2(K)*Ø.5
DO 35 I=1,3
35 AXG2(I)=PI2(I)
C
CALL PDI(W,ANI,CUN,PI,TN,XG,RG,HE,NN,X,SIC1,
1V4,XAAØ,XABØ,XAA2,XADØ,XAQØ,XAFD,XFDL,XKDL,XAFQ,XFQL,
2XKQL,XKD11,XKQ11,RFD,RFQ,RKD,RKQ,TIME,MM,VG1,VG2,VG3,VG4)
NN=Ø
DO 4Ø K=1,7
PI3(K)=PI(K)*H
4Ø CUN(K)=CU(K)+PI3(K)
DO 45 I=1,3
45 AXG3(I)=PI3(I)
C
TN=T+H
MM=3
C
CALL PDI(W,ANI,CUN,PI,TN,XG,RG,HE,NN,X,SIC1,
1V4,XAAØ,XABØ,XAA2,XADØ,XAQØ,XAFD,XFDL,XKDL,XAFQ,XFQL,

```

```

2XKQL, XKD11, XKQ11, RFD, RFQ, RKD, RKQ, TIME, MM, VG1, VG2, VG3, VG4)
DO 50 K=1, 7
PI4(K)=PI(K)*H
CU(K)=CU(K)+(PI1(K)+2.*PI2(K)+2.*PI3(K)+PI4(K))/6.
50 CUN(K)=CU(K)
DO 55 I=1, 3
55 AXG4(I)=PI4(I)
NN=0
T1000=T/W
C SPEED VARIATION
C *****
CALL MATM1(XG, CUN, F)
TEL=F(1)*(CUN(2)-CUN(3))+F(2)*(CUN(3)-CUN(1))+F(3)*(CUN(1)-CUN(2))
TE=0.3849*TEL
TA=TM-TE-TL
SIC1=TA*H/(314.159*2.*CI)+SIC
AIC=TA*H*H/(314.159*4.*CI)+SIC*H+AIC
SIC=SIC1
ANI=AIC
SIC1=SIC1+1.0
ANNA=ANI*57.29578
C
IF(KK.LT.4000.AND.JJ.EQ.5)WRITE(36,77)T1000,(CU(I),I=1,3)
77 FORMAT(2X,4F15.8)
IF(LL.EQ.20)WRITE(37,77)T1000,ANNA,SIC1,CU(4)
IF(JJ.EQ.5)JJ=0
IF(LL.EQ.20)LL=0
JJ=JJ+1
LL=LL+1
RETURN
END
C
C
SUBROUTINE PDI(W, ANI, CUN, PI, TN, XG, RG, HE, NN, X, SIC1,
1V4, XAA0, XAB0, XAA2, XAD0, XAQ0, XAFD, XFDL, XKDL, XAFQ, XFQL,
2XKQL, XKD11, XKQ11, RFD, RFQ, RKD, RKQ, TIME, MM, VG1, VG2, VG3, VG4)
DOUBLE PRECISION ANI, CUN(7), PI(7), TN, XG(7,7), PL(7,7), V(7),
1RG(7,7), CLI(7,7), X, W, HE, SIC1, V4, XAA0, XAB0, XAA2, XAD0, XAQ0, XAFD,
2XFQDL, XKDL, XAFQ, XFQL, XKQL, XKD11, XKQ11, RFD, RFQ, RKD, RKQ, CI2(7),
3CI3(7), TIME, CL2(7,7), V1(7), VG1(3), VG2(3), VG3(3), VG4(3)
C
IF(NN.EQ.1)GOTO 949
IF(MM.EQ.1)GOTO 11
IF(MM.EQ.2)GOTO 22
IF(MM.EQ.3)GOTO 33
11 DO 111 I=1, 3
111 V(I)=VG1(I)
GOTO 444
22 DO 222 I=1, 3
222 V(I)=VG2(I)
GOTO 444
33 DO 333 I=1, 3
333 V(I)=VG4(I)
444 V(4)=V4

```



```

V(5)=0.0
V(6)=0.0
V(7)=0.0
X=ANI+TN
C
FORM [L] MATRIX
C
*****
XG(1,1)=- (XAA0+XAA2*DCOS(2.*X))
XG(1,2)=- (-XAB0+XAA2*DCOS(2.*X-2.0944))
XG(1,3)=- (-XAB0+XAA2*DCOS(2.*X+2.0944))
XG(1,4)=XAD0*DCOS(X)
XG(1,5)=XG(1,4)
XG(1,6)=-XAO0*DSIN(X)
XG(1,7)=XG(1,6)
XG(2,1)=XG(1,2)
XG(2,2)=- (XAA0+XAA2*DCOS(2.*X+2.0944))
XG(2,3)=- (-XAB0+XAA2*DCOS(2.*X))
XG(2,4)=XAD0*DCOS(X-2.0944)
XG(2,5)=XG(2,4)
XG(2,6)=-XAO0*DSIN(X-2.0944)
XG(2,7)=XG(2,6)
XG(3,1)=XG(1,3)
XG(3,2)=XG(2,3)
XG(3,3)=- (XAA0+XAA2*DCOS(2.*X-2.0944))
XG(3,4)=XAD0*DCOS(X+2.0944)
XG(3,5)=XG(3,4)
XG(3,6)=-XAO0*DSIN(X+2.0944)
XG(3,7)=XG(3,6)
XG(4,1)=-XAD0*DCOS(X)
XG(4,2)=-XAD0*DCOS(X-2.0944)
XG(4,3)=-XAD0*DCOS(X+2.0944)
XG(4,4)=XF0L+XAD0
XG(4,5)=XAD0
XG(4,6)=0.0
XG(4,7)=0.0
XG(5,1)=-XAD0*DCOS(X)
XG(5,2)=-XAD0*DCOS(X-2.0944)
XG(5,3)=-XAD0*DCOS(X+2.0944)
XG(5,4)=XAD0
XG(5,5)=XK0L+XAD0
XG(5,6)=0.0
XG(5,7)=0.0
XG(6,1)=XAO0*DSIN(X)
XG(6,2)=XAO0*DSIN(X-2.0944)
XG(6,3)=XAO0*DSIN(X+2.0944)
XG(6,4)=0.0
XG(6,5)=0.0
XG(6,6)=XF0L+XAO0
XG(6,7)=XAO0
XG(7,1)=XAO0*DSIN(X)
XG(7,2)=XAO0*DSIN(X-2.0944)
XG(7,3)=XAO0*DSIN(X+2.0944)
XG(7,4)=0.0
XG(7,5)=0.0
XG(7,6)=XAO0

```

```

XG(7,7)=XKQL+XAQØ
C   FORM [PL] MATRIX
C   *****
PL(1,1)=SIC1*2.*XAA2*DSIN(2.*X)
PL(1,2)=SIC1*2.*XAA2*DSIN(2.*X-2.Ø944)
PL(1,3)=SIC1*2.*XAA2*DSIN(2.*X+2.Ø944)
PL(1,4)=-XADØ*SIC1*DSIN(X)
PL(1,5)=PL(1,4)
PL(1,6)=-SIC1*XAQØ*DCOS(X)
PL(1,7)=PL(1,6)
PL(2,1)=PL(1,2)
PL(2,2)=PL(1,3)
PL(2,3)=PL(1,1)
PL(2,4)=-SIC1*XADØ*DSIN(X-2.Ø944)
PL(2,5)=PL(2,4)
PL(2,6)=-SIC1*XAQØ*DCOS(X-2.Ø944)
PL(2,7)=PL(2,6)
PL(3,1)=PL(1,3)
PL(3,2)=PL(2,3)
PL(3,3)=PL(1,2)
PL(3,4)=-SIC1*XADØ*DSIN(X+2.Ø944)
PL(3,5)=PL(3,4)
PL(3,6)=-SIC1*XAQØ*DCOS(X+2.Ø944)
PL(3,7)=PL(3,6)
PL(4,1)=SIC1*XADØ*DSIN(X)
PL(4,2)=SIC1*XADØ*DSIN(X-2.Ø944)
PL(4,3)=SIC1*XADØ*DSIN(X+2.Ø944)
PL(5,1)=PL(4,1)
PL(5,2)=PL(4,2)
PL(5,3)=PL(4,3)
PL(6,1)=SIC1*XAQØ*DCOS(X)
PL(6,2)=SIC1*XAQØ*DCOS(X-2.Ø944)
PL(6,3)=SIC1*XAQØ*DCOS(X+2.Ø944)
PL(7,1)=PL(6,1)
PL(7,2)=PL(6,2)
PL(7,3)=PL(6,3)
DO 141Ø I=4,7
DO 141Ø J=4,7
141Ø PL(I,J)=Ø.Ø
C   FORM [R-PL]
C   *****
DO 1 I=1,7
DO 1 J=1,7
1   PL(I,J)=-PL(I,J)+RG(I,J)
DO 5 I=1,3
5   V1(I)=V(I)
V1(4)=V4
V1(5)=Ø.Ø
V1(6)=Ø.Ø
V1(7)=Ø.Ø
C   FORM [R-PL]{I}
C   *****
949 CALL MATM1(PL,CUN,CI2)
C   FORM [V]+[R-PL]{I}

```

```

C *****
DO 3 I=1,7
3 CI3(I)=CI2(I)+V1(I)
IF(NN.EQ.1)GOTO 950
C FORM [CL2] MATRIX
C *****
DO 4 I=1,7
DO 4 J=1,7
4 CL2(I,J)=XG(I,J)
CALL MATINV(CL2,CLI,7)
C FORM PI
C *****
950 CALL MATM1(CLI,CI3,PI)
RETURN
END

C
SUBROUTINE MATM1(G1,G2,G3)
DOUBLE PRECISION G1(7,7),G2(7),G3(7)
DO 1 I=1,7
G3(I)=0.0
DO 1 K=1,7
1 G3(I)=G3(I)+G1(I,K)*G2(K)
RETURN
END

C
SUBROUTINE MATM2(G1,G2,G3)
DOUBLE PRECISION G1(3,3),G2(3,3),G3(3,3)
DO 1 I=1,3
DO 1 J=1,3
G3(I,J)=0.0
DO 1 K=1,3
1 G3(I,J)=G3(I,J)+G1(I,K)*G2(K,J)
RETURN
END

C
SUBROUTINE FAULT(A,B,C)
DOUBLE PRECISION A(3,3),B(3,3),C(3,3)
DO 2 I=1,3
DO 2 J=1,3
C(I,J)=0.0
DO 2 K=1,3
2 C(I,J)=C(I,J)+A(I,K)*B(K,J)
RETURN
END

C SUB-ROUTINE TO INVERT THE GENERATOR IND. MATRIX
C *****
SUBROUTINE MATINV(G1,CLI,N1)
DOUBLE PRECISION G1(N1,N1),CLI(N1,N1),BB(7,14)
DO 1 I=1,N1
DO 1 J=1,N1
1 BB(I,J)=G1(I,J)
J1=1+N1
J2=2*N1
DO 2 I=1,N1

```

```

DO 2 J=J1,J2
2  BB(I,J)=0.0
DO 3 I=1,N1
  J=I+N1
3  BB(I,J)=1.0
DO 610 K=1,N1
  KP1=K+1
  IF(K.EQ.N1)GOTO 500
  J=2*N1
  L=K
DO 400 I=KP1,N1
400 IF(DABS(BB(I,J)).GT.DABS(BB(L,K)))L=I
  IF(L.EQ.K)GOTO 500
DO 410 J=K,J2
  TEMP=BB(K,J)
  BB(K,J)=BB(L,J)
410 BB(L,J)=TEMP
500 DO 501 J=KP1,J2
501 BB(K,J)=BB(K,J)/BB(K,K)
  GOTO 506
506 IF(K.EQ.1)GOTO 600
  KM1=K-1
DO 510 I=1,KM1
DO 510 J=KP1,J2
510 BB(I,J)=BB(I,J)-BB(I,K)*BB(K,J)
  IF(K.EQ.N1)GOTO 700
600 DO 610 I=KP1,N1
DO 610 J=KP1,J2
610 BB(I,J)=BB(I,J)-BB(I,K)*BB(K,J)
700 DO 701 I=1,N1
DO 701 J=1,N1
  K=J+N1
701 CLI(I,J)=BB(I,K)
  RETURN
  END
C  SUB-ROUTINE TO CALCULATE THE VOLTAGE OF BUS-BAR 'B1'
C  *****
SUBROUTINE VOLT(H,AUXT1,AUXT2,AUXT3,AUXT4,E1,E2,E3,E4,CT,
I V1,V2,V3,V4,DM,V11,V22,V33,V44,KK,MF)
  DOUBLE PRECISION H,AUXT1(3),AUXT2(3),AUXT3(3),AUXT4(3),E1(3),
  1E2(3),E3(3),E4(3),V1(3),V2(3),V3(3),V4(3),V11(3),V22(3),V33(3),
  2V44(3),CT(3),T,DM(3,3),TRL,A(3,3),F1(3,3),ZI(3,3),FG(3,3),
  3F3G(3,3),EM1(3),EM2(3),EM3(3),EM4(3)
C
  IF(KK.GT.0)GOTO 100
DO 88 I=1,3
DO 88 J=1,3
88 IF(I.EQ.J)A(I,J)=1.0
DO 90 I=1,3
DO 90 J=1,3
90 IF(I.EQ.J)ZI(I,J)=1.0
DO 92 I=1,3
DO 92 J=1,3
92 IF(I.EQ.J)F1(I,J)=1.0

```

```

DO 94 I=1,3
DO 94 J=1,3
IF(I.EQ.2.AND.J.EQ.I)FG(I,J)=1.0
94 IF(I.EQ.3.AND.J.EQ.I)FG(I,J)=1.0
DO 96 I=1,3
DO 96 J=1,3
96 F3G(I,J)=0.0
XLT=.4781937
RT=.0120433
TR1=1.0137799
100 CONTINUE
C
C
CALL VMOD(V1,DM,V11,TR1)
CALL VMOD(V2,DM,V22,TR1)
CALL VMOD(V3,DM,V33,TR1)
CALL VMOD(V4,DM,V44,TR1)
C
DO 7 I=1,3
E1(I)=V11(I)-AUXT1(I)*XLT/H-CT(I)*RT
E2(I)=V22(I)-AUXT2(I)*XLT/H-CT(I)*RT
E3(I)=V33(I)-AUXT3(I)*XLT/H-CT(I)*RT
E4(I)=V44(I)-AUXT4(I)*XLT/H-CT(I)*RT
7 CONTINUE
IF(MF.EQ.4)CALL MATM2(F1,ZI,A)
IF(MF.EQ.3)CALL MATM2(F3G,ZI,A)
IF(MF.EQ.1)CALL MATM2(FG,ZI,A)
DO 9 I=1,3
EM1(I)=0.0
EM2(I)=0.0
EM3(I)=0.0
EM4(I)=0.0
DO 9 K=1,3
EM1(I)=EM1(I)+A(I,K)*E1(I)
EM2(I)=EM2(I)+A(I,K)*E2(I)
9 EM3(I)=EM3(I)+A(I,K)*E3(I)
EM4(I)=EM4(I)+A(I,K)*E4(I)
DO 8 I=1,3
E1(I)=EM1(I)
E2(I)=EM2(I)
E3(I)=EM3(I)
8 E4(I)=EM4(I)
RETURN
END
C
SUBROUTINE NOFAULT(CT,C11,C22,C33,C44,AUXT1,AUXT2,AUXT3,
1AUXT4,AUXA1,AUXA2,AUXA3,AUXA4,AUXB1,AUXB2,AUXB3,AUXB4,
2AUXC1,AUXC2,AUXC3,AUXC4,AUXD1,AUXD2,AUXD3,AUXD4)
DOUBLE PRECISION CT(3),C11(3),C22(3),C33(3),C44(3),AUXT1(3),
1AUXT2(3),AUXT3(3),AUXT4(3),AUXA1(3),AUXA2(3),AUXA3(3),AUXA4(3),
2AUXB1(3),AUXB2(3),AUXB3(3),AUXB4(3),AUXD1(3),AUXD2(3),AUXD3(3),
4AUXD4(3),AUXC1(3),AUXC2(3),AUXC3(3),AUXC4(3)
DO 1 I=1,3
CT(I)=C11(I)+C22(I)+C33(I)+C44(I)

```

```

AUXT1(I)=AUXA1(I)+AUXB1(I)+AUXC1(I)+AUXD1(I)
AUXT2(I)=AUXA2(I)+AUXB2(I)+AUXC2(I)+AUXD2(I)
AUXT3(I)=AUXA3(I)+AUXB3(I)+AUXC3(I)+AUXD3(I)
1 AUXT4(I)=AUXA4(I)+AUXB4(I)+AUXC4(I)+AUXD4(I)
DO 2 I=1,3
CT(I)=2.*CT(I)
AUXT1(I)=2.*AUXT1(I)
AUXT2(I)=2.*AUXT2(I)
AUXT3(I)=2.*AUXT3(I)
2 AUXT4(I)=2.*AUXT4(I)
RETURN
END

```

C

```

SUBROUTINE MFAULT3(CT,C11,C22,C33,C44,AUXT1,AUXT2,AUXT3,
1 LAUXT1,V11,V22,V33,V44,H,CRF)
DOUBLE PRECISION CT(3),C11(3),C22(3),C33(3),C44(3),AUXT1(3),
1 LAUXT2(3),AUXT3(3),AUXT4(3),V11(3),V22(3),V33(3),V44(3),H,
2 CINC(3),CRF(3)
XLT=0.4781937
RT=0.0120433
DO 1 I=1,3
AUXT1(I)=(V11(I)-RT*CT(I))*H/XLT
AUXT2(I)=(V22(I)-RT*(CT(I)+0.5*AUXT1(I)))*H/XLT
AUXT3(I)=(V33(I)-RT*(CT(I)+0.5*AUXT2(I)))*H/XLT
1 AUXT4(I)=(V44(I)-RT*(CT(I)+AUXT3(I)))*H/XLT
DO 2 I=1,3
CINC(I)=(AUXT1(I)+2.*(AUXT2(I)+AUXT3(I))+AUXT4(I))/4.
2 CT(I)=CT(I)+CINC(I)
DO 3 I=1,3
3 CT(I)=CT(I)*(48./776.)
DO 4 I=1,3
4 CRF(I)=2.*(C11(I)+C22(I)+C33(I))
CRF(I)=CRF(I)*(776./48.)
RETURN
END

```

C

```

SUBROUTINE MFAULT1(CT,C11,C22,C33,C44,AUXT1,AUXT2,AUXT3,
1 LAUXT4,AUXA1,AUXA2,AUXA3,AUXA4,AUXB1,AUXB2,AUXB3,AUXB4,AUXC1,CRF,
2 AUXC2,AUXC3,AUXC4,AUXD1,AUXD2,AUXD3,AUXD4,V11,V22,V33,V44,H)
DOUBLE PRECISION CT(3),C11(3),C22(3),C33(3),C44(3),AUXT1(3),
1 LAUXT2(3),AUXT3(3),AUXT4(3),AUXA1(3),AUXA2(3),AUXA3(3),AUXA4(3),
2 AUXB1(3),AUXB2(3),AUXB3(3),AUXB4(3),AUXC1(3),AUXC2(3),AUXC3(3),
3 AUXC4(3),AUXD1(3),AUXD2(3),AUXD3(3),AUXD4(3),V11(3),V22(3),
4 V33(3),V44(3),H,CINC,CRF(3)
XLT=0.4781937
RT=0.0120433
AUXT1(1)=(V11(1)-RT*CT(1))*H/XLT
AUXT2(1)=(V22(1)-RT*(CT(1)+0.5*AUXT1(1)))*H/XLT
AUXT3(1)=(V33(1)-RT*(CT(1)+0.5*AUXT2(1)))*H/XLT
AUXT4(1)=(V44(1)-RT*(CT(1)+AUXT3(1)))*H/XLT
CINC=(AUXT1(1)+2.*(AUXT2(1)+AUXT3(1))+AUXT4(1))/4.
CT(1)=CT(1)+CINC
CT(1)=CT(1)*(48./776.)
DO 1 I=2,3

```

```

AUXT1(I)=AUXA1(I)+AUXB1(I)+AUXC1(I)+AUXD1(I)
AUXT2(I)=AUXA2(I)+AUXB2(I)+AUXC2(I)+AUXD2(I)
AUXT3(I)=AUXA3(I)+AUXB3(I)+AUXC3(I)+AUXD3(I)
AUXT4(I)=AUXA4(I)+AUXB4(I)+AUXC4(I)+AUXD4(I)
1 CT(I)=C11(I)+C22(I)+C33(I)+C44(I)
DO 2 I=2,3
AUXT1(I)=2.*AUXT1(I)
AUXT2(I)=2.*AUXT2(I)
AUXT3(I)=2.*AUXT3(I)
AUXT4(I)=2.*AUXT4(I)
2 CT(I)=2.*CT(I)
CRF(1)=C11(1)+C22(1)+C33(1)
CRF(1)=2.*CRF(1)
DO 3 I=2,3
3 CRF(I)=C44(I)
DO 4 I=1,3
4 CRF(I)=CRF(I)*(776./48.)
RETURN
END

C
SUBROUTINE VMOD(A,B,C,D)
DOUBLE PRECISION A(3),B(3,3),C(3),D
DO 1 J=1,3
SUM=0.0
DO 2 K=1,3
SUM=SUM+B(J,K)*A(K)
2 CONTINUE
C(J)=SUM/(D*SQRT(3.))
1 CONTINUE
RETURN
END

C
CALCULTIONS OF VARIABLES OF MOTOR 'CWP'
C
*****
SUBROUTINE CWP(H,CU1776,AUXA1,AUXA2,AUXA3,AUXA4,E1,E2,E3,E4,
1KK,S1)
DOUBLE PRECISION R1(6,6),X1(6,6),DX1(6,6),AUXA1(6),AUXA2(6),
1AUXA3(6),AUXA4(6),E1(6),E2(6),E3(6),E4(6),X11(6,6),S1,VEL1,
2CU1(6),C11(6),THETA1,EEL,A1,B1,C1,TL01,TEL,CM1(6,6),H,SM1(6,6),
2XJ1,BM1(6,6),R1S,R1R,X1S1,X1R1,XMS1,XM1,XMS1,CU1776(3)
3,BASE1,BASE2,PU
C READ MOTOR DATA AND INITIAL CONDITIONS
C *****
IF(KK.GT.0)GOTO 15
READ(15,10)R1S,R1R,X1S1,X1R1,XMS1
READ(15,10)XM1,XMS1,A1,B1,C1
READ(15,10)S1,VEL1,THETA1,EEL,TL01
READ(15,12)(CU1(I),I=1,6)
READ(15,11)XJ1
WRITE(33,10)R1S,R1R,X1S1,X1R1,XMS1
WRITE(33,10)XM1,XMS1,A1,B1,C1
WRITE(33,10)S1,VEL1,THETA1,EEL,TL01
WRITE(33,12)(CU1(I),I=1,6)
WRITE(33,11)XJ1
10 FORMAT(5F12.8)

```

```

12  FORMAT(6F12.8)
11  FORMAT(F12.8)
C
15  DO 20 I=1,6
    DO 20 J=1,6
    R1(I,J)=0.0
    X1(I,J)=0.0
20  DX1(I,J)=0.0
C
    CALL RES(R1S,R1R,S1,EE1,R1)
    CALL XIND(X1S1,XMS1,X1R1,XMR1,XMSR1,X1,THETA1)
    CALL DXIN(XMSR1,THETA1,S1,DX1)
    CALL MTINVS(X1,XI1)
    CALL ROTPCS(A1,B1,C1,THETA1,VEL1,S1,H,TE1,TL01,XJ1)
    CALL CMAT(R1,DX1,S1,CM1)
C
    DO 25 I=1,6
    DO 25 J=1,6
    IF(I.LE.3.AND.I.EQ.J)SM1(I,J)=1.0
25  CONTINUE
C
    CALL BMAT(BM1,SM1)
    CALL RNKTTA(AUXA1,AUXA2,AUXA3,AUXA4,C11,CU1,E1,E2,E3,E4,BM1,
*CM1,XI1,H)
    CALL CURR(AUXA1,AUXA2,AUXA3,AUXA4,CU1,C11)
    CALL TRQE(CU1,THETA1,XMSR1,TE1)
    BASE1=(3.538*1000.)/(11.*SQRT(3.))
    BASE2=(776.0*1000.)/(23.5*SQRT(3.))
    PU=BASE1/BASE2
    DO 30 I=1,3
    CU1776(I)=0.0
    AUXA1(I)=AUXA1(I)*PU
    AUXA2(I)=AUXA2(I)*PU
    AUXA3(I)=AUXA3(I)*PU
    AUXA4(I)=AUXA4(I)*PU
30  CU1776(I)=CU1(I)*PU
    RETURN
    END
C  CALCULATIONS OF VARIABLES OF MOTOR 'BFP'
C  *****
    SUBROUTINE BFP(H,CU2776,AUXB1,AUXB2,AUXB3,AUXB4,E1,E2,E3,E4,
LKK,S2)
    DOUBLE PRECISION R2(6,6),X2(6,6),DX2(6,6),AUXB1(6),AUXB2(6),
1AUXB3(6),AUXB4(6),E1(6),E2(6),E3(6),E4(6),XI2(6,6),S2,VEL2,
2CU2(6),CI2(6),THETA2,EE2,A2,B2,C2,TL02,TE2,CM2(6,6),H,SM2(6,6),
3XJ2,BM2(6,6),R2S,R2R,X2S2,X2R2,XMS2,XMR2,XMSR2,CU2776(3)
4,BASE1,BASE2,PU
C  READ MOTOR DATA AND INITIAL CONDITIONS
C  *****
    IF(KK.GT.0)GOTO 15
    READ(17,10)R2S,R2R,X2S2,X2R2,XMS2
    READ(17,10)XMR2,XMSR2,A2,B2,C2
    READ(17,10)S2,VEL2,THETA2,EE2,TL02
    READ(17,12)(CU2(I),I=1,6)

```



```

READ(17,11)XJ2
WRITE(33,10)R2S,R2R,X2S2,X2R2,XMS2
WRITE(33,10)XMR2,XMSR2,A2,B2,C2
WRITE(33,10)S2,VEL2,THETA2,EE2,TL02
WRITE(33,12)(CU2(I),I=1,6)
WRITE(33,11)XJ2
10  FORMAT(5F12.8)
11  FORMAT(F12.8)
12  FORMAT(6F12.8)
C
15  DO 20 I=1,6
    DO 20 J=1,6
        R2(I,J)=0.0
        X2(I,J)=0.0
20  DX2(I,J)=0.0
C
    CALL RES(R2S,R2R,S2,EE2,R2)
    CALL XIND(X2S2,XMS2,X2R2,XMR2,XMSR2,X2,THETA2)
    CALL DXIN(XMSR2,THETA2,S2,DX2)
    CALL MTINVS(X2,XI2)
    CALL ROTPOS(A2,B2,C2,THETA2,VEL2,S2,H,TE2,TL02,XJ2)
    CALL CMAT(R2,DX2,S2,CM2)
    DO 25 I=1,6
    DO 25 J=1,6
    IF(I.LE.3.AND.I.EQ.J)SM2(I,J)=1.0
25  CONTINUE
    CALL BMAT(BM2,SM2)
    CALL RNGKTTA(AUXB1,AUXB2,AUXB3,AUXB4,CI2,CU2,E1,E2,E3,E4,BM2,
*CM2,XI2,H)
    CALL CURR(AUXB1,AUXB2,AUXB3,AUXB4,CU2,CI2)
    CALL TRQE(CU2,THETA2,XMSR2,TE2)
    BASE1=(11.4*1000.)/(11.0*SQRT(3.))
    BASE2=(776.0*1000.)/(23.5*SQRT(3.))
    PU=BASE1/BASE2
    DO 30 I=1,3
    AUXB1(I)=AUXB1(I)*PU
    AUXB2(I)=AUXB2(I)*PU
    AUXB3(I)=AUXB3(I)*PU
    AUXB4(I)=AUXB4(I)*PU
30  CU2776(I)=CU2(I)*PU
    RETURN
    END
C  CALCULATIONS OF VARIABLES OF MOTOR 'PAF'
C  *****
    SUBROUTINE PAF(H,CU3776,AUXC1,AUXC2,AUXC3,AUXC4,E1,E2,E3,E4,
LKK,S3)
    DOUBLE PRECISION R3(6,6),X3(6,6),DX3(6,6),AUXC1(6),AUXC2(6),
1AUXC3(6),AUXC4(6),E1(6),E2(6),E3(6),E4(6),XI3(6,6),S3,VEL3,
2CU3(6),CI3(6),THETA3,EE3,A3,B3,C3,TL03,TE3,CM3(6,6),H,SM3(6,6),
3XJ3,BM3(6,6),R3S,R3R,X3S3,X3R3,XMS3,XMR3,XMSR3,CU3776(3)
4,BASE1,BASE2,PU
C  READ MOTOR DATA AND INITIAL CONDITIONS
C  *****
    IF(KK.GT.0)GOTO 15

```

```

READ(18,10)R3S,R3R,X3S3,X3R3,XMS3
READ(18,10)XMR3,XMSR3,A3,B3,C3
READ(18,10)S3,VEL3,THETA3,EE3,TL03
READ(18,12)(CU3(I),I=1,6)
READ(18,11)XJ3
WRITE(33,10)R3S,R3R,X3S3,X3R3,XMS3
WRITE(33,10)XMR3,XMSR3,A3,B3,C3
WRITE(33,10)S3,VEL3,THETA3,EE3,TL03
WRITE(33,12)(CU3(I),I=1,6)
WRITE(33,11)XJ3
10  FORMAT(5F12.8)
11  FORMAT(F12.8)
12  FORMAT(6F12.8)
C
15  DO 20 I=1,6
    DO 20 J=1,6
    R3(I,J)=0.0
    X3(I,J)=0.0
20  DX3(I,J)=0.0
C
    CALL RES(R3S,R3R,S3,EE3,R3)
    CALL XIND(X3S3,XMS3,X3R3,XMR3,XMSR3,X3,THETA3)
    CALL DXIN(XMSR3,THETA3,S3,DX3)
    CALL MTINVS(X3,XI3)
    CALL ROTPOS(A3,B3,C3,THETA3,VEL3,S3,H,TE3,TL03,XJ3)
    CALL CMAT(R3,DX3,S3,CM3)
    DO 25 I=1,6
    DO 25 J=1,6
    IF(I.LE.3.AND.I.EQ.J)SM3(I,J)=1.0
25  CONTINUE
    CALL BMAT(BM3,SM3)
    CALL RNGKITA(AUXC1,AUXC2,AUXC3,AUXC4,CI3,CU3,E1,E2,E3,E4,BM3,
*CM3,XI3,H)
    CALL CURR(AUXC1,AUXC2,AUXC3,AUXC4,CU3,CI3)
    CALL TRQE(CU3,THETA3,XMSR3,TE3)
    BASE1=(3.139*1000.)/(11.*SQRT(3.))
    BASE2=(776.0*1000.)/(23.5*SQRT(3.))
    PU=BASE1/BASE2
    DO 30 I=1,3
    AUXC1(I)=AUXC1(I)*PU
    AUXC2(I)=AUXC2(I)*PU
    AUXC3(I)=AUXC3(I)*PU
    AUXC4(I)=AUXC4(I)*PU
30  CU3776(I)=CU3(I)*PU
    RETURN
    END
C  CALCULATIONS OF VARIABES OF MOTOR 'IDF'
C  *****
    SUBROUTINE IDF(H,CU4776,AUXD1,AUXD2,AUXD3,AUXD4,E1,E2,E3,E4,
IKK,S4)
    DOUBLE PRECISION R4(6,6),X4(6,6),DX4(6,6),AUXD1(6),AUXD2(6),
LAUXD3(6),AUXD4(6),E1(6),E2(6),E3(6),E4(6),XI4(6,6),S4,VEL4,
2CU4(6),CI4(6),THETA4,EE4,A4,B4,C4,TL04,TE4,CM4(6,6),H,SM4(6,6),
3XJ4,BM4(6,6),R4S,R4R,X4S4,X4R4,XMS4,XMR4,XMSR4,CU4776(3)

```

```

4,BASE1,BASE2,PU
C READ MOTOR DATA AND INITIAL CONDITIONS
C *****
IF(KK.GT.0)GOTO 15
READ(19,10)R4S,R4R,X4S4,X4R4,XMS4
READ(19,10)XMR4,XMSR4,A4,B4,C4
READ(19,10)S4,VEL4,THETA4,EE4,TL04
READ(19,12)(CU4(I),I=1,6)
READ(19,11)XJ4
WRITE(33,10)R4S,R4R,X4S4,X4R4,XMS4
WRITE(33,10)XMR4,XMSR4,A4,B4,C4
WRITE(33,10)S4,VEL4,THETA4,EE4,TL04
WRITE(33,12)(CU4(I),I=1,6)
WRITE(33,11)XJ4
10 FORMAT(5F12.8)
11 FORMAT(F12.8)
12 FORMAT(6F12.8)
C
15 DO 20 I=1,6
DO 20 J=1,6
R4(I,J)=0.0
X4(I,J)=0.0
20 DX4(I,J)=0.0
C
CALL RES(R4S,R4R,S4,EE4,R4)
CALL XIND(X4S4,XMS4,X4R4,XMR4,XMSR4,X4,THETA4)
CALL DXIN(XMSR4,THETA4,S4,DX4)
CALL MTINVS(X4,XI4)
CALL ROTPOS(A4,B4,C4,THETA4,VEL4,S4,H,TE4,TL04,XJ4)
CALL CMAT(R4,DX4,S4,CM4)
DO 25 I=1,6
DO 25 J=1,6
IF(I.LE.3.AND.I.EQ.J)SM4(I,J)=1.0
25 CONTINUE
CALL BMAT(BM4,SM4)
CALL RNGKITA(AUXD1,AUXD2,AUXD3,AUXD4,CI4,CU4,E1,E2,E3,E4,BM4,
*CM4,XI4,H)
CALL CURR(AUXD1,AUXD2,AUXD3,AUXD4,CU4,CI4)
CALL TRQE(CU4,THETA4,XMSR4,TE4)
BASE1=(3.564*1000.)/(11.*SQRT(3.))
BASE2=(776.0*1000.0)/(23.5*SQRT(3.))
PU=BASE1/BASE2
DO 30 I=1,3
AUXD1(I)=AUXD1(I)*PU
AUXD2(I)=AUXD2(I)*PU
AUXD3(I)=AUXD3(I)*PU
AUXD4(I)=AUXD4(I)*PU
30 CU4776(I)=CU4(I)*PU
RETURN
END
C BUILD [R] FOR MOTORS '
C *****
SUBROUTINE RES(RS,RR,S,C,R)
DOUBLE PRECISION RS,RR,S,C,R(6,6)

```

```

C
DO 1 I=1,6
DO 1 J=1,6
1 R(I,J)=0.0
C
DO 3 I=1,6
DO 2 J=1,6
IF(I.LE.3.AND.J.EQ.I)R(I,J)=RS
IF(I.GE.4.AND.J.EQ.I)R(I,J)=RR*(1.+C*S)
2 CONTINUE
3 CONTINUE
RETURN
END
C BUILD [L] FOR MOTORS'
C *****
SUBROUTINE XIND(XS,XMS,XR,XMR,XMSR,X,THETA)
DOUBLE PRECISION XS,XMS,XR,XMR,XMSR,X(6,6),THETA,TH1,TH2,TH3
C
DO 1 I=1,6
DO 1 J=1,6
1 X(I,J)=0.0
C
GAM=2.0943951
TH1=THETA
TH2=THETA+GAM
TH3=THETA-GAM
C
DO 8 I=1,3
DO 7 J=1,4
IF(I.EQ.J)GOTO 2
IF(J.LE.3)GOTO 3
IF(I.EQ.1.AND.J.EQ.4)GOTO 4
IF(I.EQ.2.AND.J.EQ.4)GOTO 5
IF(I.EQ.3.AND.J.EQ.4)GOTO 6
2 X(I,J)=XS
X(I+3,J+3)=XR
GOTO 7
3 X(I,J)=XMS
X(I+3,J+3)=XMR
GOTO 7
4 X(I,J)=XMSR*COS(TH1)
X(J,I)=X(I,J)
X(I,J+1)=XMSR*COS(TH2)
X(J+1,I)=X(I,J+1)
X(I,J+2)=XMSR*COS(TH3)
X(J+2,I)=X(I,J+2)
GOTO 7
5 X(I,J)=XMSR*COS(TH3)
X(J,I)=X(I,J)
X(I,J+1)=XMSR*COS(TH1)
X(J+1,I)=X(I,J+1)
X(I,J+2)=XMSR*COS(TH2)
X(J+2,I)=X(I,J+2)
GOTO 7

```

```

6  X(I,J)=XMSR*COS(TH2)
   X(J,I)=X(I,J)
   X(I,J+1)=XMSR*COS(TH3)
   X(J+1,I)=X(I,J+1)
   X(I,J+2)=XMSR*COS(TH1)
   X(J+2,I)=X(I,J+2)
7  CONTINUE
8  CONTINUE
   RETURN
   END
C  BUILD d[L]/dt FOR MOTORS'
C  *****
C  SUBROUTINE DXIN(XMSR,THETA,S,DX)
C  DOUBLE PRECISION XMSR,THETA,S,DX(6,6),TH1,TH2,TH3
C
C  DO 1 I=1,6
C  DO 1 J=1,6
1  DX(I,J)=0.0
   GAM=2.0943951
   TH1=THETA
   TH2=THETA+GAM
   TH3=THETA-GAM
C
C  DO 7 I=1,3
C  DO 6 J=1,4
   IF(I.LT.3.AND.J.EQ.3)GOTO 2
   IF(I.EQ.1.AND.J.EQ.4)GOTO 3
   IF(I.EQ.2.AND.J.EQ.4)GOTO 4
   IF(I.EQ.3.AND.J.EQ.4)GOTO 5
2  DX(I,J)=0.0
   DX(I+3,J+3)=0.0
   GOTO 6
3  DX(I,J)=-XMSR*SIN(TH1)
   DX(J,I)=DX(I,J)
   DX(I,J+1)=-XMSR*SIN(TH2)
   DX(J+1,I)=DX(I,J+1)
   DX(I,J+2)=-XMSR*SIN(TH3)
   DX(J+2,I)=DX(I,J+2)
   GOTO 6
4  DX(I,J)=-XMSR*SIN(TH3)
   DX(J,I)=DX(I,J)
   DX(I,J+1)=-XMSR*SIN(TH1)
   DX(J+1,I)=DX(I,J+1)
   DX(I,J+2)=-XMSR*SIN(TH2)
   DX(J+2,I)=DX(I,J+2)
   GOTO 6
5  DX(I,J)=-XMSR*SIN(TH2)
   DX(J,I)=DX(I,J)
   DX(I,J+1)=-XMSR*SIN(TH3)
   DX(J+1,I)=DX(I,J+1)
   DX(I,J+2)=-XMSR*SIN(TH1)
   DX(J+2,I)=DX(I,J+2)
6  CONTINUE
7  CONTINUE

```

```

RETURN
END
C   INVERT MOTOR INDUCTANCE MATRIX
C   *****
SUBROUTINE MTINVS(X,XI)
DOUBLE PRECISION X(6,6),XI(6,6),WKSPCE(10)
C
DO 1 I=1,6
DO 1 J=1,6
1  XI(I,J)=0.0
DO 2 I=1,10
2  WKSPCE(I)=0.0
IFL=1
CALL F01AAF(X,6,6,XI,6,WKSPCE,IFL)
IF(IFL.EQ.0)GOTO 5
WRITE(30,4)IFL
4  FORMAT(1X,'ERROR IN F01AAF= ',1X,I2)
5  RETURN
END
C   UP-DATE MOTORS' ROTOR POSITION
C   *****
SUBROUTINE ROTPOS(A,B,C,THETA,VEL,S,H,TE,TL0,XJ)
DOUBLE PRECISION A,B,C,THETA,VEL,S,AA,AA1,AA2,AA3,AA4,VELI
1,H,TL0,XJ,TE
C
XJJ=XJ*2.*100.*3.14159
AA=A*(1.+B*S+C*S*S)
AA1=H*(TE-AA-TL0*VEL)/XJJ
AA2=H*(TE-AA-TL0*(VEL+0.5*AA1))/XJJ
AA3=H*(TE-AA-TL0*(VEL+0.5*AA2))/XJJ
AA4=H*(TE-AA-TL0*(VEL+AA3))/XJJ
VELI=0.0
VELI=(AA1+2.*AA2+2.*AA3+AA4)/6.
VEL=VEL+VELI
S=1.-VEL
DVEL=(TE-AA-TL0*VEL)/XJJ
THETA=THETA+H*VEL+(H*H*DVEL)/2.
RETURN
END
C   BUILD [R + d[L]/dt]
C   *****
SUBROUTINE CMAT(R,DX,S,CM)
DOUBLE PRECISION R(6,6),DX(6,6),S,CM(6,6)
C
DO 1 I=1,6
DO 1 J=1,6
1  CM(I,J)=0.0
C
DO 2 I=1,6
DO 2 J=1,6
2  DX(I,J)=(1.-S)*DX(I,J)
C
DO 3 I=1,6
DO 3 J=1,6

```

```

3   CM(I,J)=R(I,J)+DX(I,J)
   RETURN
   END

C
C
SUBROUTINE BMAT(BM,SM)
DOUBLE PRECISION BM(6,6),SM(6,6),BMT(6,6)

C
DO 1 I=1,3
DO 1 J=1,3
IF(I.LE.3.AND.I.EQ.J)BMT(I,J)=1.
1  CONTINUE
C
DO 4 I=1,3
DO 3 J=1,3
SUM=0.0
DO 2 K=1,3
SUM=SUM+SM(I,K)*BMT(K,J)
2  CONTINUE
BM(I,J)=SUM
3  CONTINUE
4  CONTINUE
RETURN
END

C   RUNGE-KUTTA ROUTINE SOLVING OF THE CURRENT DERIVATIVE VECTOR
C   *****
SUBROUTINE RNGKTTA(AUX1,AUX2,AUX3,AUX4,CI,C,E1,E2,E3,E4,BM,
1CM,XI,H)
DOUBLE PRECISION AUX1(6),AUX2(6),AUX3(6),AUX4(6),CI(6),C(6),
1E1(6),E2(6),E3(6),E4(6),BM(6,6),CM(6,6),BR(6),CR(6),TM(6),H,
2XI(6,6),COF1,COF2,COF3,COF4

C
COF1=-0.5+1./SQRT(2.)
COF2=1.-1./SQRT(2.)
COF3=-1./SQRT(2.)
COF4=1.+1./SQRT(2.)

C
DO 510 I=1,6
BR(I)=0.0
DO 505 J=1,6
BR(I)=BR(I)+BM(I,J)*E1(J)
505 CONTINUE
510 CONTINUE
C
DO 520 I=1,6
CR(I)=0.0
DO 515 J=1,6
CR(I)=CR(I)+CM(I,J)*C(J)
515 CONTINUE
520 CONTINUE
C
DO 525 I=1,6
525 TM(I)=0.0
C

```

DO 527 I=1,6
527 TM(I)=BR(I)-CR(I)

C

DO 530 I=1,6
AUX1(I)=0.0
DO 528 J=1,6
AUX1(I)=AUX1(I)+XI(I,J)*TM(J)
528 CONTINUE
AUX1(I)=H*AUX1(I)
530 CONTINUE

C

DO 540 I=1,6
BR(I)=0.0
DO 535 J=1,6
BR(I)=BR(I)+BM(I,J)*E2(J)
535 CONTINUE
540 CONTINUE

C

DO 550 I=1,6
CR(I)=0.0
DO 545 J=1,6
CR(I)=CR(I)+CM(I,J)*(C(J)+0.5*AUX1(J))
545 CONTINUE
550 CONTINUE

C

DO 555 I=1,6
555 TM(I)=0.0
DO 560 I=1,6
560 TM(I)=BR(I)-CR(I)

C

DO 565 I=1,6
AUX2(I)=0.0
DO 562 J=1,6
AUX2(I)=AUX2(I)+XI(I,J)*TM(J)
562 CONTINUE
AUX2(I)=H*AUX2(I)
565 CONTINUE

C

DO 570 I=1,6
BR(I)=0.0
DO 568 J=1,6
BR(I)=BR(I)+BM(I,J)*E3(J)
568 CONTINUE
570 CONTINUE

C

DO 575 I=1,6
CR(I)=0.0
DO 572 J=1,6
CR(I)=CR(I)+CM(I,J)*(C(J)+COF1*AUX1(J)+COF2*AUX2(J))
572 CONTINUE
575 CONTINUE

C

DO 580 I=1,6
580 TM(I)=0.0


```

C
DO 581 I=1,6
581 TM(I)=BR(I)-CR(I)
DO 585 I=1,6
AUX3(I)=Ø.Ø
DO 582 J=1,6
AUX3(I)=AUX3(I)+XI(I,J)*TM(J)
582 CONTINUE
AUX3(I)=H*AUX3(I)
585 CONTINUE

C
DO 595 I=1,6
BR(I)=Ø.Ø
DO 59Ø J=1,6
BR(I)=BR(I)+BM(I,J)*E4(J)
59Ø CONTINUE
595 CONTINUE

C
DO 6Ø5 I=1,6
CR(I)=Ø.Ø
DO 6ØØ J=1,6
CR(I)=CR(I)+CM(I,J)*(C(J)+COF3*AUX2(J)+COF4*AUX3(J))
6ØØ CONTINUE
6Ø5 CONTINUE
DO 61Ø I=1,6
61Ø TM(I)=Ø.Ø
DO 615 I=1,6
615 TM(I)=BR(I)-CR(I)

C
DO 625 I=1,6
AUX4(I)=Ø.Ø
DO 62Ø J=1,6
AUX4(I)=AUX4(I)+XI(I,J)*TM(J)
62Ø CONTINUE
AUX4(I)=H*AUX4(I)
625 CONTINUE
RETURN
END

C
UP-DATE MOTOR'S CURRENT VECTOR
C
*****
SUBROUTINE CURR(AUX1,AUX2,AUX3,AUX4,CC,CII)
DOUBLE PRECISION AUX1(6),AUX2(6),AUX3(6),AUX4(6),CC(6),CII(6),
1COF2,COF4

C
COF2=1.-1./SQRT(2.)
COF4=1.+1./SQRT(2.)
DO 1 I=1,6
1 CII(I)=Ø.Ø
DO 2 I=1,6
2 CII(I)=(AUX1(I)+AUX4(I))/6.+(COF2*AUX2(I)+COF4*AUX3(I))/3.
DO 3 I=1,6
3 CC(I)=CC(I)+CII(I)
RETURN
END

```

```

C   CALCULATE THE AIR-GAP TORQUE
C   *****
C   SUBROUTINE TRQE(C, THETA, XMSR, TE)
      DOUBLE PRECISION C(6), THETA, XMSR, TE, T11, T12, T13, T14, T1Ø, TH1, TH2,
1 TH3, TX, T21, T22, T23, T2Ø, TY, T31, T32, T33, T3Ø, TZ

```

```

C   GAM=2.Ø943951
      TH1=THETA
      TH2=THETA+GAM
      TH3=THETA-GAM

```

```

C   T11=C(1)*C(4)
      T12=C(2)*C(5)
      T13=C(3)*C(6)
      T1Ø=T11+T12+T13
      TX=T1Ø*SIN(TH1)
      T21=C(1)*C(5)
      T22=C(2)*C(6)
      T23=C(3)*C(4)
      T2Ø=T21+T22+T23
      TY=T2Ø*SIN(TH2)
      T31=C(1)*C(6)
      T32=C(2)*C(4)
      T33=C(3)*C(5)
      T3Ø=T31+T32+T33
      TZ=T3Ø*SIN(TH3)
      TE=-(TX+TY+TZ)*XMSR
      RETURN
      END

```

```

C - UP-DTAE VOLTAGE OF BUS-BAR 'B2'
C   *****
      SUBROUTINE SYSTEM(AUXT1, AUXT2, AUXT3, AUXT4, AXG1, AXG2,
1 AXG3, AXG4, CT, CU, VG1, VG2, VG3, VG4, T, H, KK, DM, DMT)
      DOUBLE PRECISION VB1(3), VB2(3), VB3(3), VB4(3), VB11(3), VB22(3),
2 VB33(3), VB44(3), AXS1(3), AXS2(3), AXS3(3), AXS4(3), CUS(3), DMT(3,3),
3 AUXT1(3), AUXT2(3), AUXT3(3), AUXT4(3), AXG1(3), AXG2(3), AXG3(3),
4 AXG4(3), CT(3), CU(7), VG1(3), VG2(3), VG3(3), VG4(3), T, H, AXT1(3),
5 AXT2(3), AXT3(3), AXT4(3), E, TR1, TR2, XS, RS, CTM(3), DM(3,3), TIME
6, A(3,3), ZI(3,3), F1(3,3), F23(3,3), V1(3), V2(3), V3(3), V4(3)
7, F21(3,3), F22(3,3), RSS, XSS, RL, XLX, XIS

```

```

C   IF(KK.GT.Ø)GOTO 119
      NK=Ø
      KC=4
      DO 88 I=1,3
      DO 88 J=1,3
88  IF(I.EQ.J)A(I,J)=1.Ø
      DO 99 I=1,3
      DO 99 J=1,3
      IF(I.EQ.J)ZI(I,J)=1.Ø
99  IF(I.EQ.J)F1(I,J)=1.Ø
      DO 1Ø9 I=1,3
      DO 1Ø9 J=1,3
1Ø9 F23(I,J)=Ø.Ø

```

```

DO 111 I=1,3
DO 111 J=1,3
IF(I.EQ.2.AND.J.EQ.3)F21(I,J)=1.0
IF(I.EQ.3.AND.J.EQ.2)F21(I,J)=1.0
IF(I.EQ.2.AND.J.EQ.2)F21(I,J)=2.0
111 IF(I.EQ.3.AND.J.EQ.3)F21(I,J)=2.0
DO 112 I=1,3
DO 112 J=1,3
112 IF(I.EQ.3.AND.J.EQ.3)F22(I,J)=1.5
TIME=0.0525
E=0.989
XS=.0667604
RS=0.0033552
RL=0.00077
XLX=0.0267
XIS=0.0766
XSS=XS+XLX+XIS
RSS=RS+RL
TR1=1.0137799
TR2=1.0781304
119 IF(KK.EQ.111)KC=1
IF(KK.EQ.1070)KC=4
VB1(1)=E*DCOS(T+TIME+1.5708)
VB1(2)=E*DCOS(T+TIME+1.5708-2.0944)
VB1(3)=E*DCOS(T+TIME+1.5708+2.0944)
VB2(1)=E*DCOS((T+TIME+0.5*H)+1.5708)
VB2(2)=E*DCOS((T+TIME+0.5*H)+1.5708-2.0944)
VB2(3)=E*DCOS((T+TIME+0.5*H)+1.5708+2.0944)
VB3(1)=VB2(1)
VB3(2)=VB2(2)
VB3(3)=VB2(3)
VB4(1)=E*DCOS((T+TIME+H)+1.5708)
VB4(2)=E*DCOS((T+TIME+H)+1.5708-2.0944)
VB4(3)=E*DCOS((T+TIME+H)+1.5708+2.0944)
C
CALL CMOD(AUXT1,DMT,AXT1,TR1)
CALL CMOD(AUXT2,DMT,AXT2,TR1)
CALL CMOD(AUXT3,DMT,AXT3,TR1)
CALL CMOD(AUXT4,DMT,AXT4,TR1)
CALL CMOD(CT,DMT,CTM,TR1)
IF(KC.EQ.3)GOTO 33
DO 3 I=1,3
AXS1(I)=AXG1(I)-AXT1(I)
AXS2(I)=AXG2(I)-AXT2(I)
AXS3(I)=AXG3(I)-AXT3(I)
AXS4(I)=AXG4(I)-AXT4(I)
3 CUS(I)=CU(I)-CTM(I)
GOTO 12
33 CALL L3GFAULT(VB11,VB22,VB33,VB44,AXS1,AXS2,AXS3,
1AXS4,RSS,XSS,H,CUS,CU)
12 CONTINUE
T1000=T/314.16
C IF(KK.LT.4000.AND.NK.EQ.5)WRITE(40,999)T1000,CUS(1)
IF(NK.EQ.5)NK=0

```

```

NK=NK+1
C999  FORMAT(2X,4F15.8)
C
CALL VMOD(VB1,DMT,VB11,TR2)
CALL VMOD(VB2,DMT,VB22,TR2)
CALL VMOD(VB3,DMT,VB33,TR2)
CALL VMOD(VB4,DMT,VB44,TR2)
DO 4 I=1,3
VG1(I)=VB11(I)+XS*AXS1(I)/H+RSS*CUS(I)
VG2(I)=VB22(I)+XS*AXS2(I)/H+RSS*CUS(I)
VG3(I)=VB33(I)+XS*AXS3(I)/H+RSS*CUS(I)
4  VG4(I)=VB44(I)+XS*AXS4(I)/H+RSS*CUS(I)
IF(KK.EQ.111.AND.KC.EQ.1)CALL FAULT(F21,ZI,A)
IF(KK.EQ.111.AND.KC.EQ.2)CALL FAULT(F22,ZI,A)
IF(KK.EQ.111.AND.KC.EQ.3)CALL FAULT(F23,ZI,A)
IF(KK.EQ.1070)CALL MATM2(F1,ZI,A)
DO 7 I=1,3
V1(I)=0.0
V2(I)=0.0
V3(I)=0.0
V4(I)=0.0
DO 7 K=1,3
V1(I)=V1(I)+A(I,K)*VG1(K)
V2(I)=V2(I)+A(I,K)*VG2(K)
V3(I)=V3(I)+A(I,K)*VG3(K)
7  V4(I)=V4(I)+A(I,K)*VG4(K)
DO 8 I=1,3
VG1(I)=V1(I)
VG2(I)=V2(I)
VG3(I)=V3(I)
8  VG4(I)=V4(I)
C  WRITE(3,888)(VG4(I),I=1,3)
C888  FORMAT(2X,3F15.8)
RETURN
END

```

```

C
C
SUBROUTINE CONMAT(DM,DMT)
DOUBLE PRECISION DM(3,3),DMT(3,3)
DO 1 I=1,3
DO 1 J=1,3
IF(I.EQ.J)DM(I,J)=1.0
IF(I.EQ.1.AND.J.EQ.2)DM(I,J)=-1.0
IF(I.EQ.2.AND.J.EQ.3)DM(I,J)=-1.0
IF(I.EQ.3.AND.J.EQ.1)DM(I,J)=-1.0
1  CONTINUE
DO 2 I=1,3
DO 2 J=1,3
2  DMT(I,J)=DM(J,I)
RETURN
END

```

```

C
C
SUBROUTINE CMOD(A,B,C,D)

```

```

DOUBLE PRECISION A(3),B(3,3),C(3),D
DO 1 J=1,3
SUM=0.0
DO 2 K=1,3
SUM=SUM+B(J,K)*A(K)
2 CONTINUE
C(J)=SUM/((SQRT(3.))*D)
1 CONTINUE
RETURN
END

```

C
C

```

SUBROUTINE L3GFAULT(VB11,VB22,VB33,VB44,AXS1,AXS2,AXS3,
LAXS4,RS,XS,H,CUS,CU)
DOUBLE PRECISION VB11(3),VB22(3),VB33(3),VB44(3),AXS1(3),
LAXS2(3),AXS3(3),AXS4(3),RS,XS,H,CUS(3),CU(3),CINC(3)

```

C

```

DO 1 I=1,3
AXS1(I)=(VB11(I)+RS*CUS(I))*H/XS
AXS2(I)=(VB22(I)+RS*(CUS(I)+0.5*AXS1(I)))*H/XS
AXS3(I)=(VB33(I)+RS*(CUS(I)+0.5*AXS2(I)))*H/XS
1 AXS4(I)=(VB44(I)+RS*(CUS(I)+AXS3(I)))*H/XS
DO 2 I=1,3
2 CINC(I)=(AXS1(I)+2.*(AXS2(I)+AXS3(I))+AXS4(I))/4.
DO 3 I=1,3
3 CUS(I)=CUS(I)+CINC(I)
RETURN
END

```

VOLTAGE AUXILIARIES AT THE MOTORS TERMINALS

-0.12865947	0.89978567	-0.77112625
-0.14378880	0.90549811	-0.76170937
-0.14378880	0.90549811	-0.76170937
-0.15888269	0.91098736	-0.75210473

VOLTAGE AUXILIARIES AT THE GENERATOR TERMINALS

0.35892633	0.62941528	-0.98834181
0.34421870	0.64154938	-0.98576828
0.34421870	0.64154938	-0.98576828
0.32942622	0.65352536	-0.98295178

GENERATOR DATA

0.779	0.119	-0.898	2.053	0.0	0.0
0.0	1.0006	0.17	0.1933	2.27	2.15
0.32	2.0	0.26	0.26	0.95	0.82
0.02	0.02	0.6667	0.0	0.0314	0.3332
314.16	0.0015	0.0022	0.0019	0.0	0.3671 0 200
1.0	0.0	0.0	0.3332	0.0	1.0
3.16	0.8308				

DATA FOR MOTOR CWP

0.00711	0.0112	3.9578	3.9847	0.0
0.0	2.5533	0.85	-1.7	0.9
0.00636	0.99364	0.0667856	0.0	0.0
0.2538869	0.3425831	-0.59647	-0.0114849	-0.4499511 0.461436
1.711				

DATA FOR MOTOR BFP

0.0047	0.0084	4.5495	4.5146	0.0
0.0	2.9400	0.9	-2.0	1.0
0.00482	0.99518	0.0754331	0.0	0.0
0.2129307	0.3672873	-0.580218	-0.0014961	-0.4625283 0.4640243
1.05				

DATA FOR MOTOR PAF

0.0095	0.0121	3.7139	3.7567	0.0
0.0	2.400	0.86	-2.0	1.0
0.00711	0.99289	0.0605200	0.0	0.0
0.268745	0.3535144	-0.6222594	-0.0107619	-0.4663772 0.4771391
13.0				

DATA FOR MOTOR IDF

0.0076	0.0107	3.4201	3.4861	0.0
0.0	2.2133	0.87	-2.0	1.0
0.00632	0.99368	0.0536189	0.0	0.0
0.2908348	0.3492795	-0.6401143	-0.0103387	-0.4703054 0.4806441

```

C THIS PROGRAM SOLVES FOR THE INITIAL CONDITION OF THE SYSTEM
C OF FIG. 5.1, UNDER STEADY STATE CONDITION. THE PROGRAM ALSO
C CALCULATES THE INITIAL CONDITION OF THE SYNCHRONOUS GENERATOR
C UNDER THIS MODE OF OPERATION
C *****

```

```

DIMENSION CIT(3,3),CT(3,3)
COMPLEX SM,ZL,ZT1,ST1,SMT1,SG,SIS,SNS,V(3),XET1(3),VM(3)
COMPLEX CU(3),VC(3),CST2(3),SUM,VST2(3),ZLL,CMTH1(3)
COMPLEX ZTLV,ZT2,XE(3),AI,ARMC(3),CMT1(3),SNSC,EG(3)
COMPLEX ANGL1,ANG2,ANG3,VMT1(3),VMT1C(3),SMT1C,EQA,ANGN

```

```

C
C TOTAL MW & MVARs OF MOTORS SET
C

```

```

C DATA ARE READ FROM FILE 'WD'
  READ(15,10)PM1,PM2,PM3,PM4
  READ(15,10)QM1,QM2,QM3,QM4
10  FORMAT(4F12.8)
  PM=2.*(PM1+PM2+PM3+PM4)
  QM=2.*(QM1+QM2+QM3+QM4)
  SM=PM+(0.0,1.0)*QM
  WRITE(16,11)PM1,PM2,PM3,PM4
  WRITE(16,11)QM1,QM2,QM3,QM4
11  FORMAT(2X,4F12.8)
  WRITE(16,12)SM
12  FORMAT(2X,2F12.8)

```

```

C
C LOSSES IN MOTOR TRANSFORMER
C

```

```

  READ(15,15)RT1,XT1
15  FORMAT(2F12.8)
  ZT1=RT1+(0.0,1.0)*XT1
  PT1=(PM*PM+QM*QM)*RT1
  QT1=(PM*PM+QM*QM)*XT1
  ST1=PT1+(0.0,1.0)*QT1
  WRITE(16,12)ST1

```

```

C
C MW & MVARs INJECTED TO THE GROUP OF MOTORS & TRANSFORMER
C

```

```

  PMT1=PM+PT1
  QMT1=QM+QT1
  SMT1=PMT1+(0.0,1.0)*QMT1
  WRITE(16,12)SMT1

```

```

C
C TOTAL MW & MVARs INJECTED TO THE INFINITE SYSTEM
C

```

```

  READ(15,15)PG,QG
  SG=PG+(0.0,1.0)*QG
  SIS=SG-SMT1
  PIS=REAL(SIS)
  QIS=AIMAG(SIS)
  WRITE(16,12)SIS

```

```

C
C TAP POSITION OF THE MOTOR TRANSFORMER T1

```

```

C
A=0.0
B=0.0
C=0.0
A=PMT1*RT1+QMT1*XT1
B=PMT1*XT1-QMT1*RT1
C=1.0-A
TEMP1=SQRT(C*C+B*B)
TNT1=1./TEMP1

C
C
C
TAP POSITION OF THE GENERATOR-TRANSFORMER T2

A=0.0
B=0.0
C=0.0
READ(15,15)RT2,XT2
ZT2=RT2+(0.0,1.0)*XT2
A=PIS*RT2+QIS*XT2
B=PIS*XT2-QIS*RT2
C=1.-A
TEMP2=SQRT(C*C+B*B)
TNT2=1./TEMP2

C
C
C
LOSSES IN GENERATOR TRANSFORMER T2

PT2=(PIS*PIS+QIS*QIS)*RT2
QT2=(PIS*PIS+QIS*QIS)*XT2

C
C
C
POWER TRANSMITTED THROUGH TRANSFORMER T2

PHI=PIS-PT2
QHI=QIS-QT2

C
C
C
LOSSES IN TRANSMISSION LINE

READ(15,15)RL,XL
ZL=RL+(0.0,1.0)*XL
PL=(PHI*PHI+QHI*QHI)*RL
QL=(PHI*PHI+QHI*QHI)*XL

C
C
C
NET POWER FED INTO THE INFINITE SYSTEM

PNS=PHI-PL
QNS=QHI-QL
SNS=PNS+(0.0,1.0)*QNS
WRITE(16,12)SNS

C
C
C
INFINITE MACHINE VOLTAGE

ET=1.0
EI1=ET*ET-(PNS*RL+QNS*XL)
EI2=EI1*EI1
EI3=QNS*RL-PNS*XL
EI32=EI3*EI3

```



```

      EI=SQRT(EI2+EI32)
C
C   CALCULATE THE THREE PHASE VOLTAGE OF THE INFINITE MACHINE
C
      ANG1=(0.0,1.0)*(1.5707963)
      ANG2=(0.0,1.0)*(1.5707963-2.0943951)
      ANG3=(0.0,1.0)*(1.5707963+2.0943951)
      V(1)=EI*CEXP(ANG1)
      V(2)=EI*CEXP(ANG2)
      V(3)=EI*CEXP(ANG3)
C
C   CURRENT FED INTO THE INFINITE SYSTEM
C   I*=SNS/V i.e I=SNS*/V* WHERE * IS CONJUGATE
C
      A1=REAL(V(1))
      B1=AIMAG(V(1))
      VC(1)=A1-(0.0,1.0)*B1
      A2=REAL(V(2))
      B2=AIMAG(V(2))
      VC(2)=A2-(0.0,1.0)*B2
      A3=REAL(V(3))
      B3=AIMAG(V(3))
      VC(3)=A3-(0.0,1.0)*B3
C
      C=REAL(SNS)
      D=AIMAG(SNS)
      SNSC=C-(0.0,1.0)*D
      DO 210 I=1,3
210  CU(I)=SNSC/VC(I)
      WRITE(16,16)(CU(I),I=1,3)
      16  FORMAT(2X,2F12.8,2X,2F10.8,2X,2F10.8)
C
C   FORM CONNECTION MATRIX CIT
C
      DO 215 I=1,3
      DO 215 J=1,3
215  CIT(I,J)=0.0
      DO 220 I=1,3
      DO 220 J=1,3
      IF(I.EQ.J)CIT(I,J)=1.0
      IF(I.EQ.1.AND.J.EQ.3)CIT(I,J)=-1.0
      IF(I.EQ.2.AND.J.EQ.1)CIT(I,J)=-1.0
      IF(I.EQ.3.AND.J.EQ.2)CIT(I,J)=-1.0
220  CONTINUE
      WRITE(16,17)((CIT(I,J),J=1,3),I=1,3)
      17  FORMAT(2X,3F10.5)
C
C   CURRENT AT LOW VOLTAGE SIDE OF THE GENERATOR TRANSFORMER T2
C
      DO 230 I=1,3
      SUM=J.0+(0.0,1.0)*0.0
      DO 225 J=1,3
      SUM=SUM+CIT(I,J)*CU(J)
225  CONTINUE

```

```

      CST2(I)=SUM*(TNT2/SQRT(3.))
230  CONTINUE
      WRITE(16,16)(CST2(I),I=1,3)
C
C   THREE PHASE VOLTAGE AT L.V SIDE OF THE GENERATOR TRANSFORMER T2
C
      DO 240 I=1,3
      SUM=0.0+(0.0,1.0)*0.0
      DO 235 J=1,3
      SUM=SUM+CIT(I,J)*V(J)
235  CONTINUE
      VST2(I)=SUM/(TNT2*SQRT(3.))
240  CONTINUE
      WRITE(16,16)(VST2(I),I=1,3)
C
C   LINE IMPEDANCE AT L.V OF T/F T2
C
      ZLL=ZL/(TNT2*TNT2)
      ZTLV=ZLL+ZT2
C
C   VOLTAGE DROP AT T2 & LINE IMPEDANCES
C
      DO 250 I=1,3
250  XE(I)=CST2(I)*ZTLV
      WRITE(16,16)(XE(I),I=1,3)
C
C   VOLTAGE AT GENERATOR TERMINALS
C
      DO 255 I=1,3
255  EG(I)=VST2(I)+XE(I)
      WRITE(16,16)(EG(I),I=1,3)
C
C   TRANSPOSITION OF CONNECTION MATRIX CIT
C
      DO 260 I=1,3
      DO 260 J=1,3
      CT(I,J)=CIT(J,I)
260  CONTINUE
C
C   VOLTAGE AT L.V OF MOTOR TRANSFORMER
C
      DO 270 I=1,3
      SUM=0.0+(0.0,1.0)*0.0
      DO 265 J=1,3
      SUM=SUM+CT(I,J)*EG(J)
265  CONTINUE
      VMT1(I)=SUM/(TNT1*SQRT(3.))
270  CONTINUE
      WRITE(16,16)(VMT1(I),I=1,3)
C
C   CURRENT AT LOW VOLTAGE SIDE OF MOTOR TRANSFORMER T1
C
      AAI=REAL(VMT1(1))
      BBI=AIMAG(VMT1(1))

```

```

VMT1C(1)=AA1-(0.0,1.0)*BB1
AA2=REAL(VMT1(2))
BB2=AIMAG(VMT1(2))
VMT1C(2)=AA2-(0.0,1.0)*BB2
AA3=REAL(VMT1(3))
BB3=AIMAG(VMT1(3))
VMT1C(3)=AA3-(0.0,1.0)*BB3
C
AA=REAL(SMT1)
BB=AIMAG(SMT1)
SMT1C=AA-(0.0,1.0)*BB
C
DO 300 I=1,3
300 CMT1(I)=SMT1C/VMT1C(I)
CMT1(1)=0.013417+0.0308214*(0.0,1.0)
CMT1(2)=0.0199836-0.0270301*(0.0,1.0)
CMT1(3)=-0.0334006-0.0037913*(0.0,1.0)
WRITE(16,16)(CMT1(I),I=1,3)
C
C DROP IN MOTOR TRANSFORMER T1
C
DO 301 I=1,3
301 XET1(I)=CMT1(I)*ZT1
C
C VOLTAGE AT MOTOR TERMINAL
C
DO 302 I=1,3
302 VM(I)=VMT1(I)-XET1(I)
WRITE(16,16)(VM(I),I=1,3)
C
C CURRENT AT HIGH VOLTAGE SIDE OF MOTOR TRANSFORMER T1
C
DO 310 I=1,3
SUM=0.0+(0.0,1.0)*0.0
DO 305 J=1,3
SUM=SUM+CIT(I,J)*CMT1(J)
305 CONTINUE
CMTH1(I)=SUM/(TNT1*SQRT(3.))
310 CONTINUE
WRITE(16,16)(CMTH1(I),I=1,3)
C
C ARMATURE CURRENT
C
DO 315 I=1,3
315 ARMC(I)=CST2(I)+CMTH1(I)
WRITE(16,16)(ARMC(I),I=1,3)
C
C CALCULATE ANGLE BETWEEN 'd' AXIS & AXIS OF PHASE 'a'
C
READ(15,19)RA,XA,XAQ0
READ(15,19)XAD0,SF,XD
READ(15,19)X0,XD1,XQ
READ(15,19)TD1,W,TL
19 FORMAT(3F12.8)

```

```

EQA=EG(1)+(RA+(0.0,1.0)*(XA+XAQ0))*ARMC(1)
EQH=REAL(EQA)
EQV=AIMAG(EQA)
EQD=SQRT(EQH*EQH+EQV*EQV)
IF((EQV.GT.0.0).AND.(EQH.GT.0.0))GOTO 555
IF((EQV.GT.0.0).AND.(EQH.LT.0.0))GOTO 666
IF((EQV.LT.0.0).AND.(EQH.GT.0.0))GOTO 777
IF((EQV.LT.0.0).AND.(EQH.LT.0.0))GOTO 888
555 ANG=ATAN(EQV/EQH)
GOTO 999
666 ANG=ATAN(EQV/EQH)+3.1415927
GOTO 999
777 ANG=ATAN(EQV/EQH)+6.2831853
GOTO 999
888 ANG=ATAN(EQV/EQH)+3.1415927
999 ANGN=(ANG-1.5707963)*(0.0,1.0)
X=AIMAG(ANGN)
WRITE(16,75)EQA,EQH,EQV,EQD,X
75  FORMAT(2X,6F12.8)
AI=ARMC(1)*CEXP(-ANGN)
DAI=REAL(AI)
QAI=AIMAG(AI)
EQ=EQD+DAI*(XAD0-XAQ0)/SF
FDI=EQ*SF*1.5/XAD0
FS1=(0.666667*FDI-DAI)*(0.666667*FDI-DAI)*XAD0*XAD0/SF*SF
FS2=QAI*QAI*XAQ0*XAQ0/(SF*SF)
WRITE(16,21)FS1,FS2
21  FORMAT(1X,2F12.8)
FS=SQRT(FS1+FS2)*100.0
FDI1=FS
SFN=FDI1/FS
FDI1=FDI1/100.0
WRITE(16,23)FDI1,FDI,FS,SF,SFN,ANGN
23  FORMAT(1X,7F10.5)
C
C  CALCULATE EFD & THE INITIAL MECHANICAL TORQUE
C
XAA0=((XD+XQ-2.*XA)/SFN+2.*XA+X0)/3.0
XAB0=((XD+XQ-2.*XA)/SFN+2.*XA-2.*X0)/6.
XAA2=(XD-XQ)/(3.*SFN)
XAL0=0.666667*XAD0
XAQ0=0.666667*XAQ0
XAFD=XAL0*XAD0/((XD-XD1)*.666667)
RFD=XAFD*XD1/(W*TD1*XD)
XX=ANG-1.5707963
AAI=REAL(ARMC(1))
BI=REAL(ARMC(2))
CI=REAL(ARMC(3))
CL11=-XAA0-XAA2*COS(2.*XX)
CL12=XAB0-XAA2*COS(2.*XX-2.0943951)
CL13=XAB0-XAA2*COS(2.*XX+2.0943951)
CL14=XAD0*COS(XX)/SFN
CL22=-XAA0-XAA2*COS(2.*XX+2.0943951)
CL23=XAB0-XAA2*COS(2.*XX)

```

```

CL24=XAD0*COS (XX-2.0943951)/SFN
CL33=-XAA0-XAA2*COS (2.*XX-2.0943951)
CL34=XAD0*COS (X+2.0943951)/SFN
FA=CL11*AAI+CL12*BI+CL13*CI+CL14*FDI
FB=CL12*AAI+CL22*BI+CL23*CI+CL24*FDI
FC=CL13*AAI+CL23*BI+CL33*CI+CL34*FDI
EFD=RFD*FDI
TE=0.3849*(FA*(BI-CI)+FB*(CI-AAI)+FC*(AAI-BI))
TM=TE+TL
WRITE (16, 25) AAI, BI, CI, FA, FB, FC, TM, EFD, RFD
25  FORMAT (1X, 9F9.5)
STOP
END

```

DATA FOR THE SYSTEM OF FIG. 5.1 USED TO CALCULATE
THE INITIAL STEADY STATE CONDITION

Ø.Ø132216	Ø.ØØ3875Ø	Ø.ØØ39948	Ø.ØØ34781
Ø.ØØ24Ø21	Ø.ØØ2264Ø	Ø.ØØ64Ø34	Ø.ØØ2Ø644
Ø.Ø12Ø433	Ø.4781937		
Ø.85	Ø.52678		
Ø.ØØ39	Ø.1552		
Ø.ØØ1	Ø.Ø31		
Ø.ØØ22	Ø.17	1.98	
2.1	1.Ø	2.27	
Ø.1933	Ø.32	2.15	
Ø.95	314.16	Ø.Ø	

RESULTS OBTAINED

Ø.Ø132216Ø	Ø.ØØ3875ØØ	Ø.ØØ39948Ø	Ø.ØØ34781Ø			
Ø.ØØ24Ø21Ø	Ø.ØØ2264ØØ	Ø.ØØ64Ø34Ø	Ø.ØØ2Ø644Ø			
Ø.Ø49139ØØ	Ø.Ø262678Ø					
Ø.ØØØØ3739	Ø.ØØ148462					
Ø.Ø4917639	Ø.Ø2775242					
Ø.8ØØ82361	Ø.499Ø2758					
Ø.79658528	Ø.3371ØØ39					
Ø.34Ø8314Ø	Ø.8Ø54Ø179	Ø.527Ø8271-	.69786955	-	.86791411-	.1Ø753224
1.ØØØØØ	Ø.ØØØØØ	-1.ØØØØØ				
-1.ØØØØØ	1.ØØØØØ	Ø.ØØØØØ				
Ø.ØØØØØ	-1.ØØØØØ	1.ØØØØØ				
Ø.7523944Ø	Ø.56826391	Ø.11593378-	.93572462	-	.86832819Ø.	.36746Ø71
Ø.458689Ø8	Ø.79447273	Ø.458689Ø3-	.79447276	-	.91737811Ø.ØØØØØØØ2	
-Ø.Ø9976839	Ø.1395429Ø	Ø.17Ø73189Ø.	Ø.Ø1663Ø51	-	.Ø7Ø96351-	.15617341
Ø.35892Ø69	Ø.934Ø1564	Ø.62942Ø93-	.77784225	-	.98834162-	.15617338
-Ø.154Ø5Ø86	Ø.9749Ø922	Ø.92132158-	.354Ø4265	-	.76727Ø72-	.62Ø86656
Ø.Ø1999675	Ø.Ø536Ø182	Ø.Ø3642216-	.Ø441186Ø	-	.Ø5641891-	.ØØ948322
-Ø.12865963	Ø.9647Ø136	Ø.8997857Ø-	.37Ø92817	-	.771126Ø7-	.59377319
Ø.Ø4351899	Ø.Ø3592715	Ø.ØØ935433-	.Ø5565213	-	.Ø5287332Ø.	Ø.Ø1972497
Ø.79591339	Ø.6Ø4191Ø6	Ø.12528812-	.99137675	-	.9212Ø151Ø.	.38718569
-Ø.938339Ø9	2.64655866	-Ø.938339Ø9	2.64655866		2.8Ø798Ø23	
Ø.34Ø7233Ø	Ø.851747ØØ	Ø.361Ø8963				
1.1Ø129	2.Ø8731	11Ø.12886	1.ØØØØØ	1.ØØØØØ	Ø.ØØØØØ	Ø.34Ø72
Ø.79591	Ø.12529	-Ø.9212Ø	Ø.93535	-Ø.78ØØ2	-Ø.15532	Ø.85219
Ø.ØØ149	Ø.ØØØ71					

```

C   THIS PROGRAM IS WRITTEN TO SOLVE FOR THE INITIAL CONDITION OF
C   THE GROUP OF MOTOR CWP, BFP, PAF& DAF.
C   *****
C
C   COMPLEX Z(2,2),SUM,Y(2,2),V(2),VS,DET,CM(2)
C   COMPLEX ANS1,ANS2,ANS3,CMS1,CMS2,CMS3,ANR1,ANR2,ANR3,
C   1CMR1,CMR2,CMR3,ZLZ,ZIZ,EM,CRT(4,3),CRTT1(3)
C
C   X=-0.12865963
C   YY=0.96470136
C   ANNA=ATAN(YY/X)
C   ANNA=ANNA+3.1415927
C   VS=X+(0.0,1.0)*YY
C   WRITE(16,2)VS,ANNA
2   FORMAT(2X,3F12.8)
C   DO 10 K=1,4
C   READ(15,30)X1,X2,XM
C   READ(15,30)R1,R2,S
C   READ(15,30)A,B,C
C   READ(15,30)RAT1,RAT2,ON
30  FORMAT(3F12.8)
C
C   WRITE(16,30)X1,X2,XM
C   WRITE(16,30)R1,R2,S
C   WRITE(16,30)A,B,C
C   WRITE(16,30)RAT1,RAT2,ON
C   WRITE(16,2)VS
C
C   V(1)=VS
C   V(2)=0.0+(0.0,1.0)*0.0
C
C   DO 15 I=1,2
C   DO 15 J=1,2
15  Z(I,J)=0.0+(0.0,1.0)*0.0
C   Y(I,J)=0.0+(0.0,1.0)*0.0
C
C   R22=R2/S
C   Z(1,1)=R1+(0.0,1.0)*X1
C   Z(1,2)=0.0+(0.0,1.0)*XM
C   Z(2,1)=Z(1,2)
C   Z(2,2)=R22+(0.0,1.0)*X2
C   WRITE(16,35)((Z(I,J),J=1,2),I=1,2)
C
C   DET=0.0
C   DET=Z(1,1)*Z(2,2)-Z(1,2)*Z(2,1)
C
C   Y(1,1)=Z(2,2)/DET
C   Y(1,2)=-Z(1,2)/DET
C   Y(2,1)=-Z(1,2)/DET
C   Y(2,2)=Z(1,1)/DET
C
C   WRITE(16,35)((Y(I,J),J=1,2),I=1,2)
C
C   DO 26 I=1,2

```

```

      CM(I)=0.0
      SUM=0.0+(0.0,1.0)*0.0
      DO 24 J=1,2
      SUM=SUM+Y(I,J)*V(J)
24    CONTINUE
      CM(I)=SUM
26    CONTINUE
      WRITE(16,40)(CM(I),I=1,2)
C
35    FORMAT(2X,2F15.8,8X,2F15.8)
40    FORMAT(2X,2F12.8,8X,2F12.8)
C
C    COMPLEX CURRENT OF MOTOR SET
C
      CHS=REAL(CM(1))
      CVS=AIMAG(CM(1))
      CMODS=SQRT(CHS*CHS+CVS*CVS)
      IF((CVS.GT.0.0).AND.(CHS.GT.0.0))GOTO 101
      IF((CVS.GT.0.0).AND.(CHS.LT.0.0))GOTO 202
      IF((CVS.LT.0.0).AND.(CHS.GT.0.0))GOTO 303
      IF((CVS.LT.0.0).AND.(CHS.LT.0.0))GOTO 404
101  ANS=ATAN(CVS/CHS)
      GOTO 505
202  ANS=ATAN(CVS/CHS)+3.1415927
      GOTO 505
303  ANS=ATAN(CVS/CHS)+6.2831853
      GOTO 505
404  ANS=ATAN(CVS/CHS)+3.1415927
505  ANS1=(ANS)*(0.0,1.0)
      ANS2=(ANS-2.0943951)*(0.0,1.0)
      ANS3=(ANS+2.0943951)*(0.0,1.0)
      CMS1=CMODS*CEXP(ANS1)
      CMS2=CMODS*CEXP(ANS2)
      CMS3=CMODS*CEXP(ANS3)
      WRITE(16,989)CMS1,CMS2,CMS3
C
      CHR=REAL(CM(2))
      CVR=AIMAG(CM(2))
      CMODR=SQRT(CHR*CHR+CVR*CVR)
      IF((CVR.GT.0.0).AND.(CHR.GT.0.0))GOTO 606
      IF((CVR.GT.0.0).AND.(CHR.LT.0.0))GOTO 707
      IF((CVR.LT.0.0).AND.(CHR.GT.0.0))GOTO 808
      IF((CVR.LT.0.0).AND.(CHR.LT.0.0))GOTO 909
606  ANR=ATAN(CVR/CHR)
      GOTO 1000
707  ANR=ATAN(CVR/CHR)+3.1415927
      GOTO 1000
808  ANR=ATAN(CVR/CHR)+6.2831853
      GOTO 1000
909  ANR=ATAN(CVR/CHR)+3.1415927
1000 ANR1=(ANR)*(0.0,1.0)
      ANR2=(ANR-2.0943951)*(0.0,1.0)
      ANR3=(ANR+2.0943951)*(0.0,1.0)
      CMR1=CMODR*CEXP(ANR1)

```



```

CMR2=CMODR*CEXP (ANR2)
CMR3=CMODR*CEXP (ANR3)
WRITE (16, 989) CMR1, CMR2, CMR3
C
C REAL PART OF STATOR & ROTOR CURRENT
C
RS=REAL (CMS1)
YS=REAL (CMS2)
BS=REAL (CMS3)
RR=REAL (CMR1)
YR=REAL (CMR2)
BR=REAL (CMR3)
WRITE (16, 989) RS, YS, BS, RR, YR, BR
989 FORMAT (2X, 6F12.7)
C
C ANGLE BETWEEN STATOR & ROTOR AXIS
C
XL=XL-XM
ZLZ=R1+(0.0, 1.0)*XL
ZIZ=ZLZ*CMS1
EM=VS-ZIZ
EMH=REAL (EM)
EMV=AIMAG (EM)
EMOD=SQRT (EMH*EMH+EMV*EMV)
WRITE (3, 222) EMOD
222 FORMAT (1X, F15.7)
THM=ATAN (EMV/EMH)
THM=THM+3.1415927
THM=ANNA-THM
WRITE (16, 905) THM, EMH, EMV
905 FORMAT (2X, 3F15.7)
C
C STEADY STATE SPEED & MECHANICAL TORQUE
C
VEL=1.-S
GAM=2.*3.1415927/3.
XMM=(2./3.)*XM
TE1=(RS*RR+YS*YR+BS*BR)*SIN (THM)
TE2=(RS*YR+YS*BR+BS*RR)*SIN (THM+GAM)
TE3=(RS*BR+YS*RR+BS*YR)*SIN (THM-GAM)
TE=-(TE1+TE2+TE3)*XMM
TM=A*(1.+B*S+C*S*S)
WRITE (16, 199) TE, TM
199 FORMAT (2X, 2F12.7)
C
C STATOR CURRENT ON 776 MVA BASE
C
CMS1=CMS1*(RAT1/RAT2)*ON
CMS2=CMS2*(RAT1/RAT2)*ON
CMS3=CMS3*(RAT1/RAT2)*ON
CRT (K, 1)=CMS1
CRT (K, 2)=CMS2
CRT (K, 3)=CMS3
WRITE (16, 989) CMS1, CMS2, CMS3

```

```
WRITE(16,50)K
50  FORMAT(2X,I4)
    WRITE(16,59)
59  FORMAT(1X,'*****')
10  CONTINUE
    DO 29 J=1,3
      SUM=0.0+0.0*(0.0,1.0)
      DO 39 K=1,4
        SUM=SUM+CRT(K,J)
39  CONTINUE
      CRTT1(J)=SUM
29  CONTINUE
    WRITE(16,989)(CRTT1(J),J=1,3)
    STOP
    END
```

3.9578	3.9847	3.83
0.00711	0.0112	0.007
0.85	-1.7	0.9
4.5495	4.5146	4.41
0.0047	0.0084	0.007
0.9	-2.0	1.0
3.7139	3.7567	3.6
0.0095	0.0121	0.0075
0.87	-2.0	1.0
3.4201	3.4861	3.32
0.0076	0.0107	0.007
0.86	-2.0	1.0

DATA FOR INDUCTION MOTORS CWP, BFP, PAF& IDF
 USED TO FIND THE INITIAL STEADY STATE

RESULTS OBTAINED FOR SOLVING THE INDUCTION MOTOR EQUATIONS
IN STEADY STATE

```

-0.12865963  0.96470136  1.70338108
 3.95780000  3.98470000  3.83000000
 0.00711000  0.01120000  0.00636000
 0.85000000 -1.70000000  0.90000000
 3.53800000776.00000000  2.00000000
-0.12865963  0.96470136
  0.00711000  3.95780000  0.00000000  3.83000000
  0.00000000  3.83000000  1.76100629  3.98470000
  0.51769303 -0.3322014  -0.53435076  0.08317014
 -0.53435076  0.08317014  0.55202666 -0.08693734
 0.25388702  0.54216249 -0.01148498 -0.52618954
 0.2538869  0.5421626  0.3425831 -0.4909538 -0.5964700 -0.0512088
 -0.0114849 -0.5261895 -0.4499511  0.2730410  0.4614360  0.2531485
 0.2538869  0.3425831 -0.5964700 -0.0114849 -0.4499511  0.4614360
  0.0667856 -0.0611764  0.9283998
 0.8405799  0.8408407
 0.0023151  0.0049437  0.0031239 -0.0044768 -0.0054389 -0.0004670
 1

```

```

4.54950000  4.51460000  4.41000000
 0.00470000  0.00840000  0.00482000
 0.90000000 -2.00000000  1.00000000
11.40000000776.00000000  2.00000000
-0.12865963  0.96470136
  0.00470000  4.54950000  0.00000000  4.41000000
  0.00000000  4.41000000  1.74273859  4.51460000
  0.52822627 -0.29116996 -0.54462515  0.07418603
 -0.54462515  0.07418603  0.56177403 -0.07711317
 0.21293066  0.54704242 -0.00149609 -0.53494537
 0.2129307  0.5470424  0.3672873 -0.4579246 -0.5802180 -0.0891178
 -0.0014961 -0.5349454 -0.4625283  0.2687683  0.4640243  0.2661771
 0.2129307  0.3672873 -0.5802180 -0.0014961 -0.4625283  0.4640243
  0.0754331 -0.0533480  0.9324264
 0.8919925  0.8913449
 0.0062562  0.0160729  0.0107914 -0.0134545 -0.0170476 -0.0026184
 2

```

```

3.71390000  3.75670000  3.60000000
 0.00950000  0.01210000  0.00711000
 0.87000000 -2.00000000  1.00000000
 3.13900000776.00000000  2.00000000
-0.12865963  0.96470136
  0.00950000  3.71390000  0.00000000  3.60000000
  0.00000000  3.60000000  1.70182841  3.75670000
  0.53726719 -0.35023244 -0.55334150  0.08495342
 -0.55334150  0.08495342  0.57062443 -0.08910145
 0.26874511  0.56336316 -0.01076196 -0.54473937
 0.2687450  0.5633632  0.3535144 -0.5144216 -0.6222594 -0.0489416
 -0.0107619 -0.5447394 -0.4663772  0.2816898  0.4771391  0.2630496
 0.2687450  0.3535144 -0.6222594 -0.0107619 -0.4663772  0.4771391

```

0.0605200 -0.0670456 0.9287394
0.8575877 0.8576726
0.0021742 0.0045577 0.0028600 -0.0041618 -0.0050342 -0.0003959
3

3.42010000 3.48610000 3.32000000
0.00760000 0.01070000 0.00632000
0.86000000 -2.00000000 1.00000000
3.56400000 776.00000000 2.00000000
-0.12865963 0.96470136
0.00760000 3.42010000 0.00000000 3.32000000
0.00000000 3.32000000 1.69303797 3.48610000
0.54227557 -0.37379850 -0.55776982 0.08510529
-0.55776982 0.08510529 0.57439210 -0.08894809
0.29083495 0.57122676 -0.01033873 -0.54903092
0.2908348 0.5712268 0.3492795 -0.5374838 -0.6401143 -0.0337431
-0.0103387 -0.5490309 -0.4703054 0.2834690 0.4806441 0.2655619
0.2908348 0.3492795 -0.6401143 -0.0103387 -0.4703054 0.4806441
0.0536189 -0.0736902 0.9312475
0.8491881 0.8491640
0.0026715 0.0052470 0.0032083 -0.0049371 -0.0058798 -0.0003099
4

0.0134170 0.0308214 0.0199836 -0.0270301 -0.0334006 -0.0037913

*LIST OF REFERENCES
AND BIBLIOGRAPHY*

LIST OF REFERENCES

- 1- ALDRED, A. S.
"Electronic Analogue Computer Simulation of Multi-machine Power-System Networks"
Proc. IEE, vol. 109A, pp 195-202, June 1962.

- 2- ALDRED, A. S., and DOYLE, B. E.
"Electronic-Analogue-Computer Study of Synchronous machine Transient Stability"
Proc. IEE, vol. 104A, pp152-160, June 1957.

- 3- ASISH, K. DE-SARKER, and GUNNAR, J. B.
"Digital Simulation of Three-Phase Induction Motors"
Trans. IEEE, vol. PAS-89, No.6, pp. 1031-1037, July/August 1970.

- 4- AHMED, H. EL-ABIAD, and NAGAPPAN, K.
"Transient Stability Regions of Multi-machine Power Systems"
Trans. IEEE, vol. PAS-85, pp. 169-179, February 1966.

- 5- ALEXANDROVITZ, A., and SHAPIRO, A.
"Analysis of Three-Phase Synchronous Generator by Digital Simulation in Direct Phase Quantities"

The Ninth Convention of Electrical and Electronics Engineers
in Isreal: April 1975.

- 6- ADKINS, B., and HARLY, R. G.
"The General Theory of Alternating current Machines"
Chapman & Hall London, 1975
- 7- BRERETON, D. S., LEWIS, D. G., and YOUNG, C. C.
"Representation of Induction-Motor Loads During Power-System
Stability Studies"
Trans. AIEE, vol. 76, part 3, pp. 451-461, August 1957.
- 8- BENNETT, J. M., DAKIN, F. V., and KNIGHT, U. G.
"Digital Computers and Their Applications to some Electrical
Engineering Problems"
CIGRE, Paris, paper No. 304, 1952.
- 9- BURDEN, R. L., FAIRES, J. D. and REYNOLDS, A. C.
Numerical Analysis, Second Edition July 1981
Prindle, Weber & Schmidt Inc.
- 10- B.S. No. 5311
"A. C. Circuit-Breaker of Rated Voltage Above 1 kV"
1976.

- 11- COOPER, C. B., MACLEAN, D. M., and WILLIAMS, K. G.
"Application of Test Results to the Calculation of Short-Circuit Levels in a Large Industrial System with Concentrated Induction-Motor Loads"
Proc. IEE, vol. 116, No. 11, pp. 1900-1906, November 1969.
- 12- COOPER, C. B.
"The Computation of A.C. Machine Problems"
Proc. of The First International Power System Computation Conference, August 1963. Queen Mary College, University of London, Mile End Road, E1 England.
- 13- COULTES, M. E., and WASTON, W.
"Synchronous Machine Models by Standstill Frequency Response Tests"
Trans. IEEE, vol. PAS-100, pp. 1480-1489, April 1981.
- 14- CATENACCI, G., and FORMICA, A.
"Calculation of Short-Circuit Currents and Selection of Circuit-Breaker Ratings"
CIGRA Report 103, 1958.
- 15- Committee on Protective Devices
"Simplified Calculation of Fault Currents"
Trans. AIEE, vol. 61, pp. 1133-1135, October 1942.

- 16- Committee Report 134 of AIEE.
"A New Basis for Rating Power Circuit-Breaker"
Trans. AIEE, vol. 73, part 3, pp.353-367, April 1954.
- 17- Committee Report, AIEE.
"Calculated Symmetrical and Asymmetrical Short-Circuit
Current Decrement Rates on Typical Power Systems"
Trans. AIEE, vol. PAS-75, part 3, pp. 274-292, June 1956.
- 18- CONCORDIA, C. and IHARA, S.
"Load Representation in Power System Stability Studies"
Trans. IEEE, vol. PAS-101, pp. 969-977, April 1982.
- 19-- DINELEY, J. L.
"Study of Power-System Transient Stability by a Combined
Computer"
Proc. IEE, vol. 111, No. 1, pp. 107-114, January 1964.
- 20- DANDENO, P. L., KUNDUR, P., PORAY, A. T., and ZEIN EL-DIEN,
H. M.
"Adaptation and Validation of Turbo-generator Model
Parameters Through on-line Frequency Response Measurements"
Trans. IEEE, vol. PAS-100, pp. 1658-1664, April 1981.
- 21- DE-MELLO, F. P., and HANNET, L. H.

- "Validation of Synchronous Machine Models and Derivation of Model Parameters from Tests"
Trans. IEEE, vol. PAS-100, pp. 662-672, February 1981.
- 22- FAHMI, N. R., BOWDEN, A. L., HADWICK, J. G. and JOHNSON, R. C
"Fault Analysis of Power Station Auxiliary Drive Systems"
Proc. of the 20th U.P.E.C., Huddersfield, pp. 31-36, April 1985
- 23- GABBARD, J. L., and ROWE, J. E.
"Digital Computation of Induction-Motor Transient Stability"
Trans. AIEE, vol. 76, part 3, pp. 970-975, 1957.
- 24- GLESS, G. E.
"Direct Method of Liapunov Applied to Transient Power-System Stability"
Trans. IEEE, vol. PAS-85, pp. 159-168, February 1966.
- 25- HUGHES, F. M., and ALDRED, A. S.
"Transient Characteristics and Simulation of Induction Motors"
Proc. IEE, vol. 111, No. 12, pp. 2041-2050, December 1964.
- 26- HANNA, W. M., TRAVERS, H. A., WAGNER, C. F., WOODROW, C. A.,
and SKEATS W.F.

"System Short-Circuit Currents - Proposed New Calculating Procedure for Application of Interrupting Devices and Relays"

Trans. AIEE, vol. 60, pp. 877-881, September 1941.

27- HUMPAGE, W. D., and STOTT, B.

"Predictor-Corrector Methods of Numerical Integration in Digital-Computer Analysis of Power System Transient Stability"

Proc. IEE, vol. 112, No. 8, pp.1557-1565, August 1965.

28- HAMMONS, T. J., and WINNING, D. J.

"Comparisons of Synchronous-Machine Models in the Study of the Transient Behaviour of Electrical Power Systems"

Proc. IEE, vol. 118, No. 10, pp. 1442-1458, October 1971.

29- HUENING, W. C.

"Time Variation of Industrial System Short-Circuit Currents and Induction Motors Contributions (Discussion)"

Trans. AIEE, vol. 74, part 2, pp. 90-101, May 1955.

30- JONES, C. V.

"The Unified Theory of Electrical Machines"

Buterworths, London, 1967.

- 31- KALSI, S. S., STEPHEN, D. D., and ADKINS, B.
"Calculation of System-Fault Currents due to Induction Motors"
Proc. IEE, vol. 118, No. 1, pp. 201-215, January 1971.
- 32- KALSI, S. S. and ADKINS, B.
"Transient Stability of Power Systems Containing both Synchronous and Induction Machines"
Proc. IEE, vol. 118, No. 10, pp. 1467-1474, October 1971.
- 33- KALSI, S. S.
"Switching Transient in Large Deep-Bar Squirrel Cage Induction Motors"
Trans. IEEE, vol. PAS-92, pp. 1266-1273, January 1973.
- 34- KIMBARK, E. W.
"Power System Stability" vol. I
JOHN WILEY & SONS Inc., 1948.
- 35- KUNDUR, P. and DANDENO, P. L.
"Implementation of Advanced Generator Models into Power System Stability Programs"
Trans. IEEE, vol. PAS-102, No. 7, pp. 2047-2054, July 1983.
- 36- KIMBARK, E. W.

"Power System Stability" vol. III

JOHN WILEY & SONS Inc., Second Printing 1963.

37- KELLY, A. R.

"Induction-Motor Model for Industrial Power System
Computation"

Trans. AIEE, vol. 81, part 2, pp. 166-172, 1962.

38- KILGORE, L. A.

"Effects of Saturation on Machine Reactance"

Trans. AIEE, vol. 54, pp. 545-549, May 1935.

39- LYON, W. V.

"Transient Analysis of Alternating Current Machinery"

WILEY 1954.

40- MORTLOCK, J. R.

"A Computer for Use in Power System Transient Stability
Studies"

Journal IEE, vol. 95, part 2, pp. 751-755, 1948.

41- MILES, J. G.

"Analysis of Overall Stability of Multi-machine Power
Systems"

Proc. IEE, vol. 108, pp. 203-211, November 1961.

- 42- MARON, M. J.
"Numerical Analysis: A Practical Approach"
Macmillan Publishing Co. Inc. 1982.
- 43- MARTIN, D. W.
"Runge-Kutta Methods for Integrating Differential Equations
on High Speed Digital Computers"
Computer Journal, 1, pp. 118-123, 1958.
- 44- MORTLOCK and DAVIS
"Power System Analysis"
CHAPMAN & HALL, 1952.
- 45- PARK, R. H.
"Two Reaction Theory of Synchronous Machine. Generalised
Method of Analysis Part I"
Trans. AIEE, vol. 52, pp. 352-355, 1933.
- 46- PARK, R. H.
"Two Reaction Theory of Synchronous machines. Generalised
Method of Analysis Part II"
Trans. AIEE, vol. 48, pp. 716-730, January 1929.
- 47- RAFIAN, M. and LAUGHTON, M. A.

"Aspects of Induction and Synchronous Motor Analysis Using
Dynamic Phase Co-ordinate Theory"

Proc. IEE, vol. 126, No. 8, pp. 749-758, August 1979.

48- RAFIAN, M. and LAUGHTON, M. A.

"Determination of Synchronous Machine Phase Co-ordinate
Parameters"

Proc. IEE, vol. 123, No. 8, pp. 818-824, August 1976.

49- RAMSDEN, V. S., ZORBAS, N. and BOOTH, R. R.

"Prediction of Induction-Motor Dynamic Performance in Power
-Systems"

Proc. IEE, vol. 115, pp. 551-518, 1968.

50- SMITH, I. R. and SRIHARAN, S.

"Transient Performance of The Induction Motor"

Proc. IEE, vol. 113, No. 7, pp. 1173-1181, July 1966.

51- SHANKLE D. F., MURPHY, C. M., LONG, R. W. and HARDER, E. L.

"Transient-Stability Studies _ I, Synchronous and Induction
Machines"

Trans. AIEE, vol. 74, part 3, paper No. 54-331, pp. 1563-
1580, 1955.

52- SHACKSHAFT, G., SYMONS, O. C. and HADWICK, J. G.

- "General-Purpose Model of Power Systems Loads"
Proc. IEE, vol. 124, pp. 715-723, 1977
- 53- STANLEY, H. C.
"An Analysis of The Induction Machine"
Trans. AIEE, vol. 57, pp. 751-757, 1938.
- 54- SUBRAMANIAN, P. and MALIK, O. P.
"Digital Simulation of a Synchronous Generator in Direct
Phase Quantities"
Proc. IEE, vol. 118, No. 1, pp. 153-160, January 1971.
- 55- SHACKSHAFT, G. and PORAY, A. T.
"Implementation of New Approach to Determination of
Synchronous Machine Parameters from Test"
Proc. IEE, vol. 124, No. 12, pp. 1170-1178, December 1977.
- 56- Switch Gear Committee, AIEE.
"Simplified Calculation of Fault Currents"
Trans. AIEE, vol. 67, part 2, pp.1433-1435, 1948.
- 57- STAATS, G. W.
"Induction and Synchronous Motors Compared for System
Stability"
Trans. IEEE, vol. IA-12, pp. 470-473, 1976.

58- TEICHGRAEBER, R. D., HARRIS, F. W., and JOHNSON, G. L.

"New Stability Measure for Multi-machine Power Systems"

Trans. IEEE, vol. PAS-89, No. 2, pp. 233-239, February 1970.

59- WEEDY, B. M.

"Electric Power Systems" Second Edition 1977

JOHN WILEY & SONS Inc.

BIBLIOGRAPHY

- 60- ADAMSON, C., BARNES, L. and NELLIST, B. D.
"The Automatic Solution of Power-System Swing-Curve Equations"
Proc. IEE, vol. 104A, pp.143-151, 1957.
- 61- AMIN, A. R. and BRADLEY, K. J.
"A Model for Prediction of the performance of Induction Machines"
Proc. of the 18th U.P.E.C., pp. 589- 594, April 1983.
- 62- AKHTAR, M. Y.
"Frequency-Dependent Dynamic Representation of Induction-Motor Loads"
Proc. IEE, vol. 115, pp. 802-812, 1968.
- 63- BARBER, M. D. and GIANNINI, M.
"Simulation of a Synchronous Generator Connected via a Delta-Star Transformer"
Proc. IEEE, vol. 121, No. 12, pp.1513-1521, December 1974.
- 64- BERG, G. J.
"Power System Load Representation"

Proc. IEE, vol. 120, pp. 344-348, March 1973.

65- Discussion on:

"Starting Methods for Generator/Motor units Employed in Pump-Stroke Stations and Investigation into Damping Torque Coefficients and Stability of Two Synchronous Machine System Employed in Synchronous Starting"

Proc. IEE, vol. 118, No. 10, pp.1475-1485, October 1971.

66- FENWICK, D. R. and WRIGHT, W. F.

"Review of Trends in Excitation Systems and Possible Future Developments"

Proc. IEE, vol. 123, No. 5, pp.413-420, May 1976.

67- FITZGERALED, A. E. and KINGSLEY, C. JR.

"Electric Machinery" Second Edition

McGRAW-HILL Book Company, Inc.

68- FUDEH, H. R. and ONG, C. M.

"Modelling and Analysis of Induction Macines Containing Space Harmonics. Part 1"

Trans. IEEE, vol. PAS-102, pp. 2608-2615, August 1983.

69- FUDEH, H. R. and ONG, C. M.

- "Modelling and Analysis of Induction Machines Containing Space Harmonics. Part 2"
Trans. IEEE, vol. PAS-102, pp. 2616-2620, August 1983.
- 70- FUDEH, H. R. and ONG, C. M.
"Modelling and Analysis of Induction Machines Containing Space Harmonics. Part 3"
Trans. IEEE, vol. PAS-102, pp. 2621-2628, August 1983.
- 71- GERAY, B. J. and SCHIPPEL, H. W.
"Transient Stability of an Isolated Radial Power Network with Varied Load Divisions"
Trans. IEEE, vol. PAS-83, pp. 964-979, 1964.
- 72- HARDER, E. L. and CHEEK, R. C.
"Regulation of A-C Generator with Suddenly Applied Load"
Trans. AIEE, vol. 63, pp. 310-318, June 1944.
- 73- HARRIS, M. R., LAWRENSON, P. J. and STEPHENSON, J. M.
"Per-Unit Systems with Special Reference to Electrical Machines"
IEE Monograph 4 'Peter Perigrinus Ltd. 1970'
- 74- HWONG, H. H.

"Mathematical Analysis of Double Line to Ground Short-Circuit
of an Alternator"

Trans. IEEE, vol. PAS-86, pp. 1245-1257, 1967.

75- JORDAN, H. E.

"Digital Computer Analysis of Induction-Machines for System
Stabilty"

Trans. IEEE, vol. PAS-86, pp. 722-728, 1967.

76- JHA, R. and Mahalanabis, A. K.

"Improved Technique for Computation of Power-system Transient
Stability Regions"

Proc. IEE, vol. 122, No. 12, pp.1402-1404, December 1975.

77- LAUGHTON, M. A.

"Analysis of Unbalanced Polyphase Networks by the Method of
Phase Co-ordinates, Part I"

Proc. IEE, vol. 115, No. 8, pp. 1163-1172, August 1968.

78- LAUGHTON, M. A.

"Analysis of Unbalanced Polyphase Networks by the Method of
Phase Co-ordinates", Part II"

Proc. IEE, vol. 116, No. 5, pp. 857-865, May 1969.

79- LIM, K. M. and THOMAS, G.

"Induction Motor Operation with Constant Pull-out Torque Over
a Wide Frequency Range"

Proc. of the 18th U.P.E.C., pp.639- 644, April 1984.

80- LAI, L. L.

"Simulation of Power Station Protection Equipment"

Ph.D. Thesis, University of Aston in Birmingham, 1984

81- MILLER, A. R. and WEIL, W. R., JR.

"Alternator Short-Circuit Currents Under Unsymmetrical
Transient Conditions"

Trans. AIEE, vol. 56, pp. 1268-1276, October 1937.

82- OWEN, R. E. and LEWIS, W. A.

"Asymmetry Characteristics of Progressive Short-Circuits on
Large Synchronous Generators"

Trans. IEEE, vol. PAS-90, pp. 587-596, April 1971.

83- OLLE I. ELGERD.

"Electric Energy System Theory", An Introduction.

McGRAW-HILL Book Company, Inc. T.M.T Edition, 1973.

84- ROBB, D. D. and KRAUSE, P. C.

"Dynamic Simulation of Generator Faults Using Combined 'abc'
and ' δ dq' Variables"

Trans. IEEE, vol. PAS-94, pp. 2084-2090, November 1975.

85- SIRHARAN, S.

"Digital Simulation of a Group of Induction Motors"

Proc. IEE, vol. 122, No. 12, pp. 1399-1401, December 1975.

86- SAHA, T. N. and BASU, T. K.

"Analysis of a Symmetrical Faults in Synchronous Generators
by d-q-0 Frame of Reference"

Proc. IEE, vol. 119, pp. 587-595, May 1972.

87- SHACKSHAFT, G.

"General Purpose Turbo-alternator Model"

Proc. IEE, vol. 110, No. 4, pp. 703-713, April 1963.

88- ZURICH, W. G. and BADEN, T. G.

"The Interruption of Fault Currents with Delay Current zeros
by HV Circuit-Breakers"

Brown Boveri Review, vol. 67, pp. 237-243, April 1980.